Binding Interactions of Bile Acids and Bile Pigments with Amines

by

Xiao-Xia Zhu

A thesis submitted to
the Faculty of Graduate Studies and Research
in partial fulfillment of the requirements
for the degree of
Doctor of Philosophy

Department of Chemistry
McGill University
Montréal, Québec, Canada

May 1988

Ph.D. Chemistry

Xiao-Xia Zhu

Binding Interactions of Bile Acids and Bile Pigments with Amines

Abstract

The binding of selected bile acids and bile pigments by peptides and quaternary amines has been studied by adsorption and NMR experiments. Novel adsorbents with quaternized peptide-containing functional groups for bile acids have been prepared by solid phase peptide synthesis techniques. The adsorption studies, conducted in aqueous buffer solutions, show that these resins have an enhanced capacity, on a per active site basis, and improved specificity over cholestyramine and colestipol. The interaction between bile acid anions and the pendants is predominantly ionic linkage, although hydrophobic and other interactions are also important. An NMR study of the binding between bile acids and various ligands, including peptides, by the determination of carbon-13 spin-lattice relaxation times, confirms the ionic and hydrophobic interactions which occur cooperatively and simultaneously.

New adsorbents for bilirubin have been prepared by covalently coating a water-swellable polyamide resin with polypeptides. These resins have much higher capacities for bilirubin in aqueous buffer solution than cholestyramine and improved capacities over the resins with attached oligopeptide pendants. The binding behavior of the resin coated with poly-D-lysine is the same as that of poly-L-lysine. The amount of bilirubin adsorbed by these resins is directly proportional to the number of lysine residues on the resin, which is consistent with the formation of an ionic linkage. This is confirmed by a study of the interaction of bilirubin with an oligopeptide, L-lysyl-L-lysine, by measurements of proton and carbon-13 NMR spin-lattice relaxation times combined with nitrogen-15 NMR experiments. The ^{15}N NMR spectra of bilirubin and some related bile pigments have also been assigned by two-dimensional ^{15}N-^{1}H heteronuclear correlation experiments.

Ph.D. Chimie

Xiao-Xia Zhu

L'étude des interactions des acides et pigments biliaires avec des amines

Résumé

Les interactions de certains acides et pigments biliaires par des peptides et des amines quaternaires ont été étudiées par des expériences d'adsorption et de RMN. De nouveaux adsorbants pour les acides biliaires portant des groupes fonctionnels peptidiques quaternisés ont été préparés par la méthode de synthèse de peptides en phase solide. Les résultats des adsorptions, faites en solutions aqueuses tamponées, ont démontré que ces résines ont une plus grande capacité, lorsque calculée à partir du nombre de groupes actifs, et sont plus spécifiques que la cholestyramine et le colestipole. L'interaction entre les acides biliaires et les résines est largement due à des liaisons ioniques, mais des interactions hydrophobes et autres peuvent aussi contribuer à cette association. Une étude de RMN des interactions entre les acides biliaires et des ligands variés incluant des peptides, a été faite en mesurant les temps de relaxation spin-réseau du carbone-13. Celle-ci a confirmé les interactions ioniques et hydrophobes qui sont coopérativement et simultanément présentes.

De nouveaux adsorbants pour la bilirubine ont été préparés par l'enduit de polypeptides sur une résine de polyamide gonflée en milieu aqueux. Les adsorptions, qui ont été faites en solution aqueuse tamponnée, ont démontré que ces résines ont de plus grandes capacités que la cholestyramine et que les résines sur lesquelles sont attachées des chaînes oligopeptidiques. L'adsorption de la bilirubine par la résine enduite de poly-D-lysine est semblable à celles enduites de poly-L-lysine. Ces résultats montrent que la quantité de bilirubine adsorbée est directement proportionnelle au nombre de résidus de lysine sur la résine. Ce phénomène est en accord avec la formation de liaisons ioniques lors de l'interaction. Cette hypothèse est confirmée par une étude de l'interaction entre la bilirubine et un oligopeptide, L-lysyl-L-lysine, en mesurant les temps de relaxation spin-réseau des protons et du carbone-13 combinée avec le RMN de l'azote-15. Les spectres de RMN de ^{15}N de la bilirubine et quelques-uns des pigments biliaires apparentés ont été assignés à l'aide des expériences de corrélation hétéronucléaire ^{15}N-^{1}H en RMN bi-dimensionnelle.

Wish all things life and health, but even better help them prosper according to their nature.

Xun Kuang (313 B.C.-238 B.C.)

Acknowledgements

The heroic stories of Dr. Norman Bethune that I read in school made me feel close to the people of his homeland. This feeling has been confirmed during my studies in Canada. I appreciate the warmth and friendliness of Bethune's people who have made me feel at home in a distant and exotic land.

I am greatly indebted to my research directors, Dr. G.R. Brown and Dr. L.E. St-Pierre, whose support and guidance made my stay at McGill a valuable and memorable experience. Dr. Brown's rigorous scientific approach and Dr. St-Pierre's profound wisdom and humor have been constant sources of inspiration for my research and study.

I am grateful to McGill University for awarding me the Clifford C.F. Wong and the Dalbir Bindra Fellowships and to the Ministry of Education of China for a scholarship.

I would also like to express my gratitude to the professors and friends in the Chemistry Department and at McGill University for their help during the entire course of my study in the University. Special thanks go to Ms. R. Charron, who has been of great help during my stay in the Department.

I wish to thank the following people for their help and expertise in the research work and in the preparation of this thesis:

Dr. F. Sauriol for her assistance in performing the NMR experiments and many helpful discussions; Dr. D.F.R. Gilson for very helpful discussions concerning the NMR relaxation times; Dr. B. Belleau for the interesting discussion on the stability of peptides and for providing the thionation reagent;

Messrs. J.A. Rochemont and N. Franco, of the Clinical Research Institute of Montreal, for their aid in the analysis of the amino acid content of the peptide resins; Ms. D. Léonard for the quaternization of the poly-L-lysine coated resin et pour son aide avec la traduction du résumé de cette thèse en français; Dr. S.-D. Clas and Ms. S.V. McBride for providing the substitution of the colestipol resin as obtained by titration; Mr. T.F. Blahovici, whose ingenious touch on the

computer software made the superscripts in the text look so superb; Dr. H.S. Calderon for reading part of the manuscript; and my colleagues in the laboratory for helping to create a pleasant atmosphere.

Continued support from my professors and friends in China, especially that from Professor Ping-Lum Ho, of Nankai University, has always been an encouragement to me; the invaluable understanding and friendship with my Canadian and Chinese friends in Montreal made my stay in this city interesting and enjoyable. I thank them all.

I thank my mother and father, and my family; their immense love and support have been the most abundant wealth I have ever possessed.

Table of Contents

Part I Bile Acids

Part II Bile Pigments

Appendices

List of Figures

List of Tables

List of Abbreviations and Symbols

The abbreviations and symbols for the physical or chemical terms and units used in this thesis are in accordance with those adopted by IUPAC (International Union of Pure and Applied Chemistry), IUPAP (International Union of Pure and Applied Physics) and IUB (International Union of Biochemistry), published in the Handbook of Chemistry and Physics. The three-lettered abbreviations for amino acids are those recommended by the Joint Commission on Biochemical Nomenclature of IUPAC and IUB. Some of the abbreviations and symbols used are listed below.

Å	Angstrom (1×10^{-8} cm)
Ala	alanine
b.p.	boiling point
BOC	*tert*-butyloxycarbonyl
BR	bilirubin
BRDME	bilirubin dimethyl ester
BSA	bovine serum albumin
BTMA	benzyltrimethylammonium chloride
CA	cholic acid
CAME	cholic acid methyl ester
CDCA	chenodeoxycholic acid
CMC	critical micellar concentration
CMT	critical micellar temperature
CoA	coenzyme A
conc	concentration
COSY	correlated spectroscopy
d	density
D_1, D_2, D_3	delay of time (in NMR pulse sequences)
2-D	two-dimensional
D_2O	deuterium oxide
DCA	deoxycholic acid
DCC	1,3-dicyclohexylcarbodiimide
DCM	dichloromethane
DEA	N,N-diisopropylethylamine
DEPT	distortionless enhancement by polarization transfer

Diff	difference
DL	dilysine, L-lysyl-L-lysine
dl	deciliter
DMG	N,N-dimethylglycine
DMSO	dimethyl sulfoxide
DMSO-d_6	deuterated dimethyl sulfoxide
DP	degree of polymerization
E	energy
eq	equivalent
F	force
FT	Fourier transform
g	gram
GCA	glycocholic acid
h	hour
	Planck constant (6.6262×10^{-34} $m^2 kg\, s^{-1}$)
HETCOR	heteronuclear correlation
HOBT	1-hydroxybenzotriazole
HPLC	high performance liquid chromatography
HSA	human serum albumin
Hz	Hertz
I	quantum number of nuclear spin
INEPT	insensitive nuclei enhanced by polarization transfer
IR	infrared
J	Joule
$^1J_{CH}$	C-H coupling constant
K	binding constant
k	Boltzmann constant (1.3806×10^{-23} $m^2 kg\, s^{-2} K^{-1}$)
kJ	kilo-Joule
LCA	lithocholic acid
Lys	lysine
M	concentration in molarity (mole/liter solution)
m	discrete spin variable, magnetic sub-level
m	concentration in molality (mole/1000 g solvent)
m.p.	melting point
mg	milligram
MHz	mega-Hertz
min	minute
ml	milliliter
mM	millimole/liter
mol	mole
ms	millisecond

MW	molecular weight
N	concentration in normality
NaC	sodium cholate
NADH	reduced nicotinamide adenine dinucleotide
NADPH	reduced nicotinamide adenine dinucleotide phosphate
NaGC	sodium glycocholate
n_H	number of protons
NMR	nuclear magnetic resonance
NOE	nuclear Overhauser effect
PDL	poly-D-lysine
PLL	poly-L-lysine
PLO	poly-L-ornithine
ppm	part per million (unit for NMR chemical shift)
Q	electric charge
R	gas constant (8.3143 $m^2kg\ s^{-2}K^{-1}mol$)
RT	retention time
sec	second
T	temperature
T_1	NMR spin-lattice relaxation time
T_2	NMR spin-spin relaxation time
THF	tetrahydrofuran
TLC	thin layer chromatography
TMG	N,N,N-trimethylglycine
TMS	tetramethylsilane
tris buffer	tris(hydroxymethyl)-aminomethane-HCl buffer
TSP	sodium trimethylsilylpropionate-2,2,3,3-d_4
UDG	uridine diphosphate glucuronate
UV	ultraviolet
$[\alpha]_D$	specific rotation
γ	gyromagnetic ratio ($\gamma_H = 2.6752 \times 10^8\ kg^{-1}s\ A$)
ΔG	free energy change
ΔH	enthalpy change
ΔS	entropy change
ε_0	permittivity of vacuum ($8.85418 \times 10^{-12}\ m^{-3}kg^{-1}s^4A^2$)
ε_r	relative permittivity (dielectric constant)
λ	wavelength
μl	microliter
μs	microsecond
τ	correlation time
ω	Larmor frequency

Preface

In ancient China the amount of bile a person possessed was considered to be an indication of one's courage. Brave warriors were found, by autopsy, to have larger gallbladders. Even today, people who "have a lot of guts" are described as "having a lot of bile" or *youdanliang* in Chinese. In the Western languages, bile usually refers to one's anger, rage or bad temper. Whatever it may be, whatever influences it may have on one's personality, it is very clear that we can never overemphasize the importance of the bile in the human body and that we still have a lot more to learn about the bile, physiologically and chemically.

The major components of the bladder or hepatic bile, in addition to water, are bile salts and bile pigments. Other biliary components include small quantities of cholesterol, fatty acids and inorganic salts. Both bile acids and bile pigments have been studied extensively as their biological significance has been recognized, especially as related to their medical and clinical aspects.

This thesis concerns a chemical approach to the study of the binding and interaction of bile acids and bile pigments with biocompatible polymeric materials. Bile acids and bile pigments belong to two different species of biocompounds, though they are related closely in their existence. The thesis is therefore presented in two parts. Part I deals with the study of bile acids, and Part II with bile pigments. Each part consists of three chapters, the first being a general introduction on the biological formation, metabolism and chemical properties, the second a description of the preparation of novel adsorbents and the adsorption studies *in vitro*, and the third a study of the interactions probed by nuclear magnetic resonance techniques. Chapter 7 gives a summary of the claims to originality for this research and suggestions for future exploration of the subject. The physical properties of bile acids and pigments, the synthesis and stability of peptides, the NMR pulse sequences, etc., are listed in the appendices.

Part I
Bile Acids

1 Introduction

Coronary heart disease is the leading cause of death among adults in many countries. It is often related to a high cholesterol level in the blood, hypercholesterolemia, which is usually a consequence of inefficiency in cholesterol metabolism or excessive intake of cholesterol in the diet. It has been found that the level of cholesterol in the serum, along with smoking and hypertension, are major risk factors for the development of atherosclerosis and cardiovascular diseases (1).

Cholesterol is the biological source for the synthesis of bile acids, which are useful in the digestion of dietary fat and other food components. However, the excessive accumulation of cholesterol in human plasma can result in deposition on the wall of blood vessels because of its low solubility in aqueous media.

Over the last few decades, researchers have focussed their attention on lowering the cholesterol level in the blood to reduce the risk of cardiovascular diseases. This can be achieved with limited success by cutting back in the cholesterol intake from food sources and accelerating the elimination of cholesterol from the human body, although genetic factors can be important. The inhibition of its production in the body may also lead to a lower level of cholesterol in the serum. The major biological pathway for the elimination of cholesterol involves its conversion to bile acids and excretion as neutral sterols in the feces (2).

1.1 Metabolism of Cholesterol and Bile Acids

1.1.1 Cholesterol Formation

The chemical structures of cholesterol and the closely related cholic acid are shown in Figure 1.1. Cholesterol is a natural steroid found in almost all living organisms. The amounts found in plant sources are usually low, except for seed oils and pollen, but animal products are rich sources of cholesterol.

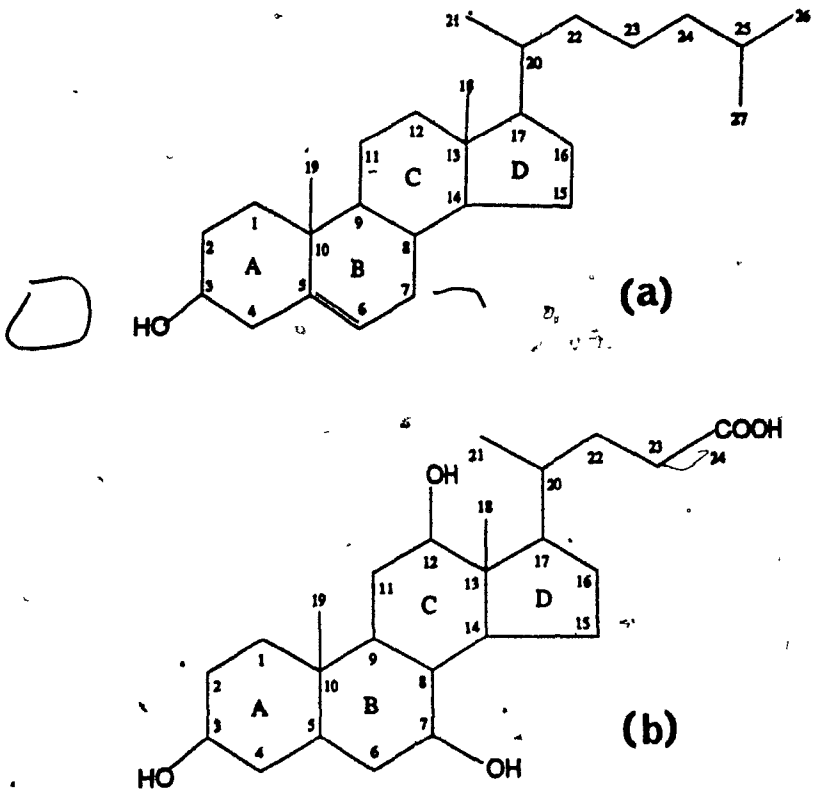

Figure 1.1 Chemical structures of (a) cholesterol and (b) cholic acid. The numbering of the steroid skeleton system is also shown.

The microsomal and cytosol fractions of all nucleated cells of the tissues are responsible for cholesterol synthesis. The parts of the body most active in the production of cholesterol are the liver, skin, intestine and testes. Figure 1.2 shows the major steps of the biosynthesis of cholesterol. These steps has been studied by asymmetric labelling and other techniques (3). Acetyl-coenzyme A, which is biologically formed from amino acids, is the biosynthetic origin of cholesterol. First, mevalonate, a six-carbon compound, is formed from the coenzyme by the reduction with enzymes. Then mevalonate is converted to isoprenoid after losing carbon dioxide. Isoprenoid is, in fact, the building block of the steroid skeleton, since six isoprenoid molecules condense to form squalene, which closely resembles the steroid skeleton. The ring closures of squalene following

enzymatic oxidation produces lanosterol. This parent steroid is finally converted to cholesterol after losing three of its methyl groups.

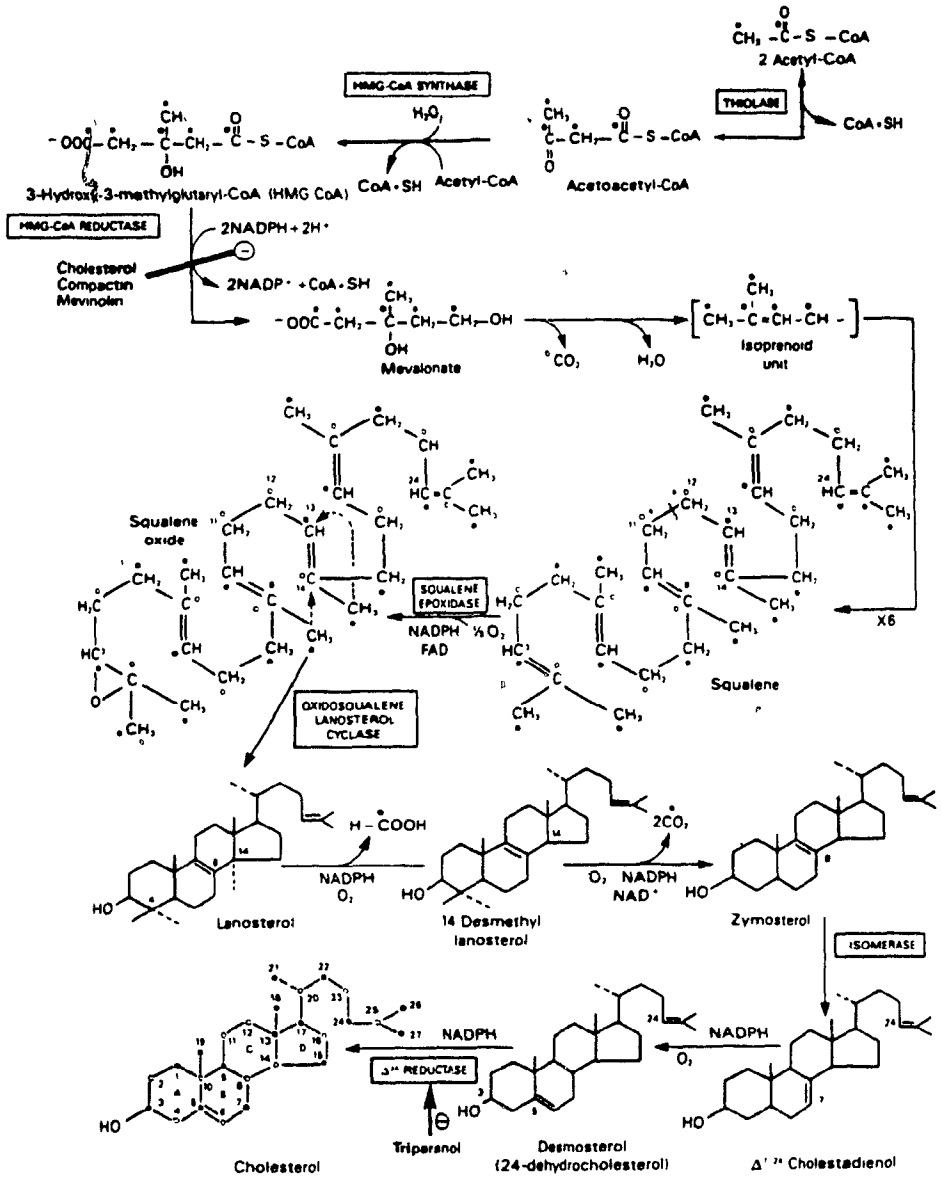

Figure 1.2 The biosynthesis of cholesterol in the human body (reference 2). The carbons with a dot represent the original methyl carbon of the acetate, and the carbons with a circle represent the original carbonyl group.

The rate of the biosynthesis of cholesterol by the human body is about one gram/day. In addition, the average daily diet in North America provides about 500 mg of cholesterol for men and 350 mg for women (4). Food of animal origin,

such as meat, liver, brain and egg yolk, is the most significant source of cholesterol. The dietary cholesterol, together with that in the intestinal fluids and bile, is absorbed in the small intestine with the aid of mixed micelles of bile salts and lecithin. An increase in the amount of fatty acids in the diet increases the efficiency of intestinal absorption of cholesterol (5). Cholesterol is usually esterified in the wall of intestine with the aid of an enzyme, cholesterol esterase.

Cholesterol exists in all living cells. Interestingly, it has been found that cancer cells produce two or three times as much cholesterol as normal cells. This over-production of cholesterol through an acquired genetic defect in turn causes the formerly normal cell to divide abnormally fast (6). It has also been reported that high cholesterol content in urine may be a clue to some cancers (7).

1.1.2 Metabolism of Bile Acids

The process of biosynthesis of bile acids from cholesterol is shown in Figure 1.3. The two main *primary bile acids*, cholic and chenodeoxycholic acids, are synthesized daily from cholesterol in the liver by several intermediate steps under the catalysis of NADPH and CoA (coenzyme A). Under normal circumstances, bile acids are synthesized by the liver at a relatively low rate of 200-500 mg/day. This rate is regulated to replace the daily loss of bile acids in the feces (8).

The bile acids usually, but not necessarily, enter the bile as glycine or taurine conjugates. In humans, the ratio of the glycine to taurine conjugates is normally 3:1. The amount of taurine conjugation depends on the availability of taurine. Because of the presence of sodium and potassium ions in the bile, which is alkaline, the bile acids and their conjugates usually exist as salts (9).

The primary bile acids, cholic and chenodeoxycholic acids, are derived directly from cholesterol. The *secondary bile acids*, deoxycholic and lithocholic acids, result from the conversion of the primary bile acids by 7α-dehydroxylating enzymes of bacterial origin during the enterohepatic circulation (Section 1.1.3). It has been found that the tri- and dihydroxylated bile acids are the predominant bile acids of most mammalian biles (10). The major bile acids present in the human bile are the glycine and taurine conjugates of cholic, chenodeoxycholic and deoxycholic acids, with minor quantities of lithocholic acid and ursodeoxycholic acid (the 7β-isomer of chenodeoxycholic acid). Although the liver does not itself

produce secondary bile acids, the presence of the secondary bile acids in the bile results from the absorption from the intestine (11).

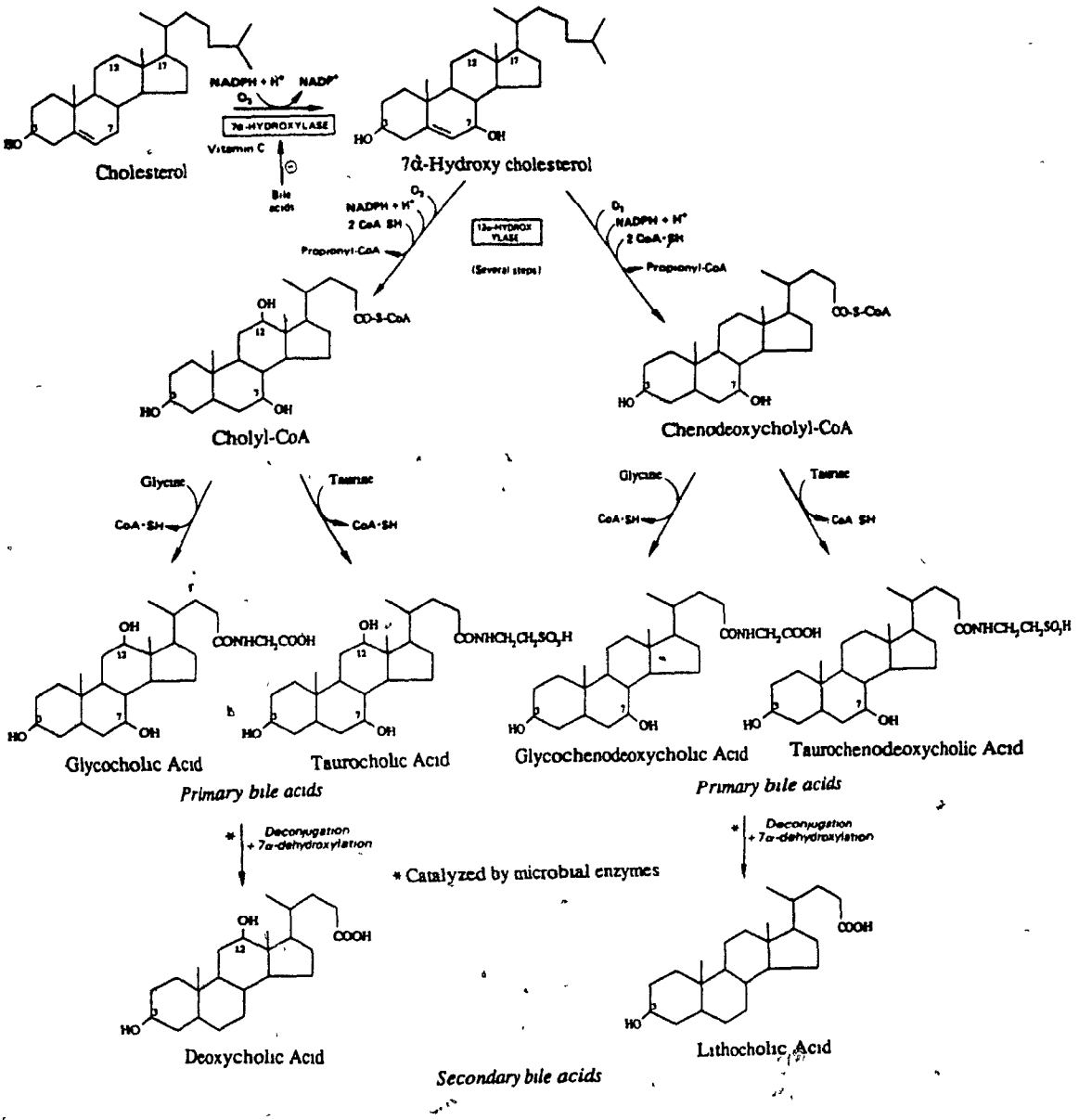

Figure 1.3 The biosynthesis of bile acids from cholesterol and their conjugation and degradation (partially from reference 8).

1.1.3 Enterohepatic Circulation

During digestion, the gallbladder contracts and excretes bile rapidly to the small intestine. The bile salts, usually in conjugated form, enter the duodenum together with cholesterol, phospholipids as well as other minor constituents of the bile. After participating in the absorption of lipids in the jejunum, the bile salts pass down to the ileum, where they are almost exclusively absorbed, complexed with proteins, and returned to the liver through hepatic portal veins (Figure 1.4). This cycle is known as enterohepatic circulation (12).

The re-absorption of bile salts in the ileum depends on a variety of factors, such as gallbladder emptying, interdigestive mobility (13), the physical state of the intestinal contents, and the structure of the bile acid molecules after modification by intestinal bacteria. In the lower ileum and colon some of the primary bile salts are converted to secondary bile salts by the deconjugation and 7α-dehydroxylation under the action of enzymes of the intestinal flora. The secondary bile salts may also reappear in the bile after being partially absorbed.

Enterohepatic circulation is a very efficient process. Each day the bile pool, which contains about 3-5 grams of bile acids, can be cycled 6 to 10 times with a small loss of bile salts, as little as 500 mg per day, corresponding to about 1% loss per cycle. Under normal conditions, they are synthesized from cholesterol by the liver at about the same rate, i.e., 500 mg/day, to maintain the pool of bile acids. This represents the only major route for the elimination of cholesterol from the human body.

The enterohepatic circulation may be interrupted by the administration of oral adsorbents or by a partial or complete ileal exclusion operation. The interruption prevents the bile salts from being reabsorbed in the ileum and consequently, more cholesterol is consumed to produce enough bile acids to maintain the bile pool. Therefore, this can lead to significant reduction of cholesterol level in the plasma of patients with hypercholesterolemia (14).

1.1.4 Functions of Bile Salts

Bile salts are essential in the body since their functions in the digestive tract are of great physiological importance. The molecular structure of bile salts determines that they can form micelles easily in an aqueous environment. The carboxylic acid group and the hydroxyl groups of the bile salts are hydrophilic, while the remaining parts of the molecules are hydrophobic. This property of bile

salts is important for the degradation and absorption of lipids in the intestine. Bile salts help to emulsify fat and solubilize lipids by forming mixed micelles. When the concentration of intestinal bile salts is low, the absorption of fat can be reduced significantly (15). They can also promote excretion of water and solutes. Therefore, they are sometimes used as laxatives.

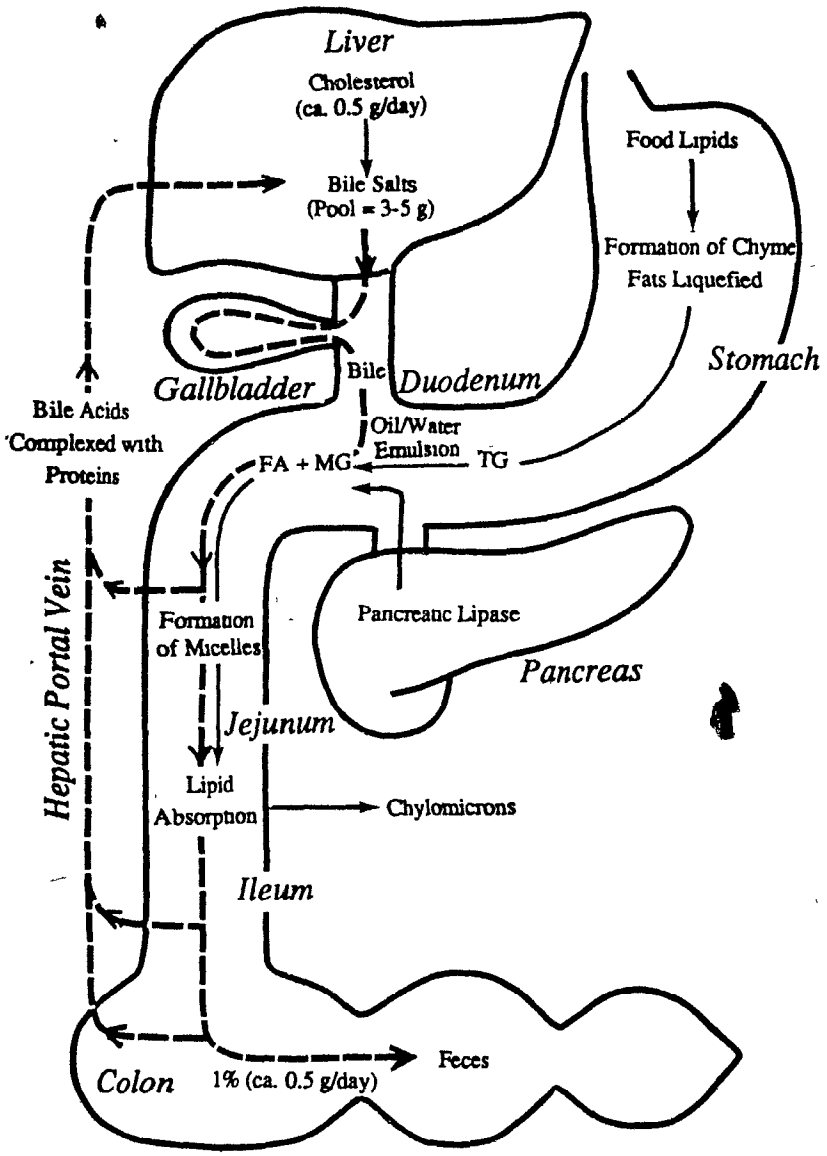

Figure 1.4 The enterohepatic circulation of bile acids and the digestion of lipids (modified from reference 8). The dashes indicate the route of the circulation of bile acids; TG: triacylglycerol; MG: monoacylglycerol; FA: long-chain fatty acid.

Another important feature of bile salts is their function in promoting the biliary excretion of cholesterol. The presence of bile salts in the bile can prevent the formation of gallstones, since bile salts together with lecithin help to solubilize cholesterol, and possibly bile pigments, in the bile.

The bile salts can also have negative effects biologically. For people who suffer from hypercholesterolemia, bile salts can elevate the cholesterol level in the plasma, while aiding the absorption of dietary cholesterol in the intestine. Bile salts can also induce diarrhea in patients with ileopathy since bile salts tend to prevent colonic water adsorption. This can be treated in most cases by bile salt binding drugs (16).

It has also been reported that the bile acids, such as lithocholate and deoxycholate, enhance tumor growth in animals (17). Studies have shown that the naturally occurring bile acids and their metabolites have a carcinogenic effect, especially after modification by the intestinal bacteria (18). It is of interest to mention that most of the adverse effects of bile salts can be reduced by bile salt binding agents, e.g., the risk of colon cancer can be reduced by such drugs (19).

1.2 Properties of Bile Acids

1.2.1 Structure

Most of the naturally occurring bile acids are C-24 saturated carboxylic acids that belong to the steroid family. The cyclopentanophenanthrene nucleus of bile acids contains 19 carbon atoms (Figure 1.1b). The side chain, located at the C17 position, consists of three to nine carbons. Therefore, the bile acids contain 22 to 28 carbon atoms, depending on their natural occurrence. The carboxylic acid group is located at the end of the side chain.

The bile acids have three six-membered rings and one five-membered ring in conjunction to form the steroid skeleton. The skeleton with a C-5 side chain is termed the cholane nucleus. Therefore, the bile acid without hydroxylic substituents is termed cholanoic acid. In the bile acids of vertebrates, the rings A and B are usually of *cis* (5β) configuration, but in some animal species the AB *trans* (5α or *allo*) configuration may occur. The BC and CD ring junctures are *trans* and the methyl group at position C13 is *cis* to that of position C10. The 5β- and 5α-configurations of cholic acid are shown in Figure 1.5.

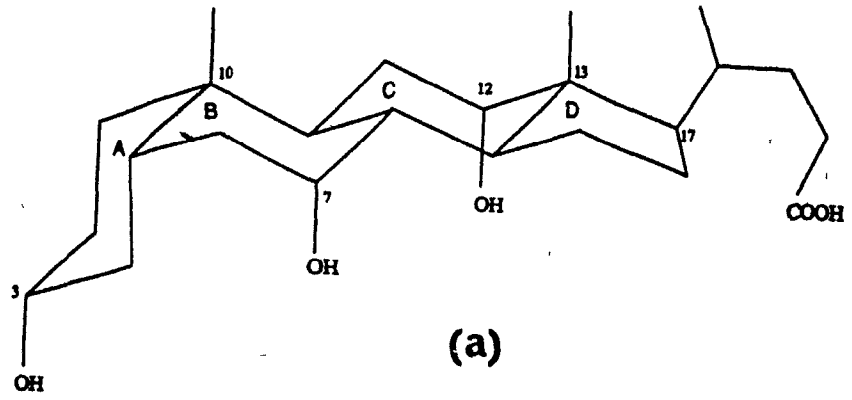

(a)

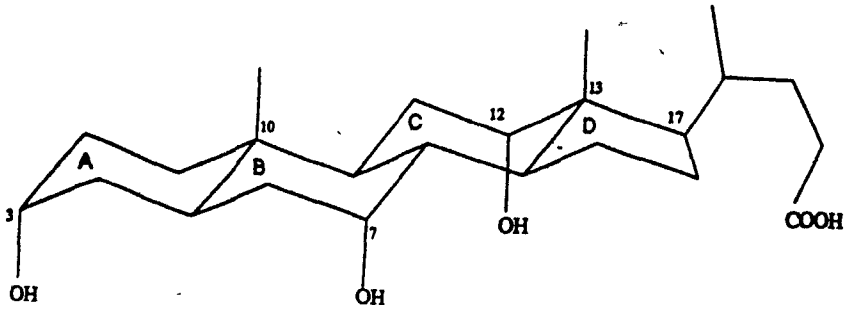

(b)

Figgure 1.5 The chemical configuration of cholic acid: (a) the commonly occurring 5β-configuration; (b) the *allo* or 5α-configuration.

As indicated in Figure 1.2, the naturally occurring primary bile acids, cholic and chenodeoxycholic acids (systematic names being 3α-, 7α-, 12α-trihydroxy cholanoic acid and 3α-, 7α-dihydroxy cholanoic acid), have three and two hydroxyl groups, respectively. The secondary bile acids, deoxycholic and lithocholic acids, possess two and one hydroxyl group(s), respectively. The hydroxyl groups are located at positions C3, C7 and C12 and are all in α- or equatorial positions. The carboxyl group is also equatorially oriented. Therefore, the hydrophilic groups, i.e., the hydroxyl and carboxyl groups, are all located beneath the plane of the steroid skeleton, while the amphiphilic methyl groups lie

on the other side of the skeleton (Figure 1.6). The planar polarity of the molecules is very important to the physico-chemical properties of bile salts.

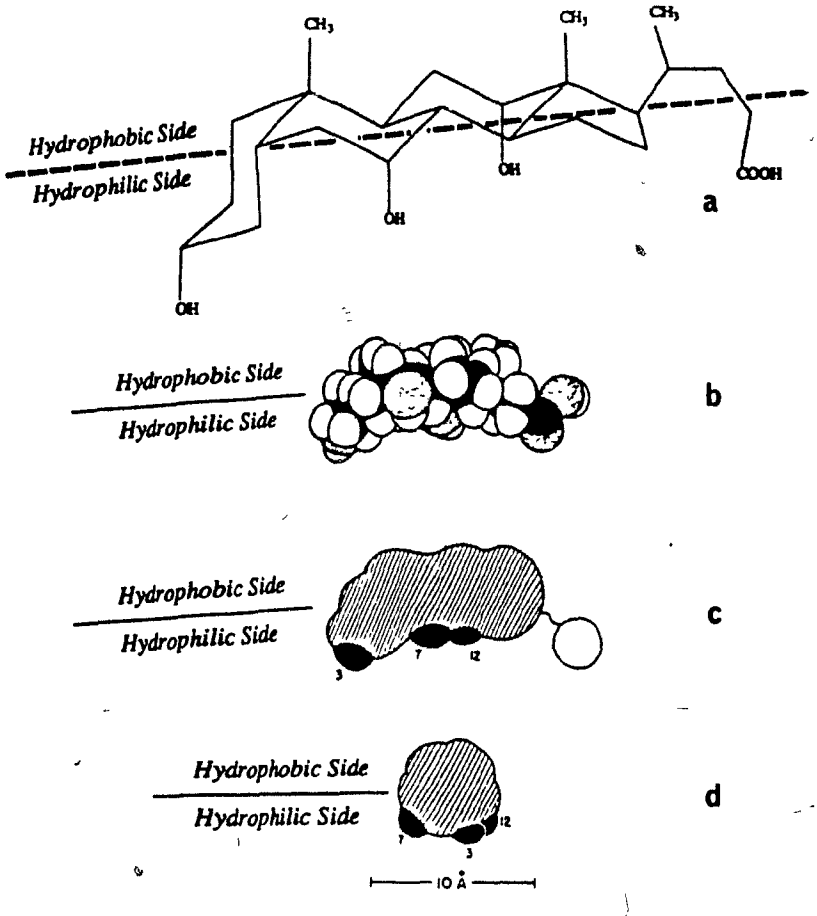

Figure 1.6 The conformation of cholic acid, indicating the hydrophobic and hydrophilic parts of the molecule: (a) perspective structure; (b) Stuart-Briegleb space filling model; (c) longitudinal and (d) transverse shorthand representations (reference 24).

1.2.2 Solubility and Micelle Formation

The physical properties of various bile acids are listed in Appendix 1. Except for bile acids conjugated with taurine, the bile acids range from sparingly soluble to practically insoluble in aqueous solutions. The solubility of bile acids has been measured to be in the range of $5x10^{-8}$ to $1.6x10^{-3}$ M (20). However, most of the bile salts are readily soluble in water (1-2 M, see Appendix 1). Regarding the different properties with respect to solubility and micelle

formation, it has been suggested that there should be a differentiation between the terms *bile acids* and *bile salts* in order to avoid confusion which may arise while using these terms (21). The water solubility of both bile acids and bile salts usually increases with increased temperature. Apart from this, it is strikingly influenced by the hydroxy groups. In general, the solubility follows the order trihydroxy > dihydroxy > monohydroxy. The positions and orientations of the hydroxyl groups can also affect the solubility significantly (22).

Depending on their molecular structure, the solubilities of bile acids in organic solvents ranges from very high to very low. Ethanol and DMSO seem to be two common organic solvents for most of the bile acids. Lithocholic acid is soluble in a number of organic solvents, including chloroform. However, taurocholic acid is practically insoluble in most organic solvents. For bile acid studies, it is important to keep the various kinds of bile acids in mind and the significant differences in their characteristics.

According to Carey (21), the apparent pK_a values of the free bile acids are higher than those of the conjugated bile acids, ranging from 5 to 6.5. The pK_a values of the glycine conjugates fall in the range of 4 to 5. The taurine conjugates have been estimated to dissociate at a much lower pH of -1.5 to 1.5. Other results have also been reported (22,23). A recent study by NMR titration has given a pK_a of 4.6 for cholic acid (23). Furthermore, the pK_a values depend on the concentration of bile salts with a remarkable increase as the concentration of bile salts reaches the critical micellar concentration (24). When the pH of the system is higher than their pK_a values, bile acids act as a detergent, as exemplified in the intestine where they are the fat-emulsifying agent. The micelle formation is largely determined by the detergent property of bile salts in aqueous media. However, bile salts behave as normal electrolytes in aqueous solutions at concentrations below their critical micellar concentration (22).

Although un-ionized bile acids exhibit high solubilities in micelles, they cannot form micelles themselves. However, the ionized form of bile acids, *bile salts*, can form micelles at the critical micellar temperature (CMT) when the concentration is above the critical micellar concentration (CMC, about 0.6-10 mM). The CMT is concentration-dependent, usually increasing with increased concentration. At temperatures lower than the CMT, phase separation may occur. The formation of micelles by bile salts has been reviewed by Carey and Small

(25). Small micelles are formed at room temperature when the concentration is less than 0.1 M. The aggregation numbers of the micelles range from 2 to 9. As the concentration increases larger micelles are formed. In the bile salt micelles, the hydrophobic part, i.e., the steroid ring, points inward, while the carboxyl group, or sulfonic acid group for taurine conjugated bile acids, which is considered to be the head group, points outward as shown in Figure 1.7 (26). In addition to these groups, the hydroxyl groups on the steroid ring make it impossible to form the ordinary type of micelles. The micelles tend to aggregate by hydrogen bonding through the hydroxyl groups. Mixed micelles are formed when molecular species other than bile salts, such as lecithin, are also present in the system (27). As indicated in Figure 1.7, lipids, cholesterol and many other substances with low solubility in water can be solubilized by forming mixed micelles with bile salts.

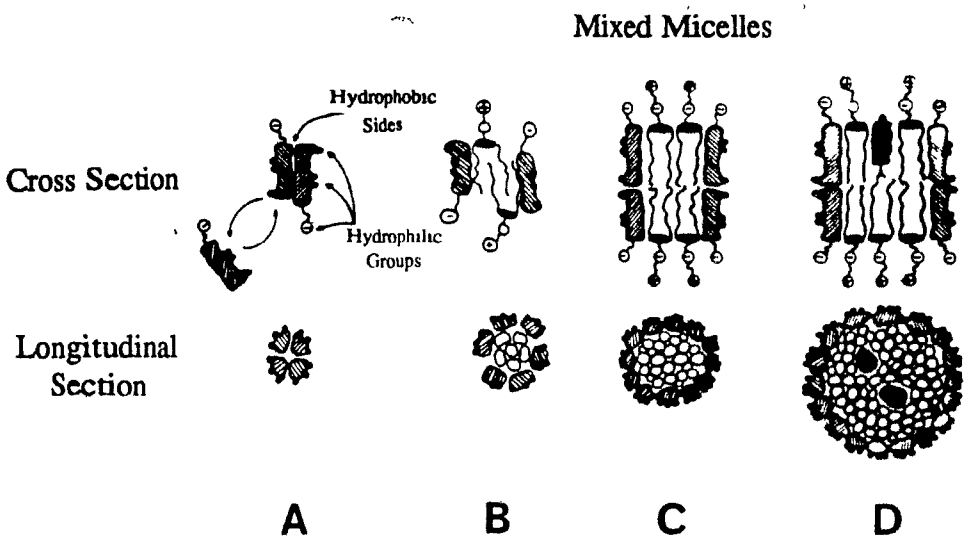

Figure 1.7 The structure of bile salt micelles (reference 26): A: a simple micelle formed by bile salt molecules with back-to-back structure, the hydrophilic part points toward the environment; B, C: mixed micelles with lecithin; D: a mixed micelles of bile salt, lecithin and cholesterol.

1.2.3 Chemical Properties

As organic acids, the carboxyl group of bile acids can be esterified, reduced and converted to amides by reaction with various chemical reagents under selected conditions (28). It has been reported that mono- and dihydroxylated bile acids, like bilirubin, may form glucuronides on the carboxylic side chain, or at the C3 position (29,30).

The hydroxyl groups of bile acids exhibit very different reactivity when esterified or oxidized, subject to their locations on the steroid skeleton. It has been reported that the hydroxyl group of bile acids at C3 is selectively esterified by acids containing polymerizable groups followed by homo- and co-polymerization of the ester. These kinds of polymers can be used for medical purposes (31).

The amide bond of the conjugated bile acids can be hydrolyzed to generate free bile acids when treated with aqueous alkali such as sodium or potassium hydroxide solutions (32). Sometimes higher temperatures are needed for rapid, complete hydrolysis.

1.3 Analytical Methods for Bile Acids

A variety of techniques, with different accuracy and applicability, have been applied for the quantitative analysis of bile acids. A summary of the available methods for bile acids analysis appeared in a recent review (33).

1.3.1 Colorimetric Methods

The colorimetric method is essentially a modification of the Pettenkofer reaction (34). The bile acids normally do not absorb UV-visible light. However, all of the bile acids show absorbance in the UV region after treatment with concentrated sulfuric acid (65-70%). The absorbance of relatively low concentrations of bile acids obeys Beer's law. The advantage of this detection method is that, because of its simplicity, it does not require advanced instrumentation.

1.3.2 High Performance Liquid Chromatography (HPLC)

High performance liquid chromatography (HPLC) is a more sensitive and precise method for bile acid analysis (35). Ion exchange columns and reversed-phase silica columns (36) can be used for the separation of bile acids. Recent

development of HPLC allows a direct separation of bile acids from biological fluids (37,38).

Most of the detection methods of the HPLC systems require precolumn derivatization (39), post-column enzymatic reactions (40), or ion-pair formation (41). UV spectrometers set around 200 nm are often used for the detection (42). Since free bile acids do not show strong UV absorbance, derivatives consisting of substituted phenyl groups are usually prepared for the detection (32). Direct detection of bile acids using a UV detector has also been reported by Ruben *et al.* (43). The differential refractometer detector is less sensitive and thus was considered to be unsuitable for detection of bile acids in serum (44). It has also been reported that the bile acids can be detected directly at a precision of 5 nmol or less by using a refractive index detector (45), thus saving laborious preparation of samples for the analysis.

1.3.3 Other Methods

Among the other available techniques for bile acid analysis, *radioimmunoassay* is very sensitive, rapid and simple (46,47). Commercial radioimmunoassay kits have been available for the routine analysis of serum bile acid determinations.

Currently, there are also many ^{14}C- or ^{3}H-labeled bile acids available commercially. These isotope-labeled bile acids are especially convenient for use in *in vitro* experiments. A double isotope derivative assay has been reported for use in serum samples (48).

The *enzymatic methods* have been used to measure the total amount of serum bile acids with a free 3α-hydroxyl group (49). Bile acids that are sulfated or glucuronidated at position C3 cannot be detected. These methods involve the reaction of certain enzymes with bile acids, to generate NADH which can be detected by spectrophotometry or spectrofluorimetry.

1.4 Treatments for Hypercholesterolemia and the Binding of Bile Acids

1.4.1 Treatments for Hypercholesterolemia

The cholesterol level in humans varies between individuals, depending on dietary and genetic factors. In the Western countries, the average plasma cholesterol level in adults is about 200 mg/dl. The average cholesterol level in

serum is different for men and women. For men it usually rises with age until the sixth decade of life and declines thereafter. For women, the cholesterol level is lower but rises continuously with age (50).

Over the years, many investigators have demonstrated that heart disease is directly linked to the level of cholesterol in the blood and that the lowering of the plasma cholesterol levels remarkedly reduces the incidence of fatal coronary heart disease and atherosclerosis in humans (51). Hypertension, obesity, smoking, high-fat diet, lack of exercise, or a combination of these factors can contribute to the development of coronary heart disease (52). In cases where the disease is not serious, patients are often instructed to watch their diets. In more severe cases, the diseases can be treated clinically by oral drugs, surgery, hemoperfusion or a combination of these treatments. The interruption of the enterohepatic circulation can be accomplished by the surgical exclusion of the lower third of the small intestine, where the bile salts are mainly reabsorbed (14).

The available prescription drugs include mainly two types, according to their biological functions. They interrupt either the biosynthesis of cholesterol in the body or the enterohepatic circulation of bile acids.

A number of oral drugs have been developed, acting as inhibitors of the biosynthesis of cholesterol. One of the recently prepared drugs, lovastatin (mevinolin), is an enzyme inhibitor which stops the formation of cholesterol in the body. It has been reported to be able to lower the serum cholesterol level by as much as 39%. However, it can cause malfunction of the liver as well as ocular lens opacities and cataracts (53). The other well-known inhibitors of this kind include gemfibrozil (54), sodium 2-phenylbutyrate and ethyl-*p*-chlorophenoxyisobutyrate (clofibrate or Atromid-S) (55), which act as inhibitors at various steps of the cholesterol biosynthesis. Their clinical usefulness is limited due to some of the untoward side effects (56). Other drugs that are considered to increase the fecal excretion of cholesterol and bile acids include dextrothyroxine (Choloxin), neomycin (57) and nicotinic acid (58). The chemical structures of some of these hypocholesterolemic drugs are shown in Figure 1.8.

Polymeric adsorbents for bile salts, such as cholestyramine (Questran) and colestipol, have been developed in the last 30 years. The best among them, cholestyramine, was first used in the treatment of hypercholesterolemia by Bergen *et al.* in 1959 (59). It is normally taken orally to adsorb bile salts in the

gastrointestinal tract, blocking the reabsorption of the bile acids. The fecal excretion of bile acids is enhanced under the effect of cholestyramine and, therefore, the conversion of cholesterol to bile acids is accelerated to maintain the pool of bile salts (60,61). However, cholestyramine, which is a sand-like insoluble resin, must be taken 3-6 times a day with a daily dosage of 12-36 grams, depending on the severity of the disease. Many patients experience some of its side effects: nausea, vomiting, constipation, bloating and gas, etc. (4,62). Similar adsorbents of this type have been developed and are discussed in Section 1.4.4.

Other materials, such as aluminum hydroxide, have been reported to bind bile salts as well as bilirubin from the bile, especially at a lower pH (63). However, the effect of aluminum hydroxide to enhance fecal excretion of bile salts in some cases is doubted (19).

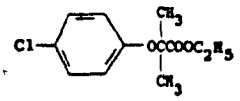

Clofibrate

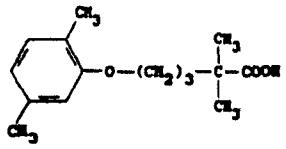

Gemfibrozil

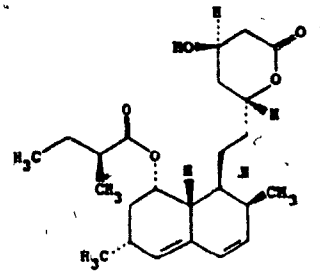

Mevinolin

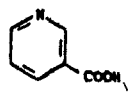

Nicotinic Acid

Figure 1.8 The chemical structures of selected hypocholesterolemic drugs.

1.4.2 Binding of Bile Acids to Proteins

Bile acids are known to be bound to a number of proteins, such as albumin (64), ligandin (glutathione S-transferase) (65) and lipoproteins (66). Other bile acid binders have only recently been identified (67).

Serum albumin is a carrier for a multitude of bio-compounds in the blood, including bilirubin and many weakly acidic drugs. A detailed discussion of the structure of serum albumin is presented in Section 4.4.2 of this thesis. Whether or not the bile acids are extensively bound to albumin in the plasma has been questioned (68). However, there is no doubt that albumin has a high affinity for bile acids. A study of the binding between deoxycholate and bovine serum albumin has shown that there are four principal binding sites and about 14 weaker sites for each ligand (69).

Ligandin, which is identified as glutathione S-transferase (or Y protein) (70), is a basic protein (pI = 9.0) found in mammalian liver, kidney and small intestinal mucosa. It is named ligandin because it binds a wide variety of ligands, mostly organic anions, such as bile acids and bilirubin. Different bile salts have been reported to bind to a single site on ligandin with association constants of the order of 10^4 M^{-1} (71).

The binding of bile acids to plasma proteins was identified as early as 1957 (72). Although the exact mechanism of binding is not known, it has been suggested that the positively charged amino groups on the side chains of the basic amino acids in proteins are attracted by the negatively charged carboxylate groups of the bile salts, while hydrogen bonds may also be formed between the hydroxy-substituted bile salts and the protein (73). Rudman and Kendall have proposed that the side chain amino groups of lysine residues in the protein form electrostatic bonds with the carboxylate groups of bile salts (74).

Hydrophobic bonding is assumed to be a dominant mechanism in the binding of small molecules by biological macromolecules since it confers thermodynamic stability on the conformation of proteins (75). In aqueous solutions, the more lipophilic bile acids are expected to exhibit a significant affinity for the hydrophobic centers in the proteins. It has been found that the binding decreases as the number of hydroxyl groups of the bile salt is increased. Bovine serum albumin exhibits the highest affinity for lithocholate, which has only one hydroxyl group, among all of the common bile salts (74,76). A similar

hydrophobic effect has also been observed for ligandin: the addition of polar groups to the hydrophobic moiety of the ligand reduces the binding affinity. Cholate has a lower binding affinity to ligandin compared with deoxycholate (71).

1.4.3 Binding of Bile Acids to Dietary Fibers

Dietary fibres have been reported to eliminate bile acids by adsorption from the gastrointestinal tract (77). Although this has been disputed, the inclusion, rather than deletion of dietary fibers from the diet, is generally considered to be beneficial in reducing the risk of cardiovascular disease (78).

Most fibers are polysaccharides from vegetable food sources. The binding of bile acids has been mostly studied *in vitro* and it seems that the method used for the preparation of the fibers prior to adsorption and the pH of the solution influences the binding capacity (79). The binding process may involve the interaction with the mixed micelles of bile salts (80).

Lignin, which is responsible for the woody texture of plants, has been found to bind both cholesterol and bile acids (81). Since lignin is an insoluble phenylpropane polymer, the hydrophobic interaction between lignin and bile acids may play an dominant role in the binding if it is indeed a better binder for bile acids than other plant fibers, as shown by Eastwood and Hamilton (82). However, the results have been disputed. It also has been reported that *pectic fibers*, rather than lignin, are more important for the binding of bile acids and, therefore, hydrogen bonding rather than hydrophobic interaction plays a major role in the binding process (83). Compared with water-soluble dietary fibres, the insoluble lignin and cellulose are thought to be less effective in the binding of cholesterol and bile acids (84). *In vitro* studies have shown that the dietary fibers exhibit higher capacities for un-ionized bile acids than for the ionized salt form (79,83).

1.4.4 Binding of Bile Acids to Polymeric Resins

Since bile acids are organic acids that exist in their salt forms in the intestine, polymeric resins with organic bases has been used for their adsorption. These materials usually have high molecular weights so that they cannot be absorbed in the digestive tract. *Cholestyramine*, the most widely used adsorbent for bile acids (85), is a copolymer of polystyrene and divinylbenzene with quaternary ammonium groups as functional groups. Being a typical strongly

basic ion exchange resin, its counterions of the quaternary ammonium, usually chloride ions, are exchanged with the bile salt anions during the binding.

The binding of bile salts with cholestyramine has been extensively studied by researchers all over the world. Most of these studies, however, have been focussed mainly on *in vivo* experiments (86-88). It has been demonstrated unambiguously in animals and clinically in man that cholestyramine can increase the fecal excretion of bile salts by interrupting the enterohepatic circulation and thereby reduces the cholesterol level in serum (89,90). However, *in vitro* studies which may lead to a clearer understanding about the binding mechanism have received limited attention. Blanchard and Nairn reported the binding of sodium cholate and glycocholate in saline solutions (91). It was found that sodium cholate had a higher affinity to cholestyramine than glycocholate. Johns and Bates have reported a series of *in vitro* adsorption studies of bile salts using cholestyramine (92-94). These studies were done in aqueous media with various bile salts. The results suggested a primary electrostatic interaction reinforced by a secondary "nonelectrostatic interaction", which is dependent on the hydrophobicity of the bile salt molecules.

Cholestyramine resin is limited by its poor biocompatibility, since its backbone is not water-swellable. Attention has been focussed on finding a replacement with better water swellability. *Colestipol*, a copolymer of tetraethylene-pentamine and epichlorohydrin (or 1-chloro-2,3-epoxypropane), is a water-swellable anion exchanger (95) with a better biological acceptability (96); however, it appears to be less effective in terms of the binding capacity for bile salts (97). This is probably due to the fact that its functional groups of colestipol, located mainly on the polymer backbone, are less accessible to the binding substrates. These functional groups are secondary and tertiary amine groups, therefore, it is not a strongly basic ion-exchanger.

Many other polymeric sorbents with quaternary functional groups and backbones similar to that of colestipol have also been reported, such as crosslinked ethylenediamine copolymers (98), linear quaternary cationic polymer segments bonded to small porous polymer beads (99), quaternary poly-alkyliminoalkylene linear polymers (100), and cholacrylamine, a water-soluble quaternary ammonium salt with polyacrylate skeleton (101,102). All of these adsorbents have been tested *in vitro* or *in vivo* with various degrees of success.

One common feature of these materials is that they are all synthetic polymers, whose application is limited either because of a lack of biocompatibility or a low binding capacity.

It is known that the bile acid binding proteins interact with bile acid with high affinity and specificity. This suggests that the ideal adsorbent would be immobilized proteins, such as albumin and ligandin. This would create no problem in biocompatibility or specificity. However, since only a small part of the protein molecule is likely to be responsible for the binding of bile acids, the capacity would be unacceptably low. A solution to this is to utilize small peptides, related in some cases to the primary structural sequence of proteins, bound to a insoluble polymer backbone as adsorbents. These materials containing oligopeptide sequences would hopefully have similar biocompatibility to the proteins, but would manifest considerably higher binding capacity.

The binding of bile acids to polymeric materials is still incompletely understood with respect to the nature of the interaction that occur. Further investigations of the binding of bile acids, however, can be carried out based on the knowledge of the studies of bile acids accumulated to date. This understanding is essential to the design and preparation of improved adsorbents. The present research concerns two aspects: (1) the study of specific interactions, by spectroscopic methods, of bile acids with selected model compounds that resemble the functional groups of the polymeric adsorbents; and (2) the characteristics of the adsorption of bile acids by peptide sequences immobilized on suitable polymeric beads.

In Part I of this thesis, the preparation of novel water-swellable polymer resins with quaternized peptide-containing functional groups and an adsorption study for bile salts using these resins are described in Chapter 2. The binding behaviors of these resins are compared with the commercial resins such as cholestyramine. Based on these results, the mechanism of the interactions is proposed. This work is complemented by the application of nuclear magnetic resonance techniques to study the interaction between the binding substrates in solutions, which is presented in Chapter 3. The measurements of the carbon-13 spin-lattice relaxation times provide more direct evidence for the nature of the interactions between bile acids and selected ligands in the binding process.

References

1. S.M. Grundy, *JAMA*, **256**, 2849, 1986
2. P.A. Mayes, **Chap. 18, Metabolism of Lipid**, p. 244, in *Harper's Review of Biochemistry*, 19th ed., D.W. Martin, Jr., P.A. Mayes & V.W. Rodwell, eds., Lange Medical Publications, Los Altos, CA, 1983
3. G.F. Gibbons, K.A. Mitropoulos & N.B. Myant, **Chap. 5, Biosynthesis**, p. 131, in *Biochemistry of Cholesterol*, Elsevier Biomedical Press, Amsterdam-New York, 1982
4. C. Wallis *et al.* (reporters), *Time*, **123** (13), 56, 1984
5. E. Heftmann, **Chap. 2, Cholesterol**, p. 11, in *Steroid Biochemistry*, Academic Press, NY-London, 1970
6. F. Sebba, *Montreal Star*, p. C4, June 29, 1974
7. H.F. Acevedo, B.A. Vela, E.A. Campbell, D.W. Hayeslip, J. Gilmore & J. Frich, *JAMA*, **212**, 1290, 1970
8. P.A. Mayes, **Chap. 41, Digestion/Absorption in the Gastrointestinal Tract**, p. 546, in *Harper's Review of Biochemistry*, 19th ed., D.W. Martin, Jr., P.A. Mayes & V.W. Rodwell, eds., Lange Medical Publications, Los Altos, CA, 1983
9. R.H. Palmer, **Bile Salts and the Liver**, p. 221, in *Progress in Liver Diseases, Vol. VII*, H. Popper & F.S. Schaffner, eds., Grune & Stratton, NY, 1982
10. J.M. Street, D.J. Trafford & H.L.J. Makin, *J. Lipid Res.*, **24**, 491, 1983
11. G.F. Gibbons, K.A. Mitropoulos & N.B. Myant, **Chap. 6, Further Metabolism**, p. 189, in *Biochemistry of Cholesterol*, Elsevier Biomedical Press, Amsterdam-New York, 1982
12. D.M. Small, R.H. Dowling & R.N. Redinger, *Arch. Intern. Med.*, **130**, 552, 1972
13. T.L. Peeters, G. Vantrappen & J. Janssens, *Gastroenterology*, 79, 678, 1980
14. S.M. Grundy, *Arch. Intern. Med.*, **130**, 638, 1972
15. I.E. Danhof, *Am. J. Clin. Nutr.*, **18**, 343, 1966
16. *Bile Acid Quantitation I, Chemical and Practical Aspects of Gastroenterology*, Nyegaard, Distr. by Accurate Chem. & Sci. Corp., 300 Sharnes Dr., Westebury, NY 11590, 1982
17. E.L. Wynder, *J. Am. Diet. Ass.*, 71, 385, 1977
18. R. Lewis & S. Gorbach, *Arch. Intern. Med.*, **130**, 545, 1972
19. A. Sali, *Lancet*, **2**, 424, 1978
20. A. Fini, A. Roda, R. Fugazza & B. Grigolo, *J. Sol. Chem.*, **14**, 595, 1985
21. M.C. Carey, *Hepatology*, **4**, 66s, 1984
22. A. Roda & A. Fini, *Hepatology*, 4, 72s, 1984
23. D.J. Cabral, J.A. Hamilton & D.M. Small, *J. Lipid Res.*, **27**, 334, 1986
24. D.M. Small, **Chap. 8, The Physical Chemistry of Cholanic Acids**, p. 249, in *The Bile Acids, Vol. 1*, P.P. Nair & D. Kritchevsky, eds., Plenum Press, New York, 1971
25. M.C. Carey & D.M. Small, *Arch. Intern. Med.*, **130**, 506, 1972
26. D.M. Small, **Chap. 7, Bile Salts in Blood**, p. 91, in *Liver and Bile*, L. Bianchi, W. Gerok & K. Sickinger, eds., University Park Press, Baltimore, 1977
27. G. Lindblom, P.-O. Eriksson & G. Arvidson, *Hepatology*, **4**, 129s, 1984
28. C.W. Shoppee, p. 115, in *Chemistry of the Steroids*, Butterworths, Washington, 1964

29. H. Martern & S. Marten, *Biochim. Biophys. Acta*, **921**, 1, 1987
30. A. Radominska-Pyrek, P. Zimniak, M. Chari, E. Golunski, R. Lester & J. St.Pyrek, *J. Lipid Res.*, **27**, 89, 1986
31. M. Ahlheim, M.L. Hallensleben & H. Wurm, *Polymer Bulletin*, **15**, 497, 1986
32. G.A.D. Haslewood, **Chap. 3, Methods of Isolation, Identification and Analysis**, p. 26, in *Bile Salts*, Methuen & Co., London, 1967
33. J.M. Street, D.J.H. Trafford & H.L.J. Makin, *J. Lipid Res.*, **24**, 491, 1983
34. P. Metais, H. Deiss & J. Warter, *Bull. Soc. Chim. Biol.*, **39**, 321, 1957
35. W.H. Elliott & R. Shaw, p. 1, in *Steroid Analysis by HPLC*, M.P. Kautsky, ed., Dekker, N.Y., 1981
36. F. Nakayama & M. Nakagaki, *J. Chromatogr.*, **183**, 287, 1981
37. C.N. Carducci, M. Matejka, H. Erguven, N. Labonia & A. Mamianetti, *J. Chromatogr.*, **337**, 91, 1985
38. M. Hayashi, *J. Chromatogr.*, **338**, 195, 1985
39. F. Stellard, D.J. Hachey & P.D. Klein, *Anal. Biochem.*, **87**, 359, 1978
40. S. Itoh, S. Onishi, K. Isobe, M. Manabe & K. Inukai, *Biochem. J.*, **204**, 141, 1982
41. H.J. Wildgrube, U. Fussel, H. Laurer & H. Stockhausen, *J. Chromatogr.*, **282**, 603, 1983
42. W.H. Elliott & R. Shaw, p. 51, in *Methods in Enzymology, Vol. 3*, Academic Press. N.Y., 1985
43. A.T. Ruben & G.P. van Berge-Henegouwen, *Clin. Chim. Acta*, **119**, 41, 1982
44. C.A. Bloch & B. Watkins, *J. Lipid Res.*, **19**, 510, 1978
45. A.D. Reid & P.R. Baker, *J. Chromatogr.*, **247**, 149, 1982
46. A.A. Mihas, J.G. Spenney, B.I. Hirschowitz & R.G. Gibson, *Clin. Chim. Acta*, **76**, 389, 1977
47. L.M. Demers & G. Hepner, *Clin. Chem.*, **22**, 602, 1976
48. J.F. Pageaux, B. Duperray, M. Dubois & H. Pacheco, *J. Lipid Res.*, **22**, 725, 1981
49. O. Fausa, *Scand. J. Gastroent.*, **11**, 537, 1976
50. E.L. Wynder, F. Field, N.J. Haley, *JAMA*, **256**, 2839, 1986
51. H.A. Tyroler, *Am. J. Cardiol.*, **54**, 14c, 1984
52. T.A. Miettinen, **Chap. 7, Clinical Implications of Bile Acid Metabolism in Man**, p. 191, in *The Bile Acids, Vol. 2*, P.P. Nair & D. Kritchevsky, eds., Plenum Press, NY-London, 1973
53. The Lovastatin Study Group II, *JAMA*, **256** (20), 2829, 1986 and related reports
54. B.M. Rifkind, *New Engl. J. Med.*, **317**, 1279, 1987 and related reports
55. L. Horlick, B.J. Kudchodkar & H.S. Sodhi, *Circulation*, **43**, 299, 1971
56. E. Heftmann, *Steroid Biochemistry*, Academic Press, N.Y., 1970
57. W.G.M. Hardison & I.H. Rosenberg, *J. Lab. Clin. Med.*, **74**, 564, 1969
58. D. Kritchevsky, p. 149, in *Metabolic Effects of Nicotinic Acid and Its Derivatives*, K.F. Gey & L.A. Carlson, eds., Huber, Berne, 1971
59. S.S. Bergen, T.B. van Itallie, D.M. Tennent & W.H. Sebreli, *Proc. Soc. Exp. Biol. Med.*, **102**, 676, 1959

60. J.B. Carey & G. William, *JAMA*, **176**, 432, 1961
61. J.M. Dietschy & J.D. Wilson, *New Engl. J. Med.*, **282**, 1128, 1970
62. E.R. Pinckney, *Lancet*, **1**, 634, 1984
63. J. Wenger & S. Heymsfield, *J. Clin. Pharm.*, **14**, 163, 1974
64. C.W. Burke, B. Lewis, D. Panveliwalla & S. Tabaqchali, *Clin. Chim. Acta*, **32**, 207, 1971
65. H. Takikawa, Y. Sugiyama & N. Kaplowitz, *J. Lipid Res.*, **27**, 955, 1986
66. G. Salvioli, R. Lugli, J.M. Pradelli & G. Gigliotti, *FEBS Lett.*, **187**, 272, 1984
67. H. Takikawa, A. Stolz, M. Sugimoto, Y. Sugiyama & N. Kaplowitz, *J. Lipid Res.*, **27**, 652, 1986
68. T. Delahunty & C. Feldkamp, *Steroids*, **36**, 439, 1980
69. S. Makino, J.A. Reynolds & C. Tanford, *J. Biol. Chem.*, **248**, 4926, 1973
70. W.H. Habig, M.J. Pabst, G. Fleischner, Z. Gatmaitan, I.M. Arias & W.B. Jacoby, *Proc. Natl. Acad. Sci. U.S.A.*, **71**, 3879, 1974
71. B. Ketterer, E. Tipping, D. Beale & J.A.T.P. Meuwissen, p. 243, in *Glutathione, Metabolism and Function*, I.M. Arias & W.B. Jakoby, eds., Raven Press, New York, 1976
72. D. Rudman & F.E. Kendall, *J. Clin. Invest.*, **45**, 187, 1957
73. P.P. Nair, **Chap. 3, Bile-Salt-Protein Interactions**, p. 29, in *The Bile Acids, Vol. 3*, P.P Nair & D. Kritchevsky, eds., Plenum Press, NY-London, 1976
74. D. Rudman & F.E. Kendall, *J. Clin. Invest.*, **36**, 538, 1957
75. W. Kauzmann, *Adv. Protein Chem.*, **14**, 1, 1959
76. R.H. Palmer, p. 172, in *Bile Salt Metabolism*, L. Schiff, J.B. Carey & J.M. Dietschy, eds., C.C. Thomas, Springfield, Illinois, 1969
77. G. Gallaher & R.O. Schneeman, *Am. J. Physiol.*, **250**, G420, 1986
78. I.H. Ullrich, *J. Am. Col. Nutr.*, **6**, 19, 1987
79. M. Eastwood, *Lancet*, **2**, 150, 1981
80. M.M. Cassidy, F.G. Lightfoot & G.V. Vahouny, *Adv. Lipid Res.*, **19**, 203, 1982
81. G.V. Vahouny, *Fed. Proc.*, **41**, 2801, 1982
82. M.A. Eastwood & D. Hamilton, *Biochim. Biophys. Acta*, **152**, 165, 1968
83. R.R. Selvendran, *Chem. Indus.*, 428, June 1978
84. R.M. Kay, *J. Lipid Res.*, **23**, 221, 1982
85. B.M. Rifkind, *Am. J. Cardiol.*, **54**, 30c, 1984
86. S.M. Grundy, E.H. Ahrens, Jr. & G. Salen, *J. Lab. Clin. Med.*, **78**, 94, 1971
87. D.J. Nazir, L. Horlick, B.J. Kudchodkar & H.S. Sodhi, *Circulation*, XLVI, 95, 1972
88. K. Einarsson, K. Hellstrom & M. Kallner, *Europ. J. Clin. Invest.*, **4**, 405, 1974
89. W.T. Beher, M.E. Beher & B. Rao, *Proc. Soc. Exp. Biol. Med.*, **122**, 881, 1966
90. Lipid Research Clinics Program, *JAMA*, **251**, 351, 1984 and related reports
91. J. Blanchard & J.G. Nairn, *J. Phys. Chem.*, **72**, 1204, 1968
92. W.H. Johns & T.R. Bates, *J. Pharm. Sci.*, **58**, 179, 1969
93. W.H. Johns & T.R. Bates, *J. Pharm. Sci.*, **59**, 329, 1970
94. W.H. Johns & T.R. Bates, *J. Pharm. Sci.*, **59**, 789, 1970
95. N.A. Nelson, *US Patent*, 3692895, 1972

96. E.E. Cooper & A.M. Michel, *South. Med. J.*, **68**, 303, 1975
97. M.M. Cassidy, F.G. Lightfoot, L.E. Grau, T. Roy, J.A. Story, D. Kritchevsky & V. Vahouny, *Dig. Dis. Sci.*, **25**, 504, 1980
98. D. Lednicer & C.Y. Peery, *US Patent*, 3803237, 1974
99. A. Rambaum, *US Patent*, 4046750, 1977
100. G.W. Kuron, N. Grier, & J.W. Huff, *Atherosclerosis*, **37**, 353, 1980
101. D.M. Tennent, H. Siegel, M.E. Zanetti, G.W. Kuron, W.H. Ott & F.J. Wolf, *J. Lipid Res.*, **1**, 469, 1960
102. D.M. Tennent, S.A. Hashim & T.B. van Itallie, *Fed. Proc., Fed. Am. Soc. Exp. Biol.*, **21**, Supp., **11**, 77, 1962

2 Adsorption Studies of Bile Salts

2.1 Introduction

A common feature of the currently known polymeric adsorbents for bile acids is that all are synthetic materials. Over the years,both *in vivo* and *in vitro* tests have shown them to possess different degrees of efficiency in adsorbing bile salts. Cholestyramine and colestipol represent the two major types of commercial synthetic sorbents for adsorption of bile salts in the alimentary tract.

Cholestyramine is an orally administered adsorbent for the elimination of bile acids. The matrix of cholestyramine is polystyrene reticulated with 2% divinylbenzene, as shown in Figure 2.1a. It contains quaternary ammonium functional groups, so that it is a strongly basic anion exchanger. The hydrophobic nature of the polymer backbone result in a poor biocompatibility. As a consequence, adverse side effects have been experienced by hypercholesterolemic patients.

Colestipol is a copolymer composed of tetraethylene-pentamine and epichlorohydrin, as shown in Figure 2.1b. Since the backbone is swellable in aqueous solutions, the biocompatibility is improved. The functional groups are the secondary and tertiary amine groups. Therefore, colestipol is a weaker basic ion exchanger than cholestyramine. This, in turn, leads to a lower capacity in the binding of bile acids.

Improved adsorbents for bile acids or bile salts are greatly desired to reduce the adverse effects of the currently used bile acid binding materials. The present study is limited to *in vitro* experiments, but the ultimate goal is to apply these adsorbents in the alimentary tract. Therefore, biocompatibility is always given priority in the selection of the active binding units to minimize any foreseeable side effects to the human body. This suggests the use of naturally occurring bio-materials, such as amino acids or oligopeptides, in the preparation

of the adsorbents. An active binding site formed by a peptide may provide better biocompatibility and possibly higher binding capacity. Thus, the strategy that has been adopted is to start with a water-swellable resin onto which peptide sequences consisting of amino acids found at the potential binding sites are attached.

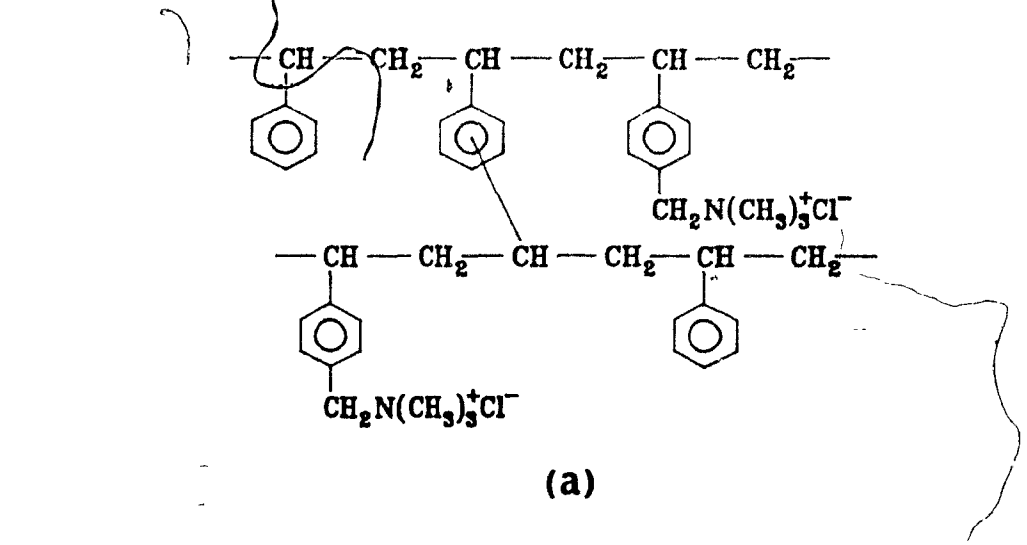

(a)

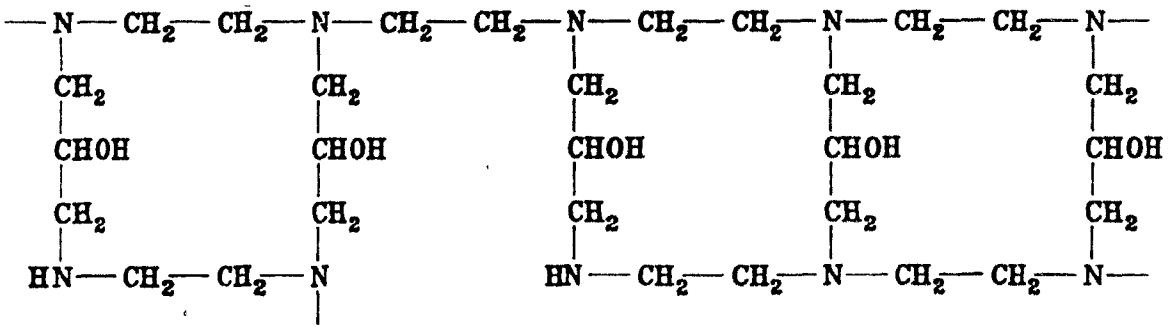

(b)

Figure 2.1 The chemical structures of cholestyramine and colestipol: (a) cholestyramine, a copolymer of styrene and divinylbenzene. Chloride anions are shown as the counterions of this ion-exchange resin; (b) colestipol, a copolymer of tetraethylene-pentamine and epichlorohydrin (reference 1).

It is well known that certain proteins bind bile acids in the heme as well as in the liver (Chapter 1). Among the bile acid binding proteins, both albumin and ligandin may bind various bio-organic ligands. Although the exact binding sites

are not confirmed, it is most likely that only the basic parts of the large protein molecules are involved in the binding of the organic anions. It has been found that the basic amino acids in serum albumin, such as lysine, arginine and histidine, play an important role in the binding of bilirubin, which is an organic dibasic acid (2,3). Peptide resins containing lysine and arginine in their sequences have already been proven to be efficient adsorbents for bilirubin (4,5).

Based on a consideration of the structure of cholestyramine, the quaternary ammonium group is likely to be important in the binding of bile salts. Thus, betaine, a natural biocompound containing a quaternary ammonium group, has potential use as the functional group in bile salt binding. Betaine occurs in sugar beet molasses and is widely distributed in plants and animals. In the human body, it is usually formed as an intermediate of the conversion of choline to glycine. This lipotropic agent has been found to be beneficial in curing fatty livers, the accumulation of lipid in the liver as a consequence of raised levels of plasma free fatty acids, or a deficiency in the production of plasma lipoproteins (6).

As for the polymer support, polyacrylamide resins seemed to be ideal because of their water-swellability. Such resins are commercially available and have been used in solid phase peptide synthesis. They are crosslinked polymers that cannot be absorbed from the gastrointestinal tract. A peptide spacer, usually a short alanine sequence, may be added to the polymer resin prior to the coupling of the active units so that the functional groups on these pendants become more accessible to the binding substrates. The chemical structures of alanine, lysine and betaine are shown in Figure 2.2.

In this chapter, the preparation of novel peptide containing polymeric adsorbents, in accordance with this strategy, is presented. The adsorption behavior of these resins in the carefully chosen bile salt system has been studied and is compared with that of cholestyramine and colestipol. Based on the experimental results, a binding mechanism is proposed with a general description of the binding between bio-compounds to peptide containing polymeric resins.

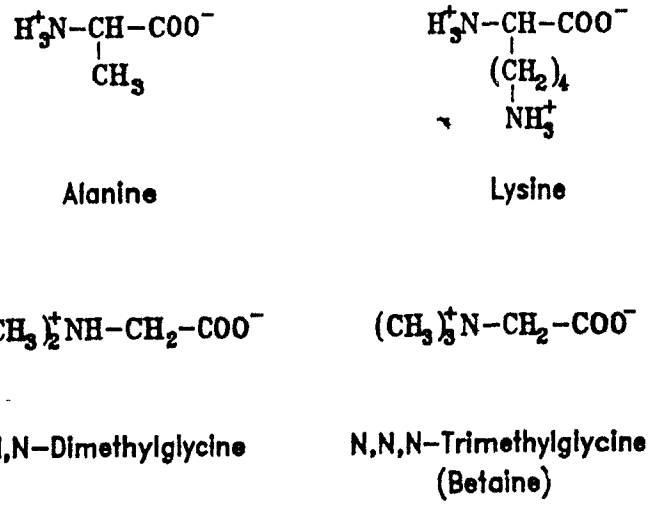

Figure 2.2 The chemical structures of alanine, lysine, dimethylglycine and betaine.

2.2 Preparation of Resins and Adsorption Experiments

2.2.1 Preparation of Quaternized Peptide Resins

A water-swellable polyacrylamide resin (from Chemalog), which is a copolymer of dimethylacrylamide and N-acryl-1,6-diaminohexane crosslinked with 11% *bis*-acryl-1,2-diaminoethane, was used as the polymer support (Figure 2.3). Sequences of peptide were synthesized onto the polymer using solid phase peptide synthesis techniques (see Appendix 2). The overall schematic diagram for the preparation of the peptide containing resins is shown in Figure 2.4.

Solid Phase Peptide Synthesis: Solid phase peptide synthesis techniques were used with a Vega Peptide Synthesizer. All the solvents used in the peptide synthesis were purchased from Aldrich and were redistilled immediately prior to the experiments, with the exception of dichloromethane and dimethylsulfoxide (DMSO), which were dried with molecular sieves (Type 4A, from Aldrich). The amino acids, N-α-t-BOC-L-alanine and N-α-t-BOC-N-ε-2,4-dichloro-CBZ-L-lysine, were purchased from Vega. The N,N-dimethylglycine in the hydrochloride form was purchased from Aldrich.

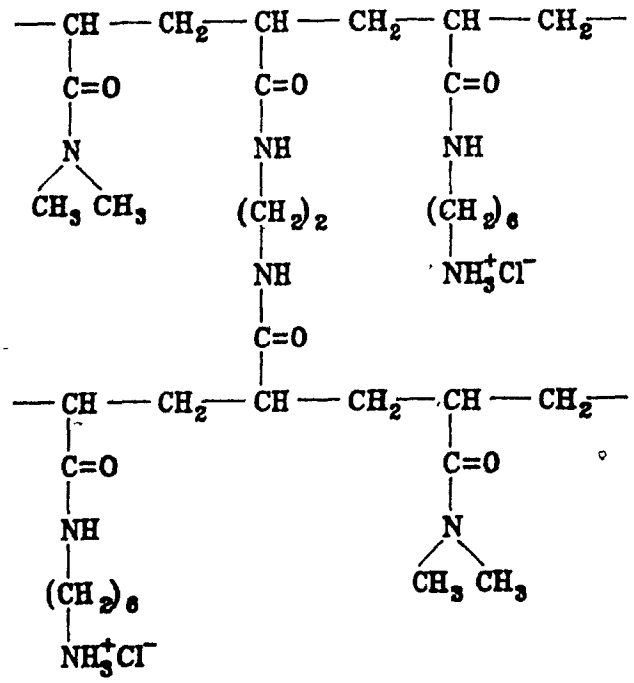

Figure 2.3 The chemical structure of the water-swellable polymer support, a copolymer of dimethylacrylamide and N-acryl-1,6-diaminohexane cross-linked with *bis*-acryl-1,2-diaminoethane.

The resin was first neutralized with an organic base, 10% N,N-diisopropylethylamine (DEA) in dichloromethane. The anhydrides of the protected amino acids (alanine and lysine) were prepared by reacting with 1,3-dicyclohexyl-carbodiimide (DCC) in dichloromethane at 0°C for 30 minutes. After filtering the urea, formed as a by-product of the reaction, the anhydride solution was added to the resin. For the coupling of alanine, a reaction period of about 3 hours was usually adequate. The addition of lysine usually takes a longer period of time and required 3-9 hours for complete coupling. The coupling of the amino acids was evidenced by a negative ninhydrin test for free amino groups (see Appendix 2). The BOC groups were then removed by reacting with 40% trifluoroacetic acid in dichloromethane. After purging the acid solution, the resin was neutralized with DEA in dichloromethane and washed successively with dimethylformamide (DMF) and dichloromethane. The deprotected amino groups gave a positive ninhydrin test. The coupling of amino acids was repeated until the desired number of amino acids was added to the sequence.

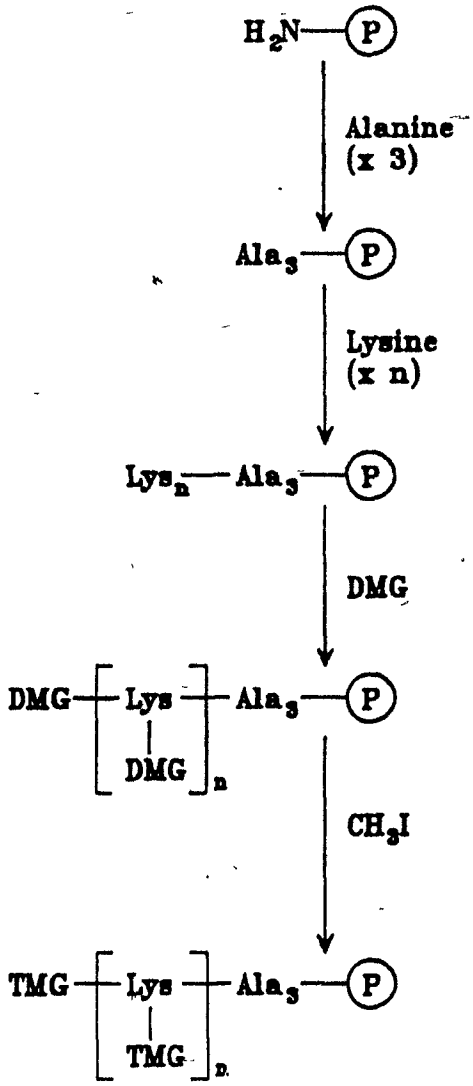

Figure 2.4 The preparation scheme for the quaternized peptide resins. P: polymer support; DMG: dimethylglycine; TMG: trimethylglycine or betaine; n = 1, 3, or 5.

The protecting groups of the amino acid side chains were removed by reacting the dried resins with anhydrous hydrofluoric acid in the presence of anisole at 0°C for 60 minutes. The fully deprotected resins gave strong positive ninhydrin tests. They were washed with anhydrous ether, dried under vacuum at room temperature, and then stored in a vacuum dessicator.

Three resins were synthesized by this method, as shown below. The difference between these resins is the different number of lysine residues on the peptide pendants.

1) Lys-Ala_3-Polymer

2) Lys_3-Ala_3-Polymer

3) Lys_5-Ala_3-Polymer

It was also observed that the color of the resin ranged from white to slightly yellow as the pendants became longer.

Coupling of Dimethylglycine and Quaternization: Before coupling of N,N-dimethylglycine (DMG) to the fully deprotected polymers with lysine pendants of various length, DMF was used to swell the resin for 30 minutes. The chloride salt form of DMG is only sparingly soluble in most of the organic solvents, such as dichloromethane and DMF. Therefore, DMSO was used to dissolve DMG and even in this solvent neutralization with organic base caused precipitation. A 10% DCC solution was added to the DMG solution in DMSO to form the anhydride. The mixture was added to the resin and shaken for 8-10 hours. The resins, after being washed successively with DMF, methylene chloride and anhydrous ether, showed a pale blue color upon testing with ninhydrin and after repeated coupling showed no appreciable decrease in the intensity of this color.

The methylation of the peptide resins was done by reacting with methyl iodide (7). The method was modified for the peptide resins. A small amount of DMF was used to swell the DMG-coupled peptide resins for 30 minutes prior to methylation. Excess methyl iodide (molar ratio about 200:1) was added to the resin, followed by stirring at room temperature for 72-96 hours in a reaction flask covered with aluminum foil to exclude light. The mixture was then filtered and the resin was washed successively with DMF, methylene chloride and anhydrous ether. The quaternized resins showed a yellow color unless washed with water. Ninhydrin tests gave total negative results, indicating that there were no free amine groups on the resins. Since dimethylglycine was coupled to the amino groups of lysine residues, upon methylation, a terminal trimethylglycine (TMG) should be formed. Thus, the terminal TMG resembles the structure of betaine (Figure 2.2) and possesses a quaternary ammonium group with iodide anion as its

counterion. The resins were dried under vacuum overnight and stored in a vacuum dessicator.

Analysis of the Quaternized Peptide Resins: The percentage of methylation was determined by potentiometric titration of the iodide ions with silver nitrate solution, previously standardized with standard sodium chloride solution. The results are listed in Table 2.1.

Table 2.1 The Number of Binding Sites of the Quaternized Peptide Resins

Resin	Number of Binding Sites (mmol/g)
$Cl^-NH_3^+$-Polymer	0.22
TMG-Polymer	0.16
TMG-Polymer (re-methylated)	0.19
TMG-Ala_3-Polymer	0.16
TMG-Lys-Ala_3-Polymer	0.18
TMG-Lys_3-Ala_3-Polymer	0.19
TMG-Lys_5-Ala_3-Polymer	0.17

Note: TMG, the iodide form of trimethylglycine

The number of active binding sites of these resins is all very close to but slightly less than the substitution of the commercial polyamide resin (0.22 mmol/g). The degree of methylation can be enhanced by prolonged reaction time. Thus, some of the resins were methylated twice to increase the percentage of quaternization.

It had been expected that each side chain of the lysine residues in the peptide sequence would be coupled with a betaine residue. However, the results (Table 2.1) indicate that, on average, there is only one active site per peptide pendant. Difficulties could arise in the step of the coupling of dimethyl glycine to the peptide. Since the neutralization of the hydrogen chloride form of DMG caused precipitation, DMG was used in its unneutralized form. The acidity of the mixture might in fact prevent the successful coupling of DMG to the side chain amino group of lysine. Therefore, it is possible that DMG was mainly coupled to the amino group on the end of the peptide chain which remained unprotonated

since it is somewhat less basic than the amine groups on the side chains. As a consequence, the number of quaternary groups on the peptide resins is lower than expected.

To analyze the amino acid contents of the peptide resins, the peptide pendants on the different resins were first hydrolyzed. All glassware used in the experiment was washed with 6 M HCl solution and rinsed with undenatured ethanol. It was then dried at 110°C under vacuum for 12 hours. Precautions had to be taken in handling the glassware to avoid possible contamination from any sources of proteins and amino acids. The peptide resins were weighed in quantities of milligrams (usually about one milligram or even less) and transferred into small culture tubes (from Pyrex) together with an internal standard, L-norleucine (Aldrich). The addition of an internal standard prior to hydrolysis is particularly useful since it covers any possible losses during the hydrolysis and sample transfer. The tubes containing the peptide resins were placed in the reaction vial which contained one ml of 6 M HCl. The system was degassed and then placed in an oven at 110°C. The peptide resins were hydrolyzed for 36 hours followed by the evaporation of the HCl solution. The residues were dissolved in 0.2 N sodium citrate sample dilution buffer (pH 2.20, from Pierce) and centrifuged to remove the solid residues. The solution of the amino acids was appropriately diluted (about 2 mM) with the same buffer. A 20 µl sample, which contained about 0.1-10.0 nmol of amino acid, was injected for analysis.

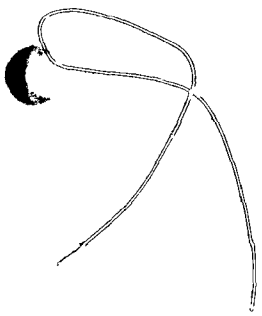

The HPLC system used was a Varian Amino Acid Analyzer (Vista 5500 Liquid Chromatograph) which utilizes an ion exchange column with a UV detector. The analyzer was programmed for a gradient eluent with three solutions, two citrate buffers (buffer 1, pH 3.25, 0.2 N and buffer 2, pH 7.40, 1.0 N) and a 0.2 N carbonate-free sodium hydroxide solution, to elute the amino acids with different polarities. After reacting with the ninhydrin solution (Pickering) in a heated post-column mixer at 110°C, the primary amino acids were detected at 570 nm and the secondary amines at 440 nm. An external standard consisting various amino acids (Amino Acid Standard H, from Pierce) was used as a reference for the analysis of the alanine and lysine residues.

The amino acid contents of the resins were analyzed after quaternization with methyl iodide. The results from the analysis proved that the alanine residues

attached as the spacer on the resin was successfully coupled with a yield of >90%. This is consistent with the previous results obtained for a similar sequence (5). However, the lysine residue content appeared to be lower than the expected number. But previous experience showed that the coupling of lysine also gives a high yield (5). Therefore, this result is an indication that the coupling of dimethylglycine to the amino groups on the lysine side chains was not complete and some of the amino groups reacted directly with methyl iodide. Consequently, this portion of lysine residues is not detected by the post-column UV detector. This in turn, explains the lower substitution of the quaternized peptide resins evidenced by titration with silver nitrate.

2.2.2 Preparation of Commercial Resins for Adsorption

Cholestyramine (Dowex 1X2, mesh size 200-400, from Aldrich) was stirred in methanol for 12 hours followed by 1.0 M hydrochloric acid solution and deionized distilled water. Most of the organic or inorganic impurities can be removed by this washing process. A portion of the resin was washed with 0.1 M sodium iodide solution to replace the chloride counterions with iodide anions. The resin was finally washed with dichloromethane and ether and then dried under vacuum at 110°C overnight. A portion of the resin with iodide counterions was converted back to the chloride form and the titration showed no changes in substitution of the resin because of this treatment.

Colestipol (Colestid, in the hydrochloride drug form, kindly donated by the Upjohn Company of Canada) was pretreated similarly with organic and aqueous solutions to remove any soluble additives. The resin was finally washed with 0.1 M sodium chloride solution and distilled water followed by dichloromethane and ether. Colestipol was dried under vacuum at room temperature for at least 24 hours.

The number of active binding sites of cholestyramine and colestipol was determined by potentiometric titration with silver nitrate solution, standardized with sodium chloride solutions. The results are listed in Table 2.2. Among all the resins cholestyramine resin has the highest number of functional groups on a per gram basis.

The cholestyramine in its chloride form has a substitution of 3.3 mmol/g. Based on this value, conversion to the iodide form, taking into account the addition of weight, gives a theoretical substitution of 2.6 mmol/g. Potentiometric

titration with silver nitrate gave a substitution of 2.7 mmol/g, which is indicative of the reliability of the titration method in the determination of the number of functional groups of the resins.

Table 2.2 The Substitutions of the Commercial Resins

Resin	Number of Binding Sites (mmol/g)
Cholestyramine (Cl)	3.3
Cholestyramine (I)	2.7
Colestipol (Cl)	2.2

2.2.3 Analysis of Bile Salts

Both the colorimetric method and HPLC were used for the analyses. They generally gave identical results except in the presence of iodide ions, which interfered with the colorimetric analysis.

The *colorimetric method* detects the UV absorbance of bile acid solution mixed with concentrated sulfuric acid solution. Typically, 0.4 ml of the adsorbate (0.01-0.40 mM) was mixed with 2 ml of 70% sulfuric acid. The mixture was agitated and allowed to stand for one hour. The absorbance of the mixture was determined using a UV spectrophotometer set at a wavelength of 318 nm. The absorbance was compared with the absorbance values of standard solutions. This method requires relatively pure samples since certain materials which absorb in the UV region can create severe interference for the detection. The iodide ions, present in some of the peptide resins, were found to interfere in the analysis. The absorbance of the bile acid solution was usually lower than normal values in the presence of iodide. In cases where iodide ions are present as the counterions of the resin, HPLC analysis is thus more reliable.

For the analysis of bile acids with *HPLC*, samples of 50 µl (0.01-0.40 mM) were injected to a C-6 reverse phased column (from CSC). The pump was adjusted so that the flow rate was approximately 1 ml/min. A differential refractometer (Waters model 410) was used as a detector, which was interfaced with a microcomputer (Varian DS 604) as a multiuser system. A mixture of

methanol and 0.1 M acetic acid solution was used as eluent. The aqueous buffer fraction, being the most polar component, was always eluted first and exhibited large, complex peaks. It is noteworthy that the buffer peak on the HPLC chromatogram could affect the baseline of the bile acid peak when the concentration of the buffer was efficiently high. Thus, a dilute buffer of about 0.005 M was preferable for the adsorption experiments.

Depending on the composition of the adsorption solutions, different compositions of eluent were selectively used to obtain a stable baseline and a symmetrical sample peak, which permitted the peak area to be calculated with the required precision. The retention times were adjusted to be around 6-7 minutes so that the sample peak would appear at a stable baseline. This was achieved by changing the methanol content in the eluent. A 75:25 mixture of methanol-acetic acid (0.1 M) was found to be most suitable for cholic acid and 70:30 was good for glycocholic acid. After each sample, the system was purged with eluent until a stable baseline was attained. A computer program was installed to integrate the peak area and to optimize the baseline of the chromatogram. A typical HPLC chromatogram is shown in Figure 2.5, in which the big solvent (buffer) peaks appears at a retention time of about 2-5 minutes and the bile acid, being much less polar, appears at a retention time of about 6-7 minutes, depending on the composition of the eluent.

To test the retention times of the different bile acids, a mixture of bile salts was dissolved in water and the mixture was injected into the HPLC column (C-18, from CSC), using methanol-acetic acid (0.1 M) mixture (70:30) as eluent. The retention times of the bile acids ranged from 1 to 45 minutes (Table 2.3), although the peaks became wider as the retention time increased. The order is that of increasing hydrophobicity. The polarity of the bile acids, as shown in Table 2.3, generally follows the order trihydroxy > dihydroxy > monohydroxy and the order taurine conjugates > glycine conjugates > unconjugated.

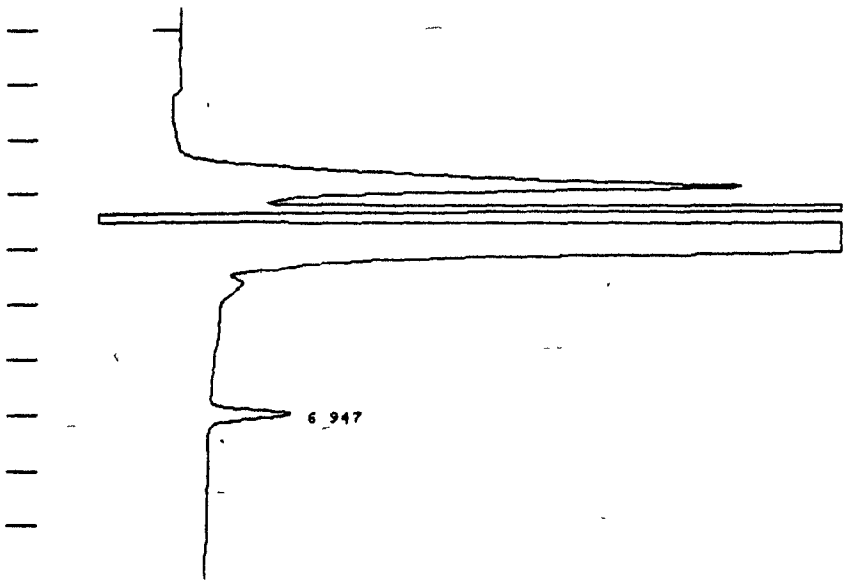

CHANNEL: 1B - 1 TITLE: ANALYSIS 17:14 12 MAR 87

SAMPLE: STD1 METHOD: CAL CALCULATION: A% - CALIB

PEAK NO	PEAK NAME	RESULT AREA%	TIME (MIN)	TIME OFFSET	AREA COUNTS	SEP CODE	W1/2 (SEC)
1		100.0000	6.947		1494996	BB	10.00
TOTALS:		100.0000			1494996		

DETECTED PKS: 1 REJECTED PKS: 0

MULTIPLIER: 1.00000

NOISE: 217.1 OFFSET: 1407

NOTES:
METHANOL.HAC(0.1M)
37:13
P-TMG/CS/12-3-87

POST RUN:
SAVE FILE: RAW CAL385

Figure 2.5 An HPLC chromatogram showing the peak of cholic acid at a retention time about 7 minutes. The large peak that elutes before the bile acid is the buffer peak. Column: C-6 reverse phased column from CSC; Eluent: Methanol-HAc (0.1 M) (74:26); Flow rate: 1 ml/minute.

Table 2.3 The HPLC Retention Times of Bile Acids

Bile Acid	Retention Time (min)
taurocholic acid	1.7
taurochenodeoxycholic acid	1.9
glycocholic acid	5.5
cholic acid	9.1
glycochenodeoxycholic acid	9.3
chenodeoxycholic acid	17.9
deoxycholic acid	18.7
lithocholic acid	43.8

2.2.4 Adsorption Experiments

Buffers: Since the resins are intended for ultimate use in the gastrointestinal tract, it was desirable that the adsorption studies should be done in a similar environment. Although the acidity of the intestine depends on the diet and the influence of nerves, etc., it is generally agreed that the pH of the intestine lies in the neutral range of about 7 to 8 (8). The most abundant ions in the intestinal fluids are chloride and bicarbonate anions, and sodium cations. Phosphate anions are also present in the fluids of the jejunal loops (9).

Both buffer and non-buffer (saline solutions) systems have been used by other researchers in adsorption studies (10,11). Since the pH of the adsorption environment can be controlled easily in buffer solutions, a buffer system was selected for the present adsorption study. *Tris*(hydroxymethyl)-aminomethane-HCl buffer (tris buffer) and KH_2PO_4-NaOH buffer (phosphate buffer) were the buffers of choice. Both of these buffers are used commonly in biochemical studies, and more importantly, their normal pH range (Table 2.4) is ideal to imitate the acidity of the intestine.

To imitate similar biological conditions of the ileum, where the pH is about 7-8, buffer solutions (0.005 M, pH 7.0-7.4) of bile acids were generally used. The phosphate buffer system was used since its content and pH range resemble closely condition of the gastrointestinal fluid where phosphate anions do exist. Tris buffer, an organic buffer, provides a similar pH range and thus was also used in the studies. The pH range was also appropriate for the analysis on

the HPLC system, where a pH range of 6.5 to 7.5 was recommended for the column.

Table 2.4 The pH Ranges of Tris and Phosphate Buffers

Buffer	Normal pH Range
Tris buffer	7.00-9.00
Phosphate buffer	5.80-8.00

Bile Salts: To choose appropriate adsorbates for the adsorption experiments, the normal composition of bile salts in the intestinal tract must be considered. Although many species of bile acids have been found in the human body, the most common bile salts in the body, especially the gastrointestinal tract, are tri- and dihydroxylated bile salts in normal cases (12,13). Furthermore, the glycine conjugates of bile acids are more abundant than the taurine conjugates (14). Therefore, the commonly existing cholic acid salt and glycocholic acid salt were selectively used for the adsorption studies.

A phenomenon that was observed in the experiments is that in some glassware glycocholate undergoes self-hydrolysis at room temperature, as evidenced by the presence of cholic acid peak in the HPLC chromatogram (Figure 2.6). This reaction takes place in the solution slowly and appeared to reach completion after adequate time. It has been reported that the peptide bond can be hydrolyzed in non-silanized glassware (15), since the glass surface is inherently basic. Old glass is particularly bad. Evidently this kind of hydrolysis happened to the amide bond in glycocholic acid, which is in fact also a peptide bond. Therefore, precautions were taken in preparation and storage of solutions of glycocholate. Silanization of the glassware is preferred since it stabilizes the glass surface.

Adsorption Experiments: Bile salts were normally used to prepare the adsorbate solutions because of their greater solubility. The concentration of the stock solution used was about 10-20 mg/dl (0.2-0.4 mM). The basicity of the bile salts does not affect the pH of the buffers significantly, e.g., the 0.4 mM sodium cholate solution changed the pH by about 0.1, compared with the original 0.005

M tris buffer (pH = 7.4).

The stock solution was then diluted with the buffer of use into different fractions and 3 ml of each was added to a known amount of resin (10-20 mg). The adsorption was performed with agitation at room temperature (20°C) for two hours and the resin in the solution was then allowed to settle before the supernatant was taken for analysis.

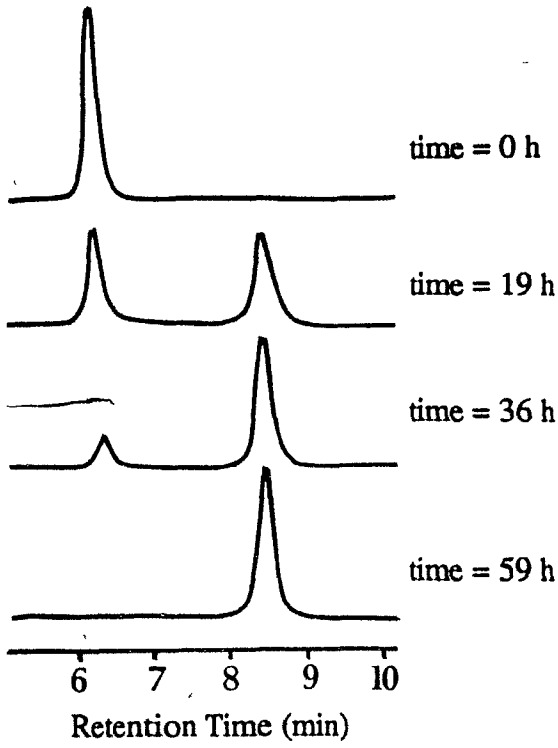

Figure 2.6 The HPLC chromatograms showing the gradual decomposition of glycocholic acid during its storage in glass containers. RT = 6.5 minutes, glycocholic acid; RT = 8.5 minutes, cholic acid.

Processing of Experimental Results: A computer program which provided detailed calculation results and graphics was written to process the results of adsorption after analysis (Appendix 4). Experimental data can be read from a diskette or entered manually and saved on the diskettes for later retrieval. Different scales for the graphics may be selected at user's choice. The program also generates a brief report which fits into the experimental records easily. The error for the adsorption experiments was estimated to be within ±10%.

2.3 Adsorption of Bile Salts Using Cholestyramine and Colestipol

2.3.1 Comparison of Different Buffers

To minimize the effect of pH, both phosphate and tris buffers were restricted in the pH range of 7.0 to 7.4. The adsorption capacity of the resins is not affected by small changes of pH in this range. Cholestyramine in its chloride form was tested for the adsorption of sodium cholate in both buffers (0.005 M). As shown in Figure 2.7, the adsorption capacity of cholestyramine in tris buffer is much higher than in phosphate buffer.

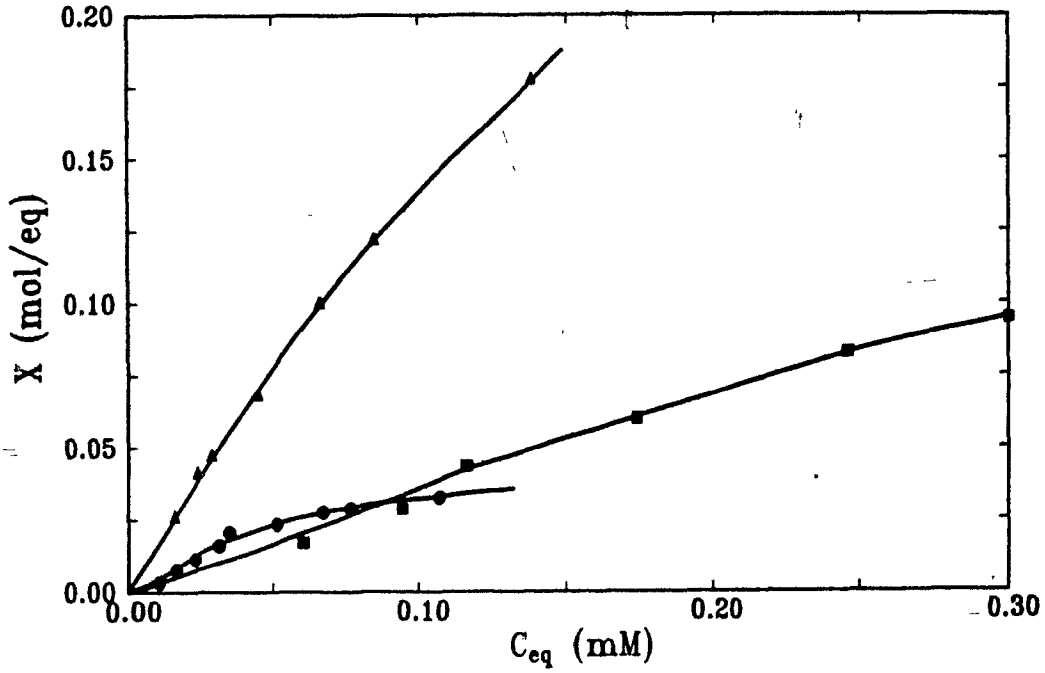

Figure 2.7 The adsorption isotherms for sodium cholate using cholestyramine (Cl) at 20°C. ▲ in 0.005 M tris buffer; ■ in 0.005 M phosphate buffer; ● in 0.050 M phosphate buffer.

As a typical ion-exchange resin, cholestyramine is capable of replacing its mobile counterion, chloride, with other anions in the system. However, this exchange process is determined largely by the selectivity of different organic or inorganic anions (16). In tris buffer, the only chloride anion comes from the buffer source. Therefore, the binding process involves only the replacement of chloride with bile salt anions on the cholestyramine resin. However, in phosphate

buffer at pH 7.4, the phosphate exists mainly as HPO_4^{2-} and $H_2PO_4^-$ anions and these ions have strong binding affinities to the resin, as shown by the selectivity sequence for the strongly basic ion-exchangers (17). These phosphate anions can also replace the chloride counterions of cholestyramine. It is obvious that the binding of cholate in phosphate buffer is a competitive binding process between the bile salt anions and phosphate anions. This competition does not exist in tris buffer system.

Although colestipol has a much smaller capacity for bile acids than cholestyramine, it still shows the same pattern of behavior (Figure 2.8). Thus, the binding affinity of colestipol for sodium cholate in tris buffer is higher than in phosphate buffer. This indicates a similar competition process exists between the cholate anions and the phosphate anions for the binding to colestipol.

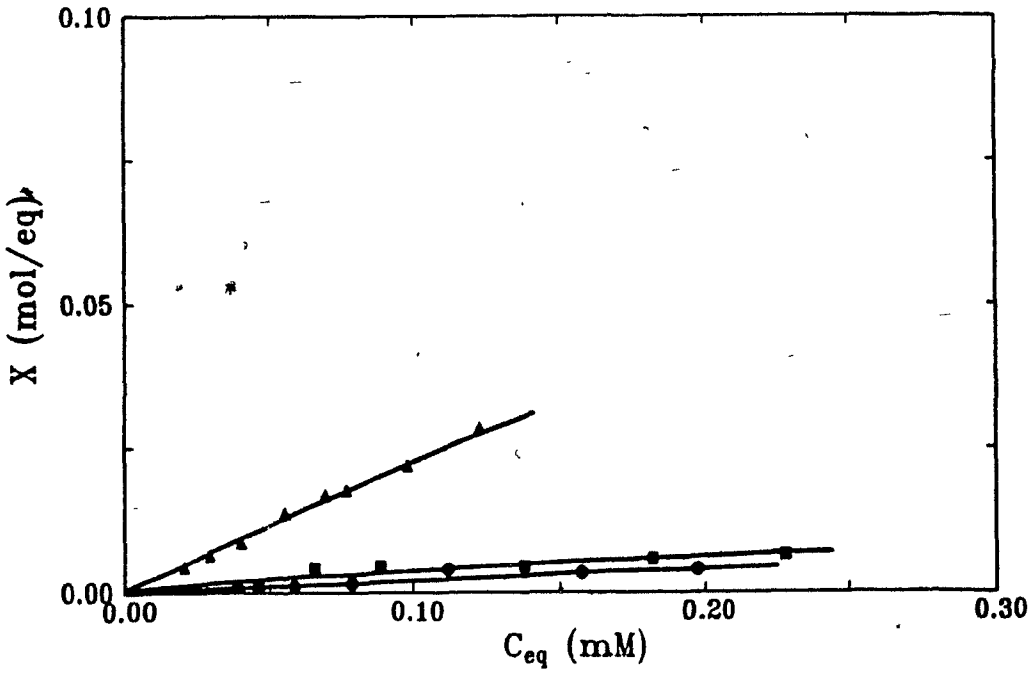

Figure 2.8 The adsorption isotherms for bile salts using colestipol (Cl) at 20°C. ▲ sodium cholate in 0.005 M tris buffer; ■ sodium cholate in 0.005 M phosphate buffer; ● sodium glycocholate in 0.005 M phosphate buffer.

2.3.2 Effect of Ionic Strength

The adsorption isotherm of cholestyramine for cholate in a more concentrated phosphate buffer solution (0.050 M) is shown in Figure 2.7 as a comparison to a dilute phosphate buffer system (0.005M). This dependence on buffer concentration is attributed to the different ionic strengths of the buffer solutions.

In a solution of high ionic strength, the charge density of the resin surface can be reduced by the neutralization with the abundant inorganic anions in the environment. The probability of their participation in ionic interactions with the bile salt anions is thus greatly reduced. This effect of ionic strength on the adsorption capacity of the resins also indicates that the interaction between bile salts and cholestyramine is primarily the formation of ionic linkage since other forms of interactions such as the hydrophobic interaction are expected to be affected less by the ionic strength of the solutions.

The effect of ionic strength can also help to explain the lower affinity of cholestyramine to bile salt in phosphate buffer than in tris buffer. Given the same concentration, it is obvious that the ionic strength of the phosphate buffer is much larger than that of the tris buffer since the tris buffer is an organic buffer and the ions in the phosphate buffer carry more charges because of the dissociation of KH_2PO_4. Therefore, in addition to the competitive binding process (Section 2.3.1), the higher ionic strength of the phosphate buffer can also reduce the binding of bile salt to a certain extent.

Johns and Bates have reported that the addition of bicarbonate or chloride anions to the aqueous solution of bile salt greatly reduced the extent of binding of the trihydroxy bile salt anions to cholestyramine (18). A similar effect was also observed for the adsorption of glycocholic acid with cholestyramine upon the addition of electrolyte (19). Our result is consistent with these observations. The increase of the ionic strength of the adsorption media was also reported to cause decreased rate of interaction (20), which is indicative of the reduced ionic bonding as well as a contributory role of nonelectrostatic interactions.

2.3.3 Effect of the Mobile Counterions of the Resin

As indicated in Figure 2.9, in tris buffer cholestyramine in the chloride form shows a somewhat greater affinity for bile salts than in the iodide form. The chloride and iodide anions are known to have different binding affinities to basic

ion exchangers. The affinity of strong anion exchangers for iodide is known to be higher than for chloride (21). Therefore, displacement of chloride mobile ions by bile salt anions should be easier than the displacement of iodide ions. In this study, the slightly lower affinity of cholestyramine in its iodide form can be explained by this selectivity order. Using this argument, it appears that cholestyramine resins have a higher affinity for bile salt anions than for the chloride and iodide anions. But it is preferable to have chloride anions as the counterions of the resins.

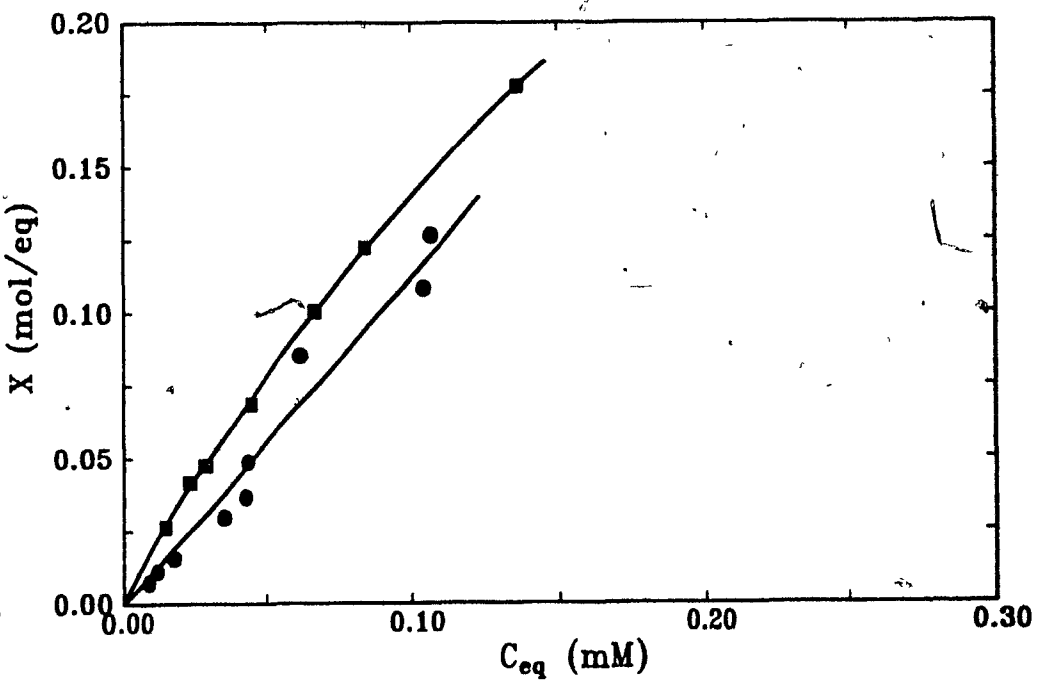

Figure 2.9 The adsorption isotherms of cholestyramine showing the counterion effect. Temperature: 20°C. Adsorbate: sodium cholate in 0.005 M tris buffer. ■ cholestyramine (Cl); ● cholestyramine (I).

2.3.4 Comparison of the Binding Ligands

In tris buffer, the adsorption capacity of cholestyramine for cholate is slightly above that for glycocholate (Figure 2.10). However, as indicated in the figure, for tris buffer neither of the isotherms gives indication of attaining the maximum capacity in the adsorption within the range of equilibrium concentrations that was used.

When tested in 0.050 M phosphate buffer, where it is easier to reach the adsorption equilibrium, it is clearly seen that cholestyramine has a greater affinity for cholate than for glycocholate (Figure 2.10).

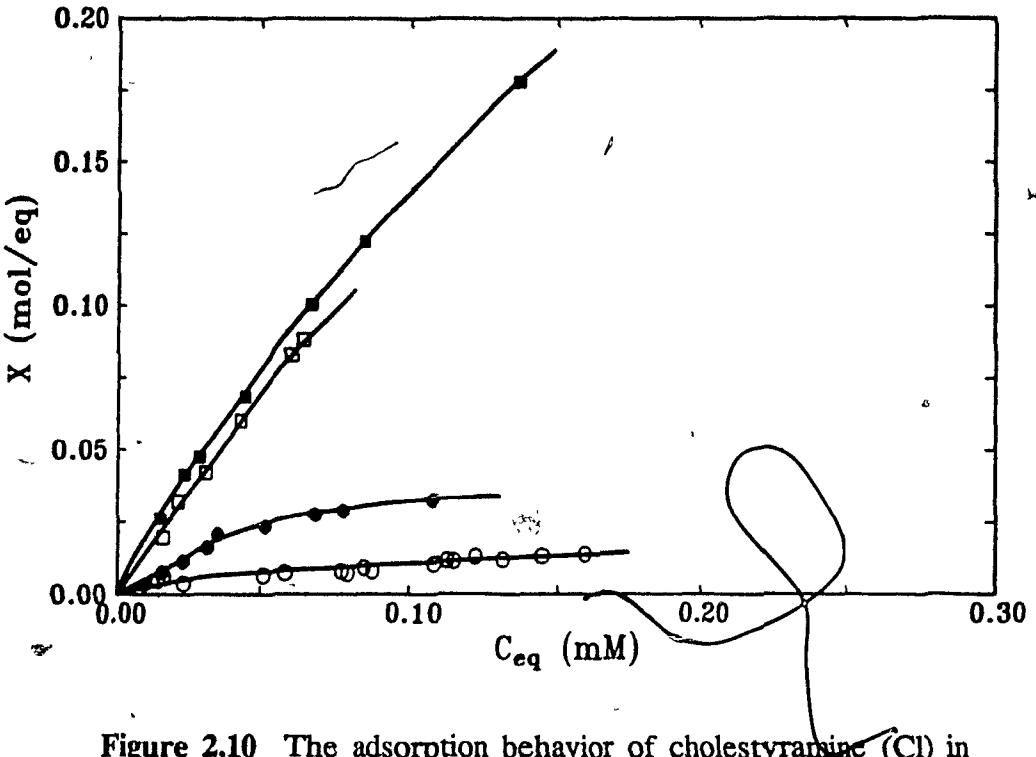

Figure 2.10 The adsorption behavior of cholestyramine (Cl) in different buffers. ■ sodium cholate in 0.005 M tris buffer; □ sodium glycocholate in 0.005 M tris buffer; ● sodium cholate in 0.050 M phosphate buffer; ○ sodium glycocholate in 0.050 M phosphate buffer.

Colestipol was tested in a dilute phosphate buffer solution (0.005 M). The binding affinity of colestipol for cholate is also greater than for glycocholate (Figure 2.8).

These findings are in agreement with the reported results, showing that in saline solutions cholestyramine showed a higher capacity for cholate than for glycocholate in 0.01 M NaCl solution (10).

Glycocholic acid is the glycine conjugate of cholic acid. Its structure resembles that of cholic acid except for the extended side chain where glycine is coupled to the carboxyl group by an amide bond. As was seen in Table 2.4, the addition of glycine to the side chain remarkably increases the polarity of the bile

acid. The difference in retention times of glycocholic acid and glycochenodeoxycholic acid is 3.8 minutes, while the difference between their respective parent bile acids, cholic and chenodeoxycholic acids is 8.8 minutes. The much smaller difference between the two glycine conjugates means the glycine residue affects the polarity of the bile acids significantly. The effect of the hydroxyl group is obscured by the presence of the glycine residue.

The fact that the resins have a stronger affinity for cholate than for glycocholate can be explained by the amphiphilic interactions. As described in Chapter 1, this behavior has been observed in the binding of bile salts to proteins. Regardless of the backbone structure, the less polar cholate is bound more strongly than its glycocholate counterpart. It has also been reported that the binding affinity of bile salt to cholestyramine decreases as the number of hydroxy substituents on the steroid skeleton increases (22). For example, cholestyramine has a higher affinity for the dihydroxy bile salts than for the trihydroxy (18). Therefore, it was concluded that the binding mechanism of bile salts involves a primary electrostatic component reinforced by a secondary nonelectrostatic interaction, the strength of the latter force being dependent on the degree of hydrophobicity of the adsorbate molecule (22).

The lower affinity of glycocholate can also be attributed to its higher solubility in water solution. The solubility effect of the adsorbates has been demonstrated by He in an adsorption study of phenol and mono-, di- and tri-chlorophenols, where the least soluble trichlorophenol has shown the highest affinity to the polymer adsorbent (21). The higher solubility of a compound indicates a high affinity with the medium, its affinity with the adsorbent is therefore reduced.

2.3.5 Comparison Between Cholestyramine and Colestipol

In the assignment of the basicity of anion exchange resins, the primary and secondary amine groups are considered to be weak bases, the tertiary amines are intermediate bases, and the quaternary ammonium is a strong base (16). Cholestyramine, which possesses the quaternary ammonium group as the functional group has a high capacity for bile salts, especially in tris buffer. Colestipol, on the other hand, has only secondary or tertiary amine groups. Although the amine groups outnumber the substitution of cholestyramine, they are less effective in the binding of bile salts. The fact that the amine groups of

colestipol are located within the polymer chains may also be disadvantageous since this makes the functional groups less accessible to the interacting substrates.

Is the strong base, i.e., the quaternary ammonium group, important in the binding of bile salts? Colleagues in our laboratory have tried to modify the functional groups of colestipol by methylation with methyl iodide. Preliminary results have shown that the colestipol resin after methylation has an increased binding capacity for glycocholate (23). The increase in basicity of the resin thus leads to an increase in the adsorption of bile salts.

The matrix of cholestyramine is a copolymer of styrene and divinylbenzene. The hydrophobicity of the backbone may be an important advantage in the binding of bile salts. Upon forming a salt linkage, which is thought to be the driving force in the binding process, the amphiphilic moiety of bile salt interacts favorably with the hydrophobic backbone of cholestyramine. Colestipol has a backbone of a water-swellable copolymer composed of tetraethylene-pentamine and epichlorohydrin. Although this backbone has a better biocompatibility, it does not favor hydrophobic interaction with bile salts. Hydrogen bond formation between the hydroxyl groups of bile salt and the polar groups on the colestipol matrix may involve the change of the configuration of bile salts since the three hydroxyl groups are located on different positions on the steroid skeleton. The lower binding affinity of colestipol for bile salts is possibly a consequence of the combination of weaker basicity and lack of hydrophobicity.

The importance of the ionic linkage has also been demonstrated by the study of the pH effect (19). The amount of glycocholic acid ($pK_a \approx 4.0$) bound to cholestyramine increased greatly as the pH was changed from 1 to 4 , while the capacity of cholestyramine for taurocholic acid ($pK_a \approx 2.0$) was high even at low pH values. Therefore, the ionization of bile acids is important in the binding of bile acids to anion exchange resins. On the other hand, in the binding of deoxycholic acid ($pK_a \approx 5.3$) to soya bean flour, wheat bran and lucerne, where non-ionic interactions were expected, the increase in pH leads to decreases in the binding capacity (24). In this case, the solubility of the bile acid at higher pH is greater and hence low pH values favor the non-ionic interactions. Therefore, it can be concluded that the binding of bile acids depends on the basicity of the anion exchange resin as well as on its own ionization status. Hydrophobic

interactions, on the other hand, may also facilitate the binding of bile acids to the resin. These conclusions will be further verified in Section 2.4.

2.4 Adsorption of Bile Salts Using the Quaternized Peptide Resins

2.4.1 Comparison of the Quaternized Peptide Resins

The adsorption of the quaternized peptide resins was tested with sodium cholate. Three of the resins, i.e.,

I^-TMG^+-Polymer

I^-TMG^+-Lys-Ala_3-Polymer

I^-TMG^+-Lys_3-Ala_3-Polymer

show little difference in their adsorption capacities when tested in 0.005 M tris buffer (Figure 2.11). This indicates that the binding sites are independent in the binding process when the peptide sequence is relatively short. In this circumstance, it is easier for the peptide chain to retain its randomly extended

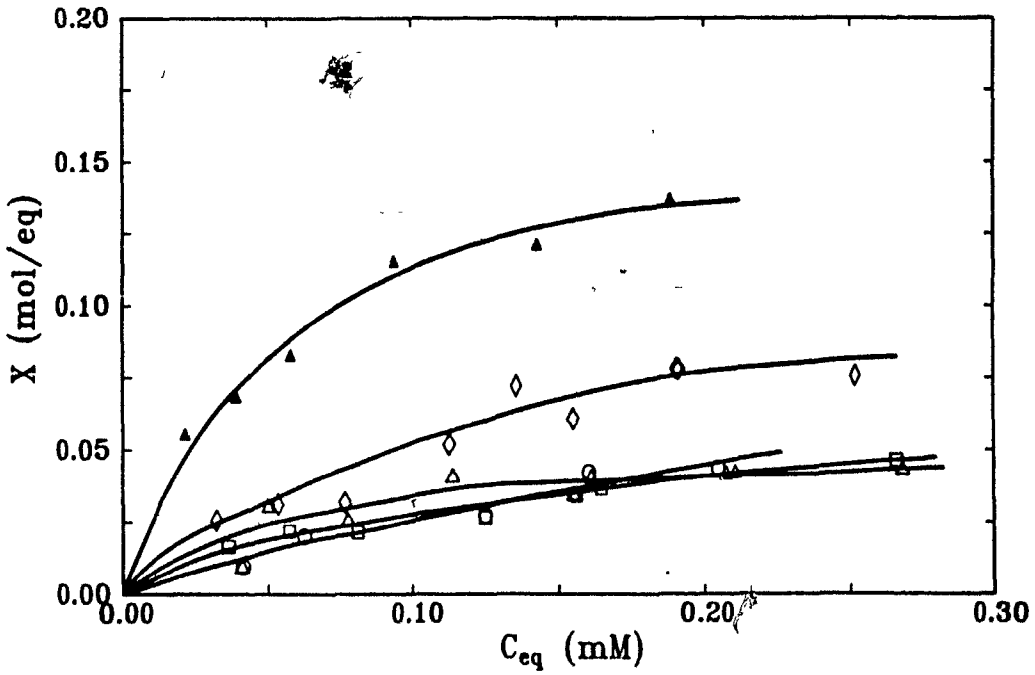

Figure 2.11 The adsorption isotherms of the quaternized peptide resins in tris buffer at 20°C. Adsorbate: sodium cholate in 0.005 M tris buffer. ○ TMG-P; □ TMG-Lys-Ala_3-P; Δ TMG-Lys_3-Ala_3-P; ◊ TMG-Lys_5-Ala_3-P; ▲ TMG-Lys_5-Ala_3-P (ground).

state. However, the quaternized peptide resin containing the lysine-5 sequence demonstrates a much greater capacity than the other quaternized peptide resins.

This series of resins also showed similar behavior when tested for the adsorption of glycocholate in 0.050 M phosphate buffer, where the resins fall in the order of TMG-Lys_5-Ala_3 > TMG-Lys_3-Ala_3 ≈ TMG-Lys-Ala_3 ≈ TMG-Ala_3 > TMG (Figure 2.12). The resin with TMG directly connected to the backbone functional groups has the lowest capacity on a per binding site basis. This indicates the addition of the alanine-3 spacer makes the binding sites more accessible and thus enhances the binding capacity of the quaternized peptide resins.

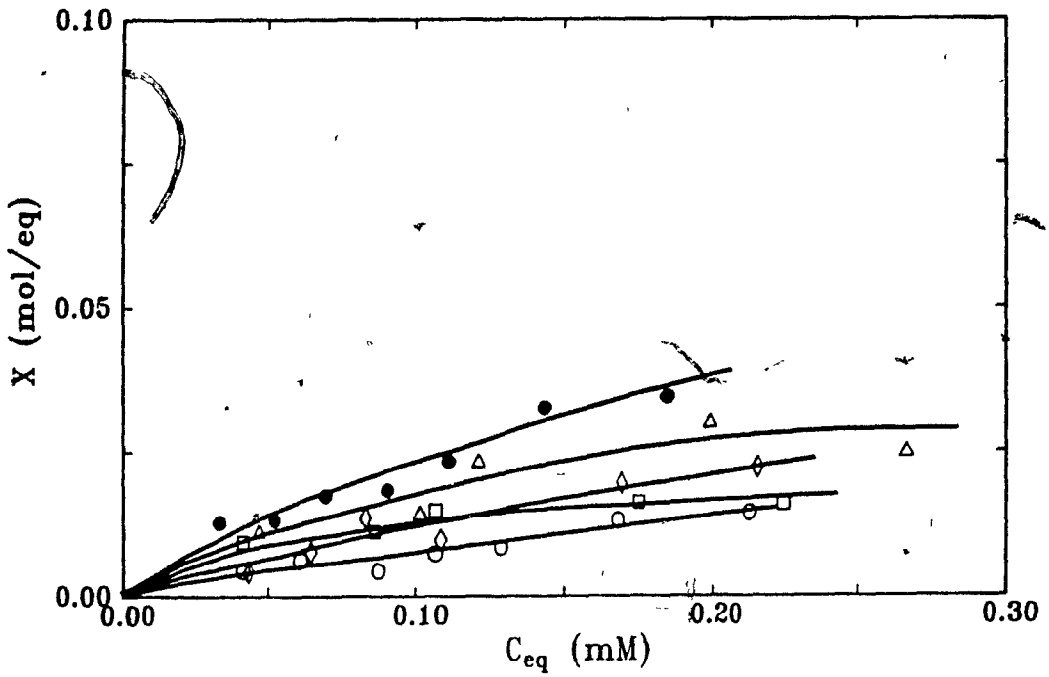

Figure 2.12 The adsorption isotherms of the quaternized peptide resins in phosphate buffer at 20°C. Adsorbate: sodium glycocholate in 0.050 M phosphate buffer. ○ TMG-P; □ TMG-Ala_3-P; Δ TMG-Lys-Ala_3-P; ◊ TMG-Lys_3-Ala_3-P; ● TMG-Lys_5-Ala_3-P.

It is obvious that the active binding sites become more accessible to the binding substrates as the peptide chain becomes longer. However, when the peptide chain is short, the binding affinity of the resin depends only on the

primary structure, i.e., the amino acid content, of the peptide-containing pendant. As the peptide chain becomes longer, long enough to adopt a certain form of conformation, the secondary structure may become important in the binding process. The secondary structure refers to the conformation of the peptides by hydrogen bonding, such as the formation of the helical structure, etc. The interaction with bile salts may very well be facilitated by such conformational changes. The importance of peptide conformation of the longer peptide pendant has also been observed in the binding of bilirubin with peptide resins, where binding capacity increases markedly as the peptide pendant grows longer (25).

2.4.2 Effect of the Resin Particle Size

For the adsorption of sodium cholate, both the bead form and ground powder of the quaternized peptide resin containing the lysine-5 sequence have been used. The binding capacity was remarkably enhanced when the ground resin was used (Figure 2.11).

The ground form of the resin has a larger surface area than the bead form. For the quaternized peptide resins, the binding capacity is about 0.13 moles per equivalent of binding sites as equilibrium is reached at the plateau of the adsorption isotherm. If the binding sites are independent, this number is a mathematical average for all the possible binding sites. In fact, a large number of the possible binding sites remain intact from the ligands in the binding process, simply because it is difficult for the bile salt anions, being rigid molecules of fairly large size, to get close to these binding sites. However, when the surface area increases, the number of quaternary ammonium groups located on the surface of the resin is also increased. Therefore, more binding sites are exposed to the bile salt anions. This, in turn, facilitates the interaction between the resin and the ligands, thus resulting in a higher binding capacity. On the other hand, the force of the ionic interaction is inversely proportional to the square of the distance between the interacting groups. When the functional groups are on the surface of the resins, it is possible that the interaction with bile salt carboxyl groups is increasingly strengthened as the distance between the interacting groups becomes shorter. These data also suggest that even in the swollen state the matrix of the beads cannot be penetrated by the bile salt anions. The effect of resin surface area has been observed in the adsorption of unconjugated bilirubin (26) as well as in organic synthesis where polymeric resins are used as catalysts (27).

2.4.3 Comparison of Different Buffers

Like cholestyramine, the adsorption by the quaternized peptide resins is little affected by small changes of pH of the buffer (pH 7.0-7.4). However, the binding affinity of the quaternized peptide resin containing lysine-5 in its sequence is essentially identical in tris and phosphate buffer systems (Figure 2.13). This is an indication of the specificity of the peptide containing resins in the binding of bile salts.

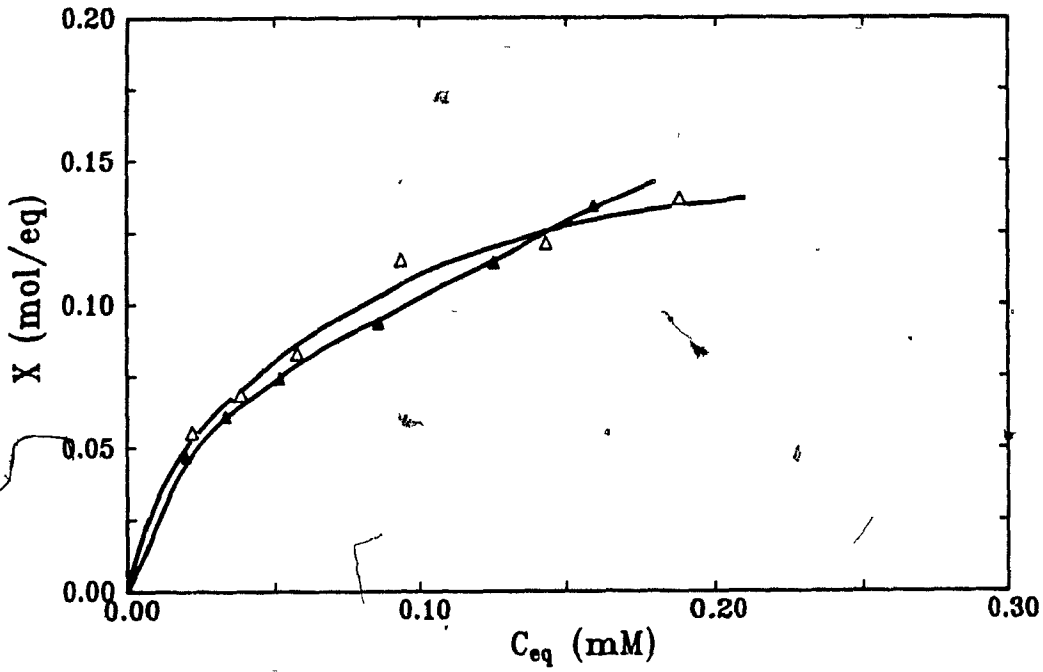

Figure 2.13 The adsorption isotherms of the quaternized peptide resin containing lysine-5 (TMG-Lys_5-Ala_3-P/ground) in different buffers. Temperature: 20°C. Δ sodium cholate in 0.005 M tris buffer; ▲ sodium cholate in 0.005 M phosphate buffer.

As discussed in Section 2.3.1, cholestyramine and colestipol behave very differently from the peptide-containing resins in the two buffers. The adsorption capacity of cholestyramine for bile salt in phosphate buffer is greatly reduced since this anion exchanger is also a good adsorbent for inorganic anions, such as $H_2PO_4^-$ and HPO_4^{2-} anions in the buffer solution. Compared with cholestyramine, the quaternized peptide resin containing the lysine-5 sequence is a much better

adsorbent in the phosphate buffer. The binding affinity of this resin for bile salts remains the same regardless of the existing anions of the buffer system.

The specificity of the quaternized peptide-containing resin for bile salts is an indication that the binding is not merely an ion exchange process, as in the cases of cholestyramine and colestipol. The peptide sequence, possibly the peptide conformation, is important for the binding of organic anions. The peptide-containing resins apparently do not have a high affinity for the inorganic anions.

Based on this observation, the low binding affinity of cholestyramine for bilirubin, also an organic acid, compared with peptide resins (25) can also be attributed to the lack of specificity when tested in phosphate buffers (pH 7.8, 0.050 M) solutions, where inorganic anions exist in large abundance. The peptide resins were little affected by these phosphate anions.

2.4.4 Effect of Ionic Strength

The affinity of the quaternized peptide resins in the binding of bile salts is affected by the ionic strength of the buffer. When tested in phosphate buffer, as shown in Figure 2.14, the binding of bile salts to quaternized peptide resins is reduced by the increase in the buffer concentration (from 0.005 to 0.050 M).

The increased ionic strength also reduces the binding affinity of bile acids for cholestyramine, as discussed in Section 2.3.2. The high concentration of the inorganic anions in the solution also reduces the charge density of the positively charged quaternary ammonium groups, thus, leading to a reduced binding affinity for bile salts. The energy of the electrostatic interactions varies inversely with the dielectric constant of the media. Therefore, the ionic bond would be expected to be weakened by the higher ionic strength of the solution.

It is also necessary to point out that the specificity of the peptide-containing resins for bile salts does *not* exclude the possibility of the binding of other anions onto these resins. This specificity implies only a preference in the binding process. Given other anions in high concentrations, the resin will naturally bind whatever anions are available in the immediate surroundings. In this case, a simple mass action or concentration dependence dominates the binding process.

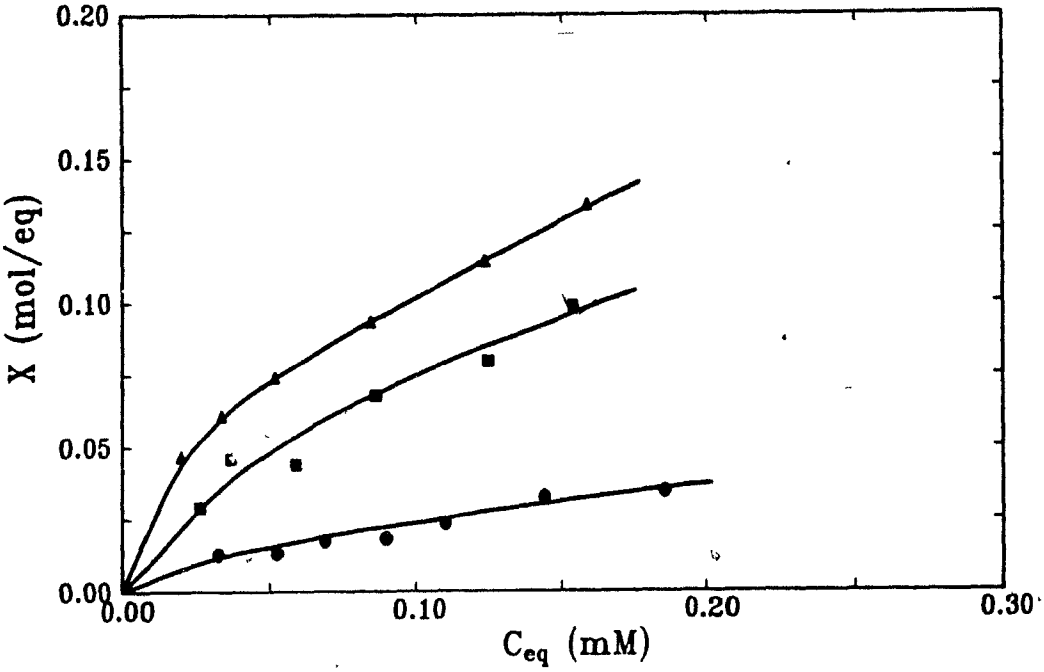

Figure 2.14 The adsorption isotherms of the quaternized peptide resin containing lysine-5 (TMG-Lys_5-Ala_3-P/ground) showing the effect of ionic strength and of different ligand. Temperature: 20°C. ▲ sodium cholate in 0.005 M phosphate buffer; ■ sodium glycocholate in 0.005 M phosphate buffer; ● sodium glycocholate in 0.050 M phosphate buffer.

2.4.5 Comparison of Different Ligands

It had been expected that the quaternized peptide-containing resins might have a higher affinity for glycocholate than for cholate because this bile salt has an amide bond which closely resembles the peptide bond. Glycocholate was tested for adsorption with the quaternized peptide resin containing the lysine-5 sequence in 0.005 M phosphate buffer. The resin shows a lower affinity for glycocholate than for cholate (Figure 2.14). This behavior is very similar to that of cholestyramine as discussed in Section 2.3.4.

The binding of bile salts with polymeric resins does not only involve the interaction between the resin and the bile salt. The binding process actually involves the competition of interaction among all the existing species in the solution. These species include the water, various anions and cations of the buffer, the bile salt and the resin. The stereostructure of bile acids indicates that

they are rather rigid molecules which have a hydrophilic side and a hydrophobic side. To bind well to the resin, both the hydrophilic and hydrophobic moieties of the molecule must adjust to have the lowest conformational energy.

It is well known that glycocholic acid has a higher solubility in water than cholic acid. This higher solubility is largely attributed to its hydrophilicity as it has an extra hydrophilic amide linkage which can readily form hydrogen bonds with water. More hydrogen bonds can be formed between glycocholate and water than between cholate and water. More energy is needed to break the hydrogen bonds between glycocholate and water for the binding between the resin and glycocholate to take place. The extra energy needed for the binding process determines that the glycocholate always has a lower binding affinity for the resins. In other words, glycocholate has a lower affinity to the resin not because it is less attracted to the resin but because it prefers the water. The same would be true if the trihydroxylated bile acids are compared with the dihydroxylated bile acids. Therefore, the hydrophobicity of the bile salt anions plays an important role in the bile process. It can be expected that the quaternized peptide resins would have a higher affinity for di- and mono-hydroxy bile salts.

2.5 The Interactions Between Polymeric Resins and Bile Salts

Three types of resins, i.e., cholestyramine, colestipol, and quaternized peptide-containing water-swellable resins, have been tested as adsorbents for bile salts in aqueous buffer solutions. Cholestyramine has a hydrophobic backbone and quaternary ammonium functional groups. Colestipol has a water-swellable backbone with secondary and tertiary amine functional groups. The quaternized peptide-containing resins have a water-swellable backbone and quaternary ammonium functional groups. Another significant difference of the quaternized peptide resins is the inclusion of peptide sequences, which appears to contribute to the binding of bile acids.

Though cholestyramine shows a rather high capacity for bile salts in tris buffer, this capacity is significantly reduced in the presence of phosphate anions, especially at a higher concentration. Colestipol shows a limited capacity for bile salts under the experimental conditions selected in this study. Its binding behavior is rather similar to that of cholestyramine. The synthesized resins containing peptide sequences show an increased capacity for bile salts. This type

of resin is much less affected by the adsorption medium because of its binding specificity. The alanine spacer is useful in improving the accessibility of the binding sites of the resins. Peptide resins containing a peptide chain long enough to accommodate conformational changes have a higher affinity for bile salts than those with shorter peptides. One common observation for all of these resins is that the hydrophobic interaction appears, in fact, to play an important role in the binding.

2.5.1 The Interactions Between the Binding Species

The adsorption of bile acids is a very complicated process. As proposed by many researchers in the past (28), three possible interactions for the binding between biological molecules include: salt linkage, hydrogen bonding and hydrophobic interactions (Figure 2.15).

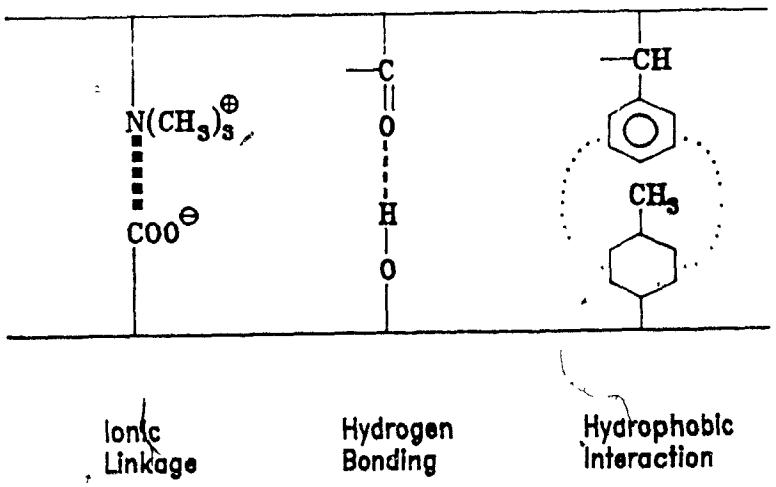

Figure 2.15 The three kinds of possible interactions between the polymeric resins and bile salts.

(1) Ionic Interaction

The predominant interaction among the three is the salt linkage, or ionic interaction. This interaction is electrostatic in nature and is usually considered as the main driving force in the binding process. The energy of the electrostatic binding follows Coulomb's law. Therefore, the strength of the ionic bond is inversely proportional to the square of the distance between the interacting groups,

$$F = \frac{1}{4\pi\varepsilon_0\varepsilon_r} \cdot \frac{Q_1 Q_2}{r^2} \qquad \text{(Equation 2.1)}$$

where r is the distance between the oppositely charged groups, Q is the charge of the respective group, ε_0 is the permittivity of vacuum and ε_r is the relative permittivity (dielectric constant). This equation is normally used to describe the electrical interactions between two spherical ions. The oppositely charged groups of the molecules have to be located at the accessible sites on the substrates to effectively form strong binding while the less accessible groups do not participate in the interaction or participate only in weaker interactions. The conformations of the molecules involved in the interaction are of great importance in this kind of binding. Equation 2.1 offers an explanation as to why the ground resin has a larger affinity for its binding substrate than the bead form since the binding force becomes weaker as the distance between the binding species becomes larger. In the ground form, more binding sites are located on the resin surface, thus strong ionic bonds can be formed easily between the resin and the bile salt anions.

(2) Hydrogen Bonding

Hydrogen bonding is a weaker form of electrostatic interaction. It is well known that hydrogen atoms attached to highly electronegative atoms form hydrogen bonds with other electronegative atoms on a nearby group. This may occur within the same molecule (intramolecular hydrogen bonding) or between two or more molecules (intermolecular hydrogen bonding). Hydrogen bonds are very common and have an important structural function in biological molecules such as proteins and polypeptides. In fact the secondary structure of proteins, such as the α-helix and β-sheet, is determined by hydrogen bond formation. The folding and bending of the peptide chain are associated with the formation of these hydrogen bonds.

The strength of the hydrogen bond is only about 5-10% that of the normal covalent bond and is inversely proportional to the square of the distance between hydrogen and the electronegative atom, since it is also a kind of electrostatic interaction. Although the two atoms are attracted by the hydrogen bond, at the same time, they are held apart by the mutual repulsions of the peripheral electrons. One of the important restrictions in the formation of a hydrogen bond is that the hydrogen bond must be colinear to assume a lowest potential energy.

For example, a deviation of 20° in the angle of the N-H...O bond reduces the binding energy by approximately 10% (29). It is also of interest to note that the hydrogen bonds of biological importance, such as those in proteins, are much weaker than the normal hydrogen bonds (30).

The hydrogen bonding is of secondary importance for adsorption in aqueous media. Due to the abundant presence of water molecules, the polar groups of the resin pendants and bile salts tend to form hydrogen bonds with water. The rigidity of the bile salt anions favors hydrogen bonding with water rather than with the resin. This represents a direct explanation for the lower affinity for glycocholic acid in the binding. Therefore, it can be expected that an increase in the hydrophilicity of the bile salt will reduce its binding affinity onto the polymeric resin.

(3) Hydrophobic Interaction

Hydrophobic binding may be considered to be a form of dispersion forces (or in a more general sense, van der Waals forces). It is an entropy-driven process, as further discussed in Section 2.5.2, and makes a major contribution to the free energy of binding. This is especially important in the binding with proteins since the quaternary structure and the conformational state of the protein can be altered significantly to accommodate the interaction.

The hydrophobic interaction can contribute greatly to the stability of the interacting molecular species. It involves the exclusion of water from the immediate vicinity of the interacting groups. The water molecules surrounding the hydrophobic groups have a more ordered structure than in the absence of this kind of group. Therefore, the mixing of water with hydrophobic molecular species is accompanied by a negative entropy change and as a consequence this is a thermodynamically unfavorable process (31). The hydrophobic binding, on the other hand, leads to an increase in entropy in this system. The exclusion of water contributes favorably to the entropic changes of the binding process.

Bile acids are steroid related compounds. They act like a detergent in aqueous solutions. The importance of the hydrophobic interactions between macromolecules and detergents needs to be emphasized. A fact presented in a review by Breuer and Robb may well reflect the importance of the hydrophobic interactions: *nearly all studies confirm that the more hydrophobic a polymer, the greater is the adsorption of the detergent onto it* (32). In addition to the isolated

hydroxyl groups and the carboxylic acid group on the side chain of the bile acids, the hydrophobicity is thus one of the most important properties of bile acids. Therefore, hydrophobic interaction between bile salt anion and the polymeric resin is an important factor during the binding process. This interaction also promotes the precipitation of organic anions onto the polymer surface, thus leading to a high selectivity in the ionic interactions.

An important point in the consideration of the binding mechanism is that binding is a cooperative process including different types of interactions rather than an isolated independent process. In the case of protein interactions, the binding process can become even more complicated than in a simple model, e.g., some binding sites with high affinity for alkyl sulfates and sulfonates on the protein do not have high affinity for alkyl carboxylates (33).

2.5.2 Thermodynamics of the Binding Process

For a system consisting of the polymeric resin (P), the binding ligand (L) and the solvent (S), the free energy change for the overall binding process, ΔG, is

$$\Delta G = \Delta H - T\Delta S \qquad \text{(Equation 2.2)}$$

As always, binding is favored by a negative free energy change. For the consideration of the thermodynamics of the overall process, it can be divided into three separated steps:

[1] Total, or partial, desolvation of the ligand;

[2] Total, or partial, desolvation of the active site or the vicinity of the active site of the polymer, especially for water-swellable polymers;

[3] Binding of the desolvated ligand by the desolvated polymer.

Thus, the binding energy or enthalpy change, ΔH, is expressed by

$$\Delta H = \Delta H_{P\text{-}L} + \Delta H_{L\text{-}S} + \Delta H_{P\text{-}S} \qquad \text{(Equation 2.3)}$$

and the entropy change, ΔS, is expressed similarly by

$$\Delta S = \Delta S_{P\text{-}L} + \Delta S_{L\text{-}S} + \Delta S_{P\text{-}S} \qquad \text{(Equation 2.4)}$$

The enthalpy term for the binding step, i.e., step [3], $\Delta H_{P\text{-}L}$, is expected to be negative due to the formation of strong ionic bonds as well as van der Waals attractions which provide binding energy in the bonded state, and $\Delta H_{L\text{-}S}$ and $\Delta H_{P\text{-}S}$ are expected to be positive since energy is needed to break the interactions

between the solvent and the ligand. However, the contributions of the terms $\Delta H_{L\text{-}S}$ and $\Delta H_{P\text{-}S}$ are expected to be relatively small, especially when both P and L are organic species in an aqueous environment, where the interactions between L and S and between P and S are relatively weak. However, hydration of the active site of the polymer can include hydrogen bonding, in which case $\Delta H_{P\text{-}S}$ would be significantly endothermic. The overall ΔH should normally be negative since the energy of the binding between the polymer and the ligand is expected to compensate for the energy consumed in the breakage of the interactions between the solvent and the ligand.

The entropy change can play the decisive role in the binding process. In simple cases, where only the bound and the free states exist, the bound state is more ordered (lower entropy) than the free state, the entropy change $\Delta S = S_{bound} - S_{free}$ should normally be negative. However, in addition, the binding process involves the desolvation of the ligand and of the polymer. When this is also considered, the total entropy change ΔS depends on the three terms given in Equation 2.4. Compared with the free state, $\Delta S_{P\text{-}L}$ is expected to be negative; $\Delta S_{P\text{-}S}$ positive; $\Delta S_{L\text{-}S}$ is also positive. The contribution of $\Delta S_{P\text{-}S}$ can be considerable because it requires the disruption of the water at the binding site, which in the present case can include contributions due to hydrogen bonding. Similarly, the contribution of $\Delta S_{L\text{-}S}$ can be significant since, in solution, the "free" ligand exists as an entity of low entropy because the water molecules which surround a hydrophobic ligand adopt a highly ordered state, the so-called "iceberg state" (31). The binding of these ligands involves a positive entropy contribution from the destruction of the "iceberg state". The total entropy change is the sum of all these factors and can be positive or negative, depending on the relative contributions of these factors.

When ΔS is positive, the entropy term ($-T\Delta S$) is negative, which favors the bound state. Under this circumstance, the total free energy change ΔG, which defines the binding, is negative and favors the binding even when ΔH is somewhat positive. However, when ΔS is negative, the entropy term ($-T\Delta S$) is positive. In this case, at a given temperature, binding will only take place when enough binding energy is provided. Furthermore, low rather than high temperatures favor the exothermic binding process between the ligand and the polymer.

2.5.3 The Stoichiometric Binding Constants and Free Energy Changes

The affinity of the binding may be expressed by the stoichiometric binding constant, K, which is the equilibrium constant for the binding process (see Section 2.5.3). This binding constant can then be related to the free energy change by

$$\Delta G = -RT \ln K \qquad \text{(Equation 2.5)}$$

At a given temperature, the binding constant can be estimated from the adsorption isotherm, and thus the free energy change can be calculated using Equation 2.5.

At the equilibrium of adsorption, the binding capacity of all the resins tested is less than one mole per equivalent of active binding sites, based on the titration of the resins which gives the number of quaternary groups of the respective resins. It is these active groups which are important in the binding process, as shown by the data obtained. It is evident that the binding capacity of the quaternized peptide containing resins is not directly proportional to the number of active sites, i.e., the quaternary ammonium groups. For example, the quaternized resin containing lysine-5 sequence has a higher capacity than those with shorter peptide sequences. It is also known that the conformational changes of the longer pendants may be an aid in accommodating the binding (Section 2.4.1). In this case, the stoichiometric binding constants can serve as a good description of the binding affinity (34). As discussed in the text above, the binding involves a rather complicated interaction between the adsorbent (P), the ligand (L), the ions of the buffer and the water. However, from a thermodynamic point of view, the overall process of adsorption can be simplified to the binding between P and L, so that an equilibrium can be reached at the end of the adsorption. Thus

$$P + L \underset{}{\overset{K}{\rightleftharpoons}} PL$$

The stoichiometric binding constant, K, is then expressed by

$$K = \frac{[PL]}{[P]\,[L]} \qquad \text{(Equation 2.7)}$$

The moles of ligand bound per equivalent of resin, X, can be expressed by

$$X = \frac{[PL]}{[P] + [PL]} \qquad \text{(Equation 2.8)}$$

From Equation 2.7, [PL] = K [P] [L], so that Equation 2.8 can be written as

$$X = \frac{K[L]}{1 + K[L]} \qquad \text{(Equation 2.9)}$$

Using a computer program with a derivative-free least square curve-fitting procedure (35) for X as a function of [L], the stoichiometric binding constant K can be calculated for each of the resins for the different ligands as the best fit to the adsorption isotherm. The results of the calculation are shown in Table 2.5.

The free energy of the binding process can be calculated according to Equation 2.5. The temperature for the adsorption was 20°C. The results of the calculation are also listed in Table 2.5.

From Table 2.5, the following conclusions may be drawn:

(1) The binding affinity of the synthesized resins containing peptide sequences generally follows the order: TMG-Lys_5-Ala_3 > TMG-Lys_3-Ala_3 ≈ TMG-Lys-Ala_3 > TMG;

(2) The quaternized peptide resins exhibit a similar affinity for the bile salt in both tris and phosphate buffers, although the binding may be affected by the ionic strength of the buffer solution. This is an indication of their high specificity for bile salt anions even in a phosphate buffer where large amounts of inorganic anions are present;

(3) The binding affinity of cholestyramine is strongly affected by the buffer system, and is especially low in phosphate buffer. Chloride counterions are favorable for the binding;

(4) The binding affinity for glycocholate is lower than that for cholate.

Table 2.5 The Binding Constants and Free Energy Changes for the Adsorption of Bile Salts at 20°C

Resin	K x 10^{-3} (M^{-1})	ΔG ($kJ\ mol^{-1}$)	
I^-TMG^+-P	0.24	-13	(NaC, tris)
	0.071	-10	(NaGC, conc phos)
TMG-Ala_3-P	0.094	-11	(NaGC, conc phos)
TMG-Lys-Ala_3-P	0.22	-13	(NaC, tris)
	0.13	-12	(NaGC, conc phos)
TMG-Lys_3-Ala_3-P	0.23	-13	(NaC, tris)
	0.11	-12	(NaGC, conc phos)
TMG-Lys5-Ala3-P	0.43	-15	(NaC, tris)
	0.22	-13	(NaGC, conc phos)
TMG-Lys5-Ala3-P (ground)	1.1	-17	(NaC, tris)
	1.1	-17	(NaC, phos)
	0.47	-15	(NaGC, tris)
	0.76	-16	(NaGC, phos)
Cholestyramine (Cl)	1.6	-18	(NaC, tris)
	0.36	-14	(NaC, phos)
	1.5	-18	(NaGC, tris)
Cholestyramine (I)	1.2	-17	(NaC, tris)
	0.10	-11	(NaGC, conc phos)
Colestipol (Cl)	0.24	-13	(NaC, tris)
	0.033	-8.5	(NaC, phos)
	0.023	-7.6	(NaGC, phos)

TMG: the iodide form of trimethylglycine; P; polymer support; NaC: sodium cholate; NaGC: sodium glycocholate; tris: tris buffer; phos: phosphate buffer; conc phos: concentrated phosphate buffer, which refers to the 0.050 M buffer; other ones are 0.005 M.

2.5.4 Comments on the Resins - A Summary

The binding of bile salt with polymeric resins having quaternary ammonium functional groups is, in a general sense, an ion-exchange process which involves the replacement of the mobile counterion of the resins, usually chloride and iodide, with the bile salt anions. This process is largely governed by the electrostatic forces, as expressed in Equation 2.1. Therefore, the binding affinity of an ion depends on the relative charges and the ionic radii of the ions involved in the exchange. Generally, the organic anions do not seem to be

favorable for the binding since these anions are mostly large in size and carry relatively less electric charge. However, the high molecular weight organic acids can precipitate, by forming insoluble complexes, with the stoichiometric quantities of a polymeric ionic species of the opposite charges (36). The precipitation is attributed to their relatively low solubility in water because of the hydrophobic nature of the organic anions. Therefore, it is not surprising that quaternary ammonium resins have a higher selectivity for bile salt anions than for the inorganic anions. But this does not exclude the possibility of a binding competition with inorganic species such as phosphate anions.

The ion exchange process depends on the relative selectivity of the various kinds of anions in the adsorption system. However, it is certain that the quaternized peptide resins are not merely anion exchangers. The unusual binding affinity of the resin containing a lysine-5 sequence indicates that the secondary or even tertiary structure of the peptide pendant also plays an important role in the exchange process. As the peptide pendant becomes longer, the binding affinity for bile salts is greatly improved. The conformational arrangement of the longer peptide chain may enhance the binding capacity. The addition of amino acids with apolar side chains in the peptide sequence can enhance the binding between the peptide pendant and the bile salt.

Although the hydrophobic binding is evident, there is no doubt that the binding of bile salts onto the polymeric resins is predominantly an ionic interaction. From the experimental results, it is evident that the quaternary ammonium group is important in the binding as shown in the comparison between cholestyramine and colestipol. The strongly basic ion-exchangers such as cholestyramine has improved capacity than those of less basicity, such as colestipol. Therefore, a high substitution on the polymer support is crucial for an increased number of binding sites on the resin.

The importance of the resin bead size in the adsorption indicates that the matrix of the polyamide resin cannot be penetrated by bile salt. On the other hand, the water-swellability does not promote hydrophobic interactions, but the probable improved biocompatibility of these resins makes them the preferable choice as orally administered adsorbents for bile salts. With the quaternized peptide-containing pendants, the binding affinity for bile salt anions has been improved. Moreover, unlike cholestyramine, the quaternized peptide resin has

shown specific binding for bile salt anions. This implies that a water-swellable backbone does not necessarily reduce the binding affinity for the bile salts since hydrophobic interaction is not the predominant force in the binding process.

Nevertheless, the binding affinity may well be improved if part of the adsorbent has hydrophobic moieties. This hydrophobic moiety may be added chemically onto the backbone of the polymer support or on the functional pendants. This hydrophobic moiety should be relatively large in size so that it can facilitate hydrophobic interactions.

Based on the adsorption experiments, the three major types of interactions have also been discussed in detail in this chapter. The experimental results are consistent with a combination of ionic and hydrophobic interactions. A thermodynamic interpretation of the interactions was also attempted for further insight of the binding process.

References

1. M.S. Brown & J.L. Goldstein, p. 840, in *The Pharmacological Bases of Therapeutics*, 7th ed., A.G. Gillman, L.S. Goodman, T.W. Rall & F. Hurad, eds., MacMillan Publishing Co., 1985
2. C. Jacobsen, *Eur. J. Biochem.*, 27, 513, 1972
3. C. Jacobsen, *Int. J. Pept. Prot. Res.*, 7, 159, 1975
4. D.S. Henning, G.R. Brown & L.E. St-Pierre, *Int. J. Artif. Organs, 9, 33, 1986*
5. M. Bouvier, G.R. Brown & L.E. St-Pierre, *Can. J. Chem.*, **65**, 1927, 1987
6. P.A. Mayes, **Chap. 18, Metabolism of Lipid: II. Role of the Tissues**, p. 244, in *Harper's Review of Biochemistry*, 19th ed., D.W. Martin, Jr., P.A. Mayes & V.W. Rodwell, eds., Lange Medical Publications, Los Altos, CA, 1983
7. F.C.M. Chen & N.L. Benoiton, *Can. J. Chem.*, **54**, 3310, 1976
8. H.W. Florey, R.D. Wright & M.A. Jennings, *Phys. Rev.*, **21**, 36, 1941
9. E.J. de Beer, C.G. Johnston & D.W. Wilson, *J. Biol. Chem.*, **108**, 113, 1935
10. J. Blanchard & J.G. Nairn, *J. Phys. Chem.*, **72**, 1204, 1968
11. C.H. Whiteside, H.B. Fluckiger & H.P. Sarett, *Proc. Soc. Exp. Biol. Med.*, **121**, 153, 1966
12. J.M. Street, D.J.H. Trafford & H.L.J. Makin, *J. Lipid Res.*, **24**, 491, 1983
13. G. Salen & E.H. Mosbach, **Chap. 6, The Metabolism of Sterols and Bile Acids in Cerebrotendinous Xanthomatosis**, p. 125, in *The Bile Acids, Vol. 3*, P.P. Nair & D. Kritchevsky, eds., Plenum Press, New York-London, 1976
14. P.A. Mayes, **Chap. 41, Digestion/Adsorption in the Gastrointestinal Tract**, p. 546, in *Harper's Review of Biochemistry*, 19th ed., D.M. Martin, Jr., P.A. Mayes & V.W. Rodwell, eds., Lange Medical Publications, Los Altos, CA, 1983

15. J.M. Stewart & J.D. Young, p. 49, in *Solid Phase Peptide Synthesis*, Pierce, 1984
16. R. Kunin, **Chap. 4, Anion Exchange Resin Characteristics**, p. 55, in *Ion Exchange Resins*, R.E. Krieger Pub. Co., N.Y., 1972
17. H.M. Burt, E.C. Cameron, H. Erber & J.D.E. Price, *J. Pharm. Sci.*, **76**, 379, 1987
18. W.H. Johns & T.R. Bates, *J. Pharm. Sci.*, **58**, 179, 1969
19. S. Lindenbaum & T. Higuchi, *J. Pharm. Sci.*, **64**, 1887, 1975
20. W.H. Johns & T.R. Bates, *J. Pharm. Sci.*, **59**, 788, 1970
21. He B.-L., **Polymeric Adsorbents**, p. 100, in *Hemoperfusion and Artificial Organs*, T.M.S. Chang & He B.-L., eds., China Academic Publishers, Tianjin, China, 1983
22. W.H. Johns & T.R. Bates, *J. Pharm. Sci.*, **59**, 329, 1970
23. S.-D. Clas, S.V. McBride, G.R. Brown & L.E. St-Pierre, unpublished results.
24. G.D. Calvert & R.A. Yeates, *Br. J. Nutr.*, **47**, 45, 1982
25. D.S. Henning, **Ph.D. Thesis**, McGill University, 1985
26. Tong M.-R., Chen C.-Z., Liu R.-X., Yu Y.-T. & He B.-L., p. 379, in *Hemoperfusion and Artificial Organs*, T.M.S. Chang & He B.-L., eds., Tianjin, China Academic Publishers, 1983
27. He B.-L., Sun J.-T., Li H., Li Y.-Z., Zhu X.-X. & Wang Y.-Q., *Chem. J. Chin. Univ.*, **5**, 732, 1985
28. R.H Haschemeyer & A.E.V. Haschemeyer, **Chap. 6, Three-Dimensional Structure of Proteins**, p. 109, in *Proteins, A Guide to Study by Physical and Chemical Methods*, Wiley Intersciences, N.Y., 1973
29. G.C. Pimentel & A.L. McClellan, pp. 242, 282-288, in *The Hydrogen Bond*, Freeman & Co., London, 1960
30. G.E. Schulz & R.H. Schirmer, p. 34 in *Principles of Protein Structure*, Springer-Verlag, New York-Heidelberg, 1979
31. C. Tanford, p. 25, in *The Hydrophobic Effect: Formation of Micelles and Biological Membranes*, John Wiley & Sons, NY-Chichester-Brisbane-Toronto, 1980
32. M.M. Breuer & I.D. Robb, *Chem. Indus.*, **1**, 530, 1972
33. J.A. Reynolds, S. Herbert & J. Steinhardt, *Biochemistry*, **7**, 1357, 1968
34. G. Scatchard, *Ann. N.Y. Acad. Sci.*, **51**, 660, 1949
35. M.L. Ralston & R.I. Jennich, *Technometrics*, **20**, 7, 1978
36. R. Kunin, **Chap. 2, The Theory and Mechanism of Ion Exchange**, p. 31, in *Ion Exchange Resins*, R.E. Krieger Pub. Co., N.Y., 1972

3 NMR Studies of Bile Acids and Bile Salts

3.1 Introduction

Modern nuclear magnetic resonance techniques provide a powerful tool for the study of bile acids and salts in solution. In this chapter, an introduction is first given to the NMR studies of bile acids in the literature and to NMR relaxation times. Following the introduction section are the results of the assignments of the NMR spectra of bile acids, made by the use of DEPT and two-dimensional correlation experiments, and of the studies of the interaction of bile acids with different binding species by the application of the NMR spin-lattice relaxation time determinations.

3.1.1 The NMR Studies of Bile Acids

The ^{1}H and ^{13}C NMR Spectral Assignments: The study of bile acids and bile salts by nuclear magnetic resonance spectroscopy dates back to the late 1960's. The proton spectra of bile acids were partially assigned by Small *et al.* (1). A full assignment for the proton and ^{13}C spectra of sodium cholate in aqueous solution was first given by Barnes and Geckle (2). Following this report, the same group published complete ^{1}H and ^{13}C NMR assignments for selected bile acids as determined by the application of two-dimensional NMR heteronuclear correlation methods (3). In the mean time, other researchers published the NMR spectra of bile acids and related steroids. The ^{13}C spectra of bile acids in organic solvents, mainly in dichloromethane, were studied by Leibfritz and Roberts (4). They found that the chemical shifts of the ^{13}C signals of rings A and B are affected by the configuration of the molecules while those of rings C and D are not. Iida *et al.* reported a ^{13}C NMR study of the hydroxylated bile acid stereoisomers (5). These studies have been summarized in a review by Barnes and Kirk, in 1985 (6).

In the proton spectra of bile acids, the methylene and methine proton signals of the steroid skeleton are mostly overlapped. However, the methyl proton signals are sharp and clear, and thus can easily be differentiated. Therefore, proton NMR spectroscopy can be used as a rapid and simple method in the analysis of bile acids (7). Small quantities of the common bile acids have been identified by proton NMR spectra after conversions to their methyl esters or trimethylsilyl ethers (8).

The Study of Micelle Formation of Bile Salts: Another useful feature of the NMR technique is in the study of the aggregation of bile salts and the formation of micelles in solutions. The aggregation of certain bile salts in aqueous solutions has been studied by use of a fluorescent probe combined with NMR spectroscopy (9). The NMR results suggested that the formation of micelles leads to a greater immobilization of the methyl groups on C18 and C19 as compared to the C21 methyl group.

The concentration dependence of the ^{13}C chemical shift of sodium deoxycholate upon formation of micelles was reported by Murata *et al.* (10). In that study it was found that, in addition to the concentration effect, micelle formation is related to the pH of the solution. At low pH's bile salts such as sodium deoxycholate do not form aggregates or gels. The ^{13}C chemical shifts of the skeleton carbons indicated that hydrogen bonding and hydrophobic interactions are responsible for the formation of micelles. Another study by Campredon *et al.* has shown that the changes in chemical shifts are more pronounced for some groups, such as the carbons bearing the hydroxyl groups and the methyl groups, when the solutions of bile salts approach the critical micellar concentration (11). It was postulated thereby that both the hydrophilic and the hydrophobic interactions within the micelles are enhanced at higher concentrations (11).

The study of the micellar aggregates of deoxycholate by proton and ^{13}C NMR, combined with the X-ray technique, has helped to confirm a helical model of the bile salt micelles (12). It has been shown that the micelles are formed mainly through ionic interactions and hydrogen bonding; although hydrophobic interactions can also occur among the helices, they are not crucial to the formation of the micelles.

The ionization behavior of bile acids in aqueous environments has been studied by ^{13}C NMR experiments (13). The apparent pK_a's for some of the bile acids have been estimated, by monitoring the chemical shift changes upon altering the pH of the solutions, to be in the range of 4.2 to 7.3.

Interaction Studies: From Chapter 1, it is evident that bile salts and their conjugates can form mixed micelles with lipidic compounds such as cholesterol and lecithin. In fact, the formation of mixed micelles represents a specific interaction between bile acids with other substances. The solubilization of benzene and alkylbenzenes in sodium cholate by forming mixed micelles has been studied by proton chemical shift changes of the NMR spectra (14).

NMR techniques have also been used for the study of the interaction of bile acids with proteins. For example, the interaction of bile salt with porcine colipase was studied by proton NMR spectroscopy (15). The hydrophobic domain of this protein interacts with the hydrophobic side of the bile salt, as shown by the line broadening effect. The specific shifts and broadening of the proton signals of the methyl groups at positions 18 and 21 on the taurocholate skeleton were observed, indicating their involvement in the interaction with the protein. The changes in pK_a's of bile acids complexed with bovine serum albumin have been determined by monitoring the chemical shifts with ^{13}C enriched samples below the critical micellar concentration (13). An NMR pulsed-gradient spin-echo technique was used to obtain the aggregate self-diffusion coefficients for the coalescence of bile salt with lecithin in aqueous solutions (16). This study confirmed the coexistence of simple bile salt micelles and mixed micelles with lecithin under physiologic conditions. The association of sodium and calcium ions to bile salts in dilute aqueous solutions was characterized by the induced chemical shift changes upon addition of paramagnetic lanthanide (17).

A series of studies of the bile salt-phosphatidylcholine mixed micelles have been carried out by Stark *et al.* using various NMR techniques (18-20). Phosphatidylcholine, a major component of lecithin, consists of a long acyl chain on one end and a quaternary amine group on the other (21). This compound was selectively deuterated at various acyl chain sites and the interaction with deoxycholate was determined by deuterium NMR techniques (18). The ^{2}H NMR relaxation time measurements provided direct evidence for the sluggish segmental motion and tight packing of the acyl chain of phosphatidylcholine in the mixed

micelles. Restricted motion of taurocholate, as monitored by the line width of the proton signals, was observed as the solubilization limit for phosphatidylcholine is approached (19). Recently, the same authors have reported the measurements of the nuclear Overhauser effect with the aid of proton spin-lattice relaxation experiments in the study of the simple and mixed micelles of bile acids and phosphatidylcholine (22).

3.1.2 NMR Relaxation Times

A brief introduction to the general concepts of NMR relaxation is given in this section, before proceeding to the discussion of the application of the spin-lattice relaxation time measurements in Section 3.4. For a detailed bibliography, reference may be made to Appendix 3 of this thesis.

If a system at equilibrium is perturbed temporarily, it will return to its original condition when the perturbance is removed. This relaxation process takes a certain time, which depends on various factors in the physical state of the system. In the case of nuclei with spin I = 1/2, there are two energy levels at equilibrium, corresponding to m = −1/2 and m = +1/2. The population distribution follows the Boltzmann Law. When the system is perturbed by an additional radio frequency pulse, the population will be redistributed between the two energy levels. After the pulse, the spin system will resume its previous equilibrium by transferring its energy to the lattice (spin-lattice relaxation) or to another spin system (spin-spin relaxation). The rates of the relaxations can be characterized by the *spin-lattice relaxation time* (T_1, *alias* longitudinal relaxation time) and *spin-spin relaxation time* (T_2, *alias* transverse relaxation time). In NMR spectroscopy, the spin-lattice relaxation time, T_1, is a measure of the rate at which the longitudinal component of nuclear magnetization returns to its equilibrium value after perturbation by a radio frequency pulse.

For a nucleus directly bonded to another nucleus with a magnetic spin, such as a carbon atom bearing protons, the dominant mechanism of relaxation is the dipole-dipole interaction. This is the most efficient and often the only significant relaxation mechanism. The spin-rotation mechanism can become effective for small highly symmetrical entities, such as methyl groups. Contrary to the dipolar mechanism, the spin-rotation relaxation leads to an increase in relaxation time. As the temperature rises, the dipolar mechanism becomes less important but the spin-rotation relaxation becomes increasingly significant.

Protons and ^{13}C nuclei next to quadrupolar nuclei (e.g., ^{14}N, ^{2}H, Cl and Br) or paramagnetic species (such as dissolved oxygen) can also undergo electric quadrupolar or paramagnetic relaxations. Chemical shift anisotropy and scalar coupling are generally less important to the relaxation mechanisms of the organic molecules.

For a molecule in Brownian motion, the average time that it remains in any given position before any changes are caused by its random molecular motion occur is called the *correlation time*, τ_c. This correlation time is typically 10^{-11} seconds in liquids of low viscosity, corresponding to a frequency of 10^5 MHz. For a polymer it is usually several orders of magnitude longer. In molecules where motion about one axis or internal rotation can occur, two or more correlation times are applicable. In more complex molecules or molecular species, such as water in biological cells, several translational and rotational correlation times may be pertinent (23).

The spin-lattice relaxation time, T_1, can be related to the correlation time, τ_c, by the following equation (24):

$$\frac{1}{T_1} = \frac{2}{3} C \tau_c \left[\frac{1}{1 + \omega^2 \tau_c^2} + \frac{4}{1 + 4\omega^2 \tau_c^2} \right] \qquad \text{(Equation 3.1)}$$

where ω is the resonance frequency and C is a constant. The correlation time τ_c can be expressed by

$$\tau_c = \tau_o \exp (E/RT) \qquad \text{(Equation 3.2)}$$

where E is the activation energy, R is the universal gas constant and T is the temperature.

The effect of the molecular correlation time τ_c on T_1 and T_2 for a molecule undergoing dipolar relaxation is shown in Figure 3.1 (25). As the correlation time increases, which is usually a consequence of increasing molecular weight, T_1 decreases and passes through a minimum around 5×10^{-10} to 10^{-8} seconds, depending on the frequency, and then increases when the molecular motion is very slow. Unlike T_1, T_2 generally decreases with increasing τ_c. Molecules of small molecular weight lie almost exclusively to the left of the minimum on the

T_1 curve, unless the viscosity of the solution is very high. Therefore, at relatively "high" temperatures, the condition $\omega\tau_c << 1$ is generally met. This condition is called the *extreme narrowing condition.* Under this condition, the relaxation times are frequency independent. Larger molecules with molecular weights of 10,000-25,000 lie in the vicinity of the minimum. Polymer molecules of still higher molecular weight are always on the right side.

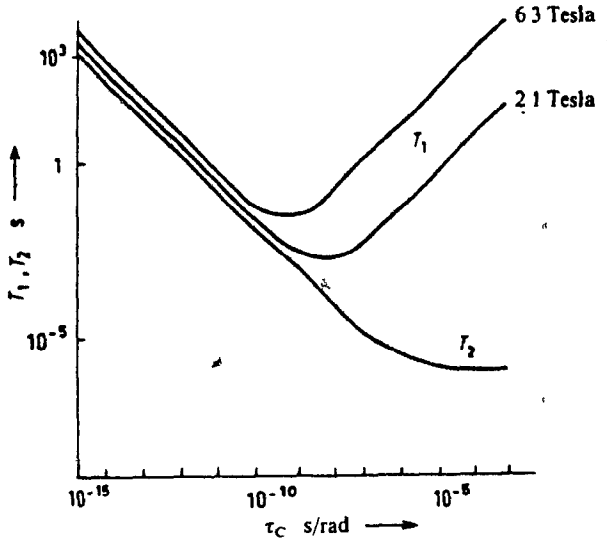

Figure 3.1 The relationship between the molecular correlation time τ_c and the dipolar relaxation times, T_1 and T_2 (reference 25). Frequency dependence of T_1 is also shown (The magnetic field strengths 2.1 and 6.3 Tesla correspond to the proton frequencies of about 90 and 270 MHz).

At the extreme narrowing condition, where $\omega\tau_c << 1$, Equation 3.1 can be simplified as

$$\frac{1}{T_1} = \frac{10}{3} C \tau_c \qquad \text{(Equation 3.3)}$$

Substitution of Equation 3.2 into 3.3, and rearrangement yields

$$\ln T_1 = -\frac{E}{R}\frac{1}{T} + \ln [3/(10C\tau_o)] \qquad \text{(Equation 3.4)}$$

Therefore, a linear relationship should be obtained when ln T_1 is plotted as a function of reciprocal T.

The spin-lattice relaxation time T_1 can be measured easily by either the inversion-recovery or the progressive saturation technique. A detailed description of the measurements is given in Appendix 3. The measurement of T_2 is more difficult since it can be influenced severely by inhomogenities in the magnetic field. Under the extreme narrowing condition, as can be seen in Figure 3.1, the T_2 values are very similar to those of T_1 (26).

The dipolar relaxation of a specific group derives from its interaction with the other nuclear magnetic dipoles of the same molecule or of neighboring molecules. Under the extreme narrowing condition, the intramolecular T_1 of ^{13}C can be related to the correlation time of the molecule (27), taking into account the number of directly bonded protons, n_H, by the following equation

$$1/T_1 = n_H \times 2.0325 \times 10^{10} \tau_c \qquad \text{(Equation 3.5)}$$

Other empirical equations are also available. The correlation time can be estimated from the measured T_1 by applying these equations.

3.1.3 The Application of the Spin-Lattice Relaxation Time Measurements

The NMR relaxation times provide important information about the molecular state of various compounds. They are very useful in the determination of the segmental motion, rotation and association of molecules in solutions. Based on the characteristic relaxation times of the various groups, the measured T_1 values can serve as an aid in assigning the NMR spectra. The intensity of an NMR signal also depends on the relaxation time of a specific group, besides the nuclear Overhauser enhancement, which is usually a consequence of dipolar interactions.

In solution the freedom of motion for molecules interacting with other molecular species will be decreased, resulting in a longer correlation time. Except for molecules with a very large molecular weight, this increase in correlation time generally leads to a decrease in the spin-lattice relaxation time (T_1) for molecules undergoing mainly dipolar relaxation. The specific groups involved in the interaction, in particular, will tumble less freely, thus having a higher relaxation rate and, of course, a shorter relaxation time. The change in

relaxation time of a specific group can be caused by increased dipolar interactions with the nucleus dipoles in the immediate vicinity.

Jardetzky *et al.* studied the binding of drugs such as sulfonamides and penicillin to bovine serum albumin in aqueous solutions by the determination of spin-lattice relaxation times (28,29). It was found that the T_1's for the protons on the functional groups involved in the binding decreased significantly. Therefore, it was concluded that the phenyl groups of the drugs are primarily involved in the interaction. Subsequently, T_1 measurements have been reported for the studies of the lipid-protein interactions (30), cellulose-water interactions (31), and calcium-parvalbumin bindings (32). Theoretical explanations, supported by experimental results, were attempted for the interactions between different molecular species (33). The binding of small ligands to macromolecules has also been explored experimentally and theoretically (34).

The NMR relaxation times of the various groups of the bile acids and salts generally reflect the freedom of segmental motion and conformational state of these molecules in solution. It thus provides a very useful probe in the study of the physical state of bile acids and salts in solution and their interactions with selected binding ligands.

3.2 Experimental Techniques

3.2.1 Instrument and Materials

The NMR experiments were performed on a Varian XL-300 NMR spectrometer, operating at 300 MHz for ^1H and 75.43 MHz for ^{13}C. The experiments were normally carried out at 25°C, unless otherwise mentioned. The temperature was controlled by the heater of the NMR probe installed with the spectrometer.

Deuterated solvents, dimethylsulfoxide (DMSO-d_6) and deuterium hydroxide (D_2O), were purchased from MSD Isotopes. As mentioned in Chapter 1, the bile salts are readily soluble in water while their acid forms can be dissolved in a variety of organic solvents, such as DMSO. Therefore, DMSO-d_6 was used for the study of bile acids and D_2O was used for bile salts in the NMR experiments. For the NMR studies with betaine, deuterated phosphate buffer solution (0.05 M, pH=7.6) was used since it is relatively easy to obtain well resolved ^{13}C signals for this compound even at high ionic strength.

The reference materials were also purchased from MSD Isotopes. In D_2O solutions, sodium trimethylsilylpropionate-2,2,3,3-d_4 (TSP) was used as the 0 ppm reference for the chemical shift. For the DMSO-d_6 solutions, the chemical shift (in ppm) was correlated to tetramethylsilane (TMS), except at high temperatures where TSP was used as a reference. The chemical shifts are accurate to about 0.005 ppm. To avoid complications, no internal reference was used for the interaction experiments.

Cholic acid, glycocholic acid, chenodeoxycholic acid and sodium glycocholate were purchased from Sigma, and deoxycholic acid, lithocholic acid and sodium cholate were purchased from Aldrich. The bile acids and salts were used without further purification. Most of the samples were prepared in 10 mm NMR tubes.

Benzyltrimethylammonium chloride was purchased from Aldrich. L-Lysyl-L-lysine (HBr salt) was purchased from Vega, poly-L-lysine (HBr salt, DP=17) and bovine serum albumin (BSA) from Sigma.

3.2.2 DEPT and Two-Dimensional Correlation Experiments

DEPT and two-dimensional correlation experiments were conducted to assign the ^1H and ^{13}C NMR spectra of bile acids in DMSO-d_6 and D_2O. A detailed description of these techniques can be found in Appendix 3. The DEPT (Distortionless Enhancement by Polarization Transfer) sequence is usually used to differentiate the carbon-13 signals bearing a different number of protons (35). This sequence is shown below:

^1H $\quad D_1\text{-}(\pi/2)_y\text{-}D_2\text{-}(\pi)_y\text{-}D_2\text{-}(\theta)_x\text{-}D_2\text{-DEC}$

^{13}C $\quad (\pi/2)\text{-}D_2\text{-}(\pi)\text{-}D_2\text{-ACQ}$

(The DEPT pulse sequence)

where D_1 is a preparation delay. An average C-H coupling constant $^1J_{CH}$ of 140 Hz was used. Based on this value, the D_2 delay was set as 3.57 ms ($1/(2^1J_{CH})$). The 90° pulse width and ^1H decoupler 90° width were calibrated prior to the experiments. The θ-pulse is dependent on the number of protons attached to the carbon. The spectra were recorded at θ-pulses of 45°, 90° and 135°. The first spectrum gives rise to all the signals of the protonated carbons, the second shows the CH carbons and the third gives positive signals for CH and CH_3 groups and

negative signals for CH_2 groups. Recalculation of the NMR spectral data gives four spectra showing the carbons bearing different numbers of protons.

Two-dimensional heteronuclear correlation (^{13}C-^{1}H) and 2-D homonuclear correlation (^{1}H-^{1}H) experiments were performed to confirm the assignments of the NMR spectra of bile acids. Proper delay time and pulse width were calibrated prior to the experiment and were carefully selected to optimize the NMR spectra.

3.2.3 Measurements of Spin-Lattice Relaxation Times

The inversion-recovery technique (Appendix 3) was used for the T_1 measurements. The NMR signals were inverted nonselectively by a pre-calibrated 180° pulse (typically 40 μsec for ^{13}C on the XL-300). Immediately after the pulse, the magnetization was allowed to recover its equilibrium condition over a preselected period of time (D_2). A 90° pulse was then applied to tilt the signals to the *xy* plane to be detected. The delay (D_1) is added to allow maximum recovery of the magnetization. The entire pulse sequence is shown below. Experimental parameters, e.g., the delay time array and irradiating pulse width, were calibrated prior to the experiment.

$$(D_1 - \pi - D_2 - \pi/2 - ACQ)_n \qquad \text{with } ACQ + D_1 > 5T_1$$

(The inversion-recovery pulse sequence)

The T_1 values were calculated using the computer software installed with the Varian instrument. The uncertainty in the T_1 values was usually within ±5% for the ^{13}C signals. At higher temperatures, some ^{13}C signals, such as the carboxyl group, had longer T_1's, therefore the uncertainties also tended to be larger, but still within ±10%.

The concentration of the bile acids and salts are expressed in molality (*m*) and varied from 0.1-0.5 *m* for T_1 studies. The ^{13}C spin-lattice relaxation times can be measured within a short period of time for samples at a concentration above 0.1 *m*. The DMSO solutions were degassed by bubbling nitrogen through the NMR tube to remove possibly dissolved paramagnetic oxygen in the solution. The D_2O solutions were usually prepared under nitrogen atmosphere to prevent oxygen from dissolving in the solution. However, the degassing was found to have little or no effect on the measured T_1 values. The NMR tubes were normally sealed during the experiments. For interaction studies, the binding substrate was

added into the solution to obtain a desired molar ratio, following the first measurement. After the resulting solution had been degassed, the second measurement was performed immediately to maintain experimental conditions identical to those for the first measurement. Selected measurements were repeated to ensure that the results were reproducible.

3.3 NMR Spectral Assignments for Bile Acids and Salts

The assignment of the ^{1}H and ^{13}C spectra of bile acids is still of remarkable importance in the NMR study since it serves as a key in the elucidation of the structure and conformation of bile acids in solution. Although certain assignments for the ^{13}C spectra of bile acids in aqueous solutions have been reported, as discussed in Section 3.1.1, some of the reported spectral data differ from each other and no systematic studies has been done for the solutions above the critical micellar concentration (CMC). Few NMR spectroscopic studies for bile acids in organic solvents have been reported. It is certainly of interest to compare the behavior of bile acids in organic solvents, where they do not form micelles, with that in aqueous solutions, where different micelles can be formed.

Deuterated water and DMSO were selected as solvents for this research as two distinct kinds of systems: aqueous and organic media. The dependence of the ^{13}C chemical shifts on temperature and concentration above CMC in water were studied. Complete assignments of bile acids in DMSO-d_6 and D_2O were established by the application of various available NMR techniques. The carbon atoms bearing 1, 2, 3 proton(s) and the quaternary carbons were differentiated by use of the DEPT sequence. Two-dimensional spectra were recorded as an aid in the assignment of the NMR spectra of bile acids.

3.3.1 The Assignments of the NMR Spectra of Bile Acids and Salts

The chemical structures of some of the primary and secondary bile acids are shown in Figure 3.2. The number and the position of hydroxyl groups represent the only major difference in their structures.

The ^{13}C Assignments Using DEPT:

The ^{13}C spectra of sodium cholate and sodium glycocholate in D_2O are shown in Figure 3.3. The carbonyl groups are most easily assigned since they

appear at the very low field. The three CHOH carbons are located at a low field of about 70-76 ppm, and therefore can also be easily recognized. The assignments at a molal concentration of about 0.25 *m* in D_2O were made in accordance with the DEPT and 2-D experiments and are shown in Table 3.1. These assignments were further verified by the characteristic spin-lattice relaxation times of the respective peaks. The assignments for the cholic acid salt are in good agreement with the previously reported results (3,11). These spectra were recorded at concentrations above the critical micellar concentration (CMC) of bile salts. Even under such conditions, a dependence of the chemical shifts on concentration as well as on temperature was observed (Sections 3.3.2 and 3.3.3), e.g., the peaks for the quaternary carbon 10 and the 23 methylene carbon exchange positions at higher temperatures. This is true for both cholic and glycocholic acid anions in aqueous solutions.

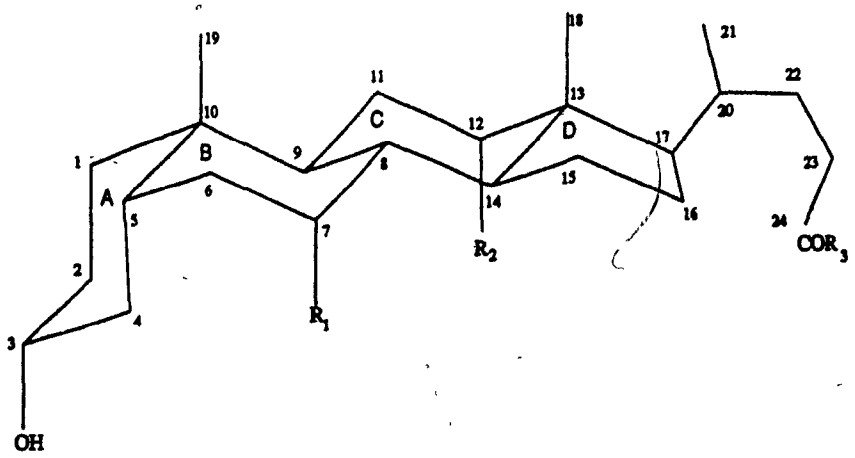

	R_1	R_2	R_3
Cholic Acid:	OH	OH	OH
Chenodeoxycholic Acid:	OH	H	OH
Deoxycholic Acid:	H	OH	OH
Lithocholic Acid:	H	H	OH
Glycocholic Acid:	OH	OH	$NHCH_2COOH$
Methyl Cholate:	OH	OH	OCH_3

Figure 3.2 The chemical structure of bile acids and cholic acid methyl ester.

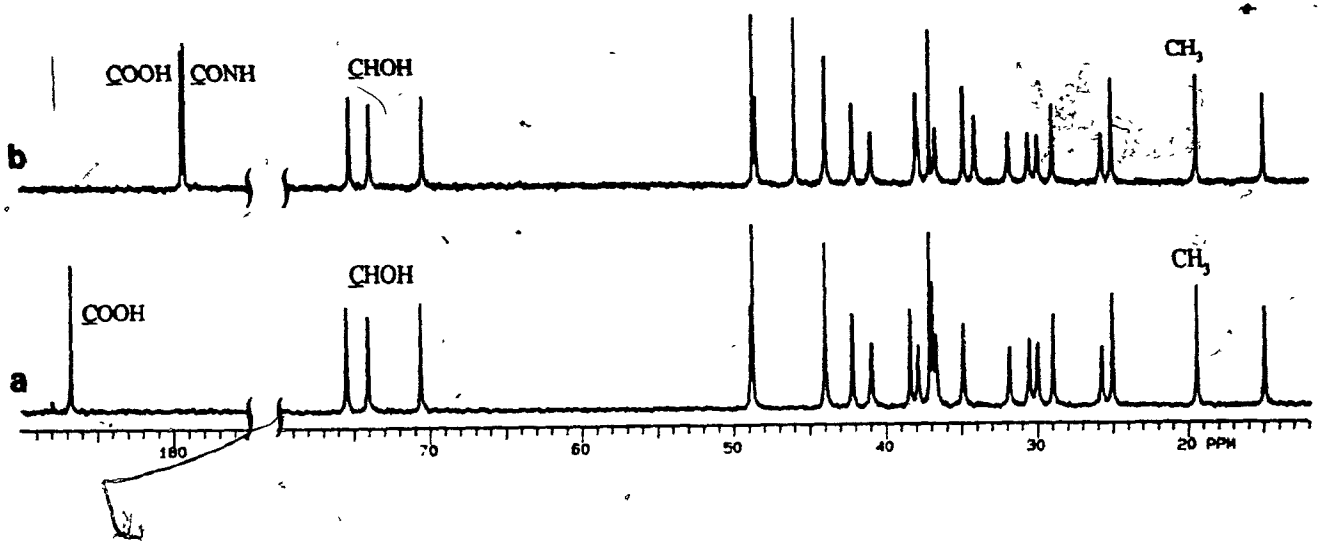

Figure 3.3 The ^{13}C NMR spectra of sodium cholate and glycocholate in D_2O: (a) sodium cholate (molal concentration: 0.27 *m*); (b) sodium glycocholate (0.25 *m*).

Table 3.1 ^{13}C NMR Spectral Assignments for Bile Salts in D_2O

Carbon	Chemical Shift (ppm)			
	Sodium Cholate		Sodium Glycocholate	
	25°C	100°C	25°C	100°C
24-C	186.75	185.87	179.20	178.55
Glycyl COOH			179.39	178.83
12-CHOH	75.48	75.52	75.37	75.44
3-CHOH	74.06	74.03	74.03	74.03
7-CHOH	70.59	70.69	70.54	70.67
17-CH	48.90	49.36	48.57	48.90
13-C	48.77	48.86	48.76	49.16
Glycyl CH_2			45.97	46.26
14-CH	44.01	44.13	43.97	44.14
5-CH	44.01	44.04	43.97	44.03
8-CH	42.23	42.27	42.22	42.27
4-CH_2	40.97	41.37	40.98	41.41
20-CH	38.42	38.15	37.99	37.76
22-CH_2	37.90	37.78	37.87	37.76
10-C	37.13	37.10	37.10	37.09
23-CH_2	36.95	37.23	34.84	35.38
6-CH_2	36.76	36.83	36.72	36.84
2-CH_2	34.91	35.01	34.11	34.05
1-CH_2	31.86	32.14	31.89	32.17
11-CH_2	30.55	30.59	30.56	30.62
16-CH_2	30.02	29.78	29.94	29.70
9-CH	28.98	29.19	28.95	29.20
15-CH_2	25.78	25.57	25.72	25.53
19-CH_3	25.04	24.81	25.01	24.77
21-CH_3	19.46	19.55	19.38	19.48
18-CH_3	14.97	14.84	14.93	14.81

Sample molal concentration: about 0.25 *m*; Reference: TSP. Assignments were made with the aid of DEPT and T_1 experiments.

Glycocholic acid is formed by the addition of a glycine residue on the side chain of cholic acid. The addition of glycine causes an upfield shift for the carbonyl group at position 24. Moreover, it also creates a shielding effect on the methylene group at position 23, causing an upfield shift of about 2 ppm (Table 3.1). However, the chemical shift of the 22-methylene group, being at the β-

position of the carbonyl group, is less affected than that of the 20-methine group (γ-position), which has an upfield shift of about 0.4 ppm.

The ^{13}C DEPT spectra of cholic acid in the form of the sodium salt in D_2O are shown in Figure 3.4. The three methyl carbon signals are located at the upper field of the spectrum. The CH carbons signals are spread over a range of about 10 ppm from 38-49 ppm, except the CH group of position 9, which appears around 29 ppm. The remainder of the ^{13}C signals belong mainly to the methylene (CH_2) groups, appearing in the region of 25-41 ppm. The quaternary carbons are suppressed in the DEPT spectra since they cannot be enhanced by proton polarization transfer.

The ^{13}C spectra of bile acids in DMSO-d_6 also show very sharp and clear signals. Although these spectra were recorded using solutions of similar molal concentrations as those in D_2O, it is unlikely that the bile acids form micelles in DMSO-d_6. Using the DEPT sequence, the huge DMSO-d_6 peaks around 39-40 ppm can be suppressed so that the peaks of bile acids hidden under the solvent peak are clearly identifiable. This is shown in the DEPT spectra of cholic acid in Figure 3.5. Figure 3.6 shows the ^{13}C spectra of some of the primary and secondary bile acids in DMSO-d_6. In this figure, the solvent peak region is selectively replaced with the spectra obtained with DEPT.

The majority of the peaks in the spectra can be assigned, especially the carbons bearing hydroxyl groups by comparing the spectra for cholic, deoxycholic, chenodeoxycholic and lithocholic acids. Table 3.2 shows the assignments of the ^{13}C spectra of selected bile acids in DMSO-d_6. The assignments are supported by the DEPT experiments and the characteristic T_1 values of the ^{13}C signals. The substitution of the carboxyl group of cholic acid affects the chemical shift of the 24-C, causing upfield shifts. This is accompanied by chemical shift changes of the side chain carbons.

In Table 3.2 it can be seen that the addition of the hydroxyl groups to the steroid rings usually affects the chemical shifts of nearby ^{13}C nuclei. The addition of an electron-withdrawing group often has a deshielding effect on the carbons at α- and β-positions, thus causing a downfield shift. However, carbons at the γ-positions of the substituent are usually affected by a shielding effect, sometimes even more significant than the deshielding effect on the β-carbons. This is known in NMR spectroscopy as the *γ-effect*. As indicated in Table 3.2, the addition of an

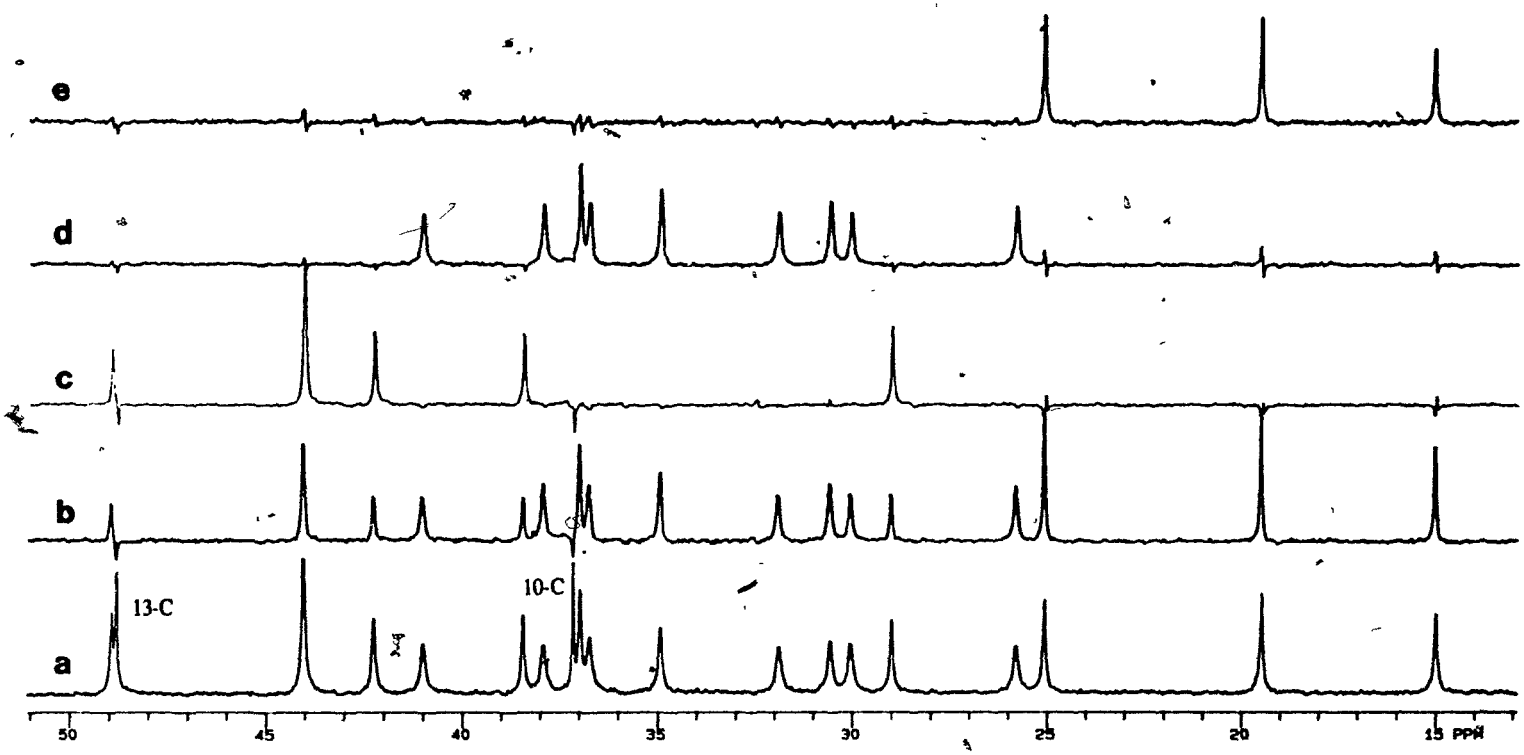

Figure 3.4 The DEPT spectra of sodium cholate in D_2O (molal concentration: 0.27 *m*): (a) the normal ^{13}C NMR spectrum; (b) the carbons with attached protons; (c) the CH's; (d) the CH_2's; (e) the CH_3's.

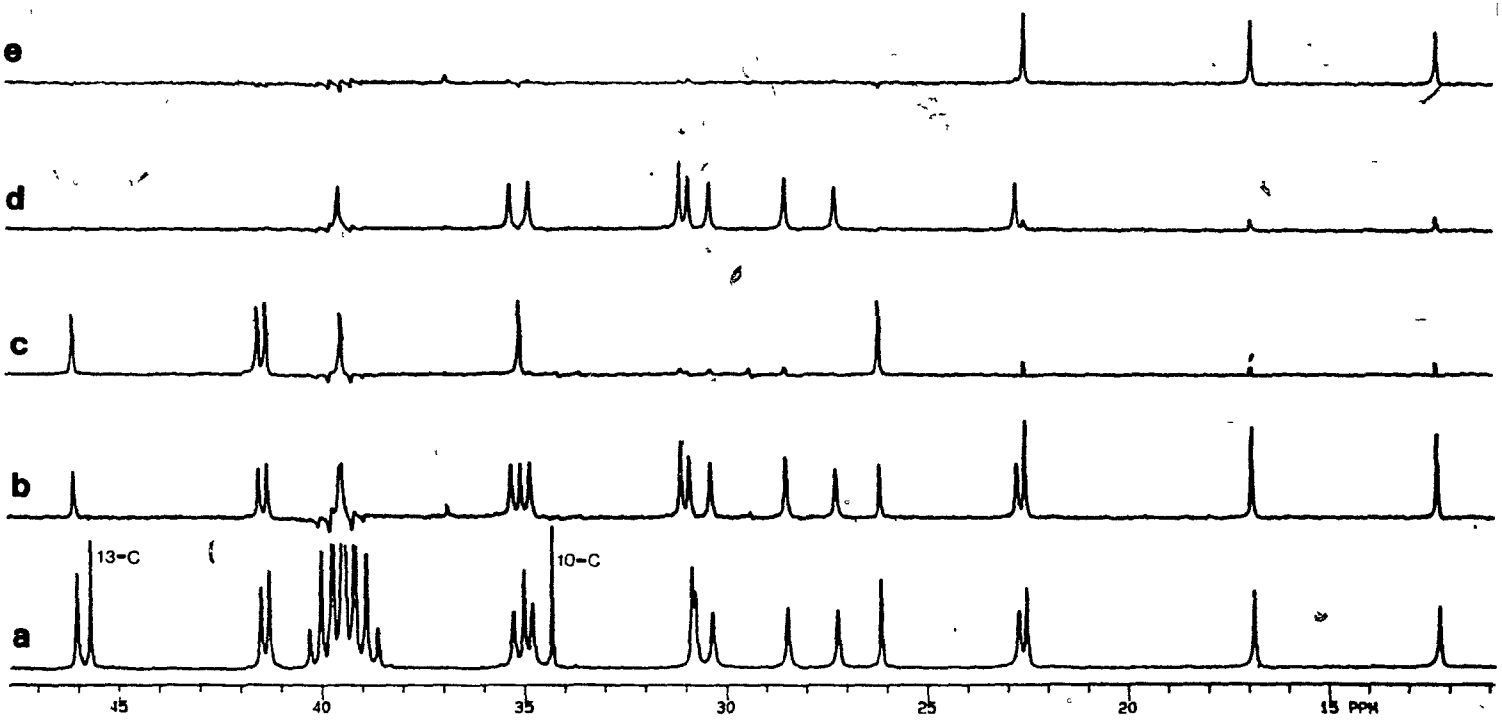

Figure 3.5 The DEPT spectra of cholic acid in DMSO-d_6 (molal concentration 0.23 *m*): (a) the normal ^{13}C NMR spectrum; (b) the carbons with attached protons, the two ^{13}C signals hidden under the DMSO-d_6 peaks are clearly shown; (c) the CH's; (d) the CH_2's; (e) the CH_3's.

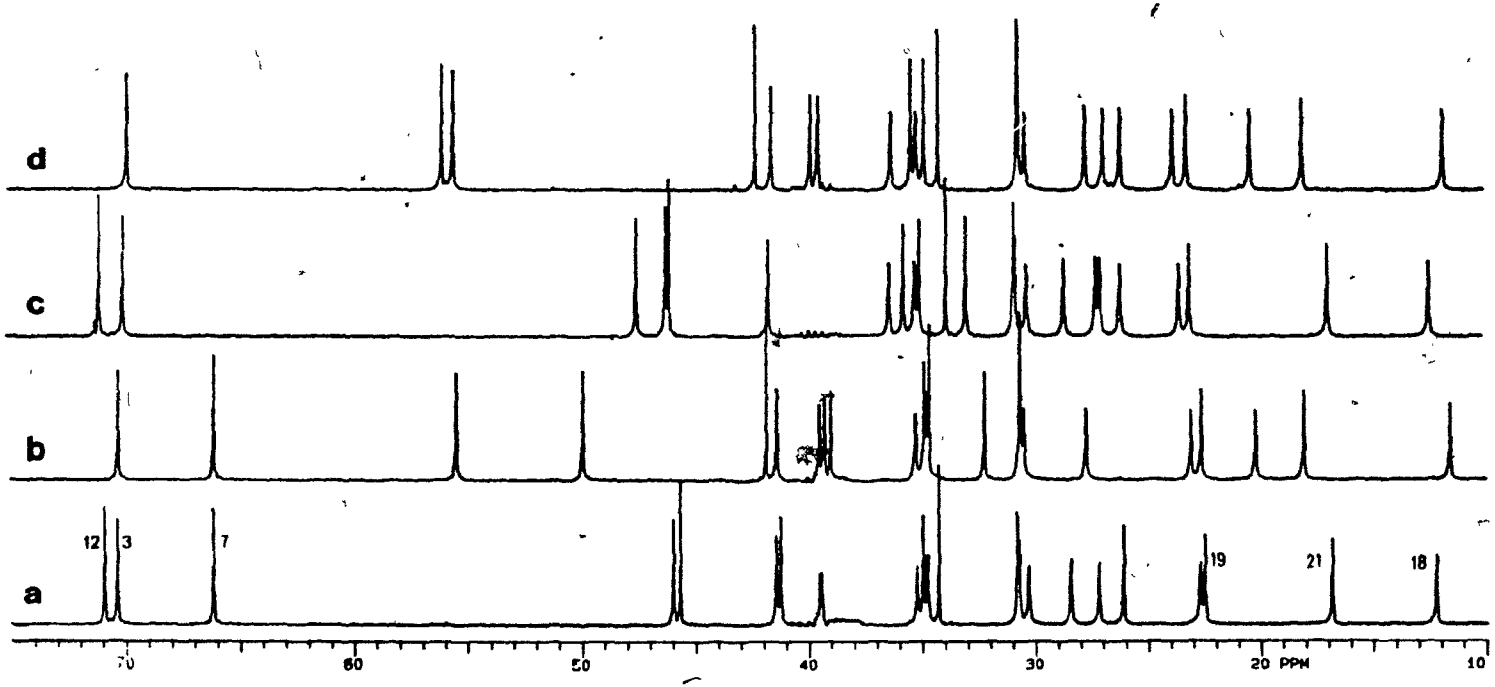

Figure 3.6 The ^{13}C NMR spectra of selected bile acids in DMSO-d_6 (molal concentration: about 0.25 *m*): (a) cholic acid; (b) chenodeoxycholic acid; (c) deoxycholic acid; (d) lithocholic acid.

Table 3.2 ^{13}C NMR Spectral Assignments for Bile Acids and Methyl Cholate in DMSO-d_6

Carbon	Chemical Shift (ppm)					
	CA	CDCA	DCA	LCA	GCA	CAME
24-C	174.90	174.27	174.83	174.73	171.35	173.72
Glycyl COOH					173.01	
12-C	70.96	39.55	70.96	39.69	70.98	70.94
3-CHOH	70.40	70.29	69.91	69.83	70.39	70.39
7-C	66.21	66.11	26.05	26.13	66.19	66.19
OCH_3						51.09
17-CH	46.03	55.47	46.09	55.52	46.07	45.96
13-C	45.70	41.85	45.94	42.23	45.67	45.70
14-CH	41.49	49.92	47.39	56.02	41.46	41.48
5-CH	41.30	41.38	41.58	41.53	41.29	41.30
Glycyl CH_2					40.47	
4-CH_2	39.52	39.35	36.23	36.25	39.45	39.50
8-CH	39.47	39.08	35.61	35.37	39.45	39.44
1-CH_2	35.28	35.27	35.10	35.14	35.24	35.26
20-CH	35.01	34.88	34.91	34.79	35.05	34.97
6-CH_2	34.82	34.75	26.94	26.88	34.80	34.81
10-C	34.32	34.65	33.74	34.16	34.30	34.31
23-CH_2	30.85	30.66	30.75	30.66	32.11	30.41
22-CH_2	30.77	30.66	30.69	30.66	31.49	30.67
2-CH_2	30.35	30.48	30.18	30.33	30.32	30.34
11-CH_2	28.47	20.20	28.54	20.39	28.47	28.46
16-CH_2	27.23	27.73	27.13	27.68	27.21	27.20
9-CH	26.15	32.22	32.87	39.96	26.14	26.15
15-CH_2	22.74	23.08	23.44	23.80	22.73	22.73
19-CH_3	22.54	22.62	23.00	23.21	22.53	22.53
21-CH_3	16.88	18.07	16.84	18.06	17.02	16.83
18-CH_3	12.25	11.56	12.35	11.79	12.26	12.23

CA: cholic acid; CDCA: chenodeoxycholic acid; DCA: deoxycholic acid; LCA: lithocholic acid; GCA: glycocholic acid; CAME: cholic acid methyl ester (methyl cholate). Molal concentration: about 0.25 *m*; CAME: 0.15 *m*.

axial hydroxyl group causes a downfield shift of about 30 ppm for the α-carbons. The β-methylene carbons are affected by a downfield shift of about 8 ppm, the methine and quaternary carbons about 3.5-4 ppm. The γ-carbons, mostly methine groups, are affected by an upfield shift of about 6-8 ppm. However, the carbon at position 5, being the γ-position of the hydroxyl groups at positions 3 and 7, does not appear to show such an effect. The reason for its indifference is probably related to the stereostructure of bile acids. In the 5β-configuration (Figure 3.2), the C5 is sterically located at a position close to the hydrophobic side and further away from the hydroxyl groups. Therefore, it is not affected by the alteration of the chemical structure on the other side (hydrophilic side) of the molecule. This is also true for the carbons at positions 1, 10 and 19, as evidenced by the limited change in chemical shifts for these carbons upon structural alternations. These carbons are located on ring A of the 5β-steroid skeleton.

Two-Dimensional Correlation:

The assignment of the proton spectra for bile acids are difficult because of the severe overlapping in the methylene and methine regions. High resolution NMR has been used in the recording of the proton NMR spectra of bile acid in aqueous solutions and assignments have been made with the aid of two-dimensional correlation with the ^{13}C spectrum (3,11).

Two-dimensional spectra of cholic acid and glycocholic acid were recorded to confirm the assignment of the ^{13}C spectra of bile acids in DMSO-d_6. The heteronuclear correlation (^{13}C-^{1}H) spectrum of cholic acid in DMSO-d_6 is shown in Figure 3.7. The correlation between the methyl carbons and protons at positions 18, 19 and 21 can be clearly seen in the contour plot. Other signals of high intensity are mostly methine groups. The correlation of the methine groups bearing the hydroxyl group at positions 3, 7 and 12 is clearly identified.

The homonuclear correlation (^{1}H-^{1}H) spectrum of cholic acid in DMSO-d_6 is shown in Figure 3.8. Because of the severe overlapping of the methylene and methine protons, the differentiation of the proton signals of this region is difficult. However, the coupling between the methine and hydroxyl protons is clearly shown in this contour plot. The assigned protons of significance are shown in Figures 3.7 and 3.8. Since the study is concerned, in the main, with ^{13}C NMR, detailed proton assignments will not be discussed.

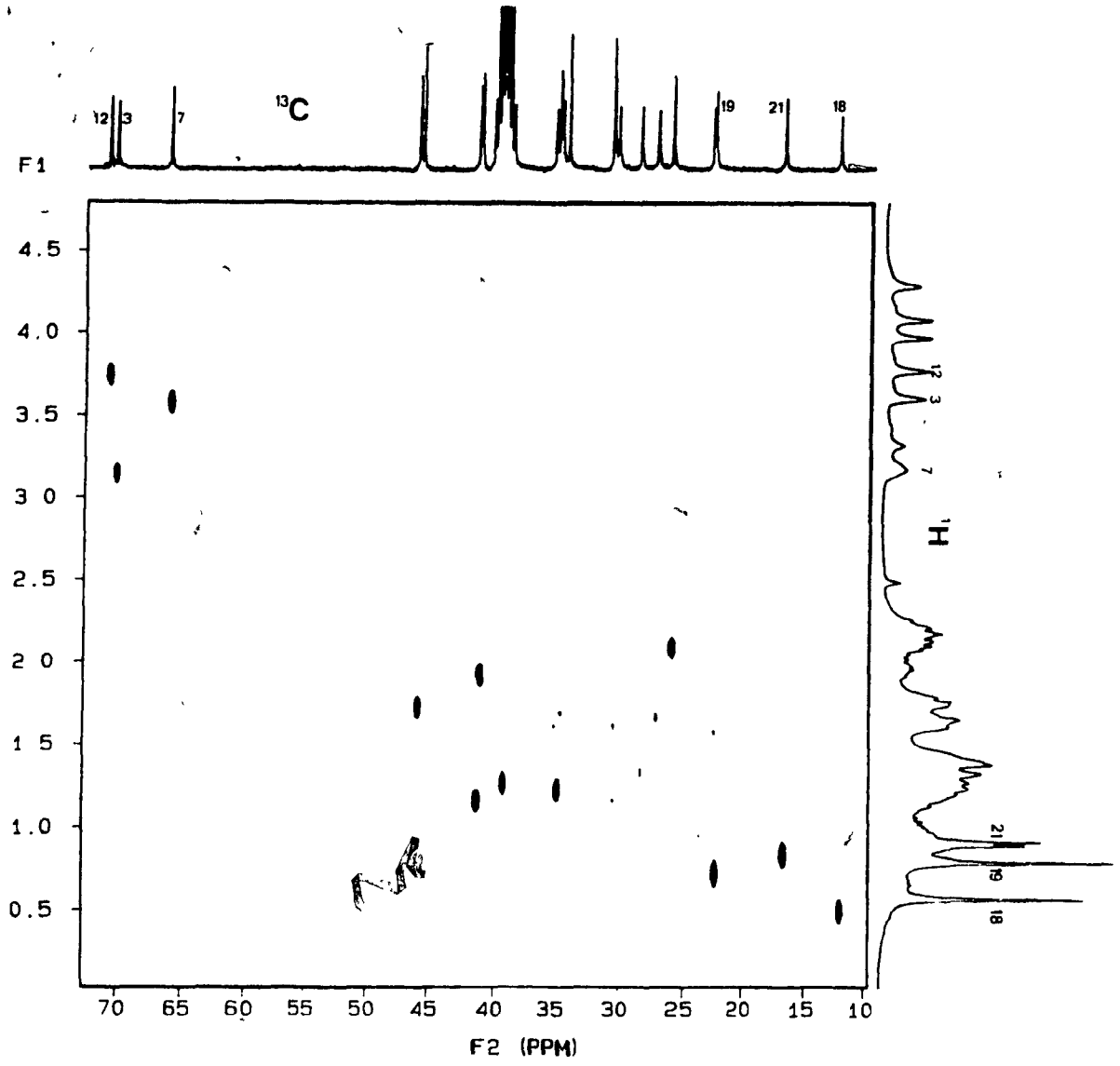

Figure 3.7 The ^{13}C-^{1}H heteronuclear correlation spectrum of cholic acid in DMSO-d_6 (molal concentration: 0.14 *m*).

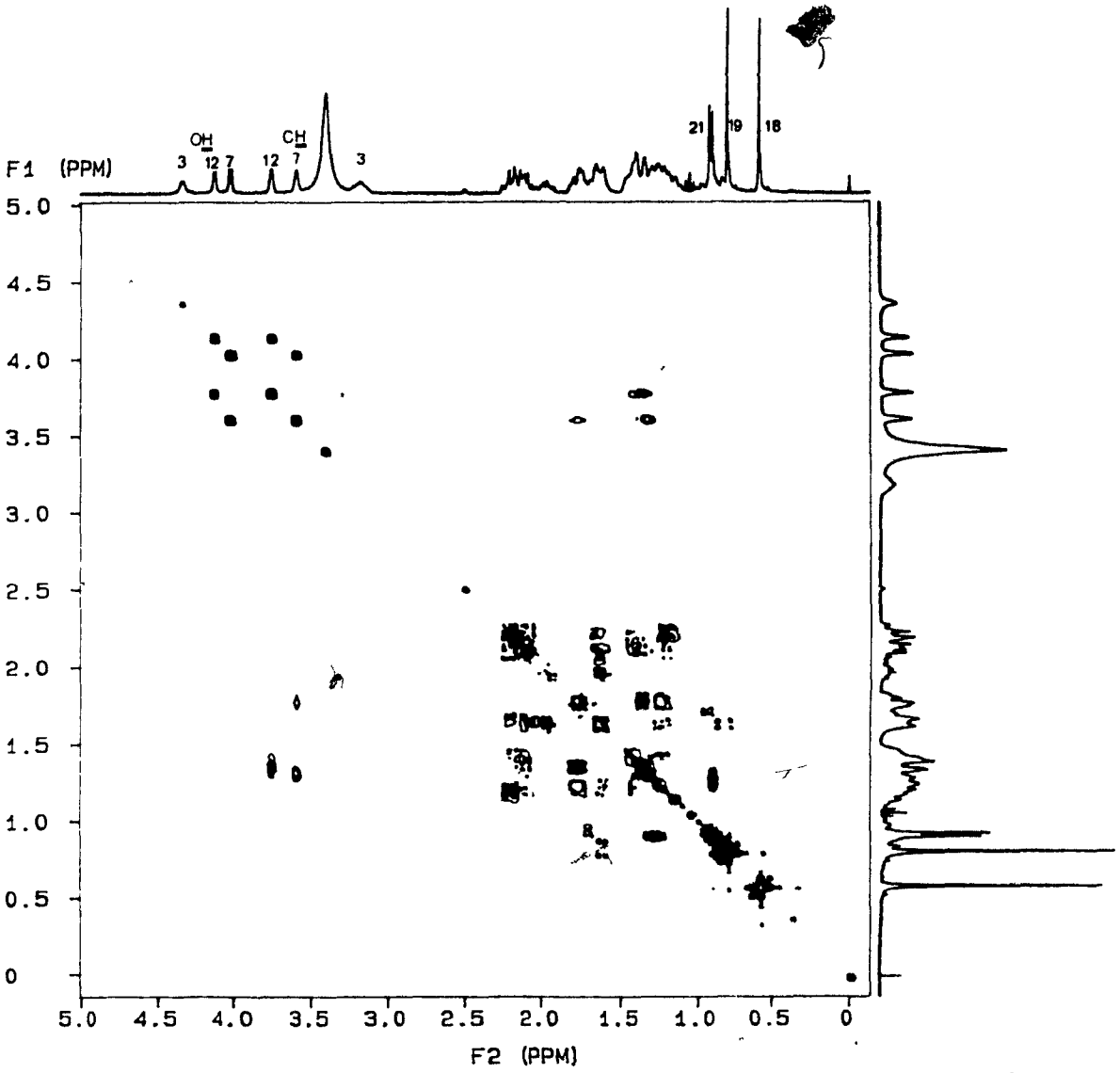

Figure 3.8 The ^1H-^1H homonuclear correlation spectrum of cholic acid in DMSO-d_6 (molal concentration: 0.09 *m*).

3.3.2 The Effect of Temperature on the Chemical Shifts

As discussed in Section 1.2.2, bile salts form micelles in aqueous solution when the concentration is above CMC (0.6-10 mM) at room temperature. Phase separation may occur at temperatures lowever than CMT. In this study, the concentration of the bile salt samples was always higher than 0.05 *m*, which is well above the CMC of the bile salts. A variable temperature study was conducted for sodium cholate and glycocholate in D_2O. The temperature of the

experiments was in the range of 25-100°C, which is also above the CMT of the bile salts.

As temperature increases, there is a general change in the chemical shifts for the ^{13}C signals of bile acids, as shown in Table 3.1. The carboxyl group undergoes an upfield shift (ca. 1 ppm from 25°C to 100°C), indicating the dissociation of hydrogen bonds with the solvent molecules. As a general rule, when the temperature increases, the carbons on the side chain and on ring D of the cholic acid skeleton are affected most in terms of the chemical shift. The 23 methylene group, appearing at about 37-38 ppm, undergoes a downfield shift as the temperature increases and passes the C10 peak from right to left, as shown in Figure 3.9, while the chemical shift for the carbon at position 10 remains unchanged. Therefore, the relative peak positions of C23 and C10 interchange at

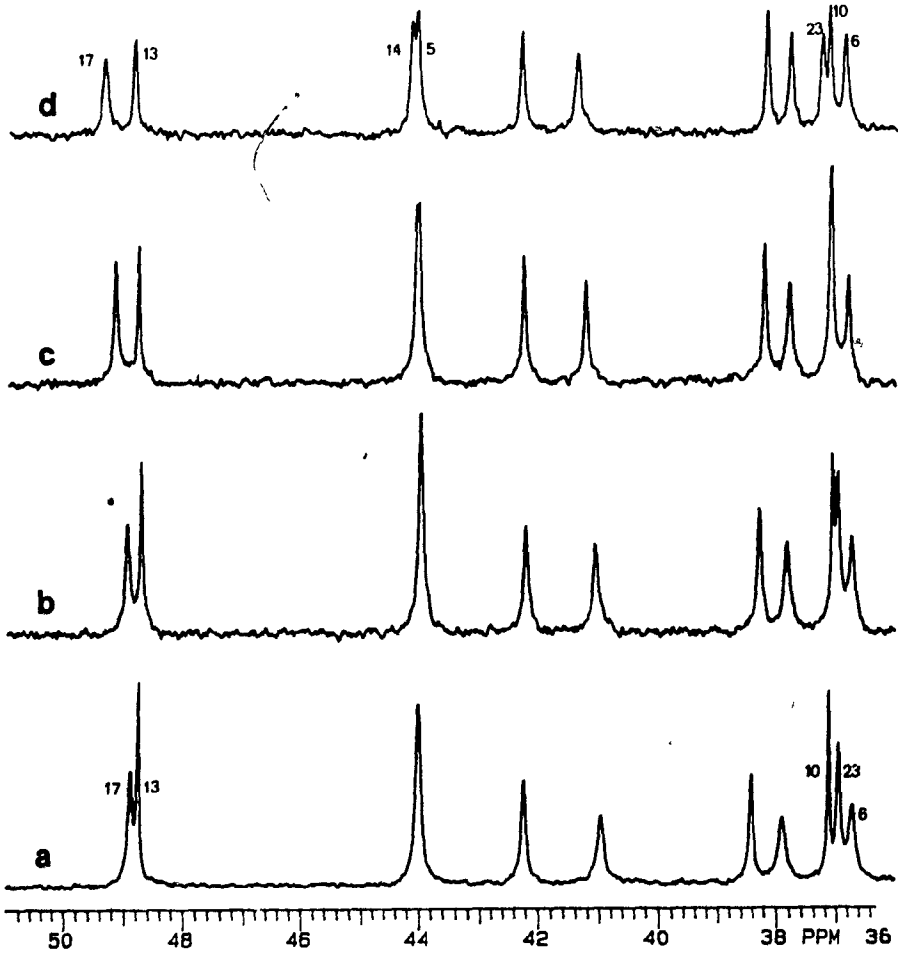

Figure 3.9 The ^{13}C NMR spectra of sodium cholate in D_2O showing the temperature effect (0.27 *m*): (a) 25°C; (b) 50°C; (c) 75°C; (d) 100°C.

elevated temperatures. The carbons at positions 14 and 17 also have similar downfield shifts, which leads to the separation of the two signals between 48-50 ppm and the splitting of the large peak around 44 ppm. These changes are probably related to the dissociation or rearrangement of the bile salt micelles in aqueous solutions at higher temperatures. Similar temperature effects are also observed for glycocholate in D_2O.

It was of interest to observe the change in the ^{13}C spectra of sodium cholate with other interacting species. The addition of benzyltrimethylammonium chloride (BTMA) to the aqueous solution caused the changes of the chemical shifts with temperature to occur at much lower temperatures (between 40-70°C), as shown in Figure 3.10. This is an indication that the addition of a quaternary

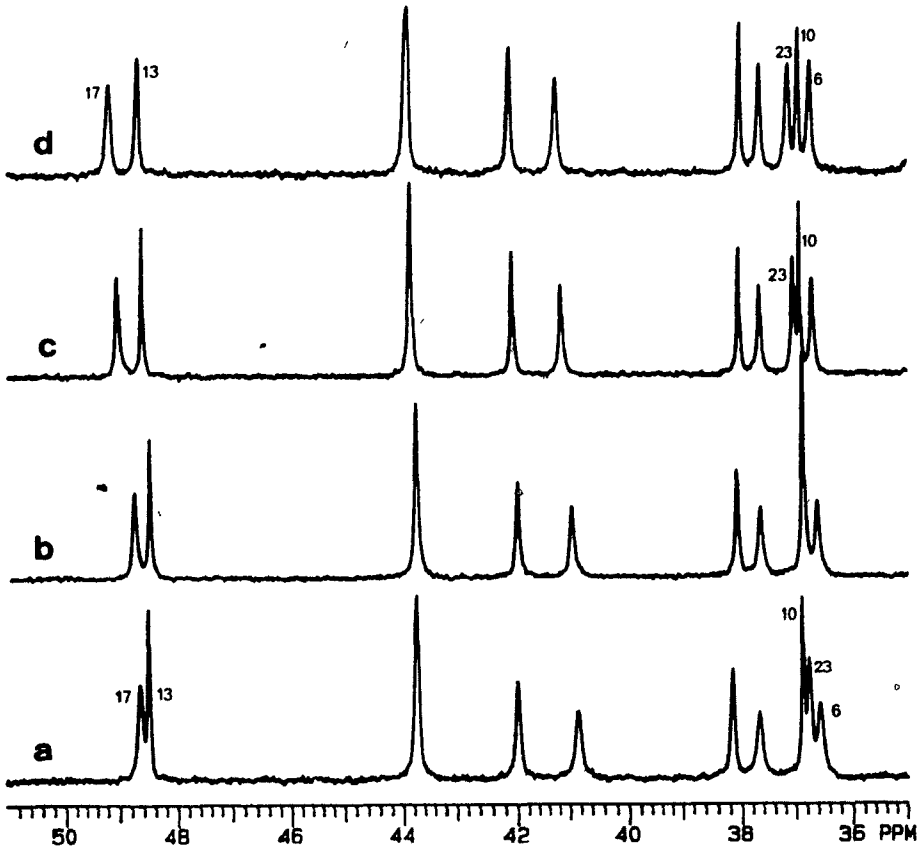

Figure 3.10 The ^{13}C NMR spectra of sodium cholate with benzyltrimethylammonium chloride in D_2O showing the temperature effect (0.27 *m*, molar ratio 1:1): (a) 25°C; (b) 50°C; (c) 75°C; (d) 100°C.

ammonium salt accelerates the dissociation or re-arrangement of the bile salt micelles, possibly by forming more complicated mixed micelles with the interacting substrate. The benzyl group of BTMA is hydrophobic and can possibly enter the "head" of the micelles with the quaternary ammonium group forming ionic linkage with the nearby carboxyl groups of bile salt on the "tail" part of the micelles.

Interestingly, the effect of increased temperature is equivalent to that of a decreased concentration of bile salt in aqueous solutions. This is further discussed in the following section.

3.3.3 The Effect of Concentration on the Chemical Shifts

It is known that, in the vicinity of the CMC of bile salts, the chemical shifts of the methyls and the carbons bearing the hydroxyl group depend significantly on the concentration (11). In this study, the concentration range of bile salts was chosen to be above the CMC. Therefore, a dependence of the chemical shifts on concentration changes was not expected. However, as shown in Figure 3.11, some of ^{13}C signals of bile salt are still affected significantly by a variation in the concentration above the CMC. The concentration effect is once again most significant for the carbons on the side chain and on ring D of cholic acid. The most obvious changes of chemical shifts involve C23, C17 and C14.

If Figure 3.11 is compared with Figure 3.9, the dilution effect of the sample of sodium cholate is seen to be almost identical to that of an increase in temperature. It is known that the aggregation number for the micelle of bile salts may change as the concentration of the solution varies (36). This provides further evidence for the variation of the size of the bile salt micelles at different concentrations. Therefore, the structures of the micelles are similar for dilute solutions or more concentrated solution at higher temperatures.

In conclusion, the bile salt micelles may undergo re-organizations upon variations of the concentration and temperature of the solution. The addition of BTMA can promote such re-organizations, indicating a possible formation of mixed micelles. It is important to be reminded that the structure of the micelles formed by bile salt anions is different from that of the simple micelles since bile salts also have hydroxyl groups in addition to the carboxyl group. This property of bile salts is important in the study of their interactions with various other binding species. It can be expected that the molecules that interact with bile salts

can involve in the formation of mixed micelles, where both hydrophilic and hydrophobic interactions may occur.

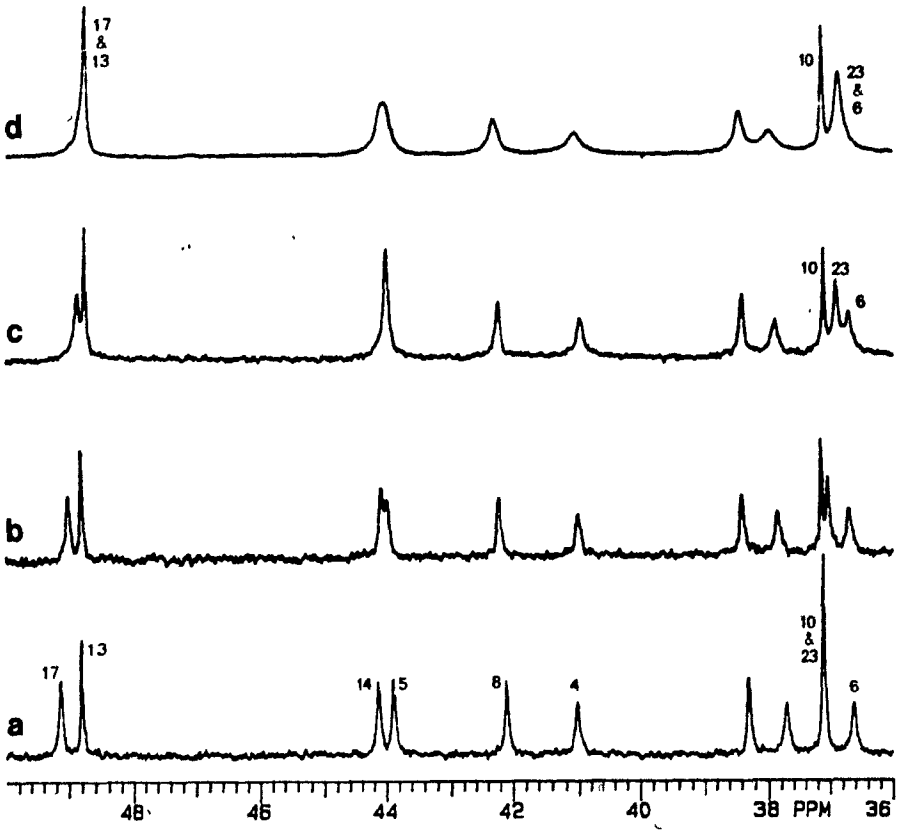

Figure 3.11 The ^{13}C NMR spectra of sodium cholate in D_2O showing the concentration effect: (a) 0.06 *m*; (b) 0.12 *m*; (c) 0.35 *m*; (d) 1.25 m.

3.4 The Determination of Spin-Lattice Relaxation Times and Interaction Studies

3.4.1 The Spin-Lattice Relaxation Times of Bile Acids and Salts

The spin-lattice relaxation times of the various groups of the interacting species were determined using the inversion-recovery technique. Cholic acid and glycocholic acids, the two major primary bile acids in the human body, were used for the T_1 studies. As a comparison, the T_1 values were measured in both aqueous and DMSO solutions. The spin-lattice relaxation times of the ^{13}C NMR signals of cholic acid and glycocholic acid in DMSO-d_6 and their sodium salts in D_2O are listed in Table 3.3.

Table 3.3 The ^{13}C T_1 Values (in Sec) of Cholic Acid and Glycocholic Acid in D_2O and DMSO-d_6

Carbon	In D_2O NaC	NaGC	In DMSO-d_6 CA	GCA
24-C	4.0	11	2.7	3.3
Glycyl COOH		2.9		2.3
12-CHOH	0.19	0.17	0.21	0.20
3-CHOH	0.19	0.16	0.23	0.20
7-CHOH	0.19	0.18	0.20	0.21
17-CH	0.20	0.27	0.23	0.22
13-C	1.75	1.6	1.9	1.9
Glycyl CH_2		0.43		0.24
14-CH	0.18	0.19	0.18	0.20
5-CH	0.17	0.16	0.26	0.21
8-CH	0.20	0.18		
4-CH_2	0.084	0.10		
20-CH	0.20	0.18	0.26	0.20
22-CH_2	0.087	0.10	0.17*	0.13
10-C	1.54	1.48	1.7	1.6
23-CH_2	0.20	0.16	0.22	0.15
6-CH_2	0.11	0.08	0.12	0.11
2-CH_2	0.12	0.12	0.088	0.098
1-CH_2	0.10	0.08	0.11	0.11
11-CH_2	0.091	0.10	0.10	0.11
16-CH_2	0.088	0.11	0.10	0.10
9-CH	0.19	0.17	0.27	0.22
15-CH_2	0.097		0.14	0.13
19-CH_3	0.60	0.62	0.55	0.56
21-CH_3	0.56	0.36	0.47	0.51
18-CH_3	0.63	0.62	0.79	0.71

NaC: sodium cholate; NaGC: sodium glycocholate; CA: cholic acid; GCA: glycocholic acid.
Samples (molal concentration): NaC/D_2O: 0.12 *m*; NaGC/D_2O: 0.14 *m*; CA/DMSO-d_6: 0.14 *m*; GCA/DMSO-d_6: 0.12 *m*. Temperature: 25°C.
* This peak is overlapped with the 23-CH_2 signal. The value is estimated from the variable temperature studies.

Owing to the spin-rotation relaxation mechanism, the methyl carbons have longer T_1 values. For the remaining carbons, the T_1's increase as the number of attached protons decreases, following the order: methylene < methine < quaternary carbons. This fact is clearly due to the dipolar relaxation with the nearby protons, which leads to decreases in T_1's. The carbons on the backbone of the steroid skeleton generally have shorter T_1's because of their limited flexibilities in motion and rotation; however, the carbons on the side chain tend to have longer T_1's, indicating increased freedom of motion. Glycocholic acid, while having a longer side chain, exhibits shorter T_1's for the corresponding carbons. The long T_1's of the carbonyl of the amide group and the glycyl methylene of glycocholate are possibly attributable to the quadrupolar relaxation mechanism involving the neighboring ^{14}N nucleus. The C=O and methyl carbons show decreases in their T_1 values going from D_2O to DMSO-d_6.

The Dependence of T_1 on Temperature:

The spin-lattice relaxation times of bile acids in DMSO-d_6 and bile salts in D_2O were measured at different temperatures from 25-100°C. The carbons on the bile acids skeleton show general increases in T_1's with increasing temperature.

As indicated in Equation 3.4, if the logarithm of T_1 is plotted against the reciprocal temperature, 1/T, a straight line should be obtained. Figure 3.12 shows the plot of ln T_1 as a function of 1/T for the carboxyl and methyl groups of sodium cholate in D_2O solutions. The methyl carbons manifest a better linear relationship than the carboxyl carbon. The deviation from the linearity of the plot is probably a result of other minor relaxations than the dipolar mechanism. It appears that the dipolar relaxation represents the major relaxation mechanism of the NMR relaxation process. Figure 3.13 shows the same linear plot for the carboxyl and methyl groups of cholic acid in DMSO.

The Dependence of T_1 on Concentration:

The spin-lattice relaxation times were measured for aqueous solutions of bile acids at different concentrations. The T_1 values for sodium cholate in D_2O in a molal concentration range of 0.1-0.5 *m* are shown in Table 3.4. It was found that the values of T_1 depend, to some extent, on the solution concentration in the concentration range of this study. There is a general trend for the T_1's to decrease as the concentration becomes higher, although this dependence is small compared

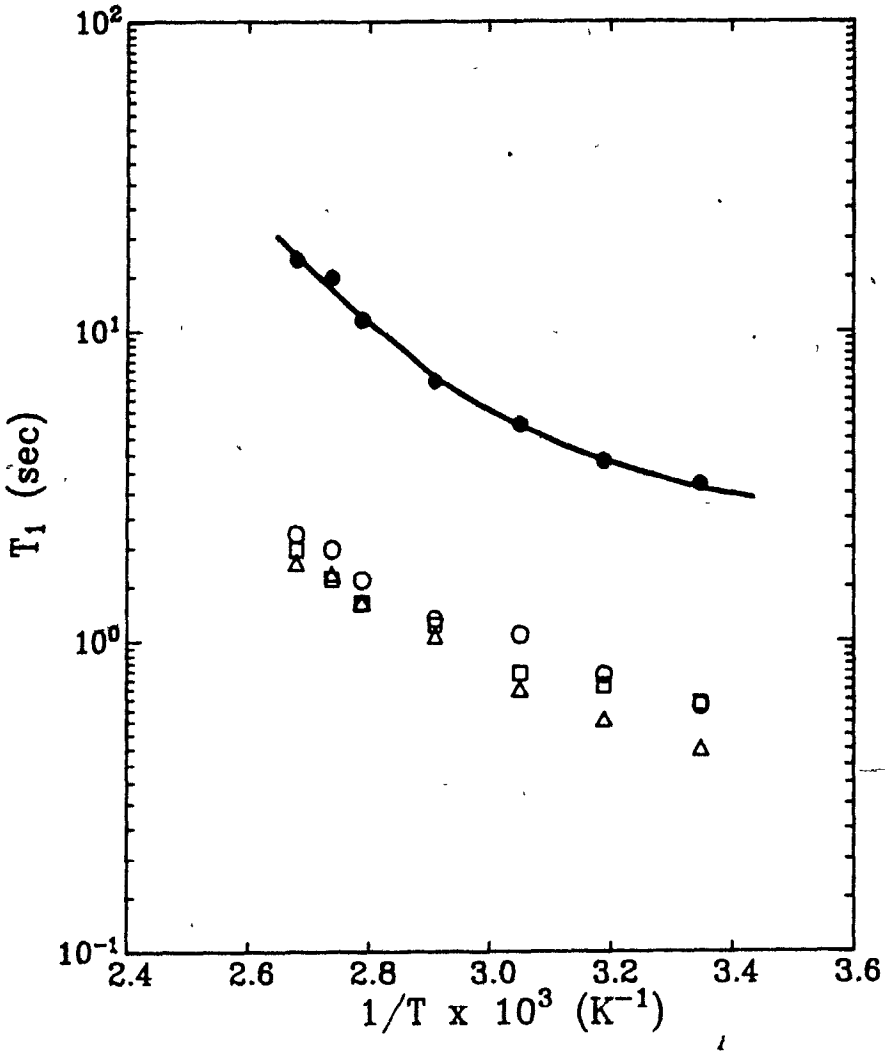

Figure 3.12 The temperature dependence of T_1 of the various groups of sodium cholate in D_2O (molal concentration 0.35 *m*): the plot of logarithm of T_1 as a function of reciprocal temperature: ● carboxyl; ○ 18- methyl; ❑ 19-methyl; Δ 21-methyl.

with the temperature effect. Since the concentration range of the solutions is above the critical micellar concentration, the alteration of the concentration results in a transfer from smaller micelles to larger ones while the basic structure of the micelles remains largely unchanged. The small dependence of T_1's on concentration can be a consequence of a combination of these factors and the experimental errors directly derived from the measurements. At even higher concentrations (e.g., molal concentration 1.6 *m*), the T_1 for the carboxyl carbon remain unchanged within experimental error (3.9 sec), while those for methyl

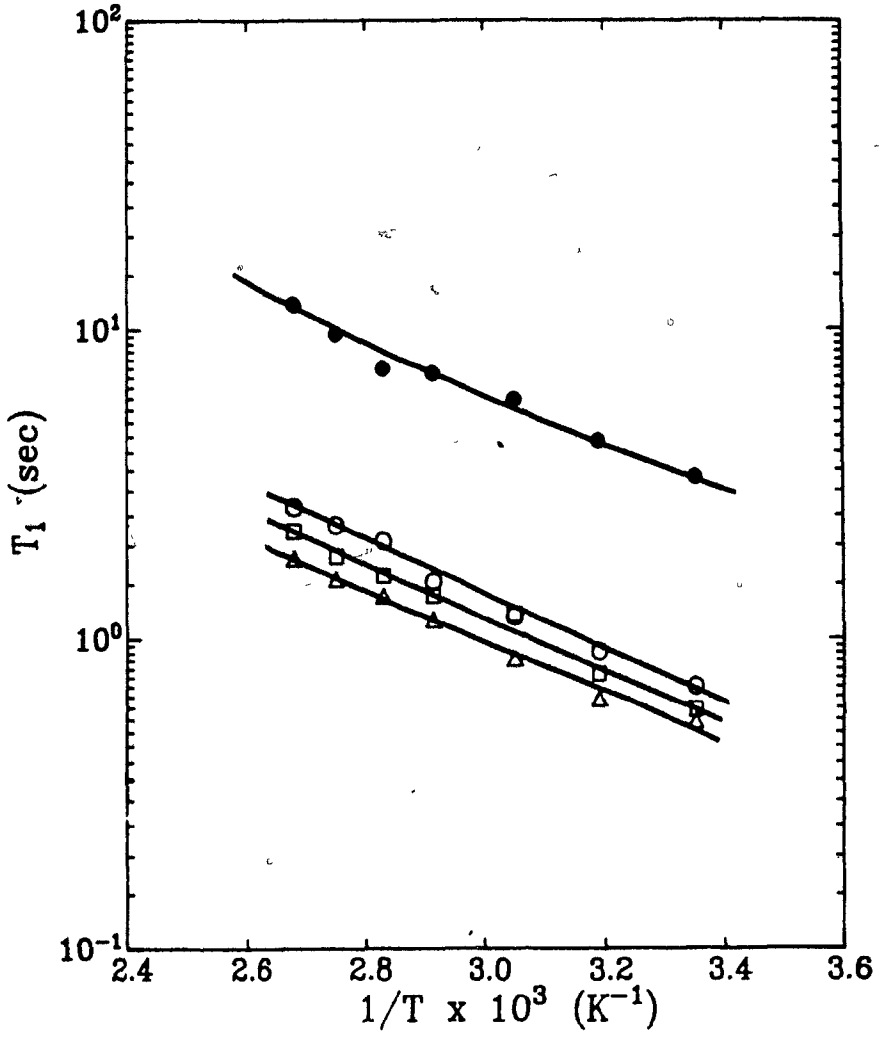

Figure 3.13 The temperature dependence of T_1 of the various groups of cholic acid in DMSO-d_6 (molal concentration 0.33 *m*): the plot of logarithm of T_1 as a function of reciprocal temperature: ● carboxyl; ○ 18- methyl; □ 19-methyl; Δ 21-methyl.

carbons become even higher. It is known that the simple bile salt micelles are formed by a back-to-back structure. At very high concentrations, the micelles of higher aggregation numbers can be formed by changing the back-to-back structure, thus allowing a higher degree of freedom of motion for the hydrophobic moiety of the bile salt molecules. Cholic acid in DMSO solution was also studied and similar results were obtained (Table 3.5).

Table 3.4 The ^{13}C T_1 Values (in Sec) of Sodium Cholate in D_2O at Different Molal Concentrations

Carbon	0.12 *m*	0.27 *m*	0.35 *m*	0.50 *m*
24-COOH	4.1	3.8	3.2	3.8
12-CHOH	0.19	0.20	0.18	0.20
3-CHOH	0.19	0.18	0.18	0.18
7-CHOH	0.20	0.19	0.20	0.19
17-CH	0.20	0.20	0.21	0.19
13-C	1.75	1.74	1.65	1.56
14 & 5-CH	0.18 0.17	0.19	0.18	0.19
8-CH	0.20	0.19	0.19	0.20
4-CH_2	0.084	0.098	0.088	0.10
20-CH	0.20	0.20	0.19	0.20
22-CH_2	0.087	0.10	0.089	0.10
10-C	1.54	1.52	1.46	1.47
23-CH_2	0.20	0.20	0.20	0.18
6-CH_2	0.11	0.10	0.12	0.11
2-CH_2	0.12	0.12	0.12	0.12
1-CH_2	0.10	0.086	0.095	0.089
11-CH_2	0.091	0.096	0.092	0.096
16-CH_2	0.088	0.11	0.098	0.10
9-CH	0.19	0.19	0.19	0.20
15-CH_2	0.11	0.10	0.097	0.10
19-CH_3	0.60	0.63	0.63	0.67
21-CH_3	0.56	0.45	0.45	0.44
18-CH_3	0.63	0.66	0.62	0.66

Temperature: 25°C.

Table 3.5 The ^{13}C T_1 Values (in Sec) of Cholic Acid in DMSO-d_6 at Different Molal Concentrations

Carbon	0.14 *m*	0.24 *m*	0.32 *m*	0.47 *m*
COOH	2.7	3.25	3.32	2.97
12-CHOH	0.21	0.21	0.20	0.19
3-CHOH	0.23	0.21	0.19	0.18
7-CHOH	0.20	0.22	0.21	0.19
17-CH	0.23	0.22	0.22	0.20
13-C	1.9	2.0	1.89	1.77
14-CH	0.18	0.20	0.19	0.17
5-CH	0.26	0.22	0.21	0.19
1-CH_2	0.11	0.12	0.11	0.11
20-CH	0.26	0.23	0.22	0.20
6-CH_2	0.12	0.13	0.12	0.11
10-C	1.7	1.7	1.68	1.54
23-CH_2*	0.22	0.18	0.17	0.15
2-CH_2	0.088	0.11	0.10	0.099
11-CH_2	0.10	0.12	0.11	0.10
16-CH_2	0.10	0.12	0.11	0.11
9-CH	0.27	0.24	0.21	0.19
15-CH_2	0.14	0.13	0.13	0.12
19-CH_3	0.55	0.59	0.59	0.59
21-CH_3	0.47	0.51	0.54	0.50
18-CH_3	0.79	0.79	0.70	0.70

* The 22-CH_2 peaks are not listed since they are mostly overlapped with 23-CH_2. Temperature: 25°C.

3.4.2 Interaction with Benzyltrimethylammonium Chloride

Benzyltrimethylammonium chloride (BTMA) is an organic compound containing a quaternary ammonium group. The molecular structures of BTMA and cholestyramine are similar and this compound has good solubilities in both aqueous and DMSO solutions. Therefore, both the ionic moiety, i.e., the quaternary ammonium group, and hydrophobic moiety, i.e., the benzyl group, can be probed by solution NMR studies. The T_1 values of the interacting species were measured to detect any specific interactions between the bile acids and BTMA.

T_1 Studies in Aqueous Solutions:

The values of T_1 were measured in D_2O. The addition of equivalent BTMA to the sodium cholate solution did not result in significant changes in T_1's for the carbons of cholic acid anions, as shown in Table 3.6. Although the ^{13}C T_1 values of bile salts in aqueous solutions tend to decrease upon mixing with other compounds, these changes are generally very small, usually within the experimental error, even upon mixing with compounds which are known to interact with bile salts.

Table 3.6 The Changes in ^{13}C T_1 Values (in Sec) of Sodium Cholate in D_2O upon Interaction with BTMA

Carbon	NaC	NaC+BTMA	Difference (%)
COOH	3.2	3.0	6.3
12-CHOH	0.18	0.19	
3-CHOH	0.18	0.18	
7-CHOH	0.20	0.19	
19-CH_3	0.63	0.65	
21-CH_3	0.45	0.45	
18-CH_3	0.62	0.60	

NaC: cholic acid; BTMA: benzyltrimethylammonium chloride.
Molal concentration of NaC in D_2O: 0.35 *m*; NaC/BTMA molar ratio = 1:1.

On the other hand, the compounds which interact with bile salts show changes in their T_1's, e.g., the ^{13}C signals of the BTMA after mixing with sodium cholate showed significant T_1 changes (Table 3.7). The large decrease of T_1 values for the carbons of the phenyl group provide direct evidence of the involvement of the hydrophobic moiety of the molecule. The methyl carbons of the quaternary ammonium group also manifest large decreases in T_1, indicating a likely involvement of these groups in the interaction. It has been known that bile salt micelles can solubilize aromatics such as alkylbenzenes by forming co-micellar aggregates (14). Therefore, a similar interaction may occur by forming mixed micelles with bile salts: the benzene ring, which is the hydrophobic moiety of BTMA, may become a part of the core of the micelles, while the quaternary

ammonium groups point toward the environment, easily forming an ionic linkage with the nearby carboxyl groups of cholic acid.

Table 3.7 The Changes in ^{13}C T_1 Values (in Sec) of BTMA in D_2O on Interaction with Sodium Cholate

Carbon	BTMA	BTMA+NaC	Difference (%)
ortho-C	5.19	1.74	66
para-C	3.18	1.16	64
meta-C	5.06	1.69	67
1-C	26	7.7	70
CH_2	2.79	0.96	66
CH_3	1.80	0.85	53

BTMA: benzyltrimethylammonium chloride; NaC: sodium cholate.
Molal concentration of BTMA in D_2O: 0.36 *m*; BTMA/NaC molar ratio = 1:1.

T_1 Studies in DMSO-d_6:

DMSO is an organic solvent with a high dielectric constant. Bile acids do not form micelles in this solvent. Therefore, it is of interest to carry out similar studies in DMSO-d_6. Unlike in aqueous solutions, on mixing BTMA with cholic acid in DMSO-d_6, the carbons of cholic acid showed significant changes in T_1's, especially the carboxyl and methyl groups. These results are listed in Table 3.8.

The most remarkable change of the T_1 values is related to the carboxyl group of cholic acid. This is an indication of its restricted freedom of motion upon interacting with BTMA. The carbons bearing hydroxyl groups can be solvated by DMSO molecules by forming intermolecular hydrogen bonds before the addition of BTMA. The small change in T_1 after mixing with BTMA, indicates a relatively small change to the physical state of these groups, namely, these groups remain solvated by DMSO. The methyl groups, however, exhibit more significant changes in their T_1 values after being mixed with BTMA. This hydrophobic interaction is also confirmed by T_1 changes of the benzyl carbons of BTMA.

The changes in T_1's of bile acids are more evident in DMSO solutions than in aqueous solutions. This difference in behavior of the bile acids in an

organic solvent is thought to be due to the fact that micelles are not formed in DMSO. Therefore, the small change in T_1's of bile salts in aqueous solutions is likely related to their micellar properties.

Table 3.8 The Changes in ^{13}C T_1 Values (in Sec) of Cholic Acid in DMSO-d_6 upon Interaction with BTMA

Carbon	CA	CA+BTMA	Difference (%)
COOH	2.9	1.7	41
12-CHOH	0.21	0.18	14
3-CHOH	0.23	0.21	9
7-CHOH	0.20	0.18	10
19-CH_3	0.55	0.34	38
21-CH_3	0.47	0.33	30
18-CH_3	0.79	0.51	35

CA: cholic acid; BTMA: benzyltrimethylammonium chloride.
Molal concentration of CA in DMSO-d_6: 0.14 *m*; CA/BTMA molar ratio = 1:1.

The cholic acid methyl ester was also studied and the results compared with that of cholic acid-BTMA interactions. The ^{13}C signals did not show significant changes in T_1, except for the ester group (OCH_3) (Table 3.9). The relatively larger decrease in T_1 for the carbons on the side chain of the methyl ester (such as the 21-methyl and OCH_3 groups) indicate a possible increased dipolar interaction which leads to shorter T_1's. However, since there is no ionic bond formed in this solution, the hydrophobic interaction is also markedly reduced.

The T_1 values of ^{13}C signals of BTMA were also measured when cholic acid was added to the solution. The various groups of BTMA generally showed decreases in their T_1 values (Table 3.10). The methyls on the quaternary ammonium functional group showed a large decrease. On the other hand, the freedom of motion for the carbons at the *para*, *meta* and *ortho* positions on the benzene ring are also restricted upon the interaction. These changes confirm both the electrostatic and hydrophobic interactions proposed in the previous discussions.

Table 3.9 The Changes in ^{13}C T_1 Values (in Sec) of Methyl Cholate in DMSO-d_6 upon Interaction with BTMA

Carbon	CAME	CAME+BTMA	Difference (%)
24-C	6.26	6.00	4.2
12-CHOH	0.26	0.24	7.7
3-CHOH	0.24	0.23	4.2
7-CHOH	0.26	0.23	12
OCH_3	2.10	1.72	18
19-CH_3	0.69	0.63	8.7
21-CH_3	0.67	0.57	15
18-CH_3	0.87	0.87	

CAME: cholic acid methyl ester; BTMA: benzyltrimethylammonium chloride.
Molal concentration of CAME in DMSO-d_6: 0.14 *m*; CAME/BTMA molar ratio = 1:1.

Table 3.10 The Changes in ^{13}C T_1 Values (in Sec) of BTMA in DMSO-d_6 upon Interaction with Cholic Acid and Its Methyl Ester

Carbon	BTMA	BTMA+CA	Diff (%)	BTMA+CAME	Diff (%)
ortho-C	1.15	0.93	19	1.02	11
para-C	0.91	0.73	20	0.77	15
meta-C	1.15	0.79	31	1.01	12
1-C	6.28	5.50	12	5.84	7.0
CH_2	0.57	0.50	12	0.54	5.0
CH_3	0.43	0.32	25	0.39	9.3

CA: cholic acid; CAME: cholic acid methyl ester; BTMA: benzyltrimethylammonium chloride; Diff: difference in T_1.
Molal concentration of BTMA in DMSO-d_6: 0.17 *m*; BTMA/CA molar ratio = 1:1; BTMA/CAME molar ratio = 1:1.

When cholic acid methyl ester, instead of cholic acid was added to the solution, the changes in T_1 values listed in Table 3.10 were evident. It can be seen that the carbons on the benzyl group are still involved in the interaction, but to a lesser extent, while the methyl carbons of the quaternary ammonium group

are much less affected than in the cholic acid solution. From these changes, two interesting points can be perceived: [1] The hydrophobic interaction still exists in the interaction of BTMA with methyl cholate while the ionic interaction is absent; [2] The lack of ionic interaction leads to a decrease in hydrophobic interaction. In other words, the ionic linkage plays a predominant role in the binding with bile acids. The secondary binding force is mainly hydrophobic interaction. However, the hydrophobic interactions only become significant in the presence of ionic or electrostatic interactions. These hydrophobic interactions probably strengthen the ionic linkages, without which the possibility for such an interaction is greatly reduced. This is to say that in the binding between bile acid with BTMA, the two kinds of interactions take place cooperatively and simultaneously.

The results presented in Tables 3.7 and 3.8 in fact support this argument. A comparison of the data in the two tables indicates the absence of ionic interactions and reduced hydrophobic interactions in the mixture of cholic acid methyl ester and BTMA.

3.4.3 Interaction of Bile Salts with Betaine and Peptides

Interaction with Betaine: In order to determine the specific interactions of bile salts with betaine, or trimethylglycine, which is the functional group of the quaternized peptide-containing resins (Chapter 2), T_1 values were measured in both D_2O and deuterated phosphate buffer solutions.

The spin-lattice relaxation times of the various groups of sodium cholate in deuterated phosphate buffer in the presence of small amount of betaine were compared with those of sodium cholate. The T_1 values of the ^{13}C signals of sodium cholate in the phosphate buffer show no significant changes, as shown in Table 3.11. Similar results were obtained in D_2O. As discussed in the previous section, the small change in T_1 values in aqueous solutions is related to the micellar properties of bile salts. This is observed in both D_2O and phosphate buffer solutions upon interaction with BTMA or betaine.

The T_1 values of the betaine carbons were measured before and after the addition of glycocholate (Table 3.12). The experiments were performed in a deuterated buffer (0.05 M, pH=7.6) since it was relatively easy to obtain good ^{13}C signals for this compound though solutions of high ionic strengths usually affect the detection of the ^{13}C signals. Obviously the involvement of the carboxyl group of the betaine molecule is very limited in the interaction with this bile salt. The

interaction between betaine and bile salts, if any, involves primarily the quaternary ammonium group, while the involvement of the carboxyl group of betaine is limited. It is unlikely that mixing with betaine could alter the structure of the bile salt micelles since it is not lipid soluble.

Table 3.11 The Changes in ^{13}C T_1 Values (in Sec) of Cholate in Deuterated Buffer upon Interaction with Betaine

Carbon	NaC	NaC+Betaine	Difference (%)
COOH	4.0	3.6	10
12-CHOH	0.16	0.19	-
3-CHOH	0.16	0.15	-
7-CHOH	0.20	0.18	10
19-CH_3	0.53	0.48	9.4
21-CH_3	0.48	0.45	6.3
18-CH_3	0.53	0.50	5.7

NaC: sodium cholate.
Molal concentration of NaC in deuterated phosphate buffer (0.05 M, pH = 7.7): 0.35 *m*; NaC/betaine molar ratio = 1:1.

Table 3.12 The Changes in ^{13}C T_1 Values (in Sec) of Betaine in Deuterated Buffer upon Interaction with Glycocholate

Carbon	Betaine	Betaine+NaGC	Difference (%)
COOH	66.8	60.9	8.8
CH_2	4.66	3.84	17.6
CH_3	3.07	2.63	14.0

NaGC: sodium glycocholate.
Molal concentration of betaine in deuterated phosphate buffer (0.05 M, pH = 7.6): 0.45 *m*; betaine/NaGC molar ratio = 10:1.

It should be noted that betaine, or trimethylglycine, is an inner salt, very small in size and lacking hydrophobicity; therefore, the interactions are limited to possible ionic or hydrophilic interactions. It is interesting, however, that lecithin,

a similar quaternary ammonium compound with a long hydrophobic acyl chain connected to the choline residue, can participate by hydrophobic interactions in forming mixed micelles (18).

Interaction with Dilysine: To study the possible interaction of bile salts with peptides in aqueous solutions, a simple basic oligopeptide, dilysine, was mixed with sodium cholate in D_2O. The T_1 values of the groups of sodium cholate show more significant changes upon the addition of dilysine than manifested for the other systems. The T_1 values listed in Table 3.13 demonstrate the participation of the carboxyl group of cholate in the interaction with this basic peptide. The T_1 changes for the carbons adjacent to the hydroxyl groups of the bile salt skeleton are generally too small to be of any significance. However, the carbon of the 21-methyl group on the side chain shows a large decrease in T_1 when dilysine is added. This can be explained by the possible involvement of this group in hydrophobic interactions with the corresponding moiety of the peptide.

Table 3.13 The Changes in ^{13}C T_1 Values (in Sec) of Cholate in D_2O upon Interaction with Dilysine

Carbon	NaC	NaC+DL	Difference (%)
COOH	4.05	2.79	30
12-CHOH	0.19	0.19	0
3-CHOH	0.19	0.18	5.3
7-CHOH	0.20	0.18	10
19-CH_3	0.60	0.56	6.7
21-CH_3	0.56	0.42	25
18-CH_3	0.63	0.59	6.3

NaC: sodium cholate; DL: dilysine.
Molal concentration of NaC in D_2O: 0.12 *m*; NaC/lysine residue molar ratio = 1:1.

It is interesting that the addition of dilysine to the aqueous solutions of bile salt, unlike in the cases of BTMA and betaine, has caused detectable T_1 decreases for the some of the ^{13}C signals. This suggests a specific interaction between the peptide and bile salt, which probably alters the structure of the existing micelles in the bile salt solutions. The ionic interaction is obvious as

shown by the significant decrease in the T_1 of the carboxyl group of sodium cholate. The ionic linkage occurs between the carboxylic acid group of the bile salt anion and the side chain amino group of the lysine residue of dilysine. This linkage seems to be facilitated by hydrophobic interactions, evidenced by the decreased freedom of motion of the methyl groups.

As already discussed in the previous chapters, it is known that the conformation of peptides may be important in their binding of bile acids. In order to investigate further the interaction between the peptide containing lysine and bile acids, *polylysine* (DP=17) was added to a glycocholate solution in D_2O (0.14 *m*) at a glycocholate-lysine residue molar ratio of 1:1. However, the addition of polylysine resulted in a cloudy, milky solution and caused a phase separation of the aqueous solution of bile salt. Both phases were in the liquid state; and the bottom layer consisted of a small drop of liquid. The supernatant, a mixture of glycocholate and polylysine, was used for a T_1 measurement. The T_1 of the carboxyl group exhibited a 25% decrease (from 2.9 to 2.2 seconds); and the amide carbonyl had a remarkable decrease of 63% (from 11 to 4 seconds). The remaining carbons did not appear to be affected within the experimental error. In fact, the phase separation phenomenon represents a unique interacting process between the peptide and the bile salt. Upon the neutralization of the negative charges of the bile salt and the positive charges of the lysine residues, the solubility of the neutralized molecules is reduced in the aqueous solution and precipitation takes place. The undissolved complex of polylysine and bile salt forms a separate phase in the mixture.

In Chapter 1, the binding of bile acids to serum albumin was discussed. Although dilysine has been shown to interact with bile salts by the T_1 measurements, similar effect was not observed for *bovine serum albumin* (BSA) with bile salts. Upon the addition of BSA into the aqueous solution of glycocholic acid (0.04 *m* GCA, GCA-BSA molar ratio 20:1), the T_1 values of glycocholic acid show no significant changes. The experiment was repeated at a different concentration (0.13 *m* GCA, GCA-BSA molar ratio 40:1) and again little difference was observed. Although interactions may occur between BSA and the bile acid, the binding of bile acids by albumin is not efficient. This is probably related to the large molecular weight of this protein (ca. 66,000). The percentage of the bile acid molecules involved in the interaction with BSA is thus not

sufficient to account for any observable changes in T_1's in the ^{13}C signals. Under these experimental conditions, the interaction between BSA and glycocholate was minimal. However, the interaction between bile acids and basic peptides such as dilysine was easily detectable. This gives a clear evidence of the inefficiency of BSA in the binding of bile acids.

3.5 Summary

The NMR spectra of bile acids in D_2O and DMSO-d_6 have been analyzed with the aid of DEPT and by comparison of the spectra of different bile acids. The T_1 measurements and two-dimensional correlation experiments confirmed the assignments. A dependence of the chemical shifts of bile salt in D_2O on temperature and concentration above the critical micellar concentration was observed, indicating dissociation and reformation of micelles under different conditions.

The interaction studies of bile acids in D_2O by measurements of the NMR spin-lattice relaxation times demonstrate a predominantly ionic interaction with selected binding species. The binding of bile salts from aqueous solutions is characterized by a combination of ionic and hydrophobic interactions. The binding of bile acids with the basic peptides containing lysine are much more efficient than the binding of bile acids with albumin.

The interaction studies in DMSO reveal more interesting aspects of the interaction between bile acid and benzyltrimethylammonium chloride. By comparison of the binding of cholic acid and its methyl ester, direct evidence of ionic and hydrophobic interactions is derived from the relaxation data. The interaction is predominantly via ionic linkages with the hydrophobic bonding being of secondary importance. In the absence of the ionic linkages, the hydrophobic interaction is also significantly weakened. Thus, the two kinds of interactions occur simultaneously and cooperatively in the binding process.

References

1. D.M. Small, S.A. Penkett & D. Chapman, Biochim. Biophys. Acta, 176, 178, 1969
2. S. Barnes & J.M. Geckle, *J. Lipid Res.*, 23, 161, 1982
3. D.V. Waterhous, S. Barnes & D.D. Muccio, *J. Lipid Res.*, **26**, 1068, 1985
4. D. Leibfritz & J.D. Roberts, *J. Am. Chem. Soc.*, **95**, 4996, 1973
5. T. Iida, T. Tamura, T. Matsumoto & F.C. Chang, *Org. Mag. Reson.*, **21**, 305, 1983
6. S. Barnes & D. Kirk, in *The Bile Acids, Vol. 4*, D. Kritchevsky, P.P.Nair & K.D.R. Setcheli, eds., Plenum Press, NY, 1985
7. P.K. Bhattacharyya & Y.G. Bankawala, *Anal. Chem.*, **50**, 1462, 1978
8. Y. Shalon & W.H. Elliott, *FEBS Lett.*, **41**, 223, 1974
9. R. Paul, M.K. Mathew & P. Balaram, *Chemistry and Physics of Lipids*, **25**, 345, 1979
10. Y. Murata, G. Suglhara, K. Fukuchima & M. Tanaka, *J. Phys. Chem.*, **86**, 4690, 1982
11. M. Campredon, V. Quiroa, A. Thevand, A. Allouche & G. Pouzard, *Mag. Reson. Chem.*, **24**, 624, 1986
12. G. Conte, R. Di Blasi, E. Giglio, A. Parretta & N.V. Pavel, *J. Phys. Chem.*, **88**, 5720, 1984
13. D.J. Cabral, J.A. Hamilton & D.M. Small, *J. Lipid Res.*, **27**, 334, 1986
14. E. Kolehmainen, *J. Colloid Interf. Sci.*, **105**, 273, 1985
15. P.J. Cozzone, P. Canioni, L. Sarda & R. Kaptein, *Eur. J. Biochem.*, **114**, 119, 1981
16. P. Schurtenberger & B. Lindman, *Biochemistry*, **24**, 7161, 1985
17. E. Mukidiam, S. Barnes & G.A. Elgavish, *J. Am. Chem. Soc.*, **108**, 7082, 1986
18. R.E. Stark, J.L. Manstein, W. Curatolo & B. Sears, *Biochemistry*, **22**, 2486, 1983
19. R.E. Stark & M.F. Roberts, *Biochim. Biophys. Acta*, **770**, 115, 1984
20. R.E. Stark, G.J. Gosselin, J.M. Donovan, M.C. Carey & M.F. Roberts, *Biochemistry*, **24**, 5599, 1985
21. D.M. Small, S.A. Penkett & D. Chapman, *Biochim. Biophys. Acta*, **176**, 178, 1969
22. R.E. Stark, R.W. Storrs, S.E. Levine, S. Yee & M.S. Broido, *Biochim. Biophys. Acta*, **860**, 399, 1986
23. E.D. Becker, p. 186, in *High Resolution NMR*, Academic Press, NY-London-Toronto-Sydney-San Francisco, 1980
24. D.F.R. Gilson & G. Gomez, *J. Organomet. Chem.*, **240**, 41, 1982
25. E. Breitmaier & W. Voelter, p. 167, in *Carbon-13 NMR Spectroscopy*, 3rd, completely rev. ed., VCH (F.R. Ger.), Weinheim-NY, 1987
26. R.J. Abraham & P. Loftus, **Chap. 6, Double Resonance Techniques and Relaxation Mechanisms**, p. 100, in *Proton and Carbon-13 NMR Spectroscopy*, Heyden & Sons Ltd., London-Philadelphia-Rhein, 1980
27. M.L. Martin, J.-J. Delpuech & G.J. Martin, p. 18, in *Practical NMR Spectroscopy*, Heyden & Son Ltd., 1980
28. J.J. Fisher & O. Jardetzky, *J. Am. Chem. Soc.*, **87**, 3237, 1965
29. O. Jardetzky & N.G. Wade-Jardetzky, *Mol. Pharmacol.*, **1**, 214, 1965
30. W. Stoffel, O. Zierenberg, B.D. Tunggal & E. Schreiber, *Hoppe-Seyler's Z. Physiol. Chem.*, **355**, 1381, 1974

31. M.F. Froix & R. Nelson, *Macromolecules*, 9, 428, 1976
32. D.J. Nelson, *Inorg. Chim. Acta*, 27, L71, 1978
33. E. v. Goldammer & H. Zorn, *Molecular Physics*, 32, 142, 1976
34. P.J. Andree, *J. Mag. Reson.*, 29, 419, 1978
35. D.M. Doddrell, D.T. Pegg & M.R. Bendall, *J. Mag. Reson.*, 48, 323, 1982
36. M.C. Carey & D.M. Small, *Arch. Intern. Med.*, 130, 506, 1972

Part II
Bile Pigments

4 Introduction

4.1 Metabolism of Bile Pigments

Bile pigments are metabolites of hemoglobin in the blood. The predominant bile pigment, bilirubin, is carried by serum albumin and excreted to the bile via the liver. These biological molecules are not only widely distributed in animals but also exist in plants (1). Their formation in mammalian systems has been extensively studied, mainly because of the toxicity properties associated with most of the bile pigments, especially bilirubin. Disorders in the metabolism of bilirubin may cause jaundice, a yellow discoloration of the skin and other tissues, which is usually an indication of a disease of the blood, liver or biliary tract. This disease is called hyperbilirubinemia since it is usually related to an elevated bilirubin level in the blood. It is especially seen among newborn infants (2).

Based on their tetrapyrrole structures, bile pigments are generally classified as porphyrin compounds. Protoporphyrin IX, which is of central importance in heme proteins such as hemoglobin and chlorophyll, is a common precursor for the bile pigments. Protoporphyrin itself is synthesized biologically from a simple amino acid, glycine, and succinyl-coenzyme A, as shown in Figure 4.1 (3).

Bile pigments occur in nature mostly as the IXα isomers. Depending on the position at which the protoporphyrin is split, there are also β, γ and δ isomers. The basic structures of these isomers are shown in Figure 4.2. Since bile pigments occur in the mammalian systems as their IXα isomers, unless otherwise specified, the terms bilirubin and biliverdin in this thesis refer to the common unconjugated bile pigment IXα isomers, bilirubin IXα and biliverdin IXα.

4.1.1 Formation of Bile Pigments

The pigments in the human body are products of the metabolism of hemoglobin of senescent red blood cells. Under normal physiologic conditions, a

70-kg human adult produces approximately 6 grams of hemoglobin daily. When hemoglobin is broken down in the body, the protein portion, globin, may be re-utilized either as a protein or in the form of its constituent amino acids. The iron of the heme is also stored for reuse. Under the catalysis of enzymes, the iron-free portion of the heme, which is protoporphyrin, is degraded mainly in the reticuloendothelial cells of the liver, spleen and bone marrow (4).

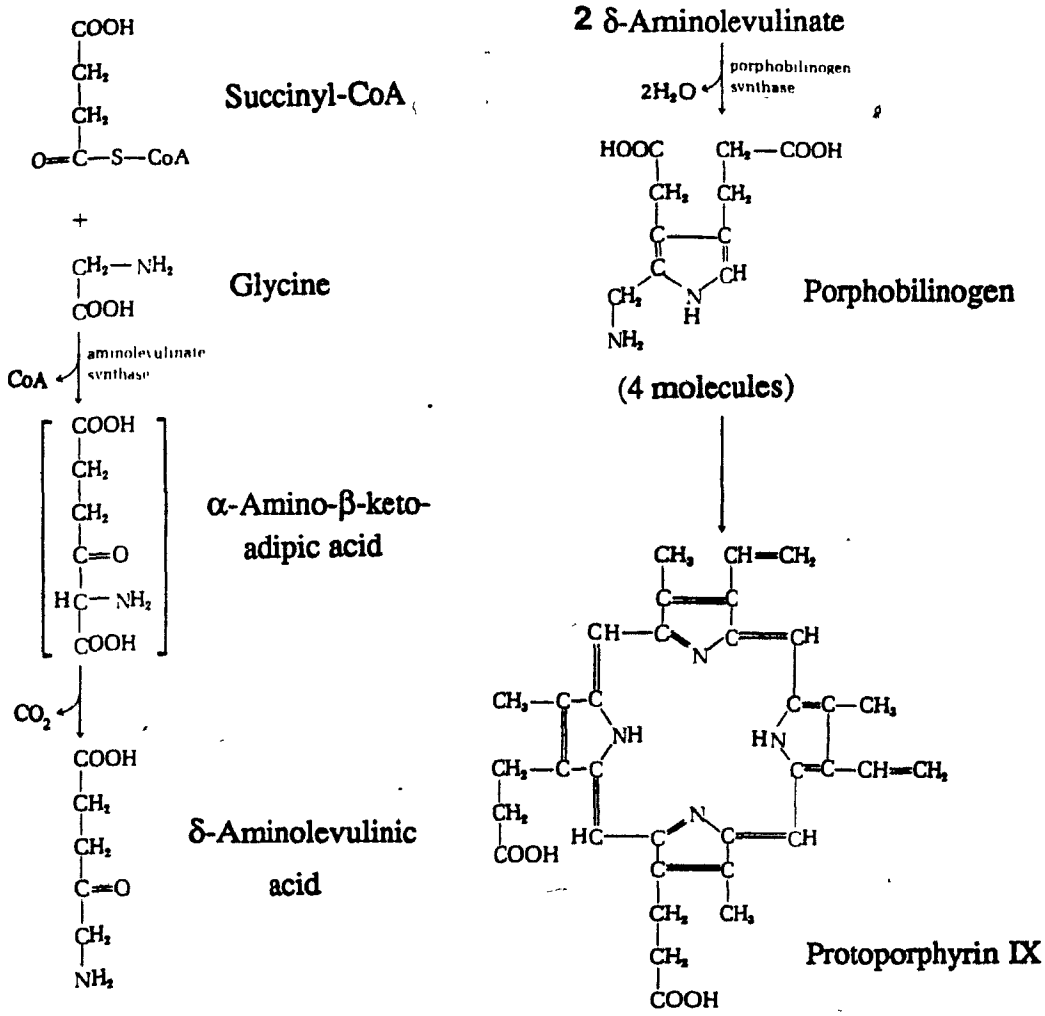

Figure 4.1 Biosynthesis of protoporphyrin IX from glycine and succinyl coenzyme A (p. 626, reference 3).

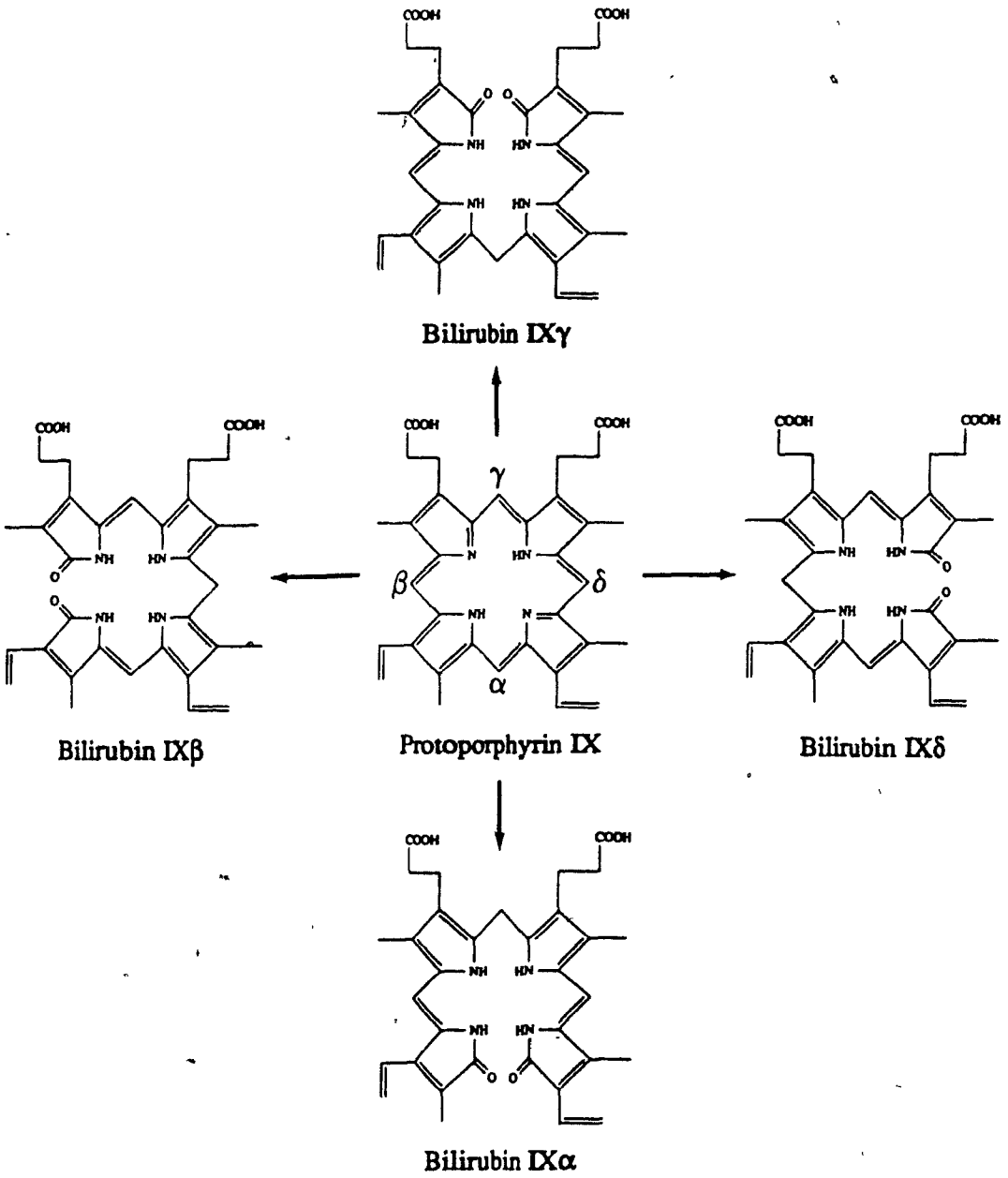

Figure 4.2 The structures of the bilirubin IX isomers, formed by splitting at different positions of the protoporphyrin IX ring.

As shown in Figure 4.1, protoporphyrin is a cyclic compound consisting of four pyrrolé rings linked through methine bridges. Further addition of oxygen to the protoheme results in the splitting of the tetrapyrrole ring with the release of

carbon monoxide and the formation of an equimolar quantity of a green pigment, biliverdin IXα (5). In birds and amphibia, biliverdin seems to be the main bile pigment and is excreted in its unconjugated form (6). Most of the biliverdin in human and rabbit bile is detected as a mono- or diglucuronide, probably formed by oxidation of conjugated bilirubin in the bile ducts (7). However, in mammals the methenyl bridge between rings B and C of biliverdin is reduced to a methylene group, under the catalysis of an enzyme called biliverdin reductase, thus forming bilirubin IXα, a reddish yellow pigment. The formation of bile pigments is schematically shown in Figure 4.3. Approximately 250-350 mg of bilirubin is produced daily by normal human adults (5).

4.1.2 Excretion of Bile Pigments

Only trace quantities of unconjugated bilirubin can be excreted in bile and urine because of its insolubility. Bilirubin is normally released into the plasma and is firmly bound to serum albumin, a protein acting as a carrier for a multitude of substances in the blood (8). In normal cases, the amount of the unbound bilirubin in plasma is very small (9). Despite the high affinity binding to serum albumin, bilirubin is rapidly transferred from the plasma into the liver.

The uptake of bilirubin by the liver cells is rapid and saturable with the aid of carrier proteins in the membrane of the hepatocyte. Most of the bilirubin is then bound to cytoplasmic anion-binding acceptor proteins; of which ligandin (alias Y protein) appears to be the most important (10). Z protein, which has a lower affinity for organic anions, is also responsible for the hepatic uptake of bilirubin (11).

Under the catalysis of uridine diphosphate glucuronate (UDG) glucuronyltransferase in the liver, the propionic acid groups of bilirubin are esterified with some sugars, mainly glucuronic acid, to form bilirubin mono- and diglucuronide (12) (Figure 4.4). The conjugated forms of bilirubin are water soluble and thus can easily be excreted. Although other forms of bilirubin conjugates may exist, bilirubin mono- and diglucuronide constitute the predominant bile pigment fraction in normal human bile (13, 14).

The conjugated bilirubin is then excreted easily into the bile. The bilirubin conjugates can aggregate with cholesterol, phospholipid, bile salts and protein (15). When the macromolecular aggregates become supersaturated, stones composed mainly of pigments and cholesterol can be formed in the

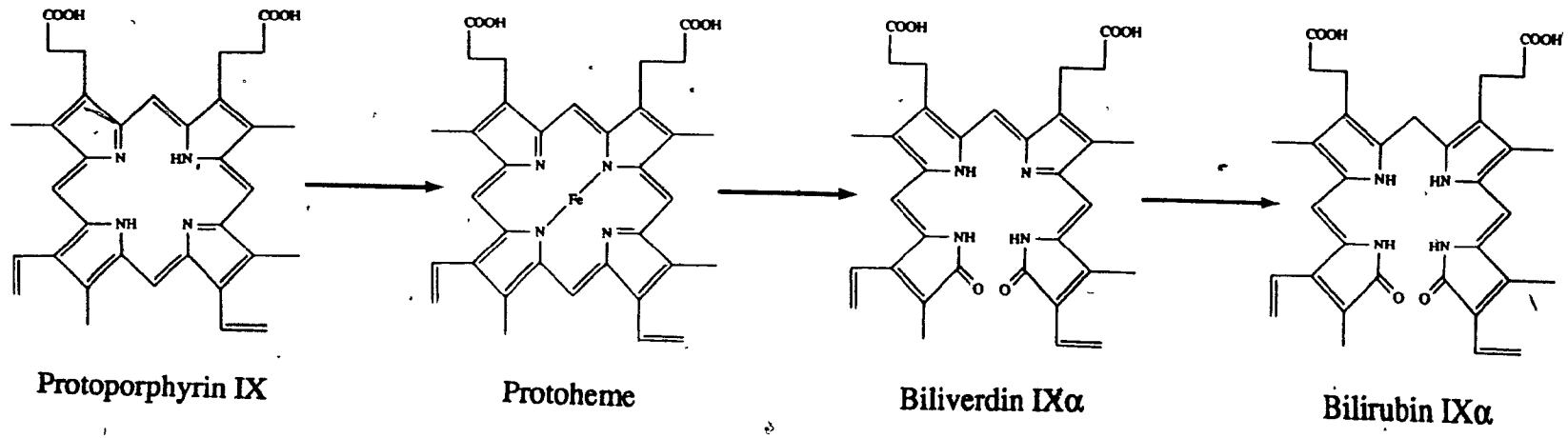

Figure 4.3 The formation of protoheme and bile pigments from protoporphyrin IX.

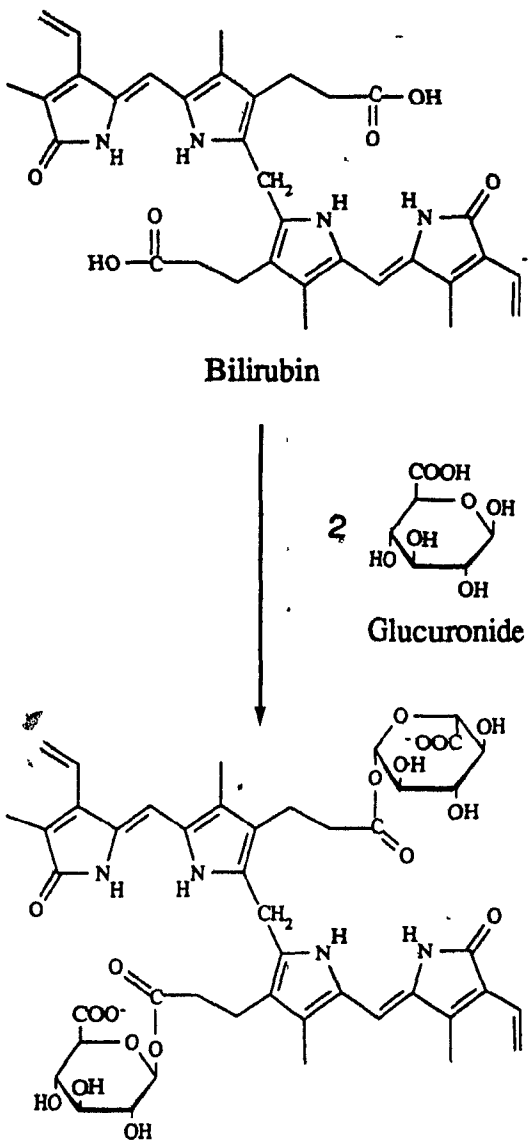

Figure 4.4 The conjugation of bilirubin with glucuronide under the catalysis of UDG-glucuronyltransferase.

gallbladder or common bile duct, which in turn may cause jaundice in the patients (16).

In normal cases, the conjugated bilirubin joins the enterohepatic circulation, together with the other constituents of bile. The glucuronides of the conjugated bilirubin are removed by bacterial enzymes in the terminal ileum and the pigment is subsequently reduced to some colorless tetrapyrrolic compounds

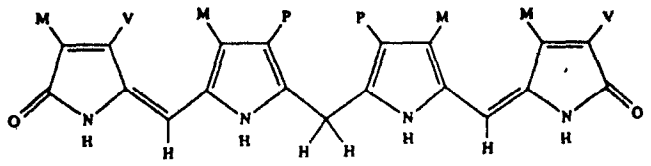

Bilirubin IXα

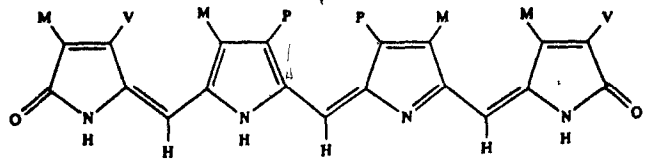

Biliverdin IXα

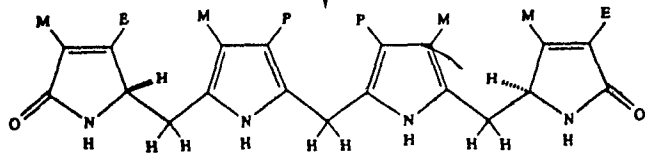

i-Urobilinogen IXα

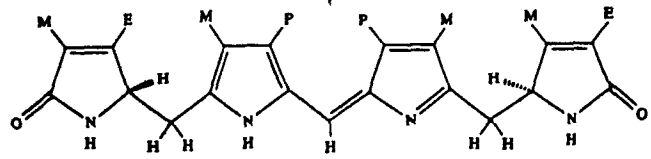

i-Urobilin IXα

Figure 4.5 The possible degradation products of bile pigments in the gastrointestinal tract (reference 17): M = CH_3; V = $CH{=}CH_2$; E = CH_2CH_3; P = CH_2CH_2COOH.

called urobilinogens (Figure 4.5) (17). Unlike bile salts, only a small fraction of the urobilinogens formed in the gastrointestinal tract is reabsorbed into the portal circulation (8). The remaining urobilinogens are oxidized in the colon to some

closely related colored compounds, urobilins, and are finally excreted in the feces. This overall process is shown in Figure 4.6 (18).

Most of the absorbed urobilinogens are re-excreted by the liver, and a small fraction is re-excreted by the kidney (19). Therefore, increased urinary excretion of urobilinogen is an indication of either liver disease or abnormal bilirubin production.

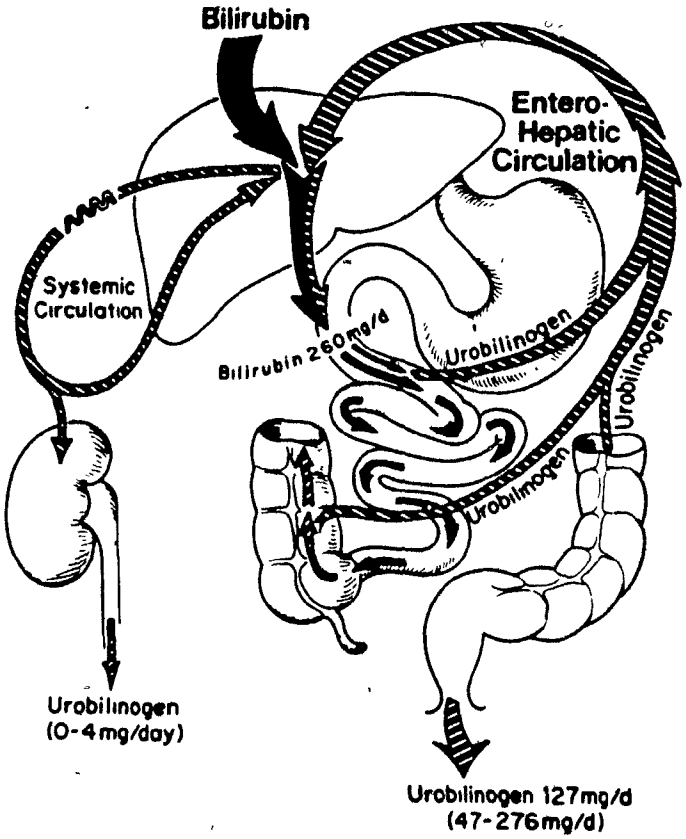

Figure 4.6 The enterohepatic circulation and excretion of bile pigments under physiological conditions (reference 18).

4.1.3 Function and Toxicity of Bile Pigments

The physiological functions of bile pigments in the human body have not been understood to date. Bilirubin seems to be merely a waste product of heme catabolism although it has been found to be toxic to some bacteria (20). However, Stocker *et al.* suggested, based on *in vitro* results, that bilirubin probably serves as a physiological, chain-breaking antioxidant (21). Bile

pigments such as bilirubin and biliverdin may possibly protect vitamin A and linoleic acid from oxidative destruction in the intestinal tract (22,23). Biliverdin serves a possible ornamental or cryptic function in birds' eggshells or fishes' scales. It has similar functions in some insects and lower animals (24).

The bile pigments of plants, however, are very important since they function as photoreceptors for photosynthesis, photomorphogenesis and many other photobiological responses. Naturally, these pigments differ slightly in structure from the bile pigments found in animals (25).

Bile pigments do not have toxic effects on the human body provided that the metabolism process functions normally, i.e., they are bound tightly to proteins in the plasma and inside the cells. However, bile pigments, especially unconjugated bilirubin, have been found to be toxic to the central nervous system and to all tissues during prolonged retention in the body (26). Biliverdin appears to be less toxic than bilirubin (27). Human neonates, especially prematurely born infants, have an undeveloped capability of conjugation and excretion of bile pigments, which results in the accumulation of bilirubin in the blood. This disease is clinically known as *hyperbilirubinemia*. About 50% of neonates are clinically jaundiced during the first five days of life (19) since the production of bilirubin is usually two or three times that of an adult on a body weight basis (2). If the serum albumin and the liver in the body are unable to handle the load of endogenous bilirubin, it is deposited in the tissues resulting in a yellow staining of the skin and icterus neonatorum. In serious circumstances, it can escape to the brain where it may result in lasting brain damage which interferes with learning functions at a later age or even death in seriously jaundiced newborns (27, 28).

Hyperbilirubinemia is not a disease restricted to newborns, it also occurs in adults. It can be a consequence of any abnormalities in the metabolism process of bile pigments since these malfunctions may cause blockage to the elimination of bile pigments from the body. This disease can also be a result of treatment with drugs, such as sulfonamides, which can be bound to serum albumin and occupy the bilirubin binding sites on the protein. Therefore, competitively bound drugs should be avoided when treating jaundiced patients (29).

Hyperbiliverdinemia has also been reported (30,31). This condition results from complications of the indomethacin therapy and phototherapy for hyperbilirubinemia. The complications of phototherapy in the neonates, such as

green jaundice or the bronze baby syndrome (32,33), are usually associated with an elevated biliverdin level in serum (32).

4.2 Properties of Bile Pigments

4.2.1 Structure and Solubility

The basic structure of bilirubin IXα was proposed by Fischer *et al.* in 1941 (34). The structure and conformation of bilirubin have been extensively studied by various techniques and the structure shown in Figure 4.7 was proposed (35) and has been generally accepted (36). Hemoperfusion and phototherapy studies have stimulated the investigations of the structure and conformation of bilirubin by various available physical techniques, e.g., nuclear magnetic resonance, infrared, electron spin resonance, mass spectra, and X-ray diffraction (24).

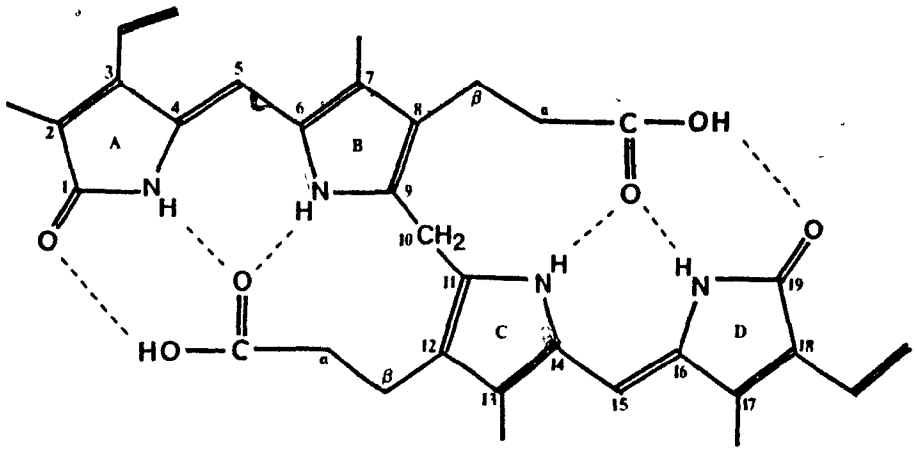

Figure 4.7 The chemical structure of unconjugated bilirubin IXα. Six intramolecular hydrogen bonds are formed between the carboxyl and NH groups.

Bilirubin, as shown, is a tetrapyrrole compound with two propionic carboxyl groups. In its unconjugated form, shown in Figure 4.7, it has six intramolecular hydrogen bonds in the solid state (37) as well as in some organic solvents such as chloroform (38). As a consequence of its hydrophobicity, it is very hard to dissolve in aqueous solutions. In strong alkaline solutions the internal

hydrogen bonds are disrupted, rendering it quite soluble. The solubility of bilirubin in aqueous solution decreases as the pH of the solution decreases so that it is virtually insoluble in water when the pH is below 7 (29). However, in the presence of detergent the solubility of bilirubin in water can be enhanced by forming mixed micelles (39). The formation of mixed micelles with bile salts is important for the transport of bilirubin in bile and prevents the formation of gallstones (40). In aqueous solutions, bilirubin dianions undergo dimerization, probably by formation of hydrogen bonds between the NH and carbonyl groups with the possible participation of the π-electrons of the dipyrrole chromophores (29). In aqueous solutions, the bile pigments tend to aggregate and precipitate by forming colloids (41). This process can be accelerated by vigorous shaking of the solution.

Bilirubin dissolves in a number of organic solvents, such as DMSO and chloroform. The solubility increases as the polarity of the solvent increases. In general, polar, aromatic solvents dissolve more bilirubin than aliphatic, apolar solvents.

The molecular structure of biliverdin is different from that of bilirubin only by the replacement of the central methylene bridge by a methenyl group with concomitant rearrangement of the double bonds. The properties of crystalline biliverdin differ from that of bilirubin. Unlike bilirubin, biliverdin is only sparingly soluble in chloroform and dichloromethane but soluble in acetic acid, dimethylformamide and methanol, an indication of the presence of strong intermolecular hydrogen bonds in the crystal that are disrupted by the hydroxylic component of the solvents (24).

4.2.2 Acid-Base Properties

The structures of bile pigment indicate that they should express both acidic and basic equilibria, depending on pH. Because of the poor solubility of bile pigments in aqueous solutions, their acid-base properties are poorly understood.

The weak acidity of the bile pigments is obviously deriving from the presence of the propionic acid side chains. There is also a more feeble acidity associated with the lactam groups. In strong alkaline solutions, the propionic acid groups are deprotonated and thus dianions of bile pigments are formed. A solution of bilirubin turns deep red when excess base is added, while biliverdin

turns yellowish green. In addition, the color changes indicate the ionization of at least one of the lactam NH protons (24).

The pK_a values for the propionic acid group in bilirubin has been investigated in many ways, often measured or estimated in mixtures of aqueous and organic solutions; therefore, the published results manifest confusion and controversy (42). It is extremely difficult to titrate bilirubin because precipitation occurs upon changes of the pH of the solution. From potentiometric titration of bilirubin in dimethylformamide and comparison with the other dicarboxylic acids with known pK_a it was estimated that the pK_{a1} and pK_{a2} for the carboxyl groups of bilirubin in water are 4.3 and 5.3, respectively (43). Biliverdin can be titrated more easily than bilirubin and gives a pK_{a1} of 5.0 and pK_{a2} of 7.2 (44). The states of dissociation of the groups of bilirubin at various pH's are shown in Figure 4.8 (44).

Hansen *et al.* (45) estimated the pK_a of bilirubin by ^{13}C NMR co-titration studies in which bilirubin was titrated in DMSO with acids of known pK_a in water in order to relate the apparent pK_a's of bilirubin to those of the acids. Analysis of the chemical shifts of the related carbons in the spectrum shows that the COOH protons of bilirubin are titrated simultaneously with *m*-hydroxybenzoic acid. Thus, they have equal pK_a values in DMSO. Conversion of the pK_a values to a different solvent yields a pK_a of 4.4 for the bilirubin carboxyls in water, which is the average pK_a of the two COOH protons of bilirubin. Similar titration and calculation gave an average value of 13.0 for the lactam protons in bilirubin.

It is often overlooked that bile pigments are not only weak acids but also weak bases. Hydrochloride salts of both bilirubin and biliverdin have been isolated. Bilirubin turns red in strongly acidic media, indicating protonation of the chromophore. The absorbance of biliverdin in the visible regions also increases upon treatment with strong acids (24). The protonation of bilirubin probably occurs on the lactam rings by forming lactim ammonium cations (46). Biliverdin has shown stronger basicity than bilirubin. Protonation of biliverdin presumably occurs at the single unprotonated nitrogen atom (47).

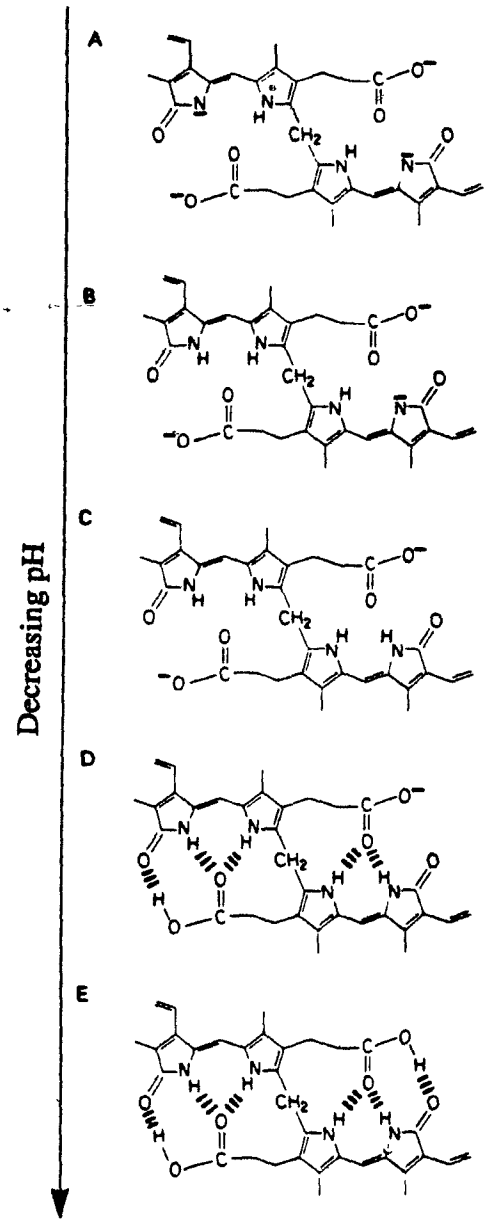

Figure 4.8 The possible configurations and electrochemical states of bilirubin in aqueous solutions at different pH's (reference 44): A: pH > 13; B: pH = 11-13; C: pH = 7-11, around neutral and slightly basic pH's; D: pH = 4-6; E: pH < 4.

4.2.3 Chemical Properties

Commercially, the bile pigments are prepared from their natural sources, e.g., bilirubin is obtained from gallstones or from bile. The purified bilirubin can

be crystallized from chloroform-methanol. Biliverdin is usually prepared by dehydrogenation of bilirubin. It can be crystallized from methanol. Since the purification of biliverdin is very difficult, the commercial sample usually contains up to 20% isomeric impurities (24).

One of the most distinct characteristics of bile pigments is their instability. The bile pigments and their derivatives, in general, are sensitive to oxygen, light and temperature. The ideal conditions for the storage of these compounds and their solutions can be best described as cold, dark and air-free. Even under these conditions they may be subject to change with time.

Bilirubin is more stable than the other bile pigments, due to the stabilization effect of the intramolecular hydrogen bonds. However, because of the sensitivity of the central bridge to electrophilic and oxidative attacks, bilirubin is unstable at room temperature. It may undergo oxidation when exposed to air or isomerization when exposed to light. The crystalline form of bile pigments can be stable for a year or two provided that they are pure and dry and are kept in cool dark places.

Bilirubin can be oxidized in the presence of trace amounts of oxygen to yield biliverdin and a number of other degradation products. It retains its intramolecular hydrogen bonds in most organic solvents, thus the solution can be stable for a limited period of time. However, the hydrogen bonding is interrupted in DMSO solution, thus leading to a slow decomposition of bilirubin at room temperature. Nonetheless, at lower temperatures bilirubin in DMSO suffers minimal degradation for periods of three days to one week.

Biliverdin is more stable in respect to autooxidation and photooxidation. Even so, solutions of biliverdin should still be protected from light and heat to avoid possible degradation.

The commonly occurring bilirubin is intramolecularly hydrogen bonded, having a Z,Z-configuration at the two double bonds of the methenyl groups which connect the two outer rings. Illumination with blue light (480 nm) can cause *cis-trans* isomerization. The formation of E,Z-, Z,E- or E,E-configuration of bilirubin partially or entirely breaks the intramolecular hydrogen bonds (36), as depicted in Figure 4.9. Photocyclization of bilirubin can produce other isomers of bilirubin (48). These bilirubin isomers, generally referred to as photobilirubin, are water soluble and can be excreted easily without conjugation. Therefore, a

phototherapy method has been used clinically for the treatment of hyperbilirubinemia (see Section 4.4.1). Photooxidation and photodegradation can also occur upon irradiating with stronger light and longer time (49,50). The by-products of photodegradation include small amounts of dipyrroles and biliverdin, which are soluble in aqueous media and can be excreted easily in bile and urine (51).

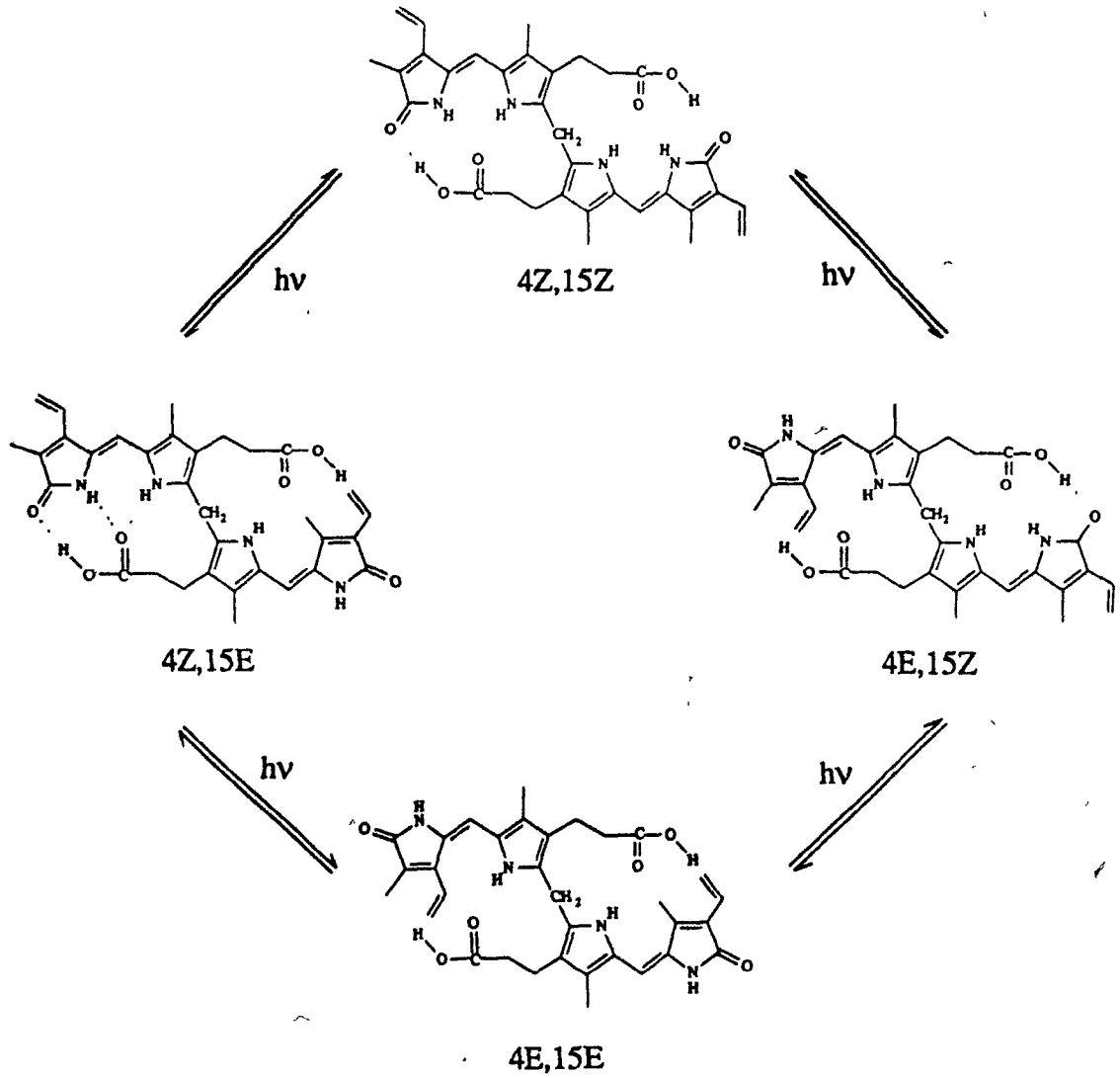

Figure 4.9 Photoisomerization of bilirubin IXα, depicting the Z-E transition which involves the disruption of the intramolecular hydrogen bonds.

Studies on derivatives of biliverdin have also shown that the all-Z conformation of the molecule can be transformed into many different isomers by rotation about any of the C-5, C-10 and/or C-15 double bonds upon irradiation with light (52).

Various derivatives of bile pigments can be prepared by reacting the respective groups of bile pigments with other reagents. *Meso*bilirubin can be prepared by the addition of hydrogen to the vinyl groups of bilirubin (53). Bilirubin esters and other conjugates can be obtained by esterification (54) and conjugation of the propionic carboxyl groups of bilirubin. Most of the derivatives of bilirubin are also unstable. Bilirubin dimethyl ester, a compound with an orange yellow color, is even more sensitive to light and oxygen than bilirubin, due to the absence of intramolecular hydrogen bonds.

4.3 Detection and Analysis of Bile Pigments

4.3.1 Light Absorption Spectroscopy

The bile pigments are colored compounds which, at certain wavelengths in the UV-visible region, absorb light with large molar extinction coefficient. The bilirubin absorbance spectrum shows a strong absorption maximum at 438-440 nm. The absorbance is insensitive to pH changes in the region of pH 8 to 11 (29). There is another weaker absorption band at about 280-300 nm. The maximum in the absorption band of free bilirubin in organic solvents varies little, while that of the dimethyl ester is sensitive to solvents (24).

The absorption spectrum of biliverdin in neutral solutions shows an absorption maximum between 380 and 400 nm with a second broad maximum at about 640-665 nm. In hydrochloric acid or in methanolic hydrogen chloride, the formation of the hydrochloride causes increased absorption of both bands and a bathochromic shift of the maximum in the visible region, together with a slight hypsochromic shift of the maximum in the ultraviolet region (55).

Addition of albumin to the bilirubin aqueous solution causes a red shift to a maximum absorption at around 460 nm, depending on the source of the protein and the method of preparing the solutions (56). The formation of complexes with proteins causes no pronounced change in the spectrum of biliverdin (57).

When the concentration is low ($\leq$ 0.20 mM), the absorbance of bilirubin has a large extinction coefficient of 4.7×10^4 l mol^{-1} cm^{-1} and obeys Beer's law

(58). Therefore, the UV-visible absorbance spectroscopy serves as a simple and rapid tool in the quantitative analysis of bile pigments. It is important to note that the presence of impurities can interfere with the bilirubin absorbance, since many substances also absorb in this region.

4.3.2 Chromatography

Thin layer chromatography (*TLC*) is still widely used for the separation of bile pigments and their derivatives (59-61). The conjugated and unconjugated bilirubin in bile has been reported to be determined quantitatively by the TLC method (62). In this method, azo-derivatives of the pigments are obtained and measured on a dual wavelength TLC scanner after diazo reactions.

High performance liquid chromatography (*HPLC*) has been used for the separation and quantitative analysis of bile pigments, mainly conjugated and unconjugated bilirubin (63-65). An eluent consisting of acetonitrile and water is generally used with a reverse-phased HPLC system. The HPLC analysis is usually a rather lengthy procedure, requiring as long as two hours (66), in addition to the treatment of samples prior to the injection into the HPLC system (65). Photoproducts of bilirubin have been separated successfully with ion-pair HPLC method on a reversed phase system at a detection wavelength of 455 nm (67), the relatively shorter separation time makes it useful for the analysis of bilirubin after its conversion to the corresponding photoproducts.

4.3.3 Infrared, Raman and NMR Spectroscopy

Various available physical techniques have been employed in the determination and analysis of bile pigments. *Infrared* (*IR*) spectroscopy has been used for the structure determination of bile pigments. The advantage of IR analysis is that it requires a small quantity of the bile pigment sample. Most of the studies have been done with solid samples (68,69). The IR spectroscopy is useful in detecting the bile pigment constituent in gallstones (70). In the IR spectrum, the carboxyl C=O appears at 1680 cm^{-1} (71), the N-H stretching is thought to be around 3410 cm^{-1} for the lactam groups and at 3265 cm^{-1} for the pyrrole groups (24). The band at 2500 cm^{-1} belongs to the carboxyl OH and the dimethyl ester does not have this characteristic band (71). It has also been observed that the IR spectra of the esters of bile pigments are shifted toward higher wave numbers, indicating the disruption of the hydrogen bonds formed by

the carboxyl groups. The ester bond has an absorption at 1740 cm^{-1}. The IR spectrum for bilirubin bound to human albumin, which suggested possible hydrogen bonding of the NH groups of bilirubin to albumin, was recorded by using dried films on thallium iodide windows (29).

There have been few reports on the analysis of bile pigments with *Raman spectroscopy*. The resonance Raman spectrum of biliverdin dimethyl ester has been recorded without band assignment (72). Hillig and Morris have recently reported a study of bilirubin and some derivatives by inverse Raman spectroscopy (73). The assignment was made by comparing with the Raman spectra of model compounds. The bilirubin spectra were recorded in organic solvents and compared with bilirubin ditauride in aqueous solution. The results confirmed the internal hydrogen bonds of bilirubin in chloroform. The solvation effects of bilirubin in DMSO and of its conjugates in water were evidenced by the hydrogen bonding with the solvent molecules. Very recently, a study of the binding of bilirubin with albumin has been reported using the surface-enhanced Raman spectroscopy (74). In this report, it was suggested that bilirubin is completely enclosed by albumin in the binding.

Nuclear magnetic resonance (*NMR*) spectroscopy has proven to be the most useful tool in the determination of the structure and properties of bile pigments. This part of the work has been reviewed by Kaplan and Navon (75). It will be further discussed in Chapter 6 of this thesis.

4.4 Treatments for Hyperbilirubinemia and the Binding of Bile Pigments

4.4.1 Treatments for Hyperbilirubinemia

Phototherapy is one of the most commonly used treatments for hyperbilirubinemia. The photoisomerization process was first observed in 1958 when the yellow pigmentation in the skin of jaundiced babies was found to be faded after exposure to sunlight (76). Subsequently this method has been applied widely in the treatment of hyperbilirubinemia (77). The patients are usually illuminated with visible light, preferably blue light, over an adequate period of time (78). This is thought to render the normally occurring bilirubin into a water-soluble form, photobilirubin, which can be excreted more easily (see Section 4.2.3 for more details). However, it had been observed that photooxidation

products of bilirubin can cause complications such as green jaundice (32) and the bronze baby syndrome (79), as mentioned above.

Hyperbilirubinemia can also be treated by *hemoperfusion*; in this technique blood is passed through a column packed with suitable sorbents to remove the toxic substances (80). Activated charcoal (81,82) and agar (83) have been tested for the adsorption of bilirubin. Charged and uncharged resins have also been used (84,85). However, the application of these materials is limited by their poor biocompatibility, lack of specificity and low capacity. Immobilizing albumin improves the biocompatibility and selectivity of these materials but does not improve the capacity (86).

Since bilirubin also joins in the enterohepatic circulation, it is expected that hyperbilirubinemia can be treated by an *orally administered adsorbent* which binds bilirubin in the gastrointestinal tract and thus blocks the re-entry of bilirubin or its metabolites into the portal veins. The reabsorption involves only a small fraction of the bilirubin metabolite, urobilinogen, while most of the urobilinogen is excreted in the feces (87). Therefore, tests with charcoal and cholestyramine have met with minimal success (88,89). The feeding of agar to jaundiced infants has been reported to reduce the bilirubin level in plasma and enhance the fecal excretion of bilirubin (90).

4.4.2 Binding of Bile Pigments to Proteins

It is universally accepted that the bile pigments are bound to protein in the body. Biliverdin also binds to the common bilirubin-binding proteins and bilirubin can be displaced by biliverdin on ligandin (91), although there seems to be no competition between bilirubin and biliverdin for a common site on albumin (92). The following text is focussed mainly on the discussion of the binding of bilirubin since the biliverdin binding is of less significance in medical applications.

Serum albumin is known to be the natural carrier of bilirubin, along with many other bio-substances and drugs in the blood, including bile acids. The binding of bilirubin to albumin has been reviewed by Brodersen (29). Bilirubin is tightly bound to serum albumin with high affinity. Nonetheless, the binding is not very efficient in terms of binding capacity. Although the reported results have been controversial, it is generally agreed that each albumin molecule, with a molecular weight of over 66,000, can only bind two bilirubin molecule strongly.

The binding affinity of albumin for bilirubin is high. It is generally agreed that binding constants of the primary site is in the order of 10^7 for the first ligand and about 10^6 for the second (93-95). There are also numerous secondary binding sites which bind bilirubin loosely (96). It is possible that bilirubin can be replaced by some drugs, such as sulfonamides, and some of the bile acids, such as cholic and lithocholic bile acids (97).

Figure 4.10 shows the structure of human serum albumin as established by Brown (98). The amino acid sequence in serum albumin is mainly in the α-helix form with three domains on the basis of the secondary structure. This has been supported by the calculated probabilities of helical structure of the amino acid sequence of albumin by McLachlan and Walker (99).

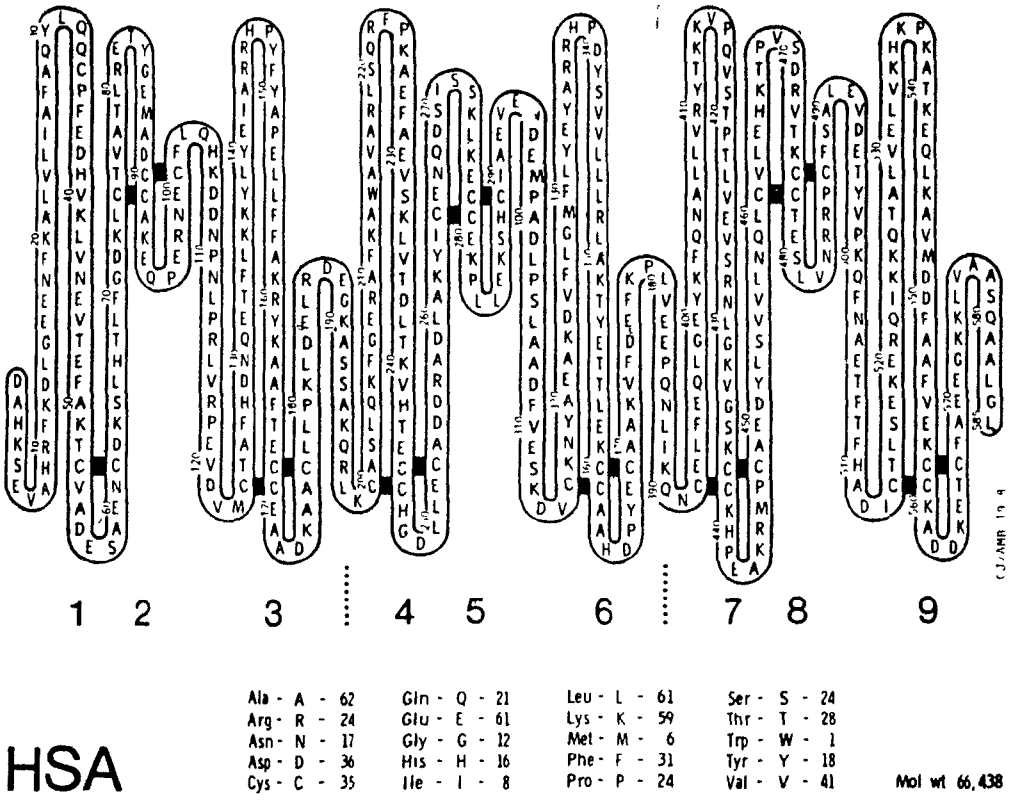

Figure 4.10 The primary structure of human serum albumin (HSA) showing the amino acid sequence and disulfide bridges (reference 29).

The exact locations of the binding sites on serum albumin have not been clearly elucidated. However, evidence suggests that basic amino acids, such as

arginine, lysine and histidine, are in the immediate vicinity of the binding sites (100-102). This suggestion is supported by the observation that polymer resins with peptide pendants containing arginine and lysine are very good adsorbents for bilirubin (103,104). Although certain mechanisms have been proposed for the binding process, the precise details are currently not fully understood. Adsorption studies, using polymeric supports with peptide pendants, indicate that the basicity of the amino acids in the pendants is an important feature. In addition, cooperative effects within the pendant are indicated, probably involving conformational changes of the peptides (104).

The lipophilic nature of the bilirubin molecules can facilitate the apolar interactions between bilirubin and albumin. Hydrophobic interactions were believed to be important in the binding process (105). Evidence suggests that the high affinity site on albumin for bilirubin is at a hydrophobic crevice located about 28 Å from the tryptophan residue (106,107). Figure 4.11 shows the enclosure of bilirubin molecules by the primary binding sites in the three-domain structure of albumin. The limited importance of carboxyl groups in the binding was supported by the binding of bilirubin dimethyl ester to albumin (108,109). However, the affinity of this kind of binding can be lower than that of bilirubin. Hydrogen bonding between the lactam groups of bilirubin and the amine groups on the protein may also contribute to the binding (110).

Based on the negative entropy changes found by Jacobsen (111), Brodersen questioned the importance of hydrophobic interactions in the binding process (29). The negative entropy change is consistent with salt linkage and other polar interactions, but it does not exclude hydrophobic interaction. As McDonagh has pointed out, *it may be inappropriate and misleading to consider bilirubin merely as a typical organic anion with respect to its complexation to albumin, at least at the high affinity site* (24). It seems safe to conclude that the binding of bilirubin to albumin at the first stage is the attraction of the oppositely charged groups of the interacting species and the subsequent conformational adjustment of albumin can accommodate the bilirubin molecule at a hydrophobic binding site. It appears that both the ionic nature and hydrophobicity of bilirubin contribute to the binding process at different stages.

There are a number of other bilirubin-binding proteins. *Ligandin* is known to bind bilirubin and other organic anions, such as bile acids in the liver.

With respect to organic anion transport, ligandin may function within the hepatocyte much as albumin does in the circulation (19). Compared with serum albumin, the purified ligandin seems to have a lower binding affinity for bilirubin (112). Nonetheless, the binding affinity of ligandin in nature is higher than in the purified form since its biological activity can be reduced after purification. It has been reported that *Z protein* (alias fatty acid binding protein), which, along with ligandin, is responsible for the binding of bilirubin in the liver, also has a high binding affinity for bilirubin (113).

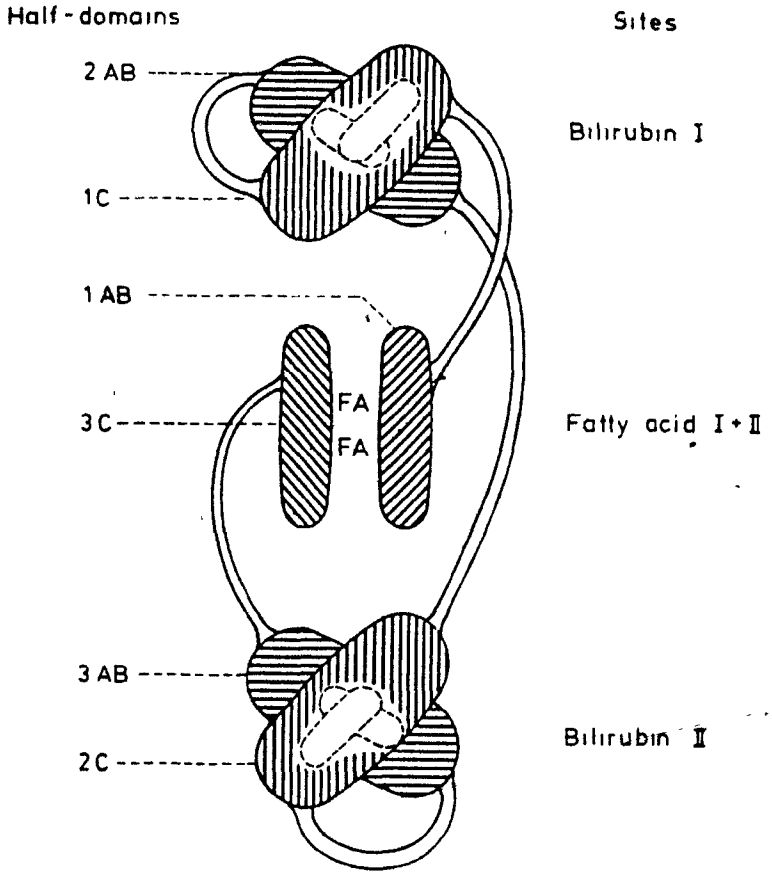

Figure 4.11 The simplified arrangement of albumin, showing the combination of six half-domains to form two binding sites for bilirubin and one site for fatty acid (reference 29).

4.4.3 Binding of Bilirubin with Polymeric Resins

For the treatment of hyperbilirubinemia, synthetic polymers have been developed for two purposes: hemoperfusion and oral administration.

Basic ion-exchange resins were mostly used for this purpose (84,85). Uncharged resins (84,114) can also adsorb bilirubin from aqueous media, indicating that bilirubin can be adsorbed without ionic salt linkage. On the other hand, charged resins are much better adsorbents for bilirubin than uncharged resins (115-117). This is an indication of the importance of the electrostatic attraction during the binding.

The porous resins generally have a higher capacity for bilirubin. Therefore, the degree of crosslinking of the resin is crucial for the binding of bile pigments. It was found that the uncharged polystyrene-divinylbenzene with large pore size and surface area has a much higher capacity than its counterpart with smaller pore size and surface area. This is supported by the results of Tong *et al.* (114), who have found that the porous non-ionic resins with an average pore diameter larger than 120 Å exhibit a higher capacity than resins with smaller pore sizes, indicating that bilirubin is probably trapped in the macroporous matrix of the resin. Similar pore size effects have also been observed with charged anion exchange resins by Sideman *et al.* (118,119). When albumin is coated on the hemoperfusion column, the compatibility can be enhanced (120). However, the adsorption capacity of the albumin coated polymer is usually very low (121).

Many polymeric materials have been tested in hemoperfusion to bind bilirubin from plasma. Others have been developed as orally administered sorbents for bilirubin in the gastrointestinal tract. The drawbacks of these polymeric materials are obvious in respect to biocompatibility, capacity and specificity. Based on these observations, water-swellable resins with peptide pendants mimicking the binding sites of albumin have been developed for the adsorption of bilirubin. Colleagues in our laboratories have been able to demonstrate that the peptide resins with arginine and lysine pendants are good adsorbents for bilirubin (103,104,122). The increment of the number of arginine and lysine residues on the pendants can augment the binding affinity of these resins. The binding of bilirubin with the arginine containing resins is of higher affinity while the lysine-containing resins demonstrated a cooperative binding effect (103,104).

The binding of biological molecules is usually a complicated process, with various interactions being very different in their nature. It may also involve

conformational rearrangements for both the macromolecules and bilirubin. Although extensive research has been conducted in the study of bilirubin binding to proteins and the removal of bilirubin with different adsorbents, there is still a gap between the understanding of the binding mechanism and the development of the novel adsorbents. The objective of this research is to apply the available knowledge of bilirubin binding in the preparation of polymeric materials with improved binding capacity and specificity, and at the same time to understand the nature of the interactions.

Previous studies have shown that bilirubin can be bound to oligopeptide pendants consisting of basic amino acids and that polymer resins with longer peptide pendants have enhanced binding affinity for bilirubin. This leads to the consideration of immobilizing polypeptides of basic amino acids onto the surface of a water-swellable resin for the study of the binding of bilirubin. This work is presented in Chapter 5 of this thesis. To understand better the nature of the binding between bilirubin and peptides, NMR experiments have also been conducted to study the mechanism of the interaction studies of bilirubin with oligopeptides and other substrates. Chapter 6 describes the application of the determination of the NMR spin-lattice relaxation times combined with nitrogen-15 NMR experiments in the study of the interactions between bilirubin and dilysine.

References

1. R.F. Troxler, p. 649, in *Bile Pigments and Jaundice*, J.D. Ostrow, ed., Marcell Decker, NY-Basel, 1986
2. J.W. Seligman, *Pediatric Clinics of North America*, **24**, 509, 1977
3. A.L. Lehninger, **Chap. 22, Biosynthesis of Amino Acids and Nucleotides**, p. 718, in *Biochemistry*, Worth Publishers, 1975
4. D.W. Martin, Jr., **Chap. 24, Porphyrin & Bile Pigments**, p. 327, in *Harper's Review of Biochemistry*, 19th ed., D.W. Martin, Jr., R.A. Mayes & V.W. Rodwell, eds., Lange Medical Publications, Los Altos, CA, 1983
5. S.B. Brown & R.F. Troxler, **Heme Degradation and Bilirubin Formation**, p. 1, in *Bilirubin, Vol. II*, K.P.M. Heirwegh & S.B. Brown, eds., CRC Press, Florida, 1982
6. T.K. With, *Bile Pigments*, Academic Press, New York, 1968
7. Z.J. Petryka & R.B. Howe, **Chap. 12, Historical and Clinical Aspects of Bile Pigments**, p. 805, in *The Porphyrins, Vol. IV*, D. Dolphin, ed., Academic Press, NY-San Francisco-London, 1979
8. J.D. Ostrow & R. Schmid, *J. Clin. Invest.*, **42**, 1286, 1963
9. R. Brodersen, *J. Clin. Invest.*, **54**, 1353, 1974
10. G. Litwack, B. Ketterer & I.M. Arias, *Nature (London)*, **234**, 466, 1971
11. A.J. Levi, Z. Gatmaitan & I.M. Arias, *J. Clin. Invest.*, **47**, 61a, 1968
12. B.H. Billing, **Chap. 3, The Role of Conjugating Enzymes in the Biliary Excretion of Bilirubin**, p. 85, in *Bilirubin, Vol. II*, K.P.M. Heirwegh & S.B. Brown, eds., CRC Press, Florida, 1982
13. E.R. Gordon, C.A. Goresky, T.-H. Chan & A.S. Perlin, *Biochem. J.*, **155**, 477, 1976
14. J. Fevery, B. van Damme, R. Michiels, J. de Groote & K.P.M. Heirwegh, *J. Clin. Invest.*, **51**, 2482, 1972
15. W.L.G. Gent, G.A.D. Haslewood & G. Montesdeoca, *Biochem. J.*, **122**, 15p, 1971
16. M.J. Whiting & J.M. Watts, *Br. J. Surg.*, **73**, 229, 1986
17. B.H. Billing, p. 255, in *Bile Pigments and Jaundice*, J.D. Ostrow, ed., Marcell Decker, NY-Basel, 1986
18. M.S. Stoll, **Chap. 4, The Formation, Metabolism, and Properties of Pyrrolic Compounds Appearing in the Gut**, p. 103, in *Bilirubin, Vol. II*, K.P.M. Heirwegh & S.B. Brown, eds., CRC Press, Florida, 1982
19. J.R. Chowdhury, A.W. Wolkoff & I.M. Arias, **Chap. 18, Heme and Bile Pigment Metabolism**, p. 309, in *The Liver: Biology and Pathobiology*, I.M. Arias, H. Popper, D. Schachter & D.A. Shafritz, eds., Raven Press, New York, 1982
20. Najib-Farah, *Lancet*, **1**, 505, 1937
21. R. Stocker, Y. Yamamoto, A.F. McDonagh, A.N. Glazer & B.N. Ames, *Science*, **235**, 1043, 1987
22. K. Bernhard, G. Ritzel & K.U. Steiner, *Helv. Chim. Acta*, **37**, 306, 1954
23. H. Beer & K. Bernhard, *Chimia*, **13**, 291, 1959

24. A.F. McDonagh, **Chap. 6, Bile Pigments: Bilatrienes and 5,15,-Biladienes**, p. 293, in *The Porphyrins, Vol. VI*, D. Dolphin, ed., Academic Press, NY-San Francisco-London, 1979
25. A. Bennet & H.W. Siegelman, **Chap. 7, Bile Pigments in Plants**, p. 493, in *The Porphyrins, Vol. VI*, D. Dolphin, ed., Academic Press, NY-San Francisco-London, 1979
26. J.A.T.P. Meuwissen & K.P.M. Heirwegh, **Chap. 2, Aspects of Bilirubin Transport**, p. 39, in *Bilirubin, Vol. II, Metabolism*, CRC Press, Florida, 1982
27. L. Johnson & T.R. Boggs, p. 122, in *Phototherapy in the New Born*, G.B. Ordell, R. Schaffer & A.P. Simopoulus, eds., National Academy of Sciences, Washington D.C., 1974
28. P.C. Scheidt, E.D. Mellits, J.B. Hardy, J.S. Drage & T.R. Boggs, *J. Pediatr.*, **91**, 292, 1977
29. R. Brodersen, **Binding of Bilirubin to Albumin**, p. 305, in *CRC Crit. Rev. Clin. Lab. Sci.*, CRC Press, 1980
30. F.F. Fenech, W.H. Bannister & J.L. Grech, *Br. Med. J.*, **3**, 155, 1967
31. S.M. Purcell, F.H. Wians, Jr., N.B. Ackerman, Jr. & B.M. Davis, *J. Am. Acad. Dermatol.*, **16**, 172, 1987
32. A.J. Greenberg, I. Brossenmaier & S. Schwartz, *Dig. Dis. Sci.*, **16**, 873, 1971
33. K.L. Tan & E. Jacobsen, *Acta Pediatr. Scand.*, **71**. 409, 1982
34. H. Fischer, H. Phenenger & O. Weissbarth, *Z. Physiol. Chem.*, **268**, 197, 1941
35. C.C. Kuenzle, M.H. Weibel, R.R. Pelloni & P. Hemmerich, *Biochem. J.*, **133**, 364, 1973
36. D.A. Lightner, **Chap. 1, Structure, Photochemistry, and Organic Chemistry of Bilirubin**, p. 1, in *Bilirubin, Vol. I, Chemistry*, K.P.M. Heirwegh & S.B. Brown, eds., CRC Press, Florida, 1982
37. R. Bonnett, J.E. Davies, M.B. Hursthouse & G.M. Sheldrick, *Proc. R. Soc. London, Ser. B*, **202**, 249, 1978
38. D. Kaplan & G. Navon, *J. Chem. Soc., Perkin II*, 1374, 1981
39. M.C. Carey & A.P. Koretsky, *Biochem. J.*, **179**, 675, 1979
40. B.F. Scharschmidt & R. Schmid, *J. Clin. Invest.*, **45**, 678, 1966
41. R. Brodersen & J. Theilgaard, *Scand. J. Clin. Lab. Invest.*, **24**, 395, 1969
42. R. Brodersen, **Chap. 3, Physical Chemistry of Bilirubin: Binding to Macromolecules and Membranes**, p. 75, in *Bilirubin, Vol. I, Chemistry*, K.P.M. Heirwegh & S.B. Brown, eds., CRC Press, Florida, 1982
43. J.J. Lee, L.H. Daly & M.L. Cowger, *Res. Commun. Chem. Pathol. Pharmacol.*, **9**, 763, 1974
44. M.C. Carey & W. Spivak, **Chap. 4, Physical Chemistry of Bile Pigments and Porphyrins with Particular Reference to Bile**, p. 81, in *Bile Pigments and Jaundice*, J.D. Ostrow, ed., Marcel Dekker, NY-Basel, 1986
45. P.E. Hansen, H. Thiessen & R. Brodersen, *Acta Chem. Scand.*, **B33**, 281, 1979
46. H. Fischer & H. Orth, p. 619, in *Die Chemie Des Pyrrols, Vol. 2*, Akad. Verlagsges., Leipzig, 1937
47. R. Lemberg & J.W. Legge, *Hematin Compounds and Bile Pigments*, Wiley (Interscience), New York, 1949

48. A.F. McDonagh & D.A. Lightner, *Pediatrics*, **75**, 443, 1985
49. D.A.Lightner, W.P. Linnane III & C.E. Ahlfors, *Pediat. Res.*, **18**, 696, 1984
50. A.O. Pedersen, F. Schonheyder & R. Brodersen, *Eur. J. Biochem.*, **72**, 213, 1977
51. L. Stern, p. 3, in *Bilirubin, Mead Johnson Symposium on Perinatal and Development Medicine*, No.19, 1982
52. S.E. Braslavsky, A.R. Holzwarth, & K. Schaffner, *Angew. Chem. Int. Engl.*, **22**, 656, 1983
53. C.C. Kuenzle, *Biochem. J.*, **119**, 395, 1970
54. D.W. Hutchison, B. Johnson & A.J. Knell, *Biochem. J.*, **133**, 493, 1973
55. C.H. Gray, A. Lichtarowicz-Kulczycka, D.C. Nicholson & Z. Petryka, *J. Chem. Soc.*, 2264, 1961
56. D. Harmatz & G. Blauer, *Arch. Biochem. Biophys.*, **170**, 375, 1975
57. Q. Chae & P.-S. Song, *J. Am. Chem. Soc.*, **97**, 4176, 1975
58. K.S. Lee & L.M. Gartner, *Pediatr. Res.*, **10**, 782, 1976
59. M.S. Stoll & C.H. Gray, *Biochem. J.*, **117**, 271, 1970
60. N. Blankaert, K.P.M. Heirwegh & F. Compernolle, *Biochem. J.*, **155**, 405, 1976
61. H. Saxerholt, T. Midtvedt & B.E. Gustafsson, *Scand. J. Clin. Lab. Invest.*, **44**, 565, 1984
62. F. Shinya, *Tohoku J. Exp. Med.*, **143**, 249, 1984
63. P.L.M. Jansen & A. Tangerman, *J. Chromatogr.*, **182**, 100, 1980
64. N. Blanckaert, P.M. Kabra, F.A. Farina, B.E. Stafford, L.J. Marton & R. Schmid, *J. Lab. Clin. Med.*, **96**, 198, 212, 1980
65. F. Li, C.K. Lim & T.J. Peters, *J. Chromatogr.*, **353**, 19, 1986
66. S. Onishi, S. Itoh, N. Kawade, K. Isobe & S. Sugiyama, *Biochem. J.*, **185**, 281, 1980
67. J.J. McCarthy, S.A. McClintock & W.C. Purdy, *Anal. Lett.*, **17(B16)**, 1843, 1984
68. B.T. Newbold & G. LeBlanc, *Can. J. Biochem.*, **42**, 1697, 1964
69. D.W. Hutchinson, B. Johnson & A.J. Knell, *Biochem. J.*, **123**, 483, 1971
70. B.P. Duggal, B.N.B. Rao, B.M.L. Kapur & N. Ananthakrishnan, *Indian J. Med. Sci.*, **33**, 313, 1979
71. J. Fog & E. Jellum, *Nature (London)*, **198**, 88, 1963
72. L. Margulies & M. Stockburger, *J. Am. Chem. Soc.*, **101**, 743, 1979
73. K.J.D. Hillig & M.D. Morris, *J. Raman Spectr.*, **15**, 288, 1984
74. Y.-Z. Hsieh, N.-S. Lee, R.-S. Sheng & M.D. Morris, *Langmuir*, **3**, 1141, 1987
75. D. Kaplan & G. Navon, *Isr. J. Chem.*, **23**, 177, 1983
76. R.J. Cremer, P.W. Perryman & D.H. Richards, *Lancet*, 1094, 1958
77. H. Moseley & D.J. Summer, *Scot. Med. J.*, **28**, 103, 1983
78. A.N. Cohen & J.D. Ostrow, *Pediatrics*, **65**, 740, 1980
79. S. Onishi, S. Itoh, K. Isobe, H. Tokari, H. Kitoh & Y. Nishimura, *Pediatrics*, **69**, 273, 1982
80. T.M.S. Chang, *Contr. Nephrol.*, **29**, 11, 1982
81. T.M.S. Chang, *Lancet*, **2**, 1371, 1972
82. B.H. Lauterburg, E.R. Dickson, A.A. Pineda, G.L. Carlson & H.F. Taswell, *J. Lab. Clin. Med.*, **94**, 585, 1979

83. C. Romagnoli, G.Polidoni, M. Foschini, L. Cataldi, P. de Turris, G. Tortorolo & R. Mastrangelo, *Arch. Dis. Child.*, **50**, 202, 1975
84. R.A. Willson, A.F. Hofmann & G.G.R. Kuster, *Gastroenterology*, **66**, 195, 1974
85. S. Sideman, L. Mor, D. Mordohovich, M. Mihich, O. Zinder & J.M. Brandes, *Trans. Am. Soc. Artif. Intern. Organs*, 27, 434, 1981
86. S. Sideman, L. Mor, M. Mihich, D. Mordohovich, S. Lupovich, J.M. Brandes & M. Zeltzer, *Contr. Nephrol.*, 29, 90, 1982
87. G.J. Dhar, p. 526, in *Chemistry and Physiology of Bile Pigments*, P.D. Berk & N.I. Berlin, eds., National Institutes of Health, Bethesda, 1977
88. R.A. Ulstrom & E. Eisenklam, *J. Pediatr.*, **65**, 27, 1964
89. R. Lester, L. Hammaker & R. Schmid, *Lancet*, **2**, 1257, 1962
90. R.L. Poland & G.B. Odell, *New Engl. J. Med.*, **284**, 1, 1971
91. P.V. Woolley, M.J. Hunter & I.M. Arias, *Biochim. Biophys. Acta*, **446**, 115, 1976
92. J.J. Lee & M.L. Cowger, *Res. Commun. Chem. Pathol. Pharmacol.*, **5**, 505, 1973
93. R. Brodersen, *J. Biol. Chem.*, **254**, 2364, 1979
94. C.B. Berde, B.S. Hudson, R.D. Simoni & L.A. Sklar, *J. Biol. Chem.*, **254**, 391, 1979
95. M. Branca, A. Gamba, P. Manitto, D. Monti & G. Speranza, *Biochim. Biophys. Acta*, **742**, 341, 1983
96. E.P. Shapovalenko & I.V. Kolosov, *Bioorganicheskaya Khimiya*, 4, 315, 1978
97. D. Bratlid, Scand. *J. Clin. Lab. Invest.*, **30**, 107, 1972
98. J.R. Brown, p. 1, in *Albumin Structure, Biosynthesis and Function*, FEBS 11th Meeting, Copenhagen, T. Peters & I. Sjoholm, eds., Pergamon Press, Oxford, 1977
99. A.D. McLachlan & G.E. Walker, *Biochim. Biophys. Acta*, **536**, 106, 1978
100. G.B. Odell, R.S. Brown & N.A. Holtzman, *Birth Defects, Orig. Artic. Ser.*, **6**, 30, 1970
101. C. Jacobsen, *Int. J. Pept. Prot. Res.*, **7**, 159, 1975
102. C. Jacobsen & J. Jacobsen, *Biochem. J.*, **181**, 251, 1979
103. D.S. Henning, G.R. Brown & L.E. St-Pierre, *Int. J. Artif. Organs*, **9**, 33, 1986
104. M. Bouvier, G.R. Brown & L.E. St-Pierre, *Can. J. Chem.*, **65**, 1927, 1987
105. G. Blauer & T.E. King, *J. Biol. Chem.*, **245**, 372, 1970
106. R.F. Chen, p. 273, in *Fluorescence Techniques in Cell Biology*, A.A. Thaer & M. Sernetz, eds., Springer-Verlag, Berlin-NY, 1973
107. J.J. Lee & M.L Coeger, *Res. Commun. Chem. Pathol. Pharmacol.*, **6**, 621, 1973
108. G. Barac, *Bull. Soc. Chim. Biol.*, **28**, 633, 1946
109. L. Kucerova, J. Jirsa & R. Papezova, *Acta Univ. Carol. Med.*, **17**, 275, 1971
110. E. Stenhagen & E.K. Rideal, *Biochem. J.*, 33, 1591, 1939
111. J. Jacobsen, *Int. J. Pept. Prot. Res.*, **9**, 235, 1977
112. K. Kamisaka, I. Lisytosky, G. Fleischner, Z. Gatmaitan & I.M. Arias, **The Binding of Bilirubin and Other Organic Anions to Serum Albumin and Ligandin (Y Protein)**, p. 156, in *Bilirubin Metabolism in the Newborn (II)*, Excerpta Medica, Amsterdam, 1976
113. K. Kamisaka, I. Listowsky, Z. Gatmaitan & I.M. Arias, *Biochim. Biophys. Acta*, 393, 24, 1975

114. Tong M.-R., Chen C.-Z., Liu R.-X., Yu Y.-T. & He B.-L., p. 379, in *Hemoperfusion and Artificial Organs*, T.M.S. Chang & He B.-L., eds., China Academic Publishers, Tianjin, 1983

115. R.A. Willson, K. Webster, A.P. Hofmann & W.H. Summerskill, *Gastroenterology*, **62**, 1191, 1972

116. K. Ouchi, W. Piatkiewic, P.S. Malchesky, W.D. Carey, R.E. Hermann & Y. Nose, *Trans. Am. Soc. Artif. Intern. Organs*, **24**, 246, 1978

117. Chen C.-Z., Wang H.-M., Tong M.-R., Yu Y.-T., Song J.-C., Qian S.-C. & Chang H.-Z., *Int. J. Artif. Organs*, **9**, 323, 1986

118. S. Sideman, L. Mor & J.M. Brandes, *Trans. Am. Soc. Artif. Intern. Organs*, **25**, 497, 1979

119. S. Sideman, L. Mor, J.M. Brandes & S. Lupovich, *J. Biomed. Mat. Res.*, **17**, 91, 1983

120. D. Bihari, R.D. Hughes, A.E.S. Gimson, P.G. Langley, R.J. Ede, G. Eder & R. Williams, *Int. J. Artif. Organs*, **6**, 299, 1983

121. B.F. Scharschmidt, J.F. Martin, L.J. Shapiro, P.H. Plotz & P.D. Berk, *J. Lab. Clin. Med.*, **89**, 101, 1979

122. D.S. Henning, G.A. Lajoie, G.R. Brown & L.E. St-Pierre, *Int. J. Artif. Organs*, **7**, 209, 1984

5 Adsorption of Bilirubin with Polypeptide-Coated Resins

5.1 Introduction

This chapter describes the immobilization of selected polypeptides onto a polymer support and the use of these materials in the adsorption for one of the toxic bile pigments, bilirubin. The first section introduces some general background and the methods used for the studies.

5.1.1 Binding of Bilirubin to Lysine-Containing Peptides

The binding of bilirubin to various proteins has been discussed in Chapter 4. It is important to recall that the basic amino acids such as lysine and arginine are thought to be located at or close to the high affinity binding site for bilirubin on albumin. The importance of the lysine residue of albumin in the binding of bilirubin was demonstrated by Jacobsen in an affinity labeling experiment (1,2), in which bilirubin was covalently attached to albumin by reacting the bilirubin-albumin complex using a carbodiimide reagent. When the amino acid contents of this albumin complex were analyzed, following enzymatic hydrolysis, it was found that the bilirubin was bound to lysine 240.

Based on these observations, water-swellable polyamide resins with peptide pendants containing lysine residues were prepared previously in this laboratory and demonstrated good binding affinities for bilirubin (3). The binding is remarkably enhanced as the peptide pendants become longer, an indication of the possible existence of positive cooperative binding, especially in the case of lysine-containing peptide pendants (3). Based on those results, it is of interest to consider the use of polymers with even longer polypeptide pendants, such as polylysine, for the adsorption of bilirubin.

Woolley *et al.* reported the binding of bilirubin to basic polypeptides, such as poly-L-lysine and poly-L-arginine in 1975 (4). The bilirubin binding to polylysine in alkaline solutions was later studied by circular dichroism (5,6).

The intrinsic dissociation constant (pK_a) for the ε-amino groups of polylysine is about 10.44 (7). At neutral pH's, the side chain groups are positively charged and the repulsion between these groups prevents the peptide from forming interchain hydrogen bonds. Therefore, the polylysine chains exist as irregular random coils instead of forming α-helices. However, between pH 10 and 11, as the charges on the side chains are neutralized, polylysine chains are transformed to the α-helix conformation, as shown in the titration curve in Figure 5.1 (8). On heating polylysine undergoes conformational changes to adopt the β-sheet form (9). Polylysine can combine electrostatically with various anionic electrolytes, which usually leads to precipitation except in solutions of high ionic strength (10,11).

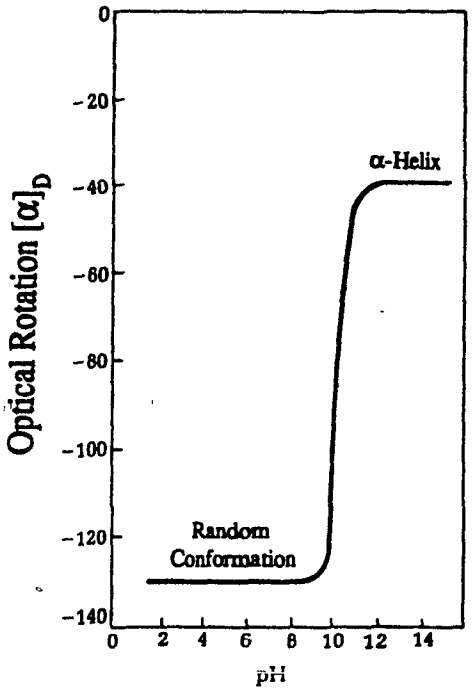

Figure 5.1 The effect of pH on the conformation of polylysine. The transition between the α-helix and the random coil conformations occurs around pH 10-11 and the unfolding of the helix is accompanied by a large change in optical rotation to a more negative value (reference 8).

Due to their excellent biocompatibility, polypeptides have found many applications in the medical and biochemical fields. The term *poly[amino acids]* is often used for the polypeptides in which all the amino acid residues are

identical. Polylysine, being a polybase, is especially useful for medical purposes. Crosslinked and non-crosslinked polylysine have been used successfully as drug carriers for a number of pharmacological purposes (12).

5.1.2 Polypeptide Coating onto Polymeric Supports

Klotz and Harris have reported that linear polylysine has a lower affinity than serum albumin when tested for the binding of small molecules. However, crosslinked polylysine has a much higher affinity than albumin (13). This effect has been attributed to the conformational changes of the polypeptide chains. It is believed that the compact conformation of the peptides increases the local concentration of the amino acid residues and thereby enhances the binding between the peptide and the substrates (13).

The enhancement of the local residue concentrations can be achieved by crosslinking of the polypeptide chains with an appropriate reagent (13), or by preparation of multichain clusters of polypeptides (14). Another way is to immobilize polypeptides onto the surface of a resin by forming covalent chemical bonds. This ensures relatively stronger adherence of the polypeptide to the resin surfaces.

The immobilization of serum albumin (15) and polylysine (16,17) dates back to the early 1960's. Polylysine was reported to be coated noncovalently to columns for use in RNA fractionations (18).

One disadvantage of noncovalent coating of polypeptides is that it can result in significant losses of the coated materials from the solid polymer support (19). Therefore, covalent coupling of the peptide to the resin support is preferable. Polylysine has been coated covalently onto polystyrene beads, by reaction with glutaraldehyde, for the study of actin assembly interactions (19). Upon chemical modification, water swellable polyacrylamide resins and positively charged glass beads are also good carriers of polylysine (20,21). These materials has been used in plasma membrane isolation (22).

5.1.3 The Present Study

This research concerns the binding behavior of peptide coated resins for the adsorption of bile pigments, especially unconjugated bilirubin. A water swellable polymeric support has been selected for biocompatibility.

Polylysine can be coupled to the resin surface by forming covalent bond linkages. An amide bond can readily be formed by reacting some of the side chain amino groups with carboxyl groups on the resin support. Since the length of the peptide chain is likely to affect its conformation, and hence have an effect on its binding behavior, polypeptides of different molecular weights were chosen to test for the effect of the degree of polymerization of the polypeptides.

While it is expected that the amount of coating will affect the absolute binding capacity of the peptide resins, it is not known if the amount of coating can influence the local concentration of the lysine residues, thus leading to different binding affinities. To test this factor, different amounts of polypeptide can be coated on the resin to verify the activity of the polypeptide coated resins during the adsorption of bilirubin in solution.

It is well known that the amino acids in nature exist mainly in the L-form. The peptide consisting of the D-amino acids can be resistant to certain enzymatic hydrolysis (Appendix 2). Therefore, poly-D-lysine was coated onto the polymer support. Being the stereoisomer of the chiral lysine residue, it is expected that poly-D-lysine will have a similar binding affinity for bilirubin to that of poly-L-lysine.

As a comparison to polylysine, poly-L-ornithine, also a basic polypeptide, can also be used for coating onto the polymer resin. The structure of ornithine is similar to that of lysine except that ornithine has three rather than four methylene groups on the side chain. Ornithine is usually obtained as a degradation product of arginine. In spite of its rare existence in humans, it is also a naturally occurring amino acid. In the ureotelic animals, which possess large amounts of arginase, ornithine is formed after the cleavage of urea from the guanidine group of arginine in the cytosol under the action of arginase, as shown in Figure 5.2 (23).

The stereostructures of L- and D-lysine, L-ornithine and L-arginine are shown in Figure 5.3.

The polypeptide coated resins have been prepared and used for the adsorption studies of bilirubin. The characteristics of these resins in the adsorption for bilirubin are discussed in Section 5.3. These results are also compared with the previous experimental data obtained using cholestyramine and the resins with oligopeptide pendants.

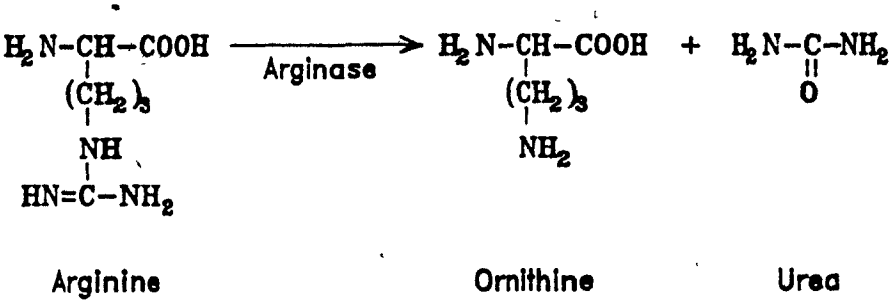

Figure 5.2 The formation of ornithine from arginine under the action of arginase.

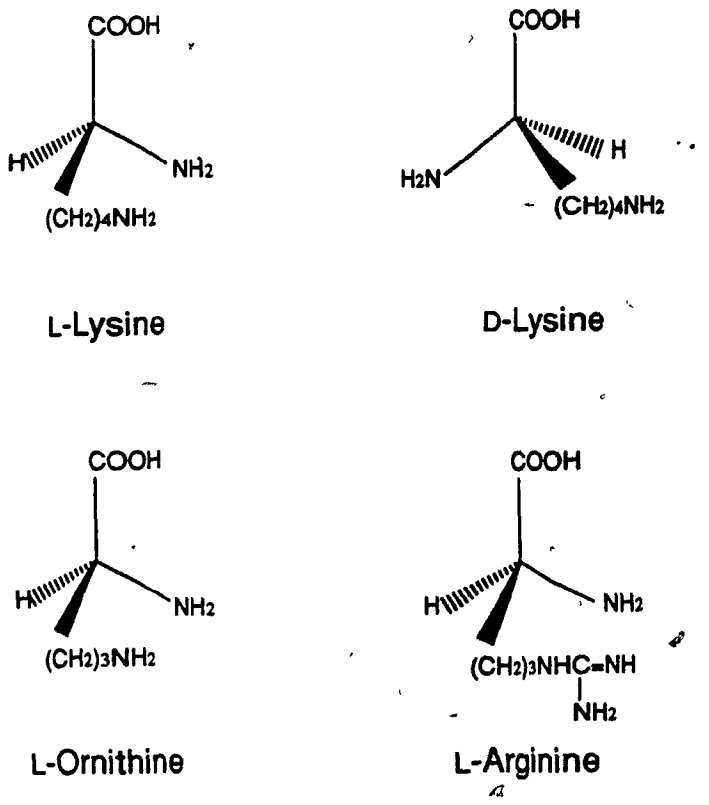

Figure 5.3 The stereostructures of lysine, ornithine and arginine.

5.2 Preparation of Polypeptide-Coated Resins for Adsorption Experiments

A polyacrylamide resin (Bio-Gel P-2, mesh size 200-400, from Bio-Rad), in its porous bead form, was used as a support for polylysine. The resin, which is a copolymer of acrylamide and N,N'-methylene-*bis*-acrylamide (Figure 5.4) (24), has amide groups as functional groups and is water swellable.

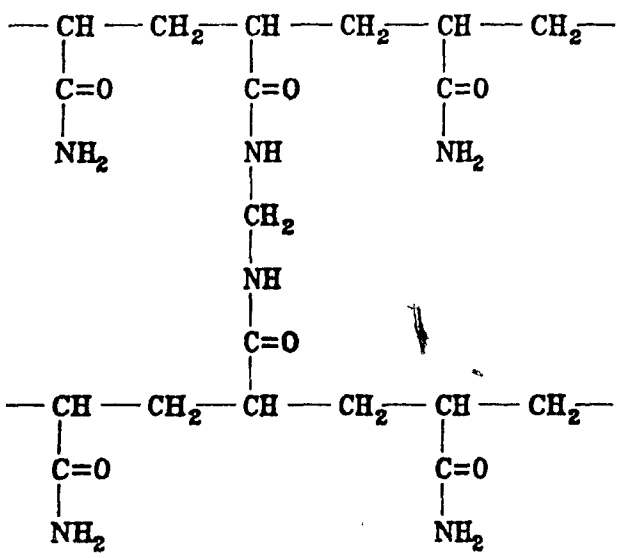

Figure 5.4 The structure of the polyacrylamide resin (Bio-Gel P), copolymer of acrylamide and N,N'-methylene-*bis*-acrylamide.

The preparation of the polypeptide coated resins is shown schematically in Figure 5.5. It was expected that lysine residues of the polylysine chain would be selectively coupled covalently to the solid polymer support. This coupling would ensure strong attachments of the polypeptide to the resin. Meanwhile, sufficient free lysine residues would be left as functional units for binding with bilirubin.

5.2.1 Treatment of the Polyamide Resin

Since the polyamide resin was obtained in the amide form, the amide functional groups were partially hydrolyzed to form free carboxyl groups onto which some of the amino groups on the side chains of the polypeptides were selectively coupled.

It is known that the hydrolysis of polyamide polymers at its first stage results in a conversion of a portion of the amide groups to carboxyl groups (25).

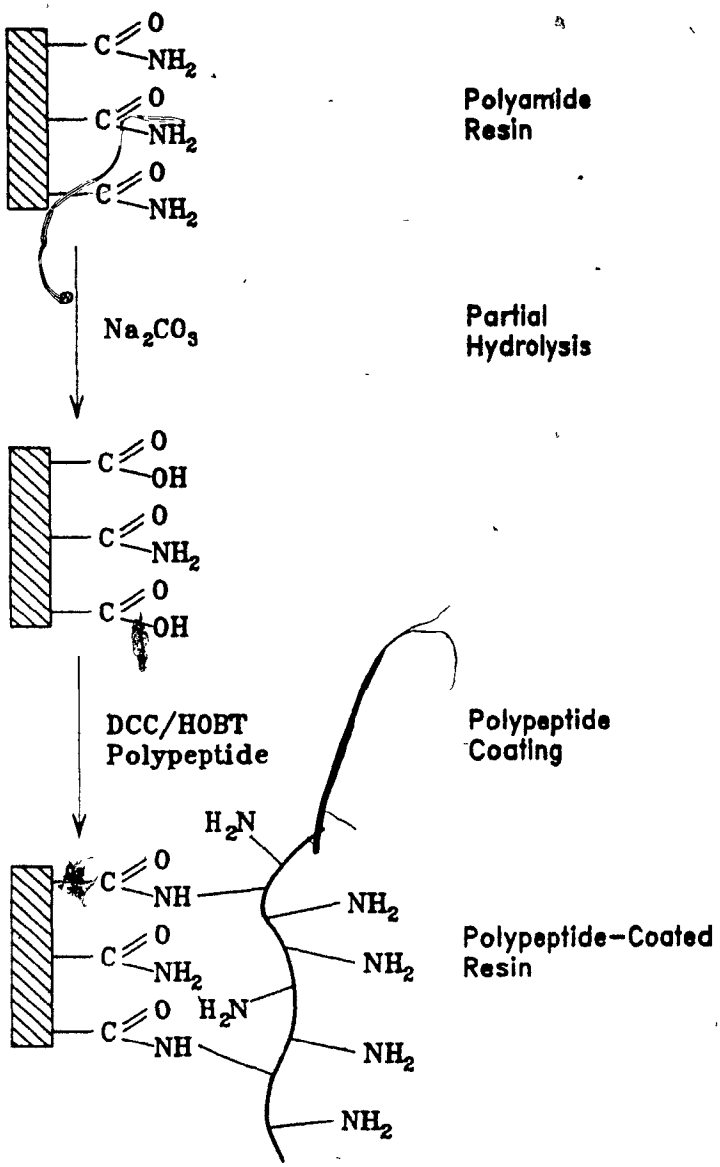

Figure 5.5 The preparation scheme of the polypeptide coated resins.

The hydrolysis of the polyamide resin was performed according to a modifications of the procedure reported by Jacobson (20). The resin was first hydrated with deionized water at 85-90°C for three hours. The supernatant was then aspirated and the mixture was cooled to 60°C. A relatively weak base, 0.5 M sodium carbonate, was used for the partial hydrolysis of the amide functional

groups. When it was added to the resin and stirred at 60°C, an odor of ammonia escaped from the solution. After 3 minutes, the supernatant was aspirated. This procedure was repeated three times, followed by incubation at 60°C for 100 minutes. The resin was then washed three times with deionized water, acetone and ether, repetitively. Finally the resin was dried under vacuum at room temperature for 24 hours.

5.2.2 Coupling of Polypeptide to the Resin

The next step was the coupling of the polypeptide to the carboxyl groups of the polyamide resin. All of the polypeptides used were purchased from Sigma Chemical Co. These polypeptides included poly-L-lysine (DP = 67, MW = 14,000), poly-L-lysine (DP = 2700, MW = 564,000), poly-D-lysine (DP = 1070, MW = 220,000), poly-L-ornithine (DP = 1000, MW = 200,000). The solvents were redistilled or pre-treated as described in Section 2.2.

About 1.5 grams of partially hydrolyzed polyamide resin was mixed with dimethylformamide (DMF) followed by stirring for 30 minutes to swell the resin. After stirring DMF was decanted. Since the carboxyl groups on the resin are sterically isolated, it was difficult to form the anhydride between these groups. Therefore, 1-hydroxybenzotriazole (HOBT, from Sigma) was used along with 1,3-dicyclohexyl-carbodiimide (DCC) to form active esters. The amount of HOBT added to the resin was calculated to render one fifth, on a molar basis, of the available side chain amino groups active for coupling. The solution of HOBT was allowed to mix with the resin for about 10 minutes. Saturated DCC (equal molarity with HOBT) solution in DMF was then added to the mixture. About 100 mg of polypeptide was then dissolved in DMF and the solution was poured into the mixture with the resin. The coupling with the HOBT active esters is usually slower than the coupling with anhydride. Therefore, the mixture was agitated overnight at room temperature to ensure complete coupling. After coating with the polypeptide, the resin was washed with 10% N,N-diisopropylethylamine (DEA) solution in dichloromethane, DMF, dichloromethane and anhydrous ether several times. The resin was finally dried under vacuum overnight. The ninhydrin test gave a blue color which indicated that free primary amino groups of the lysine side chains were present on the resin.

Poly-L-lysines (PLL) of different degrees of polymerization were selected. Poly-D-lysine (PDL) and poly-L-ornithine (PLO) were also coated onto the

hydrolyzed resin, using the same procedure. The amount of coating was increased by prolonged coupling of polypeptide or by the addition of extra DCC solution to the mixture. The former is preferred since the latter alters the number of the covalent linkages between the resin and the polypeptide chains, which, in turn, decreases the number of free amino acid residues on the resin surface.

The coupling of poly-L-ornithine appeared to be more difficult than the coupling of polylysine, since it tended to precipitate from the solution. Coupling was repeated once to ensure enough poly-L-ornithine coating on the resin.

5.2.3 The Characterization of the Polypeptide-Coated Resins

The polypeptide-coated resins showed blue colors upon testing with ninhydrin. The amino acid contents of the resins were analyzed using the HPLC method described in Section 2.2.1. An internal standard of L-norleucine (Aldrich) was used. The resins were hydrolyzed with 6N HCl solution (Pierce) for at least 48 hours. An external standard containing lysine was used as a reference for the analysis of the lysine containing resins. An ornithine standard was prepared by dissolving L-ornithine (hydrochloride salt, from Aldrich) in the same citrate buffer and was used as a reference for the analysis of ornithine. The amount of polypeptide coating was calculated in terms of moles of amino acid residue per gram of resin and the results are shown in Table 5.1.

Table 5.1 The Amount of Coating for the Polypeptide Resins

Polypeptide-Coated Resin		Amount of Peptide Coated
Resin #	Polypeptide	(mmol amino acid residue/g resin)
5-1	Poly-L-Lysine (DP=2700)	0.018
5-2	Poly-L-Lysine (DP=2700)	0.18
5-3	Poly-L-Lysine (DP=67)	0.093
5-4	Poly-D-Lysine (DP=1070)	0.28
5-5	Poly-L-Ornithine (DP=1000)	0.077

DP: degree of polymerization

In the coupling process, about 100 mg of polypeptide were added to 1.5 grams of resin, corresponding to approximately 0.30 mmol/g resin. However, the amount of coating for the resins did not reach this value. A considerable amount

of polypeptide was lost during the coupling with the resin. This loss could be a consequence of the inefficient reaction of the polypeptide side chain amino groups with the resin carboxyl groups. The coating of polyornithine was especially difficult, probably due to the shorter length of the side chain, which is less accessible to the resin backbone.

5.2.4 Quaternization of the Poly-L-Lysine Coated Resin

The functional groups of the polypeptide-coated resins are primary amine groups. To test the effect of functionality of the resin in the binding of bilirubin, one of the resins, poly-L-lysine (DP = 67) coated resin, was quaternized by reacting it with methyl iodide in methanol in the presence of potassium bicarbonate for 48 hours (26). The reaction was monitored by the disappearance of the free amino groups on the side chains of lysine residues using the ninhydrin test. A quantitative measure of the extent of the quaternization of the resin was obtained by a potentiometric titration of the iodide with standard silver nitrate in a solution containing potassium nitrate.

5.2.5 Adsorption Experiments

The polypeptide coated resins were tested for the adsorption of bilirubin in a phosphate buffer, 0.050 M KH_2PO_4-NaOH solution (pH = 7.8). The buffer was usually de-oxygenated with nitrogen and kept below 5°C in a refrigerator for a maximum storage of one week. The adsorbate was prepared by first dissolving bilirubin in small amount of 0.10 M NaOH solution in which it dissolves well. The solution was then diluted carefully with the phosphate buffer to reach a final concentration about 0.20 mM (10 mg/dl). This was used as the stock solution and was always freshly prepared for the adsorption experiments. Aliquots of the stock solution were diluted to different concentrations, ranging 0.02-0.20 mM (1-10 mg/dl). Each of these solutions were deaerated with nitrogen.

An aliquot of 20 ml of each of the sample solutions was mixed with about 10 mg of polypeptide coated resin.[9] The adsorption was conducted at 0°C under a constant flow of nitrogen. Kinetics experiments for the adsorption, performed previously by Henning (27), showed that the adsorption equilibrium could be reached within 60 minutes under such conditions. Therefore, the mixture was stirred for one hour. Vigorous stirring was avoided since it can cause precipitation of bilirubin. To prevent any possible photodegradation or

photoisomerization of bilirubin, the whole process was carried out in a dark room, using a dim red light when needed.

Since the absorbance of the bilirubin solutions obeys the Beer's law in the concentration range used for the adsorption (see Section 4.3.1), the solution of the adsorbate was analyzed using a Beckman 25 Double Beam Spectrophotometer at a wavelength of 438 nm by comparison with the standard bilirubin solutions.

Neither the polyamide resin support or the hydrolyzed form of the resin adsorbed bilirubin under the conditions described above.

5.3 Adsorption of Bilirubin Using the Polypeptide-Coated Resins

5.3.1 Poly-L-Lysine Coated Resins

(1) The Effect of the Amount of Coating

It is expected that the capacity of the resin to adsorb bilirubin should be greatly affected by the amount of polypeptide attached to the resin. As shown in Figure 5.6, the capacity of the resin on a per gram of resin basis is greatly enhanced as the amount of coating increases. However, when calculated on a basis of per mole of lysine residues, the capacities of the resins with different amounts of coating remain unchanged for the binding of bilirubin (Figure 5.7). On this basis, the adsorption isotherms for the polylysine coated resins are almost identical. If the polymer matrix of the resin were also involved in the binding of bilirubin, the calculated amount of adsorption based on the number of lysine residues in a unit weight of the resin should be different for the resins with different amounts of coating. Thus, this is consistent with the previous experiments that indicated the binding of bilirubin by the polymer matrix is minimal (Section 5.2.3). Since the Bio-Gel resin support, itself a polymer containing both aliphatic chain and hydrophilic groups, does not adsorb bilirubin from the phosphate buffer solution, it is obvious that the hydrophobic interaction or hydrogen bonding are not crucial factors in the adsorption process.

Even when the resin is coated with polypeptide, it is not likely that hydrogen bonding or hydrophobic interactions can dominate in the binding process. On the other hand, Figure 5.7 indicates that the number of bound ligands, i.e., bilirubin molecules, is directly related to the number of lysine residues, which suggests a specific interaction between bilirubin and the lysine

residues. This relation is consistent with an electrostatic interaction, which is evidenced by the NMR relaxation time measurements as discussed in Chapter 6. It is also known that the amino groups of the lysine residues are protonated under the experimental conditions (pH = 7.8). Therefore, it is possible that these groups can form ionic linkages with the carboxyl groups of bilirubin. The ionic linkage makes an important contribution to the binding, although other kinds of interactions such as hydrophobic interaction and hydrogen bonding may play lesser roles.

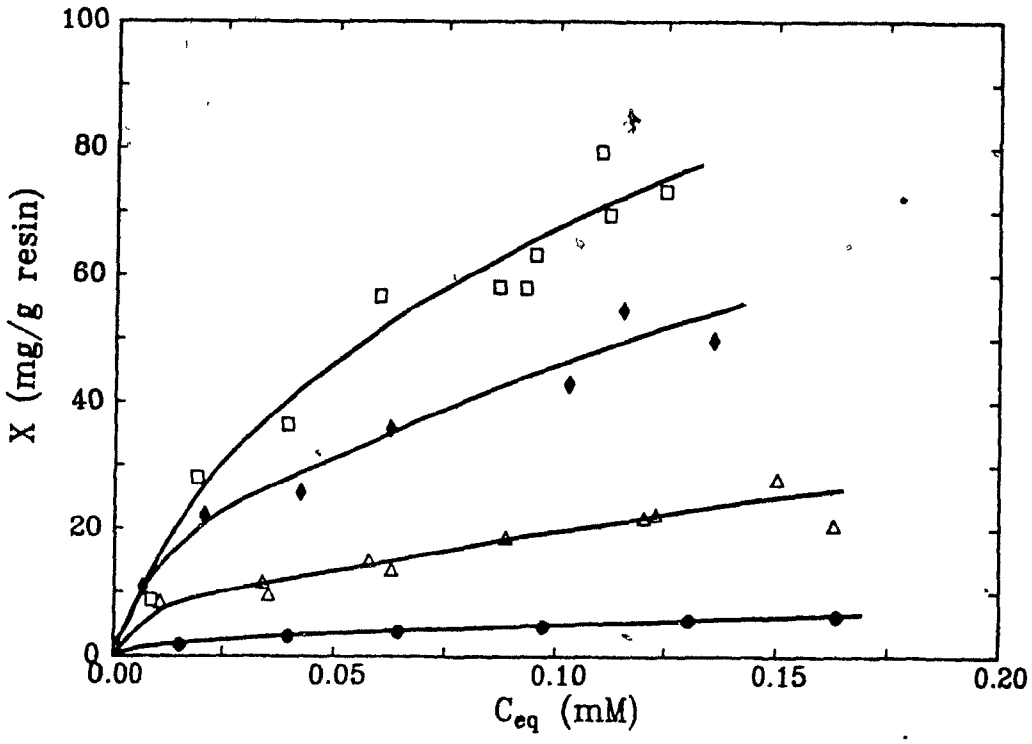

Figure 5.6 The adsorption isotherms of the polylysine-coated resins for bilirubin comparing the amount of coating. ● Resin 5-1 (PLL, DP = 2700, 0.018 mmol/g); ♦ Resin 5-2 (PLL, DP = 2700, 0.18 mmol/g); Δ Resin 5-3 (PLL, DP = 67, 0.093 mmol/g); ❑ Resin 5-4 (PDL, DP = 1070, 0.28 mmol/g).

The concentration of lysine residues at a certain defined area was reported to be important in the binding (13). If this is true, the result is an indication that the amount of coating does not alter the distribution of lysine residues in a defined local area. In other words, the local concentration of lysine residues is not affected by the amount of coating. In general, the amount of polylysine coated on

the polyamide resins is still very low. Hence, an increase in the amount of coating within a certain range is not sufficient to change the local concentration of lysine residues at a specific area. The adsorption behavior of these resins also indicates that the coated polylysine is completely permeable to bilirubin under the experimental conditions. Therefore, improved resins can be expected if more polylysine can be coated onto the surface of the resin. It can be predicted that the local concentration of lysine residues can be saturated when the resin bead is fully covered with the polypeptide chains. In practice, it is ideal to maintain the largest possible amount of polypeptide coating on the resin so that the absolute capacity of the resins in binding would be enhanced.

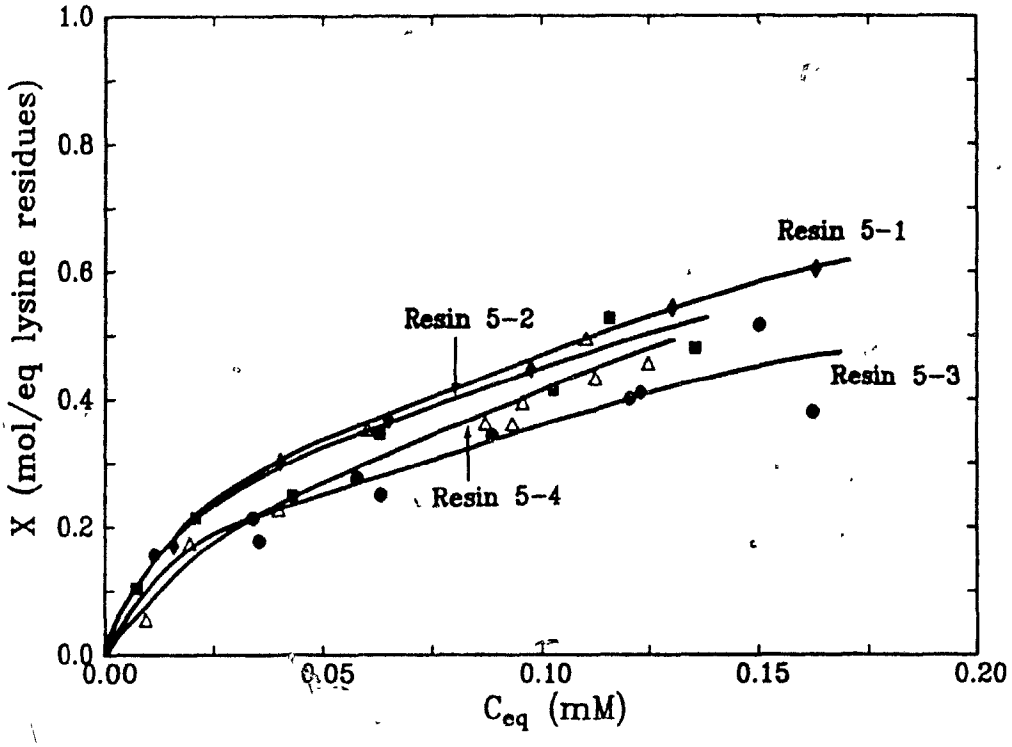

Figure 5.7 The adsorption isotherms of the polylysine-coated resins, calculated on a per lysine residue basis. ♦ Resin 5-1 (PLL, DP = 2700, 0.018 mmol/g); ■ Resin 5-2 (PLL, DP = 2700, 0.18 mmol/g); ● Resin 5-3 (PLL, DP = 67, 0.093 mmol/g); Δ Resin 5-4 (PDL, DP = 1070, 0.28 mmol/g).

(2) The Effect of the Molecular Weight of Polylysine

It has been shown that the length of oligopeptide pendant consisting of lysine can affect its binding affinity for bilirubin (3). It is of interest to know if

the number of basic amino acids (i.e., the degree of polymerization) in a polypeptide chain is still important in their role as adsorbents. To study this effect, polylysines with different degrees of polymerization (DP = 67 and 2700) were chosen for the experiments.

Since the amount of coating does not affect the adsorption capacity of the resin on a per amino acid residue basis, Resin 5-3, coated with polylysine of lower molecular weight (DP = 67) can be compared with Resin 5-2, coated with polylysine of a higher molecular weight (DP = 2700), to indicate the effect of the molecular weight of polylysine. As shown in Figure 5.7, the capacity of Resin 5-3 seems to be slightly lower than that of Resin 5-2, indicating that the resin coated with polylysine of higher molecular weight has a slightly increased capacity for bilirubin.

Although the polypeptide chains are randomly attached to the resin surface when coated, the number of lysine residues which are attached to the resin is still small as compared to the free lysine residues of long polypeptide chain. At the pH of the phosphate buffer (pH = 7.8), the side chain amino groups are positively charged and the peptide chains of polylysine exist mainly as random coils because of mutual repulsion. However, the existence of random coil does not exclude the possible conformational rearrangement of the peptide chain upon interaction with bilirubin. A higher molecular weight of polylysine, namely, an increase in the length of the peptide chain, is expected to improve the flexibility for any conformational changes. Therefore, it is reasonable that the polylysine of higher molecular weight would exhibit a higher capacity for bilirubin. This effect is consistent with the experimental results obtained in the binding of bilirubin with oligopeptide attached as pendant on the resin (3).

5.3.2 Poly-D-Lysine Coated Resin

Poly-D-lysine was used to replace poly-L-lysine to determine if there is any steric structural effect in the binding of bilirubin. A large amount of poly-D-lysine was easily coated onto the resin and Resin 5-4 has the highest amount of coating. Hence, its binding capacity on a per gram basis also ranks the highest, as shown in Figure 5.6. Each gram of this resin can be expected to adsorb as much as 80 mg of bilirubin at an adsorbate equilibrium concentration of about 0.14 mM (ca. 8 mg/dl).

When calculated on per mole of lysine residue basis, as shown in Figure 5.7, the affinity of the poly-D-lysine coated resin (Resin 5-4) is, within experimental error, identical to that of the poly-L-lysine coated resins (compare with Resins 5-1 and 5-2 in Figure 5.7). This is an indication that the binding of bilirubin depends solely on the number of lysine residues and that the stereostructure of lysine does not affect the binding behaviors of the polypeptide resin.

5.3.3 Poly-L-Ornithine Coated Resin

The structure of poly-L-ornithine differs from that of poly-L-lysine only by the shorter side chain of the amino acid residues. This difference appears to lead to a decreased solubility of polyornithine in the organic solvents. As a consequence, the ninhydrin test showed poor coupling of polyornithine after prolonged reaction, indicating the coupling of polyornithine was more difficult than that of the other polypeptides. As was seen in Table 5.1, the amount of coating for polyornithine resin is lower than that of polylysine coated resins.

Figure 5.8 shows the results obtained for the binding of bilirubin using the polyornithine coated resin. The binding capacity of Resin 5-5 is significantly lower than that of the polylysine coated resins. This decrease in adsorption is attributed to the shorter length of the side chain amino groups of the ornithine residues, which is expected to reduce the accessibility of the amino groups toward the binding ligands, the bilirubin molecules. On the other hand, repeated coupling during the coating of polyornithine can increase the number of linkages between the polyornithine and the resin, which, in turn, leads to a decrease of the number of free amino groups on the side chains. This can contribute, in part, to the decreased binding capacity of the polyornithine coated resin.

5.4 Comparison of Polylysine-Coated Resins with Other Resins

5.4.1 Comparison with the Resins Containing Lysine Pendants

A series of polymeric adsorbents with oligopeptide pendants consisting of an alanine-3 spacer and lysine residues were previously prepared in this laboratory (3,27), using the method described in Section 2.2 of this thesis. The three resins prepared had 1, 2, and 5 lysine residues in the sequence, respectively.

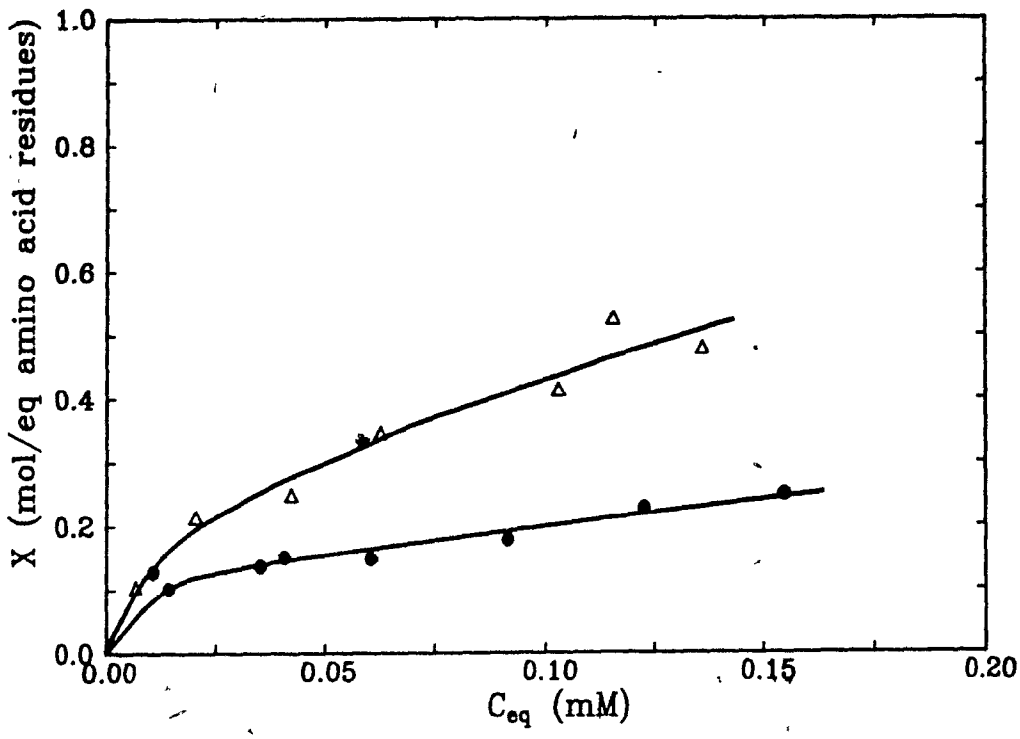

Figure 5.8 The adsorption isotherms of the resins coated with polyornithine and polylysine. ● Resin 5-5 (PLO, DP = 1000, 0.077 mmol/g); Δ Resin 5-2 (PLL, DP = 2700, 0.18 mmol/g).

Figure 5.9 shows the adsorption isotherms, calculated on the basis of the number of lysine residues. The resin containing five lysine residues has the highest binding capacity per lysine residue (ca. 0.35 mol/eq lysine residue). In this figure, it is clearly seen that the binding capacity for bilirubin is not directly proportional to the number of lysine residues in a unit weight of the resins. Thus, longer peptide pendants have a higher capacity on a per lysine residue basis than the shorter ones, i.e., the longer peptide pendants are more effective in the binding of bilirubin. If it is assumed that the resin backbone and the alanine spacer are not involved in the binding, i.e., that it is only the lysine residues in the pendants that contribute to the binding of bilirubin, this can be explained as an increased binding interaction when the local concentration of the lysine residues is enhanced. On the other hand, upon the binding of the first bilirubin molecule, the binding of the second ligand molecule may become easier. This is termed as the *positive cooperativity* in binding (28). The three isotherms in Figure 5.9 indicate increased binding capacity as the peptide chain grows longer. This was shown to

be a result of a positive cooperativity in binding, especially for the resin with lysine-5 pendants (29). This effect seems to be characteristic for the binding of bilirubin with lysine-containing peptides since it was also observed when a peptide sequence (containing lysine) from albumin was immobilized for the adsorption of bilirubin (30). It is assumed that the binding of bilirubin can be enhanced when bilirubin molecules in close proximity interact by stacking, which permits the interaction of the π-electrons on the pyrrole rings of bilirubin.

If the adsorption isotherms of the oligopeptide resins are compared with the polypeptide coated resins (such as Resins 5-1 and 5-3) in Figure 5.9, it is clear that, as a general trend, the polylysine coated resins demonstrate an increased binding capacity over that of oligopeptide pendants for the adsorption of bilirubin. Resin 5-3, coated with polylysine of lower molecular weight (DP = 67), shows a similar capacity to the resin with lysine-5 pendant, especially at higher equilibrium concentration.

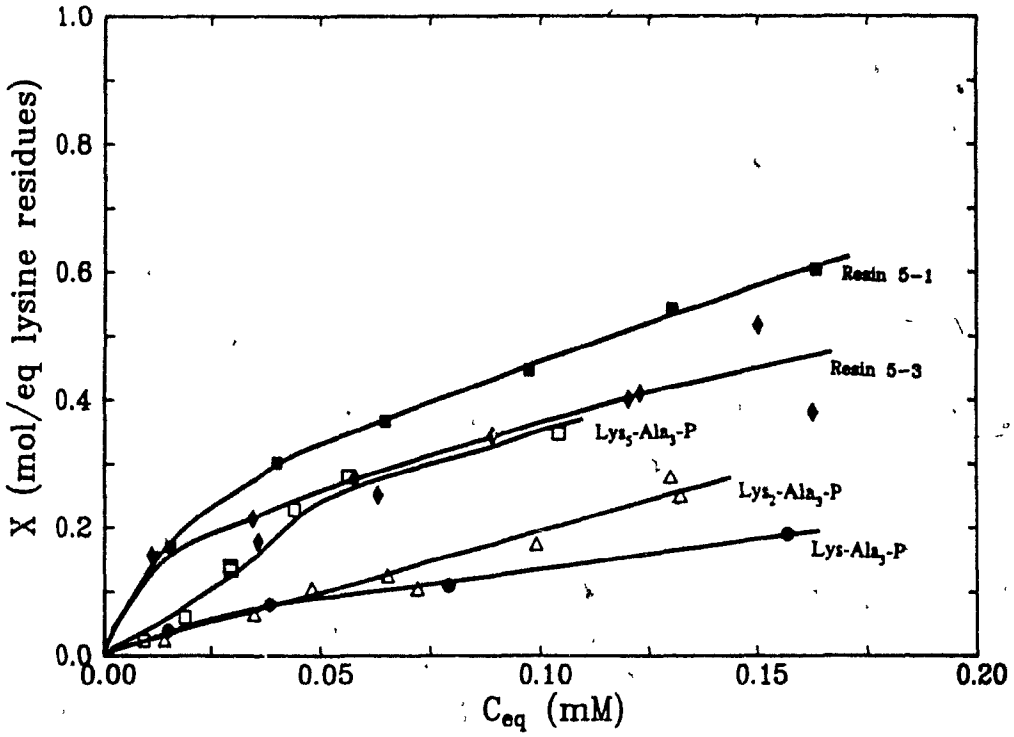

Figure 5.9 The adsorption isotherms of the resins with oligopeptide pendants containing lysine in comparison with those of the polylysine-coated resins. ● Lys-Ala_3-P; Δ Lys_2-Ala_3-P; □ Lys_5-Ala_3-P; ■ Resin 5-1 (PLL, DP = 2700, 0.018 mmol/g); ♦ Resin 5-3 (PLL, DP = 67, 0.093 mmol/g).

In the preparation of the polypeptide coated resins, the coupling reagents were added such that for every five lysine residues one lysine side chain would be coupled to the resin. Although it was impossible to control the number of free lysine residues in a sequence during coating, the average number must be no less than five. Therefore, it is very reasonable that the polylysine coated resins demonstrated similiar, or slightly better, adsorption capacities than the resin with Lys_5-Ala_3- pendants.

It has been shown that the peptide containing resins, especially those with lysine, have a positively cooperative effect in the binding of bilirubin (30,31). One of the obvious advantages of the polylysine coated resins is the enhanced possibility of cooperative binding. When cooperative binding exists for smaller peptides, the possibility of this effect can only be enhanced when the peptide chain becomes much longer. In fact, this effect may well be maximized in such circumstances, which, in turn, explains the fact that the degree of polymerization of polylysine does not affect its binding behavior significantly (Section 5.3.1). The cooperativity may be maximized as the peptide chain reaches a certain critical length.

5.4.2 Comparison with Quaternized Polylysine-Coated Resin

Cholestyramine type of resins, i.e., polymer resins with quaternary ammonium groups, have been used for the binding of bilirubin. As mentioned in Chapter 2 concerning the adsorption of bile salts, there is again a question about the importance of the quaternary ammonium group in the binding of bilirubin.

To answer this question, one of the resins coated with poly-L-lysine, Resin 5-3, was quaternized by reacting with methyl iodide in organic solvent (Section 5.2.3). It is assumed that the amino groups on the side chains of the lysine residues are methylated to form quaternary ammonium groups. This resin was also tested for the binding of bilirubin. When calculated on a per gram of resin basis, the adsorption capacity is slightly enhanced for the binding of bilirubin as shown in Figure 5.10.

The quaternary ammonium groups of the cholestyramine type of resins are considered to be the active units in the binding of organic anions. Based on the known poor capacity of cholestyramine on a per active site basis (see Section 5.4.3), it seems reasonable to conclude that, compared with other forms of protonated amines, the quaternary ammonium group has the same or slightly

higher affinity for bilirubin. This limited importance of the quaternary ammonium groups is one of the characteristics for the adsorption of bilirubin which is different from the adsorption of bile salts. As discussed earlier in Chapter 2, the basicity of the resin functional groups is very important in the binding of bile salts, therefore, the quaternary ammonium groups are preferred for these ligands. This result indicates that the binding of bile salts is different from the binding of bilirubin in term of mechanism because of the different intrinsic properties associated with these different species, bile salts and bile pigments.

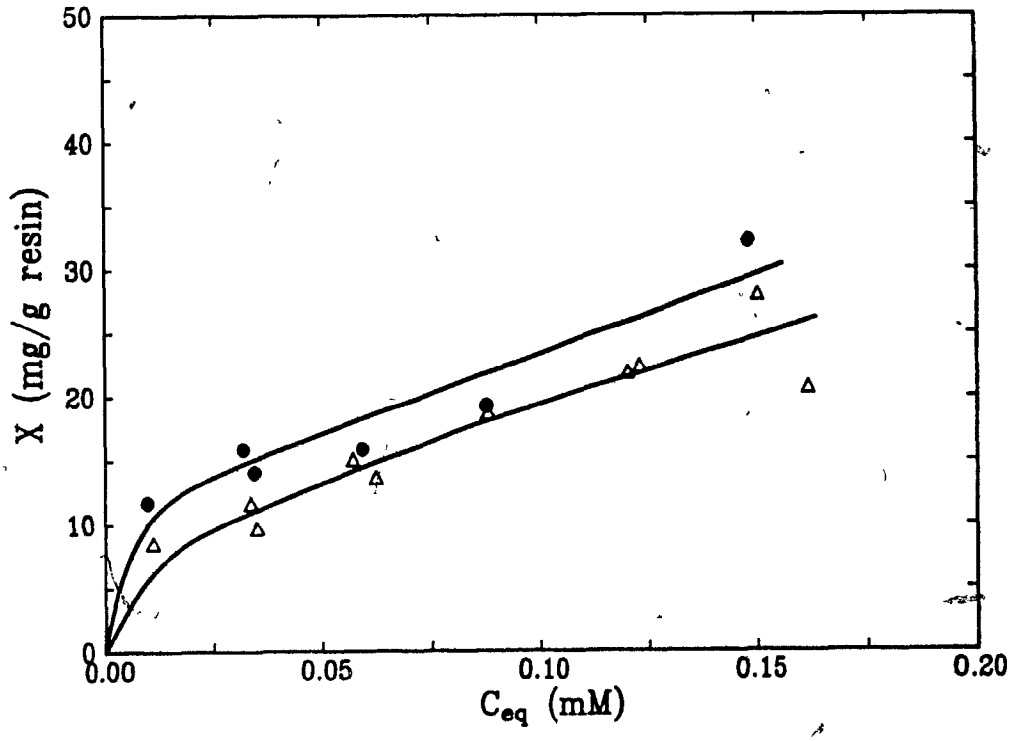

Figure 5.10 The adsorption isotherms of the polylysine-coated resin before and after methylation. ● Resin 5-3 after methylation; Δ Resin 5-3 (PLL, DP = 67, 0.093 mmol/g).

5.4.3 Comparison with Cholestyramine

Cholestyramine (Dowex 1X2, Aldrich, mesh size 200-400) was tested previously in this laboratory for the adsorption of bilirubin at various temperatures (27). Its binding capacity on a per gram basis at 0°C is shown in Figure 5.11a in comparison with Resin 5-4. The binding capacity of cholestyramine on a per gram basis is generally lower than that of the

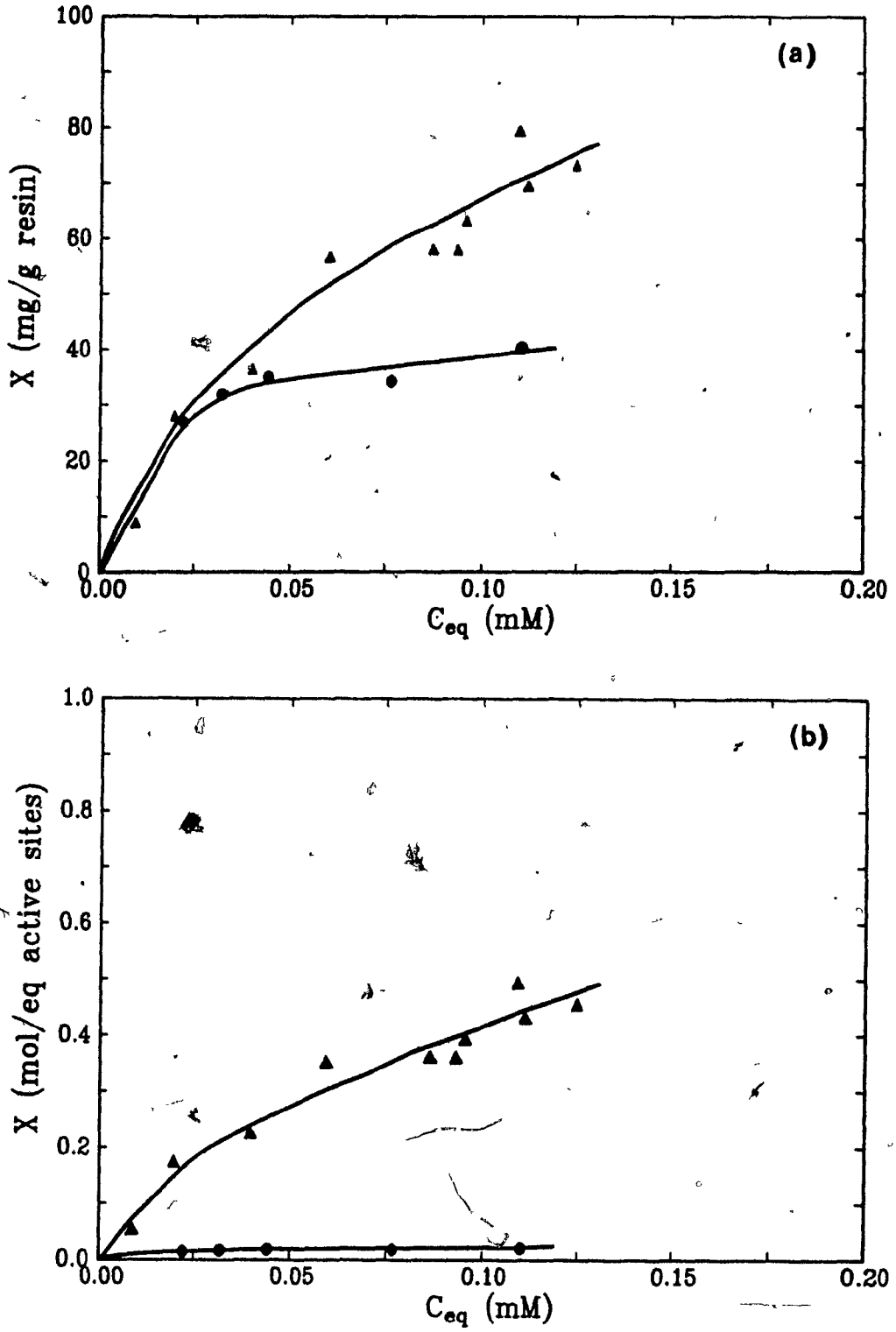

Figure 5.11 The adsorption isotherm of cholestyramine in comparison with that of the polypeptide coated resin: (a) on a weight basis; (b) on per active site basis. ● Cholestyramine; ▲ Resin 5-4 (PDL, DP = 1070, 0.28 mmol/g).

polypeptide-coated resin.

Assuming the quaternary ammonium groups are responsible for the binding, the number of active binding sites, or functionality, of cholestyramine was determined to be 3.3 mmol/g. Based on the discussion above, the active site of the polypeptide-coated resin can be regarded as the positively charged amino group on the side chain of the amino acid residue. When these results are calculated on a per active site basis, the active site being the quaternary ammonium group of cholestyramine and the side chain amino group of the lysine residue, the capacity of cholestyramine is much lower than any of the polypeptide coated resins (Figure 5.11b). This result is an indication that the quaternary ammonium groups are not very effective in the binding of bilirubin. This poor capacity of cholestyramine for bilirubin is largely attributed to the lack of specificity in the binding of organic anions. This phenomenon was also observed previously for the binding of bile salts, as discussed in Chapter 2. It is known that the strongly basic anion exchange resins have a high selectivity for phosphate anions (32). In a 0.050 M phosphate buffer solution at pH 7.8, large concentrations of phosphate anions, existing mainly as HPO_4^{2-} and $H_2PO_4^-$ anions, are present. The quaternary ammonium groups of cholestyramine can be neutralized by these phosphate ions, resulting in a reduced charge density on the resin surface. Therefore, it is expected that hydrophobic interactions between cholestyramine and the binding ligands will become increasingly important in this circumstance. On the other hand, the peptide containing resins have a high specificity for organic acids, as already demonstrated in the binding of bile acids (Section 2.4).

A variable temperature study for the adsorption of bilirubin was conducted in this laboratory (27). The previously reported adsorption isotherms, calculated on a weight basis, for the binding of bilirubin with cholestyramine at four different temperatures are recalculated on a basis of per mole of active binding sites and are shown in Figure 5.12. An enlarged scale is used to show the differences in binding capacity at various temperatures. As depicted in Figure 5.12, the binding affinity for bilirubin increases as the temperature rises.

This variable temperature study provides information on the thermodynamic aspects of the binding of bilirubin with cholestyramine. If the discussion on the thermodynamics of the binding process in Section 2.5.2 is

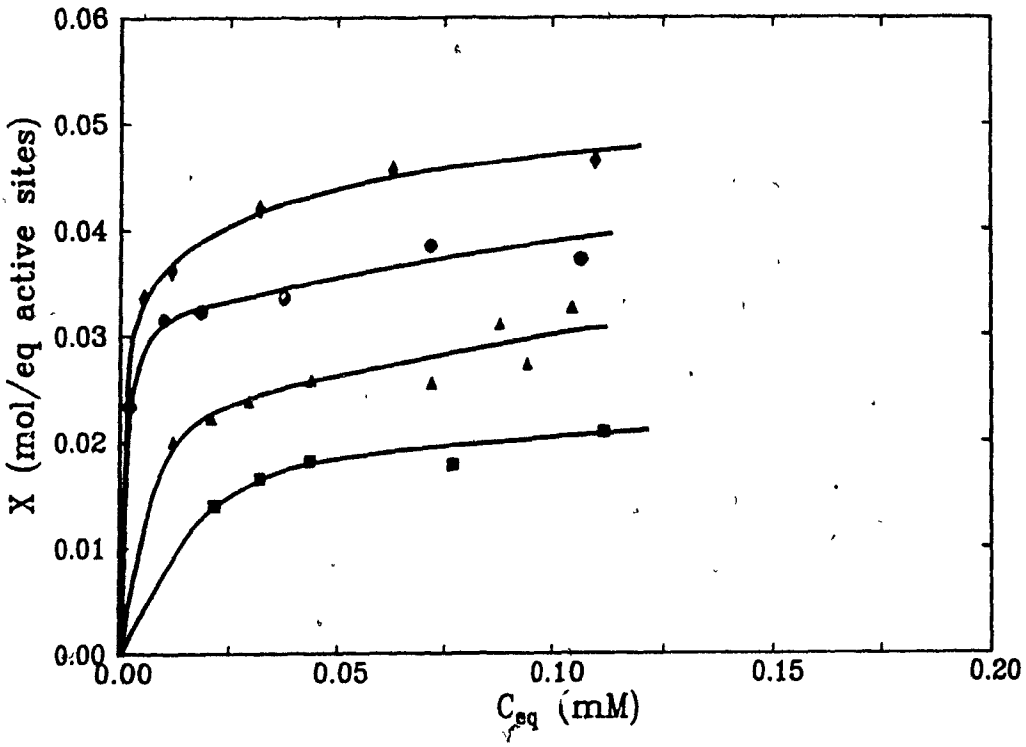

Figure 5.12 The adsorption isotherms of cholestyramine for bilirubin at different temperatures (recalculated from reference 27). ■ 0°C; ▲ 10°C; ● 20°C; ♦ 25°C.

continued, the stoichiometric binding constant, which is in fact the equilibrium constant for the binding process, can be related to temperature as follows:

Substituting Equation 2.2 into Equation 2.5 followed by rearrangement yields

$$\ln K = \frac{\Delta S}{R} - \frac{\Delta H}{R} \cdot \frac{1}{T} \qquad \text{(Equation 5.1)}$$

If both ΔS and ΔH are constant within the temperature range studied, a straight line will be obtained by plotting the logarithm of K (ln K) as a function of reciprocal temperature (1/T). From the slope and intercept of the line, the enthalpy change ΔH and entropy change ΔS for the binding, within the temperature range of the study, can be calculated.

When ln K is plotted as a function of 1/T, as shown in Figure 5.13, the negative slope of the line indicates the enthalpy change for the overall binding

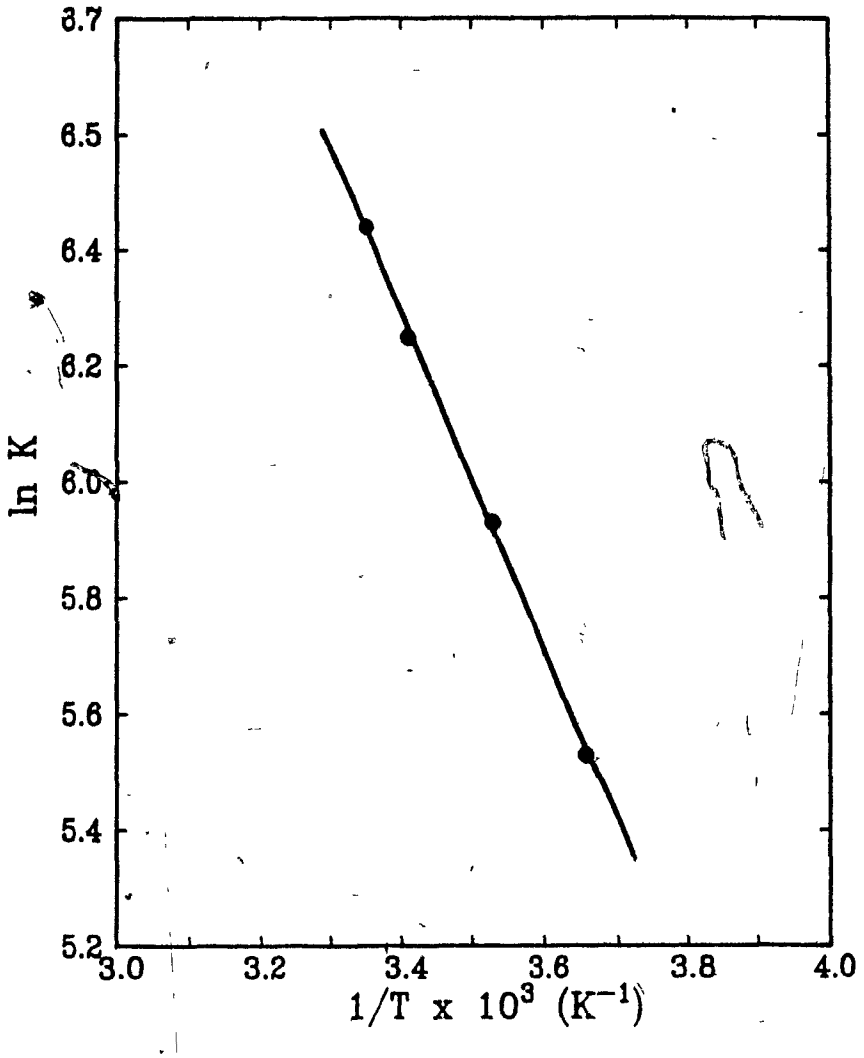

Figure 5.13 The plot of ln K as a function of reciprocal temperature for the binding of bilirubin with cholestyramine. The plot is characterized with a positive entropy change. It also indicates that the binding is an endothermic process.

process is *positive*, about 24 kJ mol^{-1}. Thus, the binding is an endothermic process. Since the formation of an ionic linkage is usually associated with a negative enthalpy change, this result suggests that, in the binding of bilirubin, the desolvation of the bilirubin molecules and of the binding sites on the resin is sufficiently endothermic so that the overall enthalpy change of the binding is positive. On the other hand, it is known from Chapter 2 that cholestyramine has a

high selectivity for the phosphate ions, such as $H_2PO_4^-$ and HPO_4^{2-}, in solution. Therefore, the adsorption is a competitve binding process among all the existing anions in the solution. The binding of phosphate ions is expected to be exothermic since it is a typical ionic bond formation process. Thus, as temperature increases, the binding of the phosphate ions becomes less favorable and this leads to an enhanced interaction between the resin and bilirubin.

From the intercept of this line, the ΔS is estimated to be approximately 130 J $K^{-1}mol^{-1}$, which strongly favors the binding. This indicates that the adsorption of bilirubin using cholestyramine resin is an entropy-driven process. The binding of bilirubin to the polymer is favored by a positive entropy change, probably related to the rearrangements of the water structure surrounding the bilirubin molecules. On the other hand, cholestyramine is a hydrophobic copolymer; therefore, its interaction is also favored by a positive entropy change for the water molecules surrounding the resin beads. Thus, the interaction between cholestyramine and bilirubin is largely determined by the positive entropy change, which is usually an indication of hydrophobic interactions. It can be concluded that the binding of bilirubin to cholestyramine involves other processes in addition to the ionic bond formation since a stronger base, such as the quaternary ammonium group, does not enhance the adsorption of bilirubin. This hydrophobic effect involved with cholestyramine is consistent with the similar effect in the binding of bile salts (Section 2.3).

5.5 The Evaluation of the Polypeptide-Coated Resins - A Summary

5.5.1 The Stoichiometric Binding Constants and Free Energy Changes

Previous results indicate that the binding of bilirubin with lysine-containing peptides is a cooperative process (3,30,31). The comparison between the polylysine-coated resins and the resins with oligopeptides pendants (Section 5.4.1) reveals that the binding capacity of the polylysine coated resins on a per lysine residue basis is somewhat higher than that of the resin with lysine-5 pendants, indicating an improved binding affinity. Since the exact length of peptide sequence consisting of free lysine residues is not known, the binding capacity was calculated on a per lysine residue basis. Thus, the stoichiometric binding constant better describes the binding of bilirubin with polypeptide coated

resins. The binding constants of the various resins for bilirubin were calculated using a derivative-free least square curve-fitting program as described in Chapter 2. The free energy changes of the binding process are calculated using Equation 2.5. These results are listed in Table 5.2.

Table 5.2 The Binding Constants and Free Energy Changes for the Adsorption of Bilirubin onto Various Resins

Resin	K x 10^{-3} (M^{-1})	ΔG (kJ mol^{-1})
Polypeptide-Coated Resins:		
5-1 Poly-L-Lysine (DP=2700)	9.3	-21
5-2 Poly-L-Lysine (DP=2700)	8.2	-21
5-3 Poly-L-Lysine (DP=67)	5.8	-20
5-4 Poly-D-Lysine (DP=1070)	7.3	-20
5-5 Poly-L-Ornithine (DP=1000)	2.7	-18
***Other Resins:**		
Lys-Ala_3-P	1.6	-17
Lys_2-Ala_3-P	2.4	-18
Lys_5-Ala_3-P	5.7	-20
Cholestyramine (Cl)	0.25	-13

Experimental conditions: 0°C in 0.050 M phosphate buffer (pH=7.8), constant stirring in dark under nitrogen for one hour.
DP: degree of polymerization; P: polyacrylamide resin.
* Result from Reference (27), recalculated on a basis of per mole of lysine residues rather than per mole of pendants; cholestyramine binding constant was calculated in accordance with the titration result, i.e., 3.3 mmol quaternary ammonium groups per gram of resin.

The polypeptide-coated resins, though having low peptide contents, exhibit excellent binding affinities for the bile pigment, bilirubin. It is to be noted that the binding constants listed in Table 5.2 are only average values for the binding equilibria with bilirubin and the adsorbents. It can be seen from Table 5.2 that the values of the binding constants for Resins 5-1, 5-2 and 5-4 are very close, indicating similar binding affinities. The difference between poly-L-lysine and poly-D-lysine is thus small in terms of binding affinity for bilirubin.

The binding constant for Resin 5-3, which was coated with a polylysine with a lower degree of polymerization, is slightly smaller than the other

polylysine coated resins. In fact, this binding constant is closer to but still higher than the binding constant of the resin with lysine-5 pendants. During the coating of polylysine, the HOBT and DCC was added quantitatively to form one amide linkage for every five lysine residues. Therefore, it is possible that the free lysine sequences in Resin 5-3 may have an average number of about five unattached lysine residues. It can be seen that the free energy changes of these resins in the binding of bilirubin are also very similar. The polyornithine coated resin has a lower affinity for bilirubin than the polylysine coated resins.

Comparing the binding constants for the resins with peptide pendants containing lysine as shown in Table 5.2, the binding affinities of these resins for bilirubin obviously fall in the order of $Lys_5 > Lys_2 > Lys$. The binding affinity for bilirubin is increased as the peptide pendants becomes longer. In the case of polypeptides, this effect is maximized since the resins show even higher affinities.

Cholestyramine resin has a greatly reduced binding affinity for bilirubin, as compared with peptide containing resins. Its poor water-swellability does not promote the diffusion of bilirubin molecules into its matrix and thus can have a negative effect on the accessibility of the binding sites to the adsorbate. This can also be an indication of the reduced importance of a stronger base, i.e., the quaternary ammonium groups, in the binding of bilirubin. On the other hand, hydrophobic interactions may play a more important role for cholestyramine than for the peptide resins.

The amino groups on the polylysine side chains remain protonated at the pH used for the adsorption studies. It is thus expected that the bilirubin dibasic acid forms an acid-base linkage with the side chains of the lysine residues. Due to the lack of information about the conformation of the polylysine chains on the surface of the polyamide resins, it is not known exactly how the lysine residues in the polypeptide chain interact with the bilirubin substrates. Previous results have shown that a positive cooperativity exists in the binding of bilirubin with resins attached with lysine-containing oligopeptide pendants (29). Therefore, it could also exist in the binding of bilirubin with polylysine coated resins.

The binding behavior of the immobilized polypeptides for bilirubin can be compared with that of albumin in a simplified way as follows. Human serum albumin, the natural carrier for bilirubin in serum, is also a polypeptide consisting of about 584 amino acid residues. Each albumin molecule, with a molecular

weight of roughly 66,300, strongly binds only two bilirubin molecules and loosely binds an additional 9-13 bilirubin molecules (33). For the polylysine coated resins, each lysine residue in the polylysine molecule can bind an average of 0.6 bilirubin molecules, corresponding to approximately 350 bilirubin molecules for every 584 lysine residues. It is thus clear that the immobilized polylysine exhibits an overwhelmingly higher capacity than albumin.

5.5.2 Summary

In conclusion, the polypeptide coated resins, especially the polylysine coated resins, exhibit high binding affinities for the bile pigment bilirubin. The binding capacity of the resin is directly proportional to the number of lysine residues, which implies a specific interaction between bilirubin and the lysine residues. The replacement of poly-L-lysine with poly-D-lysine does not affect the adsorption capacity of the resin, while the chemical and biological stability of the peptides can be enhanced (Appendix 2). The polylysine coated resins demonstrated improved binding affinity for bilirubin over the resins with lysine containing oligopeptide pendants, and much better affinity than cholestyramine. It can be expected that the polylysine coated resins, having a better biocompatibility than the commercially available adsorbents, can be applied for hemoperfusion or oral administration purposes in the elimination of the toxic bile pigments.

References

1. C. Jacobsen, *Int. J. Pept. Prot. Res.*, **8**, 295, 1976
2. C. Jacobsen, *Biochem. J.*, **171**, 453, 1972
3. D.S. Henning, G.R. Brown & L.E. St-Pierre, *Int. J. Artif. Organs*, **9**, 33, 1986
4. P.V. Woolley, III, M.J. Hunter & I.M. Arias, *Biochim. Biophys. Acta*, **393**, 24, 1975
5. P.V. Woolley, III, M.J. Hunter & I.M. Arias, *Biochim. Biophys. Acta*, **446**, 115, 1976
6. D. Marr-Leisy, K. Lahiri & P. Balaram, *Int. J. Pept. Prot. Res.*, **25**, 290, 1985
7. E. Katchalsky, M. Sela & R. Spanier, *Bull. Res. Council Isr.*, **3**, 446, 1955
8. A.L. Lehninger, p. 130, in *Biochemistry*, Worth Publishers, N.Y., 1975
9. N. Greenfield, B. Davidson & G.D. Fasman, *Biochemistry*, **6**, 1630, 1967
10. E. Katchalski & M. Sela, *Adv. Prot. Chem.*, **13**, 391, 1958
11. M. Sela & E. Katchalski, *Adv. Prot. Chem.*, **14**, 426, 1959

12. R. Duncan & J. Kopecek, **Soluble Synthetic Polymers as Potential Drug Carriers**, p. 51, in *Advances in Polymer Sciences, Vol. 57, Polymers in Medicine*, K. Dusek, ed., Springer-Verlag, Berlin-Heidelburg-NY-Tokyo, 1983
13. I.M. Klotz & J.U. Harris, *Biochemistry*, **10**, 923, 1971
14. M. Sela, E. Katchalski & M. Gehatia, *J. Am. Chem. Soc.*, **78**, 746, 1956
15. T.L. Goodfriend, L. Levine & G.D. Fasman, *Science*, **144**, 1344, 1964
16. E. Haber, L.B. Page & G.A. Jacoby, *Biochemistry*, **4**, 693, 1965
17. J. Spragg, K.F. Austen & E. Harber, *J. Immunol.*, **96**, 865, 1966
18. P.A. Bromley & R.D. Barry, *Anal. Biochem.*, **36**, 278, 1970
19. S.S. Brown, p. 291, in *Methods in Cell Biology, Vol. 24*, D.M. Prescott, ed., Academic Press, N.Y., 1982
20. B.S. Jacobson, *Biochim. Biophys. Acta*, **471**, 331, 1977
21. B.S. Jacobson, J. Cronin & D. Branton, *Biochim. Biophys. Acta*, **506**, 81, 1978
22. C.M. Cohen, D.I. Kalish, B.S. Jacobson & D. Branton, *J. Cell Biol.*, **75**, 119, 1977
23. A.L. Lehninger, p. 581, in *Biochemistry*, Worth Publishers, N.Y., 1975
24. S. Hjerten & R. Mosbach, *Anal. Biochem.*, **3**, 109, 1962
25. W.M. Thomas & D.W. Wang, **Acrylamide Polymers**, p. 192, in *Encyclopedia of Polymer Science and Technology, Vol. 1*, 2nd ed., H.F. Mark, N.M. Bikales, C.G. Werberger, G. Menges & J.I. Kroschwitz, eds., John Wiley & Sons, NY-Chichester-Brisbane-Toronto-Singapore, 1985
26. F.C.M. Chen & N.L. Benoiton, *Can. J. Chem.*, **54**, 3310, 1976
27. D.S. Henning, pp. 51-90, in *Ph.D. Thesis*, McGill University, 1985
28. R. Brodersen, **Binding of Bilirubin to Albumin**, p. 305, in *CRC Crit. Rev. Clin. Lab. Sci.*, CRC Press, Cleveland, 1980
29. S.-D. Clas, D.S. Henning, G.R. Brown & L.E. St-Pierre, in press, *Biomat., Artif. Cells, Artif. Org.*, 1988
30. M. Bouvier, G.R. Brown & L.E. St-Pierre, *Can. J. Chem.*, **65**, 1927, 1987
31. M. Bouvier, G.R. Brown & L.E. St-Pierre, submitted to *Can. J. Chem.*, 1988
32. R. Kunin, **Chap. 4, Anion Exchange Resin Characteristics**, p. 55, in *Ion Exchange Resins*, R.E. Krieger Pub. Co. N.Y., 1972
33. E.P. Shapovalenko & I.V. Kolosov, *Bioorganicheskaya Khimiya*, **4**, 315, 1978

6 NMR Studies of Bile Pigments

6.1 Introduction

6.1.1 NMR Studies of Bile Pigments

The study of bile pigments by nuclear magnetic resonance (NMR) techniques, even in its early stages has made a significant contribution in establishing and confirming the structure and conformation of bile pigments.

These studies focussed mainly on bilirubin and its derivatives and have been carried out since the 1960's (1-3). The proton spectra of bilirubin and other bile pigments were partially assigned by various authors, as reviewed by McDonagh (4). The *bis*-lactam structure, rather than the *bis*-lactim or mixed lactam-lactim tautomers, of bilirubin was confirmed by proton exchange studies (5). Proton NMR spectra showed that bilirubin and its dimethyl ester adopt different conformations in chloroform solutions, as manifested by the chemical shift of the methyl group at position 2. The chemical shift of this methyl group of bilirubin is not affected by the addition reaction of the vinyl group at C-18 with methanol, indicating that these two groups are sterically remote when bilirubin is intramolecularly hydrogen bonded. The chemical shift of the same C-2 methyl group of bilirubin dimethyl ester, however, is affected by the methanol addition, which implies a possible helical conformation (6). Bilirubin exists as two enantiomers because of the dissymmetry of the molecule, as shown in Figure 6.1. A fast interconversion process was confirmed by the study of the effect of temperature in chloroform on the splitting of the proton signal of the C-10 methylene bridge (7,8).

Owing to the instability and poor solubility of bilirubin in most solvents, the early recording, and hence the interpretation, of the NMR spectral data led to different spectral assignments and questionable structures for the bile pigments (9-11). Nonetheless, the summation of these studies has contributed to the

establishment of the chemistry of bilirubin as well as to the application of the NMR technique in the bio-medical field.

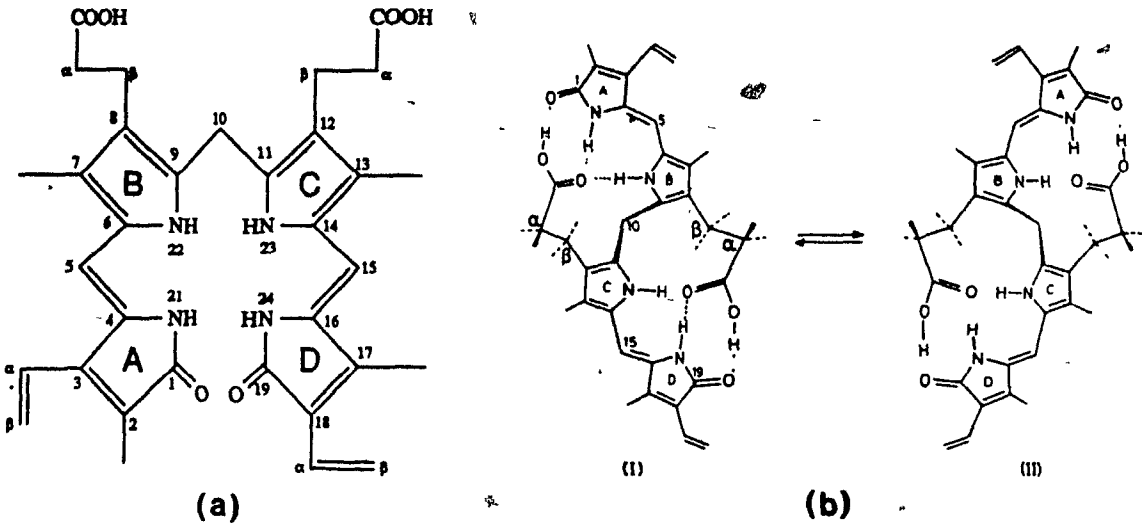

Figure 6.1 (a) The structure of unconjugated bilirubin IXα; (b) The transition between the two hydrogen-bonded bilirubin enantiomers (reference 7).

In recent years, the increasing interest in phototherapy and hemoperfusion treatments of hyperbilirubinemia has stimulated the investigation of the structure and conformation of the bile pigments by a variety of physical techniques, such as infrared and Raman spectroscopy (Section 4.3.3), circular dichroism (12,13) and optical rotatory dispersion (14), fluorescence (15,16), electron spin resonance (17), and especially by NMR. The development of the Fourier transform techniques has made possible more sophisticated NMR studies of these important biocompounds. Detailed assignments of the ^{1}H and ^{13}C spectra of some of the bile pigments have been made (18-23). The structures and conformations of bilirubin in organic solvents, such as DMSO and chloroform, have been studied extensively by proton and carbon-13 NMR. Hansen *et al.* have estimated the acidity constants of bilirubin by monitoring the chemical shift changes upon titration of a solution of bilirubin in DMSO (21). These studies have been reviewed by Kaplan and Navon (18).

The intramolecularly hydrogen bonded structure of bilirubin in chloroform and the solvation effect in DMSO, which disrupts these hydrogen bonds, were confirmed by the measurements of relaxation times and the nuclear Overhauser effect (24,25). Model compounds were prepared for the determination of the hydrogen bonding of bilirubin and some of its derivatives (26,27). These studies have provided the basis for the understanding of the structure and conformation of bilirubin and related bile pigments in organic solvents. In medical research, human bilirubin pigment gallstones were characterized chemically with the aid of solid state ^{13}C NMR techniques (28,29), since other conventional methods can easily change the nature of bilirubin.

The association between bilirubin and oligopeptides has been studied indirectly by adsorption experiments (30-32); however, NMR techniques can very well provide useful probes for the study of the specific interactions of bilirubin with these oligopeptides and perhaps other substrates.

An introduction to the general concepts of NMR relaxation and its application in the interaction studies has been given in Chapter 3. It is obvious that the binding or interaction between two molecular species in solution increases the effective molecular weight, and hence, the size of the molecule. This, in turn, leads to a longer molecular correlation time. Under the extreme narrowing conditions, the relaxation rate is inversely proportional to the correlation time, as indicated in Equation 3.3. Therefore, the restricted freedom of motion can be detected by the changes in the NMR spin-lattice relaxation times.

The general principle of changes in relaxation times that result from binding can be applied to a study of the interaction of bilirubin with oligopeptides. The adsorption studies indicate that lysine residues in the peptides are involved in the binding. It is likely that a salt linkage is formed between the amino groups of lysine and the carboxylic groups of bilirubin. However, the mechanism of the binding remains open to dispute. Other interactions such as hydrogen bonding and hydrophobic bonding may also contribute to the binding process. The determination of changes in the proton and ^{13}C spin-lattice relaxation times that result from the addition of a simple dipeptide, L-lysyl-L-lysine, to bilirubin permits a determination of the functional groups involved in

the binding and should offer direct insight into the nature of the interactions, hence the binding process.

6.1.2 Nitrogen-15 NMR Studies

Bilirubin is a rather large molecule, with a molecular weight of 585, but it is made up of only four elements, i.e., carbon, hydrogen, nitrogen and oxygen. Two of the four nitrogen atoms in the bilirubin molecule are located in the pyrrole rings with the remaining two in the lactam rings. The study of these nitrogen atoms, by NMR, should give interesting information concerning the conformation of bilirubin and its interaction with various other molecules.

Nitrogen-14, which is the most abundant isotope of nitrogen, is not ideal for NMR studies because of the line broadening (up to several kHz) associated with its quadrupolar nature. The intrinsic NMR properties of ^{15}N are much less favorable than those of ^{13}C. The ^{15}N nucleus has a spin of 1/2, but its low frequency, low natural abundance (only 0.365%), unfavorable gyromagnetic ratio (-2.7112×10^7), negative Overhauser effect and usually large T_1's make the observation of ^{15}N very difficult (33). Nonetheless, it is possible to obtain sharp ^{15}N lines, especially when sufficient sample is available and an appropriate pulse sequence is applied. Modern enhancement techniques, such as INEPT (Insensitive Nuclei Enhanced by Polarization Transfer) and DEPT (Distortionless Enhancement by Polarization Transfer) sequences, can be used to improve the signal.

The recording of ^{15}N spectra for the porphyrin compounds using isotope enriched samples has been reported in the literature since the 1970's (34,35). Hansen *et al.* reported the ^{15}N NMR spectrum for bilirubin in DMSO, with partial assignments (36), obtained by the use of a pulse sequence called SINEPT (37). The ^{15}N study for some of the pyrrole pigments at the natural abundance has also been reported recently by Falk *et al.* (38).

In this study the newly developed INEPT pulse sequence (39,40) will be applied to obtain enhanced ^{15}N signals in NMR spectra. The ^{15}N spectra of bilirubin and of some of the related pigments are assigned by means of two-dimensional heteronuclear correlation experiments. Studies of the interaction of bilirubin with benzyltrimethylammonium chloride, based on ^{15}N spectra, are also presented and compared with the interaction with dilysine.

6.2 Experimental Techniques

6.2.1 Instruments and Materials

The proton T_1 measurements were performed using a Varian XL-200 NMR spectrometer with the samples contained in 5 mm NMR tubes. Carbon-13 and nitrogen-15 experiments were normally done with samples in 10 mm tubes using a Varian XL-300 NMR spectrometer (operating at 75.43 MHz and 30.41 MHz for ^{13}C and ^{15}N, respectively), except for the measurements of T_1 for dilysine, which were done using 5 mm broad band tubes. The proton and ^{13}C chemical shifts were determined by setting the peak of the reference tetramethylsilane (TMS, from MSD Isotopes) to 0 ppm. For the ^{15}N experiment, nitromethane was used as the 0 ppm reference for the chemical shift. The reported chemical shifts are accurate to about ±0.002 ppm.

Bilirubin IXα, purchased from Sigma, was of high purity as determined by thin layer chromatography (TLC) and high performance liquid chromatography (41). Biliverdin IXα, of 85% purity, was also purchased from Sigma. Bilirubin dimethyl ester and bilirubin conjugate (ditaurate sodium salt) were purchased from Porphyrin Products (Utah, USA). The bilirubin dimethyl ester commercial product was impure as shown by a TLC test. The compounds were used without further treatment or purification since the NMR spectra of these compounds indicated acceptable purity for the desired experiments.

Benzyltrimethylammonium chloride was purchased from Aldrich. It dissolves well in both aqueous and DMSO solutions. L-Lysyl-L-lysine dihydrobromide (Vega Biochemicals) dissolves readily in aqueous solution but is insoluble in organic solvents. To render it soluble in organic solvents it was converted to the salt of trifluoroacetic acid by dissolving it in trifluoroacetic acid (ca. 1 g in 5 ml), warming the solution to 35°C before it was poured into ethyl ether (45 ml). The resulting precipitate was filtered and washed with ether (42). The product was freeze-dried overnight before use and handled in a glove bag filled with dry nitrogen to avoid moisture.

Since bilirubin in the unconjugated form is not appreciably soluble in aqueous solution, the NMR studies were conducted in fully deuterated dimethylsulfoxide (DMSO-d_6, from MSD Isotopes). The solutions were prepared immediately prior to the experiments and were covered with aluminum foil to

prevent exposure to light. Degassed bilirubin solutions kept in a refrigerator remained stable for about three days to one week.

The solutions of bile pigments in DMSO-d_6 were prepared in NMR tubes. The solutions were filtered in a glove bag filled with dry nitrogen and were degassed with nitrogen for about 10 minutes. This process was performed in a dark room, using a dim red light when necessary.

6.2.2 Proton and Carbon-13 T_1 Measurements

The inversion-recovery Fourier transform method (Appendix 3) was used in this study. For the ^{13}C experiments, a reduced spectrum window was used to ensure that the pulse was applied equally to all of the signals. The error in the proton T_1 values was always within ±5%, and in some cases less than 1%. For the ^{13}C values of T_1 the errors tended to be larger, but still within ±10%.

The concentration of the bilirubin was kept in the range of 0.015-0.028 M (10-15 mg/ml) for T_1 studies. Although bilirubin is readily soluble in DMSO, relatively low concentrations were used to minimize any viscosity effects. The measured T_1's remained unchanged within experimental error for different solutions in this restricted concentration range. The solution was degassed by bubbling nitrogen through the NMR tube to remove dissolved paramagnetic oxygen in the solution. However, the degassing was found to have little or no effect on the measured T_1 values. The NMR tubes were normally sealed during the experiments. The relaxation times were measured at 20°C over a period of about 6-8 hours. Following this measurement, sufficient dilysine was added to obtain a molar ratio of about 1:10 (dilysine : bilirubin). After the resulting solution had been degassed, the second measurement was performed immediately to maintain the experimental conditions identical to those for the first measurement. The measurements were generally repeated to ensure that the results were reproducible.

For the carbon-13 T_1 measurements of dilysine, the compound was dissolved in deuterated phosphate buffer (0.010 M, pH 7.8). The concentration of dilysine in buffer was about 0.20 M. The error for the measurements was less than 5%.

6.2.3 Nitrogen-15 NMR Experiments

The nitrogen-15 spectra were recorded with a Varian XL-300 NMR spectrometer operating at a ^{15}N frequency of 30.4 MHz. The detected ^{15}N signals all appeared upfield relative to the reference CH_3NO_2, therefore, acquiring a negative sign. The stability of the magnetic field was verified by recording the ^{15}N spectrum of dimethylacetamide (90% with DMSO-d_6) at its ^{15}N natural abundance with and without an external reference (nitromethane contained in a inner tube). Only a very small change (ca. 0.02 ppm) was detected, indicating an acceptable stability for the magnetic field.

The refocussed INEPT pulse sequence shown below was used to detect the ^{15}N signal. A detailed description of the INEPT pulse sequence can be found in Appendix 3.

^{1}H $\quad D_1\text{-}(\pi/2)_x\text{-}t_D\text{-}(\pi)_x\text{-}t_D\text{-}(\pi/2)_y\text{-}t_R\text{-}(\pi)_x\text{-}t_R\text{-DEC}$

^{15}N $\quad (\pi)\text{-}t_D\text{-}(\pi/2)\text{-}t_R\text{-}(\pi)\text{-}t_R\text{-ACQ}$

(The refocussed INEPT pulse sequence)

The 90° pulse width was calibrated using the reference sample and was found to be about 22 μsec. The delays used in the sequence were based on an average value of the N-H coupling constant ($^1J_{NH}$ = 95 Hz) observed for bilirubin (36). The value of t_D in all cases was 2.63 ms ($1/(4^1J_{NH})$). The refocussing period (t_R) was also set to 2.63 ms to maximize the detection of the NH groups. One of the advantages of the INEPT experiment is that the repetition rate of the sequence is based on the short proton spin-lattice relaxation times (T_1) of the NH groups (Table 6.1, measured at 200 MHz with the inversion-recovery experiment), thus permitting the use of a short preparation delay (D_1) of 0.4-0.5 seconds, which is usually set to 1.26 times of the T_1 of the attached protons.

Two-dimensional heteronuclear correlation experiments (Appendix 3) were then conducted to assign the nitrogen peaks for the bile pigments. The proper delay time and pulse width were calibrated prior to the experiment and were carefully chosen to optimize the spectrum.

All the ^{15}N studies were carried out using DMSO-d_6 solutions. Bilirubin solutions were prepared with the concentration of 0.03-0.04 M. More

concentrated samples for other bile pigments were used for ^{15}N studies because of their higher solubilities, e.g., the concentration of biliverdin was about 0.05 M.

Table 6.1 The T_1 Values of NH Protons of Bilirubin and Biliverdin in DMSO-d_6

Proton	Chemical Shift (ppm)	T_1 (sec)
Bilirubin		
Pyrrole NH	10.49	0.18
	10.46	0.18
Lactam NH	10.05	0.26
	9.93	0.25
Biliverdin		
Lactam NH	10.79	0.34
Pyrrole NH	10.67	0.32

Samples: Bilirubin, 0.015 M; biliverdin, 0.020 M.

6.3 Interaction Studies of Bilirubin with Dilysine by T_1 Determinations

6.3.1 Proton T_1 Measurements of Bilirubin

The proton NMR spectrum of bilirubin in DMSO-d_6 is shown in Figure 6.2. The proton peaks of bilirubin, including the carboxyl proton, are very well resolved. The stacked plot of the relaxation process of bilirubin in DMSO-d_6, determined by the inversion-recovery Fourier transform technique, is shown in Figure 6.3a. The gradual relaxation of the proton signals after a 180° inversion is clearly shown in this figure. Generally the protons on the methyl and vinyl groups of the bilirubin molecule have longer T_1's than the protons of the methylene groups and of the NH groups (Table 6.2).

Upon addition of dilysine, the relaxation times of certain protons change, as shown in Figure 6.3b. The derived values of T_1, before and after mixing the dilysine with bilirubin, for the affected protons are listed in Table 6.3. Upon addition of dilysine, only small, insignificant downfield chemical shifts (ca. 0.010 ppm) were observed.

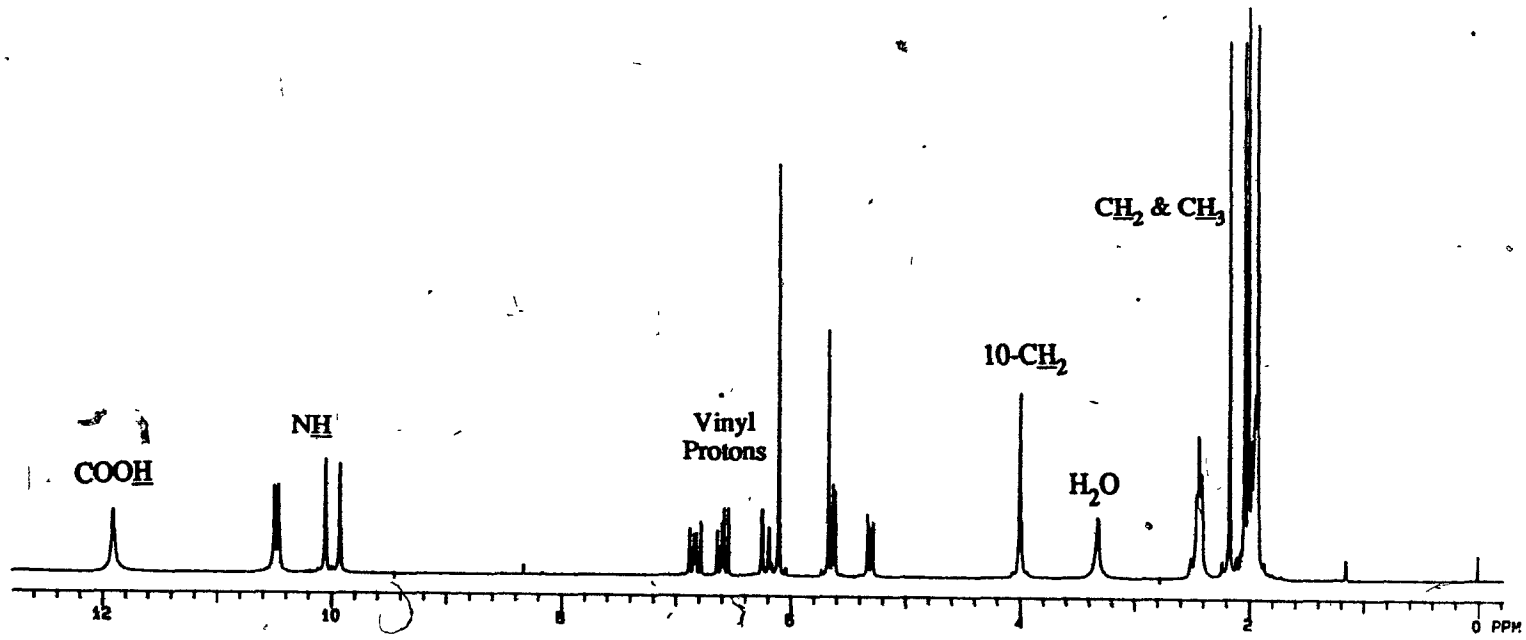

Figure 6.2 The proton NMR spectrum of bilirubin IXα in DMSO-d_6.

Table 6.2 The Chemical Shifts and T_1 Values for the Protons of Bilirubin in DMSO-d_6

Proton		Chemical Shift (ppm)	T_1 (sec)
carboxyl		11.90	1.48
22-pyrrole		10.48	0.18
23-pyrrole		10.45	0.18
21-lactam		10.04	0.26
24-lactam		9.91	0.25
5- & 15-CH		6.09	0.52
3-vinyl			
H_X H_A \ / C=C / \ H_B	H_A	5.30	0.27
	H_B	6.21	0.32
	H_X	6.58	0.69
18-vinyl	H_A	5.66	0.63
	H_B	5.61	0.61
	H_X	6.82	0.77
10-methylene		3.99	0.14
α-propionic methylene		1.94	0.21
β-propionic methylene		2.43	0.15
7- & 13-methyl		2.04	0.41
		2.00	0.40
17-methyl		2.16	0.45
2-methyl		1.92	0.37

Bilirubin sample: 0.015 M.
The coupling constants measured in this experiment:
3-vinyl group, $J_{AB} = 2.79$, $J_{AX} = 11.45$, $J_{BX} = 17.49$ Hz;
18-vinyl group, $J_{AB} = 1.80$, $J_{AX} = 11.94$, $J_{BX} = 17.12$ Hz.

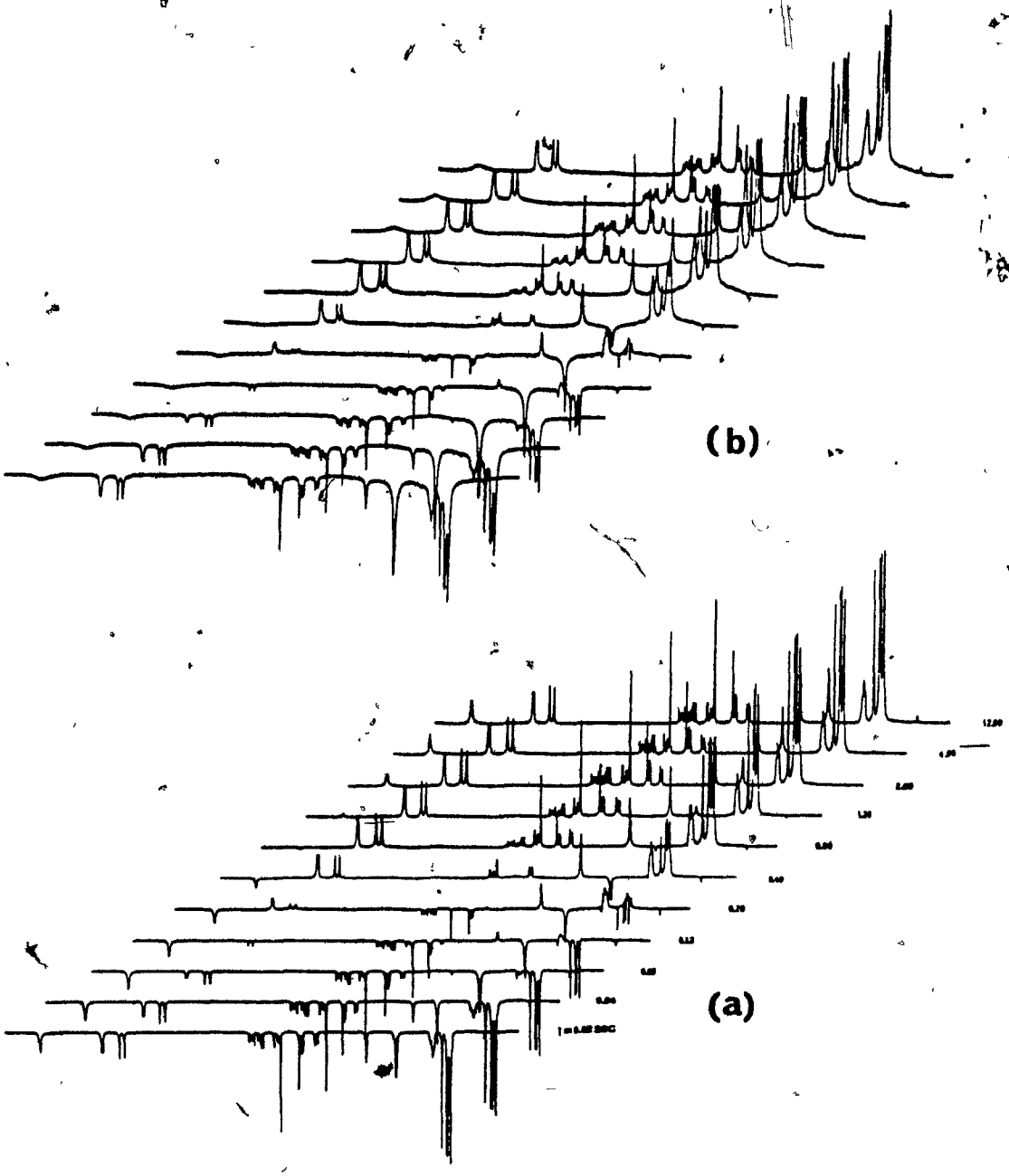

Figure 6.3 The stacked plots obtained by the measurement of the proton spin-lattice relaxation times of bilirubin and bilirubin with dilysine; 16 transients collected per spectrum; t, delay time: (a) T_1 measurement of 0.017M bilirubin in DMSO-d_6; (b) T_1 measurement of 0.017M bilirubin in DMSO-d_6 with dilysine, bilirubin/dilysine molar ratio 10:1.5.

Table 6.3 Changes in Proton T_1 Values (in Sec) of Bilirubin upon Addition of Dilysine

Proton	BR	BR+DL	Difference (%)
carboxyl	1.48	0.87	-41 [1]
	1.49	0.81	-46 [2]
10-methylene	0:14	0.16	+14
	0.14	0.15	+7
α-propionic methylene	0.21	0.25	+19
	0.21	0.25	+19
β-propionic methylene	0.15	0.17	+13
	0.15	0.17	+13
7- & 13-methyl	0.41	0.33	-20
	0.41	0.33	-20
	0.40	0.32	-20
	0.40	0.32	-20
2-methyl	0.37	0.32	-14
	0.36	0.31	-14
17-methyl	0.45	0.39	-13
	0.45	0.38	-16

BR: bilirubin; DL: Dilysine.
The two groups of data correspond to the following samples:
[1] 0.015 M BR/DMSO, BR/DL molar ratio 10:1.0;
[2] 0.017 M BR/DMSO, BR/DL molar ratio 10:1.5.

The most significant change is for the T_1 of the carboxyl protons. The substantial decrease in their T_1 indicates an interaction of these carboxyl groups with the dilysine. A strong selective broadening effect is also observed for these carboxyl protons. The DMSO used to prepare the solutions was not dried, since the use of drying reagents can introduce impurities (25). Consequently, the carboxyl protons are saturated with exchangeable protons from the water in solution prior to the addition of dilysine. Therefore, the broadening effect is indicative of an exchange between the carboxyl protons and the exchangeable protons of the dilysine. It gives added evidence of a specific interaction of the

bilirubin moiety with the dilysine. This is verified by carbon-13 NMR studies which are discussed later in Section 6.3.2.

It is of particular note that the T_1 values for the protons of the NH groups, i.e., the pyrrole and the lactam protons remained unchanged, within experimental error. On this basis it would appear that their involvement in the interaction of dilysine with bilirubin is limited, if there is any at all. Similarly, the vinyl groups on rings A and D, the methine groups at positions 4, 5, 15 and 16 of the bilirubin backbone do not seem to be involved.

The protons of the methyl groups at positions 2, 7, 13 and 17 show significant decreases in T_1 values. This decrease can be attributed to an increase in rigidity that results from the formation of a complex of bilirubin with dilysine. In solution all four methyl groups on the free bilirubin molecule point toward the environment and can tumble freely. The increase in correlation time and resulting decrease in the T_1 values is consistent with complex formation upon addition of dilysine. It is particularly interesting to notice that the percentage decrease of T_1 values for the methyl protons on positions 7 and 13 is greater than those for the methyl protons on positions 2 and 17, which are further away from the propionic side chains with the carboxyl groups. It is possible that these groups are involved in a dipolar interaction with the protons of the dilysine, thus leading to a decrease in the spin-lattice relaxation times.

In the case of the binding of two small molecules, where only one correlation time is applicable, normally only decreases in relaxation times would be expected under the extreme narrowing condition. Surprisingly, a small *increase* was observed for the T_1's of the methylene protons, i.e., for protons on the bridge at position 10 and on the propionic chains. It is important to notice the fact that bilirubin, with a molecular weight of 585, is a relatively large molecule. Upon binding with dilysine it becomes a complex, the various portions of which may have different correlation times. The correlation time of the methylene bridge at position 10 may, in fact, lie beyond the limit of extreme narrowing. (This is evidenced by an estimation as discussed in the next section.) Consequently, the changes in relaxation times that result from the interaction with dilysine may differ for the various parts of the molecule. Due to conformational changes of the molecule, the spin-lattice relaxation times for the various groups may involve increases as well as decreases. Thus, the increase in T_1 for the C-10

methylene protons may reflect an increase in correlation time for conditions where the correlation time lies in the vicinity of the minimum of T_1 as shown in Figure 3.1. This is supported by the simultaneous increase in T_1 for the propionic methylene protons.

On the other hand, the relatively small increase in T_1 of the 10-methylene protons upon the addition of dilysine suggests a decreased solvation effect of bilirubin in DMSO. The binding of dilysine to a carboxyl group of the bilirubin molecule would replace the intermolecular hydrogen bonds between bilirubin and DMSO with salt linkages between bilirubin and dilysine. The solvation effect of the bilirubin molecules by DMSO is certainly less significant than the binding between bilirubin and the basic peptide.

6.3.2 Carbon-13 T_1 Measurements of Bilirubin

The ^{13}C spectrum of bilirubin in DMSO-d_6 is shown in Figure 6.4. The ^{13}C assignments were made with the aid of DEPT and ^{13}C-^1H correlation experiments and were found to be in agreement with the assignments by Hansen *et al.* (21), but different from the recently reported results (23). The T_1 values for the assigned carbon-13 signals are listed in Table 6.4. For carbon atoms on the backbone, especially those bearing no protons, the lack of dipolar relaxation leads to longer T_1's than those with directly attached protons. Methyl groups also tend to have longer T_1's because their high symmetry allows spin-rotation relaxation.

Values of T_1 for those carbons of bilirubin affected by the addition of dilysine are given in Table 6.5. The carbons of the carboxyl groups on the propionic side chains show a large decrease in T_1. This decrease confirms the earlier suggestion that the decrease in T_1 for the carboxylic protons is not due merely to the broadening effect arising from the proton exchange process. Furthermore, it also indicates that the nature of the interaction is not exclusively hydrogen bonding or hydrophobic bonding. Since the bilirubin molecules in DMSO solution are already solvated as a result of the formation of hydrogen bonds with DMSO, it seems unlikely that the mere substitution of this hydrogen bond by another with dilysine would result in a significant change in T_1. Therefore, it would seem more probable that this is an acid-base interaction. This is also evidenced for dilysine by the T_1 changes of the methylene group on the side chain adjacent to the amine group (Section 6.3.3).

Table 6.4 The Chemical Shifts and T_1 Values for the Carbons of Bilirubin in DMSO-d_6

Carbon	Chemical Shift (ppm)	T_1 (sec)
carboxyl	173.86	2.28
C-1	171.26	1.44
C-19	170.33	1.69
C-17	141.84	1.68
C-3	140.33	1.71
C-11	131.39	1.06
C-9	130.64	1.27
C-16	128.19	1.69
C-4	127.43	1.24
α-vinyl (3')	127.34	0.60
α-vinyl (18')	127.02	0.39
C-12	124.01	1.81
C-8	123.34	1.56
C-2	123.19	1.84
C-18	122.36	1.29
C-14	122.21	1.71
C-6	122.04	1.33
β-vinyl (3')	121.92	1.41
C-13	119.73	1.77
C-7	119.52	1.33
β-vinyl (18')	117.03	1.32
C-15	99.93	0.14
C-5	99.06	0.12
α-propionic CH_2 (8'& 12')	34.19	0.13
10-methylene	23.60	0.09
β-propionic CH_2 (8'& 12')	19.20	0.09
2-methyl	9.41	1.16
17-methyl	9.19	1.98
7- & 13-methyl	9.08	1.33

Bilirubin sample: 0.028 M.

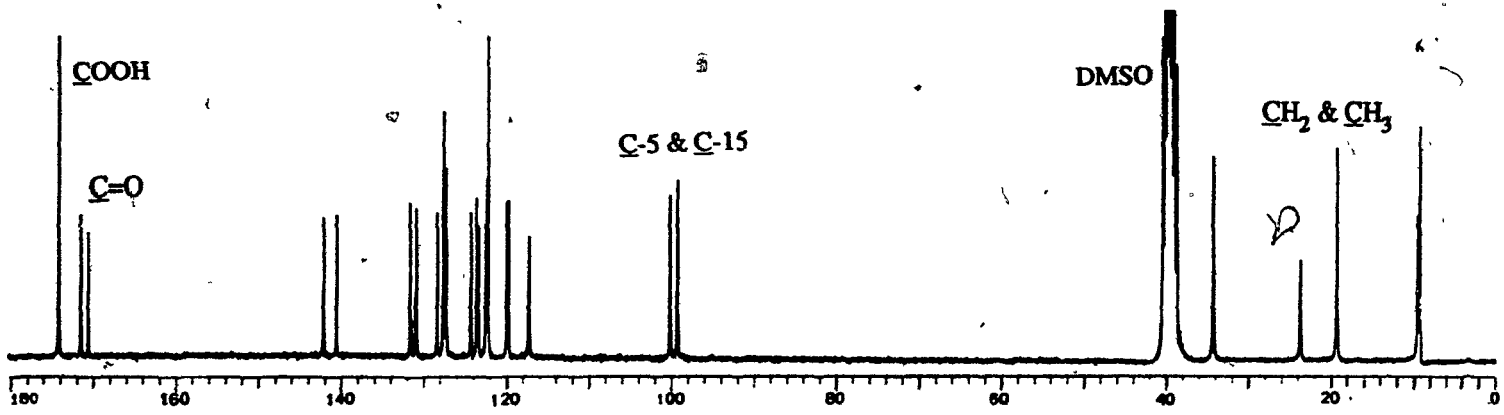

Figure 6.4 The ^{13}C NMR spectrum of bilirubin IXα in DMSO-d_6.

Table 6.5 Changes in ^{13}C T_1 Values (in Sec) of Bilirubin upon Addition of Dilysine

Carbon	BR	BR+DL	Difference (%)	
Carboxyl	2.28	1.69	−26	[1]
10-methylene	0.09	0.11	+22	[2]
α-propionic methylene	0.13	0.12	−7.7	[2]
β-propionic methylene	0.09	0.11	+22	[2]
7- & 13-methyl	1.33	1.08	−25	[1]

BR: bilirubin; DL: Dilysine.
Samples: [1] 0.028 M BR/DMSO, BR/DL molar ratio 10:2.2;
[2] 0.028 M BR/DMSO, BR/DL molar ratio 10:1.5.

It is of interest to recall that the dilysine was added to the bilirubin in the form of the salt of trifluoroacetic acid. Studies by FTIR of this salt dissolved in carefully dried DMSO solution failed to indicate the presence of the free amine group of dilysine indicating that, under these conditions, the salt is largely undissociated. However, when the solution was prepared with undried DMSO, as was done for the NMR studies, the IR spectra gave clear evidence that the amino groups on the peptide side chains exist as free primary amine groups, which, which would facilitate the formation of the salt bonds with bilirubin in the solution.

The changes in T_1 determined by the ^{13}C experiments exhibit similar trends as those for the protons. The methylene group on the central bridge, position 10, is again a very useful sensor in studying the conformation of the bilirubin molecules in solution. The increase in T_1 for the β-carbon on the propionic chain demonstrates that the side chain becomes more flexible when bilirubin is bound to dilysine. Meanwhile, the T_1 values for the α-carbons on these two side chains show a slight decrease, or remains unchanged within experimental error. This is consistent with the smaller increase observed for the T_1's of these protons relative to those of the β-carbon.

Since both bilirubin and dilysine have two functional groups, some of the bilirubin molecules can be complexed together through the dilysine linkage, forming a complex having a large effective molecular weight. This in turn leads to an increase in the correlation time for the C-10 methylene which now is on the backbone of the complex. The correlation time for the central bridge methylene group of bilirubin is estimated to be approximately 10^{-10}-10^{-9} seconds, using Equation 3.5, and is on the border line of the extreme narrowing condition. The C-10 bridge carbon shows an increased T_1 relaxation time (Table 6.5), as seen in previous T_1 measurements for attached protons. Furthermore, the increase for the C-10 carbon T_1 value is greater than that for the corresponding protons as shown in Tables 6.2 and 6.4. This discrepancy can be explained by the dependence on frequency of the T_1 values in the range where the correlation time falls around the minimum of T_1.

It should also be pointed out that the measurement error for carbon-13 T_1 values is greater than that for the proton T_1's. However, repeated experiments demonstrate the same tendency upon addition of different amounts of dilysine.

As expected, the carbons on the bilirubin backbone generally show a decrease in the relaxation times. This is obviously due to the increase in molecular weight resulting from the formation of a complex. The methyl carbons also relax faster in the presence of dilysine, which is also consistent with the results for the proton T_1's. This is also true for the vinyl carbons at positions 3 and 18.

6.3.3 Carbon-13 T_1 Measurements of Dilysine

In the previous section, it has been suggested that the binding between bilirubin and dilysine is primarily an acid-base binding. The most likely binding would be between the side chain amino groups of dilysine and the carboxyl groups of bilirubin.

To determine the involvement of dilysine, experiments were performed in which small quantities of bilirubin were added to excess dilysine. As mentioned previously, to obtain a concentration of dilysine sufficient for these experiments, the dipeptide was dissolved in deuterated phosphate buffer. This allowed observation of changes in T_1 for the carbons of the dilysine. Table 6.6 demonstrates that the T_1 for the carbon adjacent to the side chain amine group is reduced in the presence of bilirubin. This is unequivocal evidence of the

involvement of the side chain amine group in the binding of bilirubin to dilysine and strongly supports the existence of the ammonium carboxylate salt bond.

Table 6.6 Changes in T_1 Value (in Sec) of the Carbon Adjacent to the Amino Group on the Side Chain of Dilysine upon Addition of Bilirubin

	DL	DL+BR	Difference (%)
Relaxation Time	1.04	0.96	-7.7 [1]
	1.02	0.98	-4.0 [2]

BR: bilirubin; DL: Dilysine.
Samples: [1] 0.185 M DL/buffer, DL/BR molar ratio 1000:6;
[2] 0.210 M DL/buffer, DL/BR molar ratio 1000:4.

Both groups of data in Table 6.6 demonstrate a decrease of T_1 for this carbon atom. The reason for the relatively small change could be the very low solubility of bilirubin in aqueous buffer solution. Consequently, the amount of bilirubin in solution was sufficient to interact with only a very small fraction of the dilysine in the buffer solution. In addition, the formation of the complex requires the disruption of the extensive inter- and intramolecular hydrogen bonds of bilirubin in aqueous solution. Hence, a considerably smaller change would be expected than in DMSO solvent.

6.4 Nitrogen-15 NMR Spectral Assignments for Bile Pigments

The nitrogen-15 NMR study is a relatively new area. To date, only one group of researchers have reported a partially assigned ^{15}N spectrum of bilirubin (45). The study of bile pigments by ^{15}N NMR can possibly provide interesting information on the conformational changes of these compounds. These studies would rely on the correct assignments of the ^{15}N signals in the spectra of bile pigments. In this section, the assignments of the ^{15}N spectra for bilirubin and some of the related bile pigments with the aid of ^{15}N-^{1}H two-dimensional heteronuclear correlation experiments are discussed.

6.4.1 Nitrogen-15 NMR Spectra of Bilirubin and Its Dimethyl Ester

As expected, four signals, in pairs of two, were detected in the decoupled ^{15}N spectrum of bilirubin IXα in DMSO-d_6, using the INEPT techniques (Figure 6.5). The peaks in the ^{15}N spectrum of bilirubin were partially assigned by Hansen and Jakobsen in 1984 (36). That assignment is confirmed by the data obtained by a ^{15}N-^{1}H heteronuclear correlation experiment (Figure 6.5). Thus, based on the proton assignment reported by Kaplan and Navon (18), the pair located at the upper field, -249.59 and -249.02 ppm, correlate with the protons of the lactam groups, at positions 21 and 24, respectively, while the other pair at the lower field, -231.39 and -231.07 ppm, belong to the two pyrrole groups at positions 22 and 23. However, since the two pyrrole protons signals at 10.46 and 10.49 ppm, respectively, were not differentiated from one another (36), these results do not permit to make a complete assignment of the ^{15}N spectrum of bilirubin.

Table 6.7 ^{15}N Chemical Shifts of Bile Pigments in DMSO-d_6

Compound	Chemical Shift (ppm)			
	21	22	23	24
Bilirubin	-249.59	-231.07	-231.39	-249.02
BRDME	-249.70	-230.83	-231.17	-249.12
BR Ditauride	-249.56	-231.48	-231.80	-249.02
Biliverdin	-246.17	-245.44		-246.11
BR + Dilysine	-249.53	-230.99	-231.29	-249.00

BR: Bilirubin; BRDME: Bilirubin Dimethyl Ester.

To obtain the information required for this assignment, the spectrum is compared with those of its derivatives and some other related bile pigments. The proton NMR spectrum of bilirubin dimethyl ester has been published previously by Trull *et al.*, with peak assignments based on a comparison with the spectra of pyrromethenones, including a separation of the pyrrole protons (26). The ^{15}N spectrum of bilirubin dimethyl ester (Figure 6.6) is essentially identical to that of bilirubin. For the pyrrole nitrogens, there is a small downfield shift of 0.24 and

0.22 ppm, while the two lactam nitrogen atoms show slight upfield shifts of 0.11 and 0.10 ppm (Table 6.7). Interestingly, these changes in the chemical shift for ^{15}N signals are in accordance with the changes observed in the proton chemical shift; pyrrole protons shift downfield by 0.07 ppm, lactam protons shift upfield by 0.02 ppm, as shown in Table 6.8.

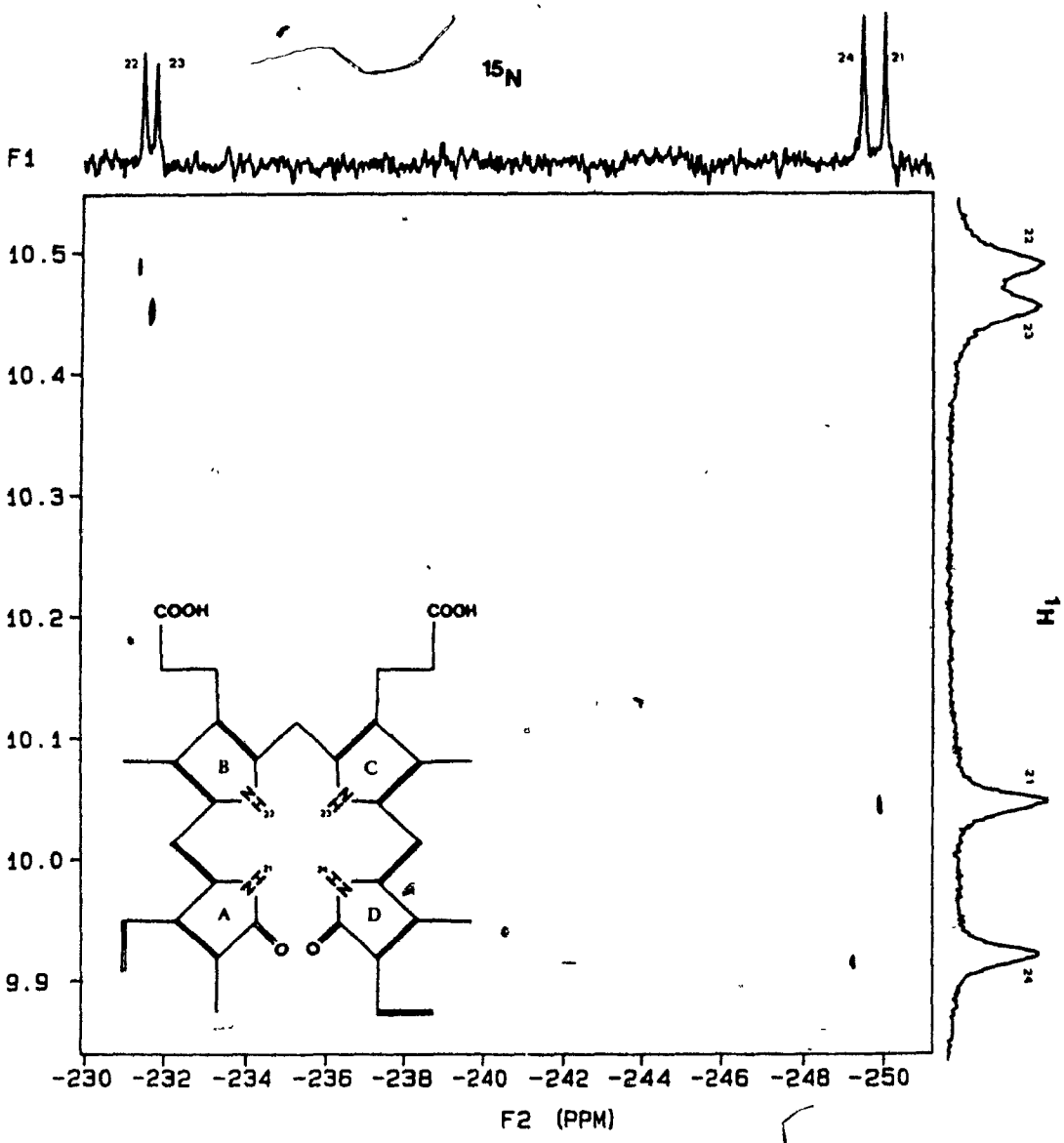

Figure 6.5 The 2-D ^{15}N-^{1}H NMR correlation spectrum of bilirubin in DMSO-d_6.

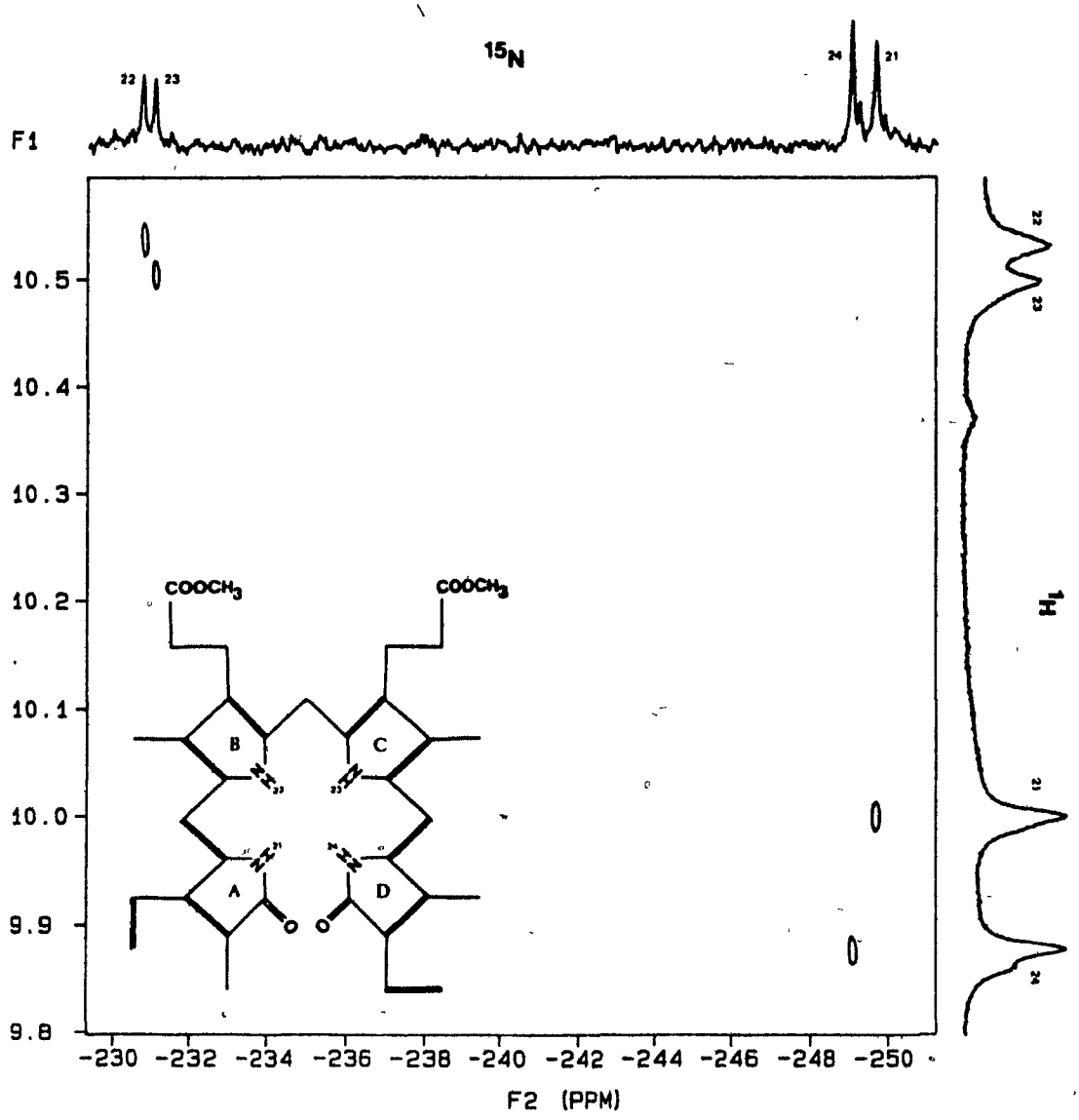

Figure 6.6 The 2-D ^{15}N-^{1}H NMR correlation spectrum of bilirubin dimethyl ester in DMSO-d_6.

The similarity of the ^{15}N spectra indicates that, in DMSO-d_6, both bilirubin and its dimethyl ester assume identical conformations, as suggested previously (25,26). The intramolecular hydrogen bonds of bilirubin are disrupted in DMSO and as a consequence there is no NOE (nuclear Overhauser enhancement) effect on the NH protons from the carboxyl protons (25). However, in chloroform solution, where bilirubin retains the intramolecular hydrogen bonds, this NOE effect does exist (24). In comparison, bilirubin

dimethyl ester dimerizes through intermolecular hydrogen bonding in chloroform solution over a large concentration range (24). In DMSO solutions, the intramolecular hydrogen bonds of bilirubin are disrupted and intermolecular hydrogen bonds are formed with the DMSO molecules, similar to those of bilirubin dimethyl ester. This solvation effect in DMSO makes both bilirubin and the ester adopt similar conformations. The similarity in conformation for these two compounds in DMSO is also characterized by similar spin-lattice relaxation times for the central bridge methylene groups, as reported by Kaplan and Navon (25).

Table 6.8 ^{1}H Chemical Shifts of the NH Groups of Bile Pigments in DMSO-d_6

Compound	Chemical Shift (ppm)			
	21	22	23	24
Bilirubin	10.05	10.49	10.46	9.93
BRDME	10.03	10.56	10.53	9.91
BR Ditauride	10.07	10.44	10.40	9.94
Biliverdin	10.79	10.67		10.79
BR + Dilysine	10.08	10.56	10.53	9.95
BR + BTMA	10.33	10.80	10.80	10.20
BR + Water	10.04	10.49	10.46	9.91

BR: Bilirubin; BRDME: Bilirubin dimethyl ester; BTMA: Benzyltrimethylammonium chloride.

The 2-D correlation spectrum for bilirubin dimethyl ester permits the complete assignment of its ^{15}N spectrum (Figure 6.6). The ^{1}H and ^{15}N spectra of bilirubin and bilirubin dimethyl ester are very similar in both dimensions, as seen in a comparison of Figures 6.6 and 6.7. The peaks in the contour plot appear at the same relative positions, so that the assignments for these compounds should be the same. Therefore, it may be concluded that, in the bilirubin ^{15}N spectrum, the pyrrole nitrogen signal that appears at the lower field belongs to the 22 NH while the one at the upper field side belongs to the NH of the 23 position (Table 6.7). Hence, in the proton spectrum the relative signal positions are reversed: the 22 NH proton appears at 10.49 ppm, the 23 NH proton at 10.46 ppm.

6.4.2 Nitrogen-15 NMR Spectra of Other Bile Pigments

The ^{15}N spectrum of a bilirubin conjugate, bilirubin ditauride (sodium salt) was also recorded, the 2-D spectrum is shown in Figure 6.7. The two signals for the lactam nitrogens remain unchanged. The pyrrole nitrogen signals are both shifted upfield by 0.41 ppm, obviously due to the substitution on the propionic side chains (Table 6.7). The two taurine amide nitrogen appeared as one sharp signal at -264.43 ppm. The correlation of the 2-D ^{15}N-^{1}H spectrum of the bilirubin conjugate is identical to those of bilirubin and bilirubin dimethyl ester.

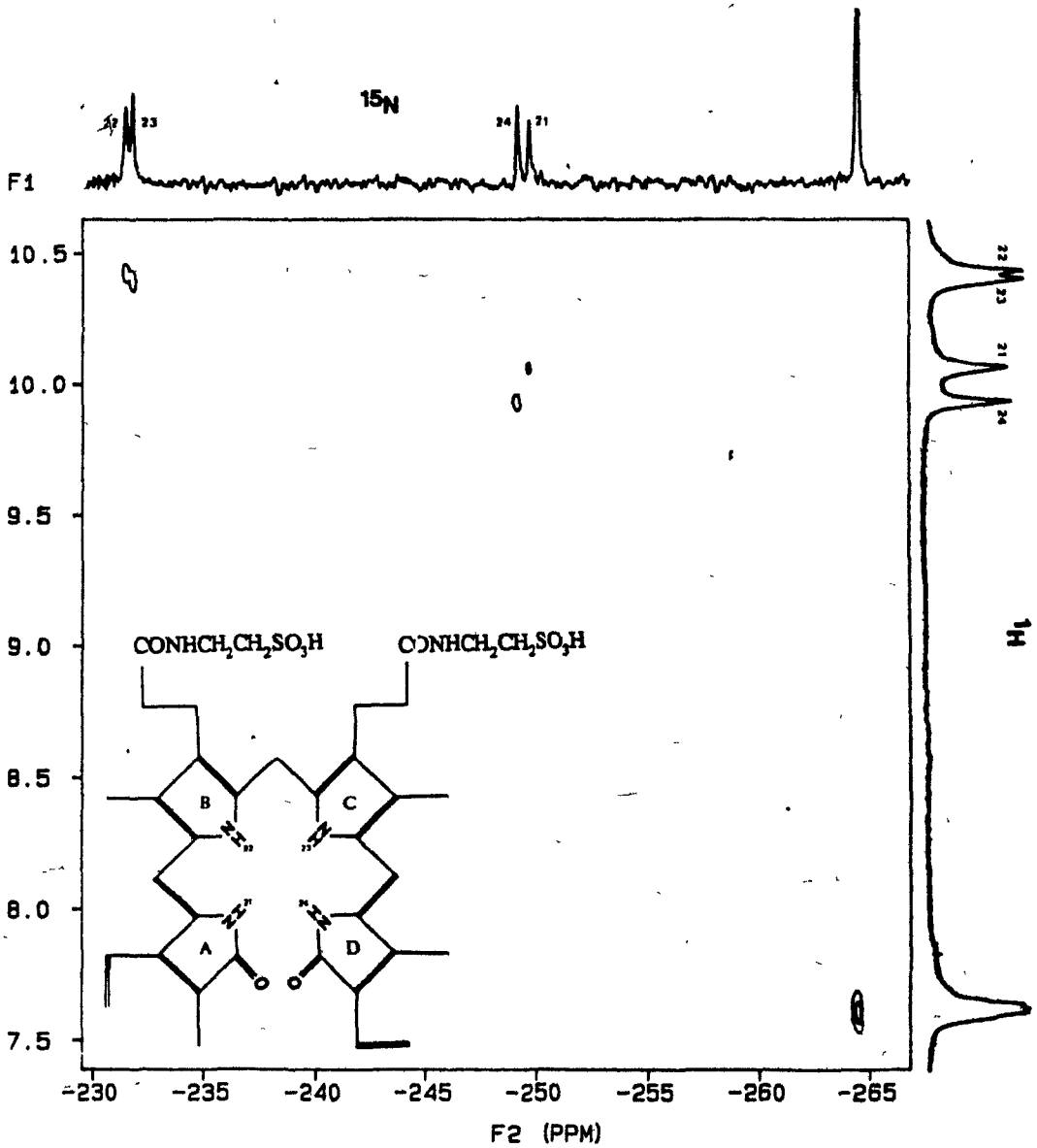

Figure 6.7 The 2-D ^{15}N-^{1}H NMR correlation spectrum of bilirubin ditauride in DMSO-d_6.

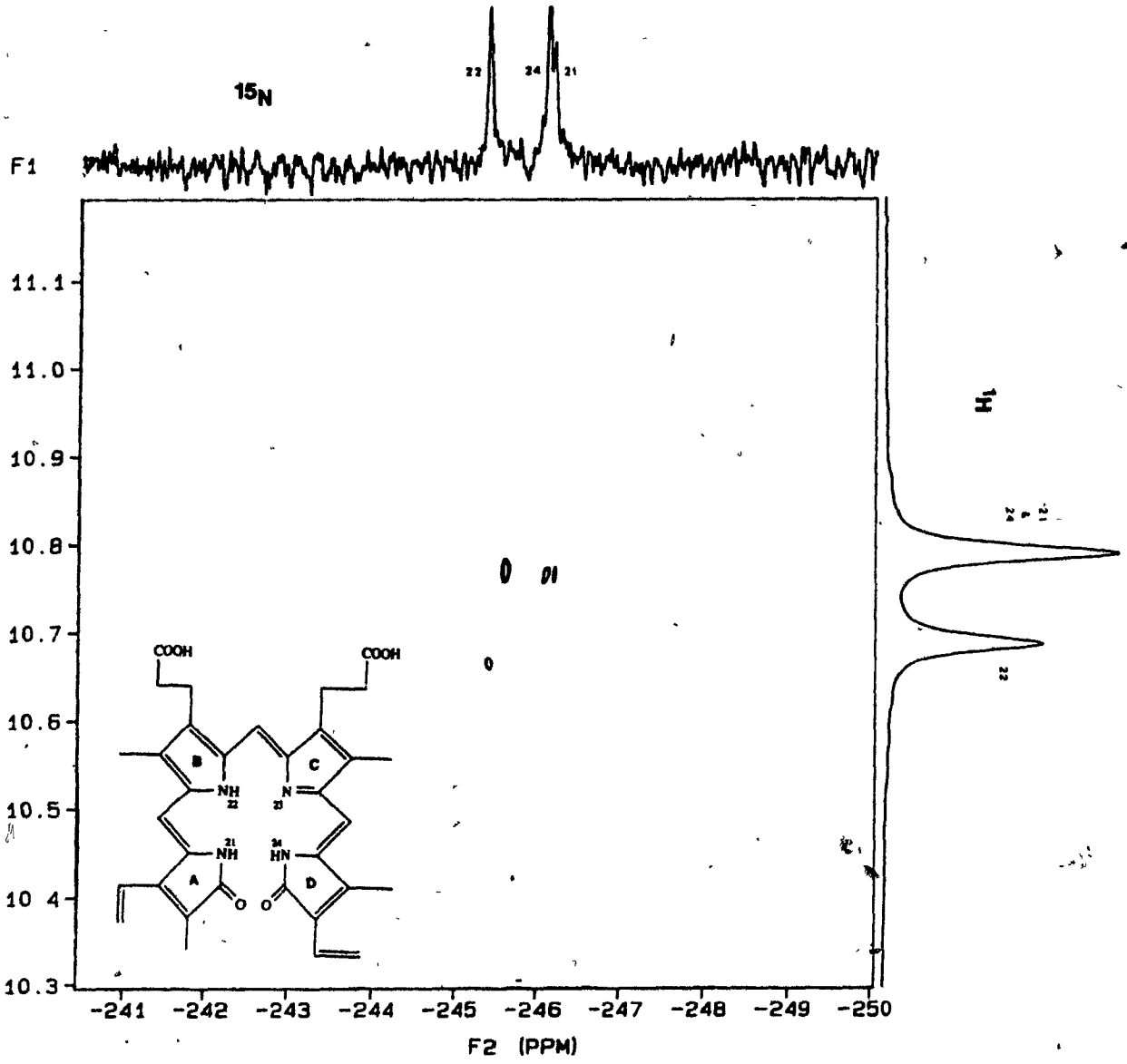

Figure 6.8 The 2-D ^{15}N-^{1}H NMR correlation spectrum of biliverdin in DMSO-d_6.

Biliverdin samples required a longer acquisition time than the other bile pigment samples, due to the relatively longer spin-lattice relaxation time of the NH groups. In the ^{15}N NMR spectrum of biliverdin, three sharp signals were detected. The signals at -246.11 and -246.17 ppm correspond to the two lactam NH groups, while the other at -245.44 ppm corresponds to the pyrrole NH group (Table 6.7). This assignment was also confirmed by a ^{15}N-^{1}H correlation

experiment (Figure 6.8). The difference between the chemical shifts of these two lactam ^{15}N peaks is only 0.06 ppm, much smaller than expected from the structural difference of the respective groups. This is indicative of similar chemical environments for both rings A and D in spite of the structural difference for these two rings, as shown in Figure 6.8. This result is consistent with a fast proton exchange process between rings B and C (38,43) (Figure 6.9). However, the rate of the exchange is still sufficiently small to allow the detection of the single pyrrole NH group of biliverdin at a lower field of -245.44 ppm.

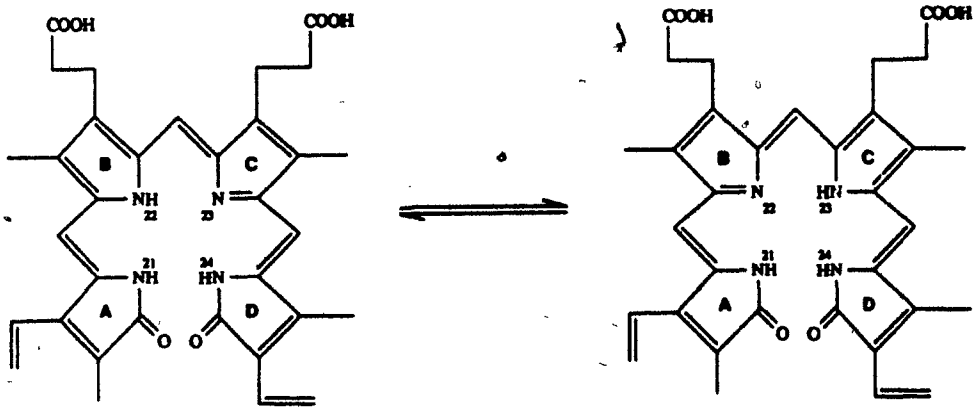

Figure 6.9 The proton exchange of biliverdin IXα in DMSO-d_6. Proton exchange occurs between rings B and C, the double bonds are rearranged accordingly.

6.5 Interaction Studies by Nitrogen-15 NMR Spectroscopy

6.5.1 Interaction of Bilirubin with Dilysine

As discussed in Section 6.3, the study of proton spin-lattice relaxation times demonstrates that bilirubin interacts with dilysine by forming an acid-base linkage through the carboxyl groups of bilirubin and the amino groups on the lysine side chains. However, there is no evidence for the involvement of the lactam and pyrrole groups of bilirubin in any interaction with dilysine. It was of interest to investigate further the interaction of bilirubin with dilysine, by considering the ^{15}N chemical shifts, generally very sensitive to environment.

The addition of dilysine does not result in significant changes in the ^{15}N spectrum of bilirubin in DMSO (Figure 6.10b). The chemical shifts for the

lactam nitrogens remained unchanged within experimental error and the signals of the pyrrole nitrogen were found to be shifted downfield about 0.08 and 0.10 ppm, respectively. The changes for the pyrrole groups of bilirubin correspond to the involvement of the nearby carboxyl groups in the interaction. This is consistent with the results obtained by the proton spin-lattice relaxation time measurements, which indicated that the NH groups of the bilirubin molecules were little involved in the interaction with the oligopeptide.

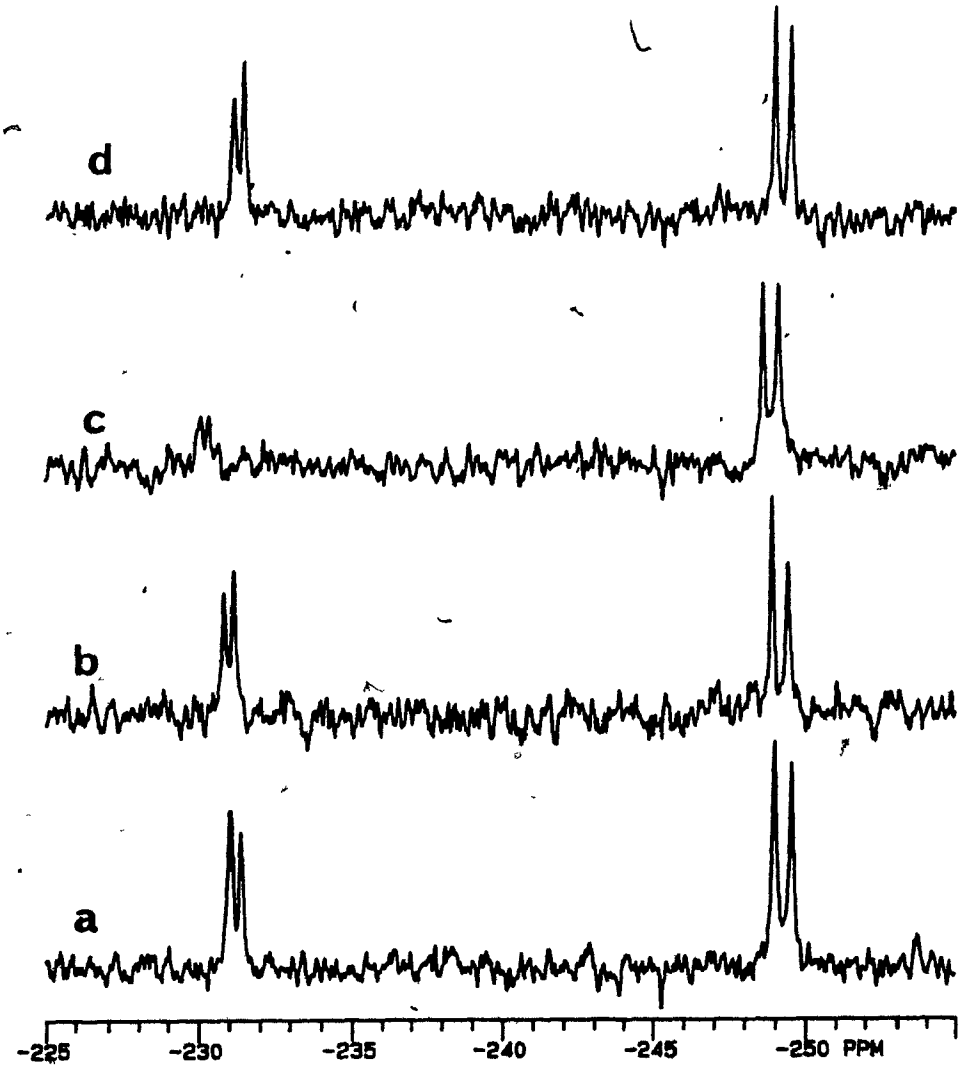

Figure 6.10 The ^{15}N NMR spectra of bilirubin upon interactions: (a) bilirubin; (b) bilirubin + dilysine; (c) bilirubin + benzyltrimethylammonium chloride; (d) bilirubin + water. Solvent: DMSO-d_6.

6.5.2 Interaction of Bilirubin with Quaternary Ammonium Salt

The interaction of amines with bilirubin is of considerable interest since it is known that cholestyramine adsorbs bile pigments, albeit with limited capacity and poor biocompatibility (Section 5.3.6). This material has benzyltrimethyl quaternary ammonium functional groups on a crosslinked polystyrene backbone. It is interesting to compare this type of interaction with that between bilirubin and dilysine. However, since solid cholestyramine resin particles cannot be used for the NMR studies in solution, a substitute of cholestyramine, benzyltrimethylammonium chloride, was chosen for the experiment. This compound resembles closely the functional groups of cholestyramine.

Upon addition of benzyltrimethylammonium chloride, the signals of the two pyrrole nitrogens diminished significantly (Figure 6.10c). Since the ^{1}H proton signals were used to enhance the intensity of the ^{15}N peaks in INEPT, this behavior is consistent with the absence of the protons on these groups. Note that there is also a chemical shift change of about 1 ppm accompanied by the diminution of the pyrrole ^{15}N signals. It is possible that the diminution is caused by proton exchange, since moisture and other exchangeable protons were present in the solution. Benzyltrimethylammonium chloride itself is very hygroscopic. The drying of the mixture with molecular sieves was attempted but caused precipitation.

To study the effect of the presence of water, small amounts of distilled water were deliberately added to the bilirubin solution in DMSO-d_6. No significant change was found for the ^{15}N signals (Figure 6.10d). On the other hand, addition of inorganic salts or acids caused precipitation of bilirubin. In fact, the proton exchange rate of pyrrole NH group of bilirubin has been reported to be much lower than that of the lactam NH group (24). Evidently, the addition of benzyltrimethylammonium chloride accelerates the proton exchange process of the pyrrole groups, while the lactam groups are less affected. This suggests a specific interaction between the quaternary ammonium salt and the pyrrole NH groups of bilirubin.

As expected, proton spectra of bilirubin in DMSO with water and with benzyltrimethylammonium chloride were characterized by the disappearance of the carboxylic proton signals on the propionic side chains. The two adjacent pyrrole NH proton peaks of bilirubin in DMSO-d_6 gradually collapse into one

single broad peak upon the addition of benzyltrimethylammonium chloride. In contrast, upon addition of water to bilirubin solution, the pyrrole protons give two separate peaks, as in pure bilirubin samples. This result is consistent with the previously reported proton exchange experiments (5). The signals of the four NH protons in the sample of bilirubin with benzyltrimethylammonium chloride are broadened, along with significant changes in chemical shifts (Figure 6.11 and Table 6.8). This downfield shift is possibly due to the deshielding effect of the π-electrons of the benzene ring when the benzene ring is aligned with the pyrrole rings of bilirubin upon interaction. This is consistent with the hydrophobic interaction characteristics between bilirubin and cholestyramine discussed in Section 5.3.6. It is unlikely that the deshielding effect is caused by hydrogen bonding since there exists a fast proton exchange for the pyrrole NH groups, as evidenced by the ^{15}N spectrum.

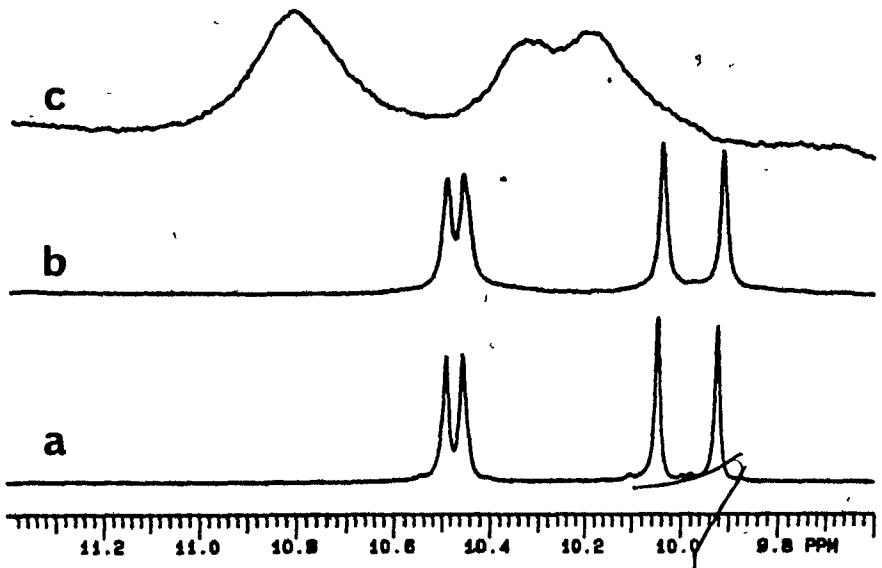

Figure 6.11 The ^{1}H NMR spectra of the NH groups of bilirubin upon interaction: (a) bilirubin; (b) bilirubin + water; (c) bilirubin + benzyltrimethylammonium chloride. Solvent: DMSO-d_6.

Unlike dilysine, benzyltrimethylammonium chloride is very soluble in DMSO so that a considerable amount can be added to the bilirubin solution. It is possible that benzyltrimethylammonium chloride interacts not only with the carboxyl groups of bilirubin but also with the π-electrons on the pyrrole rings and

with the pyrrole NH groups. However, dilysine interacts only with the propionic acid groups of bilirubin. This difference in interaction is very interesting and is consistent with the observation of the adsorption studies as discussed in Chapter 5, where the adsorption of bilirubin with cholestyramine was an entropy-driven process, indicating the significance of hydrophobic interactions between cholestyramine and bilirubin. The interaction of the π-electrons of the pyrrole rings of bilirubin with those of the benzene rings is of hydrophobic nature. For the binding of bilirubin with peptides consisting of lysine residues, the interactions through π-electrons do not exist.

6.6 The Salt Linkage - A Summary

From the study of proton and ^{13}C NMR spin-lattice relaxation times, it can be concluded that in the polar organic solvent, DMSO, the remarkable decrease of the relaxation time for the carboxyl group of the bilirubin molecule demonstrates that this group is involved in a specific interaction with dilysine. The concomitant decrease of T_1 for the carbon adjacent to the amino groups on the dilysine side chains provides evidence that the basic amino groups are involved in the binding. This is in agreement with the results of adsorption experiments in which it was found that an increase in the number of the basic amino acid residues on the resins enhances their binding capacity for bilirubin (Chapter 5). The nature of the interaction is concluded to be predominantly salt binding. The interaction process involves the dissociation of the hydrogen bonds of the bilirubin molecule and the formation of the ammonium carboxylate salt bond between bilirubin and the peptide. The proton T_1 study has also shown that the pyrrole and lactam NH groups are minimally involved, if at all, in the interaction with dilysine in DMSO.

The ^{15}N NMR study confirmed the lack of involvement of the NH groups of bilirubin in the interaction with dilysine. The addition of a quaternary ammonium salt (benzyltrimethylammonium chloride) selectively accelerates the proton exchange of pyrrole groups of bilirubin, indicating that the pyrrole NH groups are involved in the interaction with this salt. The deshielding effect of this compound for the pyrrole and lactam protons indicates a possible interaction between the π-electrons induced by the stacking of the phenyl and pyrrole rings.

The ^{15}N and proton NMR spectra of bilirubin and some of the related derivatives have been assigned successfully by 2-D ^{15}N-^{1}H heteronuclear correlation with the results shown in Tables 6.6 and 6.7. The similar conformations of bilirubin and bilirubin dimethyl ester in DMSO are confirmed by the ^{15}N NMR studies. The proton exchange between the two pyrrole rings of biliverdin molecule is identified by the ^{15}N NMR spectrum.

References

1. R. Brodersen, H. Flodgaard & J.K. Hansen, *Acta Chem. Scand.*, 21, 2284, 1967
2. A.W. Nichol & D.B. Morell, *Biochim. Biophys. Acta*, 177, 599, 1969
3. C.C. Kuenzle, M.H. Weibel, R.R. Pelloni & P. Hemmerich, *Biochem. J.*, 133, 364, 1976
4. A.F. McDonagh, **Chap. 6, Bile Pigments: Bilatrienes and 5,15-Biladienes**, p. 293, in *The Porphyrins, Vol. VI*, Part A, D. Dolphin, ed., Academic Press, 1979
5. D.W. Hutchison, B. Johnson & A.J. Knell, *Biochem. J.*, 123, 483, 1971
6. P. Manitto, G.S. Ricca & D. Monti, *Gazz. Chim. Ital.*, 104, 633, 1974
7. G. Navon, S Frank & D. Kaplan, *J. Chem. Soc., Perkin II*, 1145, 1984
8. P. Manitto & D. Monti, *J. Chem. Soc., Chem. Commun.*, 122, 1976
9. A.W. Nichol & D.B. Morell, *Biochim. Biophys. Acta*, 177, 599, 1969
10. C.C. Kuenzle, *Biochem. J.*, **119**, 395, 1970
11. C.C. Kuenzle, M.H. Wiebel & R. Pelloni, *Biochem. J.*, 133, 357, 1973
12. D. Harmatz & G. Blauer, *Arch. Biochem. Biophys.*, 170, 375, 1975
13. P.V. Woolley, M.J. Hunter & I.M. Arias, *Biochim. Biophys. Acta*, 446, 115, 1976
14. G. Blauer & T.E. King, *J. Biol. Chem.*, 245, 372, 1970
15. A.A. Lamola & J. Flores, *J. Am. Chem. Soc.*, 104, 2530, 1982
16. W. Kufer, H. Scheer & A.R. Holzwarth, *Isr. J. Chem.*, 23, 233, 1983
17. J. Subramanian, J.-H. Fuhrhop, A. Salek & A. Gossauer, *J. Mag. Reson.*, 15, 19, 1974
18. D. Kaplan & G. Navon, *Isr. J. Chem.*, 23, 177, 1983
19. V. Wray, A. Gossauer, B. Gruning, G. Reifenstahl & H. Zilch, *J. Chem. Soc., Perkin II*, 1558, 1979
20. M.S. Stoll, N. Vicker, C.H. Gray & R. Bonnett, *Biochem. J.*, 183, 139, 1979
21. P.E. Hansen, H. Thiessen & R. Brodersen, *Acta Chem. Scand., Ser. B*, 33, 281, 1979
22. D. Kaplan & G. Navon, *Org. Mag. Reson.*, 13, 59, 1980
23. N. Muller, *Mag. Reson. Chem.*, 23, 688, 1985
24. D. Kaplan & G. Navon, *J. Chem. Soc., Perkin II*, 1374, 1981
25. D. Kaplan & G. Navon, *Biochem. J.*, 201, 605, 1982
26. F.R. Trull, J.-S. Ma, G.L. Landen & D.A. Lightner, *Isr. J. Chem.*, 23, 211, 1983
27. D.A. Lightner, J.-S. Ma & X.-X. Wu, *Spectr. Lett.*, 19, 311, 1984

28. K.W. Zilm, D.M. Grant, R.C. Straight & E. Englert, Jr., *Biochem. Biophys. Res. Comm.*, **93**, 850, 1980
29. W.R. Woolfenden, D.M. Grant, R.C. Straight & E. Englert, Jr., *Biochem. Biophys. Res. Comm.*, **107**, 684, 1982
30. D.S. Henning, G.A. Lajoie, G.R. Brown, L.E. St-Pierre & S. St-Pierre, *Int. J. Artif. Organs*, **7**, 209, 1984
31. D.S. Henning, G.R. Brown & L.E. St-Pierre, *Int. J. Artif. Organs*, **9**, 33, 1986
32. M. Bouvier, G.R. Brown & L.E. St-Pierre, *Can. J. Chem.*, **65**, 1927, 1987
33. G.J. Martin, M.L. Martin & J.-P. Gouesnard, **Chap. 1, Introduction**, p. 1, in *^{15}N-NMR Spectroscopy*, Springer-Verlag, Berlin-Heidelberg-NY, 1981
34. D. Gust & J.D. Roberts, *J. Am. Chem. Soc.*, **99**, 3637, 1977
35. K. Kawano, Y. Ozaki, Y. Kyogoku, H. Ogoshi, H. Sugimoto & Z.-I. Yoshida, *J. Chem. Soc., Perkin II*, 1319, 1978
36. P.E. Hansen & H.J. Jakobsen, *Org. Mag. Reson.*, **22**, 668, 1984
37. H.J. Jacobsen, H. Bildsoe, S. Donstrup & O.W. Sorensen, *J. Mag. Res.*, **57**, 324, 1984
38. H. Falk & N. Muller, *Mag, Res. Chem.*, **23**, 353, 1985
39. G.A. Morris & R. Freeman, *J. Am. Chem. Soc.*, **101**, 760, 1979
40. G.A. Morris, *J. Am. Chem. Soc.*, **102**, 428, 1980
41. J.J. McCarthy, S.A. McClintock & W.C. Purdy, *Anal. Lett.*, **17 (16B)**, 1843, 1984
42. M.M. Ponpipom, R.L. Bugianesi, J.C. Robbins, T.W. Doebber & T.Y. Shen, *J. Med. Chem.*, **24**, 1393, 1981
43. S.E. Braslavsky, A.R. Holzwarth & K. Schaffner, *Angew. Chem. Int. Ed. Engl.*, **22**, 656, 1983

7 Contributions to Original Knowledge and Suggestions for Future Work

7.1 Contributions to Original Knowledge

This research project concerns studies of the binding of selected bile acids and bile pigments with peptides and quaternary amines by adsorption and NMR experiments. The contributions to knowledge derived from this research, which have been discussed in detail in the preceding chapters, are briefly summarized in this section.

Studies of the Binding Interactions of Bile Salts

Polyamide resins with quaternized peptide-containing pendants have been prepared and tested in tris and phosphate buffers for adsorption of various bile salts. Comparisons of these resins with commercial resins, such as cholestyramine and colestipol, in the binding of bile salts have been made. The originality of this work includes:

(1) The adsorption studies of bile salts using cholestyramine and colestipol reveal that the quaternary ammonium functional groups are important in the binding of bile salt from aqueous buffer solutions. This is indicative of the predominant ionic interactions. Ionic strength of the solution and mobile counterions of the resins have been shown to influence the binding affinity of bile salt anions by the resins;

(2) Polyamide resins with quaternized lysine pendants are shown to be less affected by the adsorption media, indicating that the resins containing peptide sequences have certain specificity for bile salt anions;

(3) The higher binding capacity of the ground form of the resin indicates the water-swellable resin matrix cannot be penetrated by the bile acid molecules and that the binding is dependent on the availability of the active sites. Longer

peptide-containing pendants have higher binding capacities for bile salts than shorter ones;

(4) The importance of the hydrophobic interactions in the binding of bile salts was evidenced by higher binding affinity for cholate anions than for glycocholate anions, as tested with all the polymeric resins;

(5) The interactions between the polymeric resins and biological molecules, i.e., the ionic linkage, hydrophobic interaction and hydrogen bonding have been elucidated based on a thermodynamic interpretation of the binding process.

The interactions of bile acids and bile salts with various ligands, including peptides, were studied by ^{13}C NMR experiments in both aqueous and DMSO solutions. This results in the following original contributions:

(1) The ^{13}C NMR spectra of selected primary and secondary bile acids in DMSO-d_6 were assigned with the aid of 2-D and DEPT experiments. The ^{13}C chemical shifts of certain carbons of bile acids in D_2O above the critical micellar concentration were found to be dependent on temperature and concentration. This dependence demonstrates the re-organization of bile salt micelles at different concentrations and temperatures;

(2) The measurements of the ^{13}C NMR relaxation times in D_2O and in DMSO-d_6 solutions revealed the relative mobility changes of the various groups of bile salts upon interaction with other species. The interactions were identified as a combination of ionic and hydrophobic interactions;

(3) A comparison of the interaction of cholic acid and its methyl ester with benzyltrimethylammonium chloride showed that the deciding factor in the interaction is the ionic linkage, without which the hydrophobic interaction is markedly weakened. Thus, the ionic and hydrophobic interactions occur cooperatively and simultaneously;

(4) The binding of bile salts with lysine containing peptides is much more efficient than with serum albumin on a weight basis.

Studies of the Binding Interactions of Bile Pigments

Polypeptides such as Poly-L-lysine and poly-D-lysine were coated onto the surface of the resin through the covalent amide bonds. The *in vitro* studies of these resins for the adsorption of bilirubin from phosphate buffer (0.050 M, pH = 7.8) showed that:

(1) Although the amounts of polypeptide coating affect the binding capacities of these resins on a weight basis, the adsorption capacity of the resins is directly proportional to the number of lysine residues, which is in accordance with the formation of an ionic linkage between the positively charged amino groups of the amino acid residues and the carboxylic groups of bilirubin;

(2) The stereostructure of lysine does not affect the binding of bilirubin with polylysine. Poly-D-lysine coated resin exhibits identical affinity for bilirubin as those coated with poly-L-lysines;

(3) The binding capacity of the polylysine-coated resins for bilirubin is higher than those with oligopeptide pendants, which indicates that the length of the peptide chain is of importance in the binding;

(4) The binding of bilirubin to cholestyramine has been shown to be an endothermic process, indicating the importance of hydrophobic nature of the binding. This result indicates the binding of bilirubin to cholestyramine and to the peptide containing resins may have different mechanisms (this is further confirmed by the ^{15}N NMR experiments).

The determinations of the ^{1}H and ^{13}C NMR spin-lattice relaxation times of the bilirubin in DMSO-d_6 and ^{15}N NMR studies revealed the following:

(1) The relatively larger changes in T_1 for the carboxyl groups of bilirubin and the CH_2 group adjacent to the amino group of dilysine upon mixing demonstrates the interaction between bilirubin and dilysine is mainly an acid-base salt bond formation process;

(2) No participation of the NH groups of bilirubin in the interaction with dilysine was detected, indicating the minimal involvement of these groups. This has been confirmed by both T_1 and ^{15}N studies;

(3) An interaction study of bilirubin with benzyltrimethylammonium chloride, an organic ammonium salt which resembles the structure of functional groups of cholestyramine, by ^{15}N and ^{1}H NMR experiments, demonstrated an involvement of the pyrrole NH groups and pyrrole rings of the bilirubin molecule in the interaction. The deshielding effect on the chemical shifts of the NH protons of bilirubin indicates interactions through the π-electrons. This interaction is different from that which occurs between bilirubin and peptides;

(4) The ^{15}N NMR spectra of bilirubin and related bile pigments in DMSO-d_6 were recorded using the INEPT sequence and were assigned by 2-D correlation

experiments with the proton spectra. The ^{15}N NMR spectrum of biliverdin confirmed the proton exchange process between rings B and C of the molecule.

7.2 Suggestions for Future Work

Further Characterization of the Interactions: Further confirmation of the hydrophobicity of bile acids in the interaction with various polymeric materials can be made by testing other commonly occurring bile acids including the secondary bile acids for adsorptions onto these adsorbents. Adsorption behavior at variable temperatures would provide further insight into the thermodynamic aspects of the binding process. Based on the thermodynamic parameters, the types of interactions may be further elucidated. Higher concentrations of bile salts, e.g., above the critical micellar concentration, can be tested for the adsorption experiments, since the formation of micelles may affect the binding characteristics of the adsorption process.

Study of the Peptide Conformations: For a better understanding of the role of peptides in the binding process, the conformation of peptides in solution as well as on the solid support should be investigated. This would provide further insight into the nature of the binding. The study would be possibly accomplished by various physico-chemical techniques, such as NMR, FTIR, Raman or a combination of these and other techniques. Conformational analysis of oligopeptides bound to polystyrene resin has been attempted by the use of IR spectroscopy (1). It should be interesting to analyze the particular peptide conformation on a water-swellable polymer resin.

***In Vivo* Studies and Peptide Stabilities:** The polymeric resins containing peptide sequences have already demonstrated very good adsorption capacities and selectivity for bile salts and bile pigments. The present studies of the adsorption by the resins are limited to *in vitro* test. It is of interest to test these resins under physiological conditions. These resins, which would be expected to have a better biocompatibility than the commercially available adsorbents, should be tested for hemoperfusion or oral administration purposes.

When these resins, or other peptide containing resins, are used for *in vivo* studies, the stability of peptides will become increasingly important. The improvement of the stability of peptides can be achieved by using the D-amino acid or modifications of the peptide bonds (Appendix 2). In fact, the modification

of the peptide bonds by thionation can possibly be done by integration into the solid phase peptide synthesis. With the application of the available methods to enhance the stability of the peptides, the new adsorbents containing peptide sequences are expected to be valuable agents for the adsorption of bile salts and bile pigments in the gastrointestinal tract and should demonstrate reasonable stability under normal conditions towards acidic or enzymatic hydrolysis and degradations.

Improvements for the Adsorbents: Since the binding of bile salts from solution involves a predominant ionic linkage and a cooperative hydrophobic interaction, resins with an enhanced number of active binding sites (the quaternary ammonium groups), can be prepared using similar procedures. Inclusion of hydrophobic moieties in the new resins is recommended to facilitate the hydrophobic interactions.

From the adsorption experiments, it is known that the surface area, i.e., the size of the resin particles, is also important for the binding. Therefore, resins with smaller mesh size are preferably selected. In the adsorption of bilirubin with the polylysine-coated resins, the fine resin (100-200 mesh) was used. The Bio-Gel resins are also commercially available in different mesh sizes (50-100, 200-400 and >400). It would be interesting to test the other resins with different mesh sizes.

The hydrolysis of polyamide at the first stage results in a partial conversion of the amide groups to carboxyl groups (2). The amount of the hydrolyzed amide groups on the resin prior to coupling with polylysine can be controlled by using different bases, or by the same base with different concentration or different reaction time (2). The degree of hydrolysis can be determined by ^{13}C NMR experiments (3). By controlling the number of carboxyl groups of the polyacrylamide resin, the average length of the free lysine sequences in the polylysine chain can be estimated. If this affects the binding behavior of the resin, a possible conformational effect of polypeptide can be verified.

References

1. M. Narita, Y. Tomotake, S. Isokawa, T. Matsuzama & T. Miyauchi, *Macromolecules*, **17**, 1903, 1984
2. W.M. Thomas & D.W. Wang, **Acrylamide Polymers**, p. 192, in *Encyclopedia of Polymer Science and Technology, Vol. 1*, 2nd ed., H.F. Mark, N.M. Bikales, C.G. Werberger, G. Menges & J.I. Kroschwitz, eds., John Wiley & Sons, NY-Chichester-Brisbane-Toronto-Singapore, 1985
3. J.A. Zurimendi, S.J. Guerrero & V. Leon, *Polymer*, **25**, 1314, 1984

Appendices

Appendix 1

Physical Properties of Bile Acids and Bile Pigments

A1.1 Bile Acids

(1) Cholic acid

3α,7α,12α-trihydroxy-5β-cholan-24-oic acid; 3α,7α,12α-trihydroxy-5β-cholanic acid; cholanic acid; 17β-(1-methyl-3-carboxypropyl)etiocholane-3α,7α,12α-triol; colalin.

$C_{24}H_{40}O_5$, MW = 408.59, pK_a = 4.98 (2 M), 5.2 (22 M).

Monohydrate, plates from dilute acetic acid. m.p. 198°C (anhydrous). Rhombic from ether; tetragonal rhombic from water or dilute alcohol solutions.

$[\alpha]^{20}_D$ +37 (alcohol, conc = 0.6%), $\lambda^{65\% \text{ sulfuric acid}}$ 318 (4.16), 377.5 (2.71).

Solubilities at 15°C (g/l): ether 1.22; chloroform, 5.08; alcohol, 30.56; benzene, 0.36; acetone, 28.24; acetic acid, 152.12; water, 0.28; also soluble in alkali hydroxides and carbonates.

Sodium salt: sodium cholate. Crystals. Very soluble in water (ca. 0.57 g/ml at 15°C).

Methyl ester: Crystals from 95% ethyl acetate and petroleum ether. m.p. 155-156°C.

(2) Glycocholic acid

N-[3α,7α,12α-trihydroxy-24-oxocholan-24-yl]glycine; N-cholylglycine.

$C_{26}H_{43}NO_6$, MW = 465.64, pK_a = 4.0 (2.2 M), 3.8 (20 M).

$[\alpha]^{20}_D$ +32.3 (alcohol, conc = 1%), $[\alpha]^{23}_D$ +30.8 (95% alcohol, conc = 7.5%), $\lambda^{65\% \text{ sulfuric acid}}$ 318 (4.18).

Needles from water. Sesquihydrate, crystals from 5% alcohol, m.p. 132-134°C (hydrate), 165-168°C (anhydrous).

Soluble in water (0.33 g/l at 15°C, 8.3 g/l at 100°C), alcohol and ether. Forms addition compounds with nitrobenzene, aniline, benzyl alcohol, benaldehyde, triolein. Hydrolyzed by acids and alkalies.

Sodium salt: sodium glycocholate. Crystals from 95% alcohol and ether, m.p. 230-240°C. Solubilities at 15°C: >0.27 g/ml in water, >0.34 g/ml.

(3) Taurocholic acid

2-{[3α,7α,12α-trihydroxy-24-oxo-5β-cholan-24-yl]amino}etanesulfonic acid; N-cholyltaurine; cholaic acid; cholyltaurine.

$C_{26}H_{45}NO_7S$, MW = 515.72, pK_a = 1.9 (19 M).

Prisms from alcohol-ether, m.p. ca. 125°C (decomposes).

$[\alpha]^{18}_D$ +38.8 (alcohol, conc = 2%), $\lambda^{\text{conc sulfuric acid}}$ 303 (3.64), 389 (4.45), 480 (3.46).

Freely soluble in water; soluble in alcohol (very soluble when hot); slightly soluble in ether and ethyl acetate.

Sodium salt: sodium taurocholate. Crystals with 1.5 and 2 moles water. Decomposes at 230°C. $[\alpha]^{20}_D$ +24 (conc = 3%). Very soluble in water and alcohol.

(4) Chenodeoxycholic acid

3α,7α-dihydroxy-5β-cholanic acid; 3,7-dihydroxycholan-24-oic acid; anthropodesoxycholic acid; gallodesoxycholic acid; 17β-(1-methyl-3-carboxypropyl)etiocholane-3α,7α-diol; chenic acid; chenodiol.

$C_{24}H_{40}O_4$, MW = 392.59, pK_a = 5.9 (2.2 M), 6.2 (23 M).

Needles from ethyl acetate-heptane, m.p. 143°C (119°C).

$[\alpha]^{20}_D$ +11.1 (alcohol, conc = 2.1%), $\lambda^{65\% \text{ sulfuric acid}}$ 272 (3.58), 380 (4.35).

Very soluble in alcohol and acetone; soluble in ether and acetic acid; insoluble in water, benzene and petroleum ether.

(5) Deoxycholic acid

3α,12α-dihydroxy-5β-cholanic acid; desoxycholic acid; 17β-(1-methyl-3-carboxypropyl)etiocholane-3α,12α-diol.

$C_{24}H_{40}O_4$, MW = 392.59, pK_a = 5.3 (2 M), 6.2 (23 M), m.p. 176-178°C.

$[\alpha]^{20}_D$ +57 (alcohol), $\lambda^{65\% \text{ sulfuric acid}}$ 310 (3.79), 380 (3.29).

Very soluble in alcohol; slightly soluble in chloroform, acetic acid, ether and acetone; insoluble in water and benzene.

(6) Lithocholic acid

3α-hydroxy-5-cholan-24-oic acid; 3α-hydroxycholanic acid; 17β-(1-methyl-3-carboxypropyl)etiocholane-3α-ol.

$C_{24}H_{40}O_3$, MW = 376.59, m.p. 186°C.

hexagonal leaves from alcohol, prism from dilute alcohol or acetic acid.

$[\alpha]^{20}_D$ +32.14 (alcohol), $\lambda^{\text{conc sulfuric acid}}$ 326 (3.53).

soluble in alcohol, very soluble when hot; soluble in chloroform, acetic acid; slightly soluble in ether, insoluble in water and ligroin.

(7) Cholesterol*

cholest-5-en-3β-ol; cholesterin.

$C_{27}H_{46}O$, MW = 386.67, m.p. 148°C (anhydrous), b.p. 360°C (decomposes), 233°C (0.5 atmosphere); $d = 1.067^{20/4}$.

$[\alpha]^{20}_D$ -31.5 (ether, conc = 2%), -39.5 (chloroform, conc = 2%), λ^{alcohol} 206 (3.53).

Monohydrate, pearly leaflets of plates from dilute alcohol solution. Becomes anhydrous at 70-80°C. Rhombic or triclinic leaves from alcohol+water, needles from ether.

Practically insoluble in water (ca. 2 mg/l). Slightly soluble in alcohol (1.29% w/w at 20°C), more soluble in hot alcohol (28% w/w in saturated 96% alcoholic solution at 80°C). Soluble in chloroform (0.29 g/ml), ether (0.36 g/ml) and pyridine (0.67 g/ml). Also soluble in benzene, petroleum ether, acetic acid, dioxane, CS_2, oils and fats. Gives intense red color with rosaniline in chloroform solution.

A1.2 Bile Pigments

(1) Bilirubin IXα

1,10,19,21,23,24-hexahydro-2,7,13,17-tetramethyl-1,19-dioxo-3,18-divinylbilin-8,12-dipropanoic acid; 8,12-*bis*(2-carboxyethyl)-10,21,23,24-tetrahydro-2,7,13,17-tetramethyl-3,18-divinyl-bilin-1,19-dione; 8,12-*bis*(carboxyethyl)-2,7,13,17-tetramethyl-3,18-divinyl(10H,21H,23H,24H)bilin-1,19-dione; 2,17-diethenyl-1,10,19,22,23,24-hexahydro-3,7,13,18-tetramethyl-1,19-dioxo-21H-biline-8,12-dipropanoic acid (Chemical Abstract).

---

* not a bile acid.

$C_{33}H_{36}N_4O_6$, MW = 584.65.

$\lambda^{chloroform}$ 454, pK_a = ca. 4.4.

Light orange to deep reddish-brown monoclinic rhomboid, prisms, plates from chloroform. m.p. 234 (decomposes), gradually blackens on heating and does not melt. Solution shows a red fluorescence in UV light. Practically insoluble in water. Soluble in chloroform, dimethyl sulfoxide, benzene, chlorobenzene, carbon disulfide, acids and alkalies. Slightly soluble in alcohol and ether.

Dimethyl ester: MW = 612.7. Crystals from methanol, m.p. 198-200°C. Soluble in chloroform, DMSO and acetone. $\lambda^{chloroform}$ 400.

(2) Biliverdin IXα

2,17-diethenyl-1,19,22,24-tetrahydro-3,7,13,18-tetramethyl-1,19-dioxo-21H-biline-8,12-dipropanoic acid (Chemical Abstract); 1,19,23,24-tetrahydro-2,7,13,17-tetramethyl-1,19-dioxo-3,18-divinylbilin-8,12-dipropanoic acid; 4,5-di(2-carboxyethyl)-1,3,6,7-tetramethyl-2,8-divinylbilatriene; dehydrobilirubin; uteroverdine.

$C_{33}H_{34}N_4O_6$ MW = 582.63.

λ^{MeOH} 376, 665, pK_a = ca. 5.0.

Dark green plates or prisms with violet surface color from methanol. Blackens and decomposes above 300°C and does not melt. Soluble in methanol, ether, chloroform, dimethyl sulfoxide, benzene, chlorobenzene, carbon disulfide and alkali hydroxides.

Dimethyl ester: MW = 610.7. Crystals from chloroform-petroleum ether, m.p. 208-209°C. Soluble in chloroform and DMSO. $\lambda^{chloroform}$ 379, 656-664.

(3) Mesobilirubin IXα

2,17-diethyl-1,10,19,22,23,24-hexahydro-3,7,13,18-tetramethyl-1,19-dioxo-21H-biline-8,12-dipropanoic acid; 1,10,19,22,23,24-hexahydro-3,7,13,18-tetramethyl-1,19-dioxo-3,18-diethylbiline-8,12-dipropanoic acid; 1,3,6,7-tetramethyl-4,5-dicarboxyethyl-2,8-diethyl-(β-13)-dihydrobilenone; 10,23-dihydromesobilin.

$C_{33}H_{40}N_4O_6$, MW = 588.70. $\lambda^{chloroform}$ 433.

Crystals from chloroform-methanol. m.p. 250°C (decomposes). Soluble in chloroform and DMSO.

(4) Protoporphyrin IX

7,12-diethenyl-3,8,13,17-tetramethyl-21H,23H-porphine-2,18-dipropanoic acid; 3,7,12,17-tetramethyl-8,13-divinyl-2,18-porphinedipropionic acid; 1,3,5,8-tetramethyl-2,4-divinylporphine-6,7-dipropionic acid; coporphyrin.

$C_{34}H_{34}N_4O_4$, MW = 562.64.

Monoclinic, brownish-yellow prisms from ether. Blackens and decomposes above 300°C and does not melt. Freely soluble in chloroform, dimethyl sulfoxide, acetic acid, hydroxychloric acid, alcohol with HCl, ether with HOAc. Somewhat soluble in dilute alkalies, aniline, pyridine. Sparingly soluble in disodium and dipotassium salts.

(5) Heme

[7,12-diethenyl-3,8,13,17-tetramethyl-21H,23H-porphine-2,18-dipropanoato(4-)-N^{21},N^{22},N^{23},N^{24}]-ferrate(2-)dihydrogen; [dihydrogen 3,7,12,17-tetramethyl-8,13-divinyl-2,18-porphinedipropionato(2-)]iron; 1,3,5,8-tetramethyl-2,4-divinylporphine-6,7-dipropionic acid ferrous complex; ferroprotoporphyrin; ferroheme; protoheme.

$C_{34}H_{32}N_4O_4Fe$, MW = 616.48.

Fine brown needles with a dark violet sheen. Sparingly soluble in acetic acid. Freely soluble in the presence of oxygen. Very unstable.

References

1. *The Merck Index: An Encyclopedia of Chemicals, Drugs, and Biologicals*, 10th Ed., M. Windholz, S. Budavari, R.F. Blumetti & E.S. Otterbein, eds., Merck & Co., Inc., USA, 1983
2. *Bilirubin, Vol I, Chemistry*, K.P.M. Heirwegh & S.B. Brown, eds., CRC Press, Florida, 1982
3. A.F. McDonagh, **Chap. 6, Bile Pigments: Bilatrienes and 5,15-Biladienes**, p. 293, in *The Porphyrins, Vol. 4*, D. Dolphin, ed., Academic Press, 1979
4. *CRC Handbook of Chemistry and Physics*, 62nd ed., R.C. Weast & M.J. Astle, eds., CRC Press, Inc., Boca Raton, Florida, 1981
5. D.M. Small, **Chap. 8, The Physical Chemistry of Cholanic Acids**, p. 249, in *The Bile Acids, Vol. 1*, P.P. Nair & D. Kritchevsky, eds., Plenum Press, N.Y., 1971

Appendix 2

Solid Phase Peptide Synthesis and the Stability of Peptides

The solid phase peptide synthesis technique was first devised by R.B. Merrifield in 1962, for which he was awarded the Nobel Prize in 1984. The method provides a simple and rapid way for the organic synthesis of peptides. It utilizes an insoluble polymer support onto which the C-terminal end of the amino acid is attached to the functional groups of the polymer. The rest of the amino acids are added stepwise until the desired sequence is completed. If desired, the final peptide sequence can be cleaved from the polymer support.

A2.1 The Protections of Amino acids

Prior to coupling of the amino acids to the solid support, either the N or the C terminal groups must be selectively protected, depending on which group is to be coupled to the polymer support. If the amino acid possesses a side group which reacts in the coupling process, this group must also be protected.

Protection of the Amino Groups: The α-amino groups of amino acids can be acylated by treatment with anhydrides or acid halides. Typically, the amino group is protected by reacting with benzylchlorocarbonate. The reaction yields the benzyloxycarbonyl derivative of the amino acid. Other protecting reagents, such as the BOC (*tert*-butyloxycarbonyl) reagent, are also available. The protection methods for the α-amino group are depicted in Figure A2.1. Usually, the acylation must be done in mild conditions to avoid racemization of the amino acid. For this reason less polar solvents are preferred for the reaction.

Protection of the Carboxyl Groups: If the amino groups are to be coupled to the solid support, the carboxyl groups need to be protected. This can be done by esterification with ethanol or benzyl alcohol.

Protection of the Side Chain Groups: The side groups of amino acids, such as the amino group of lysine, the guanidinium groups of arginine, the

carboxyl group of glutamic acid and the thiol group of cysteine, should also be protected in the solid phase peptide synthesis.

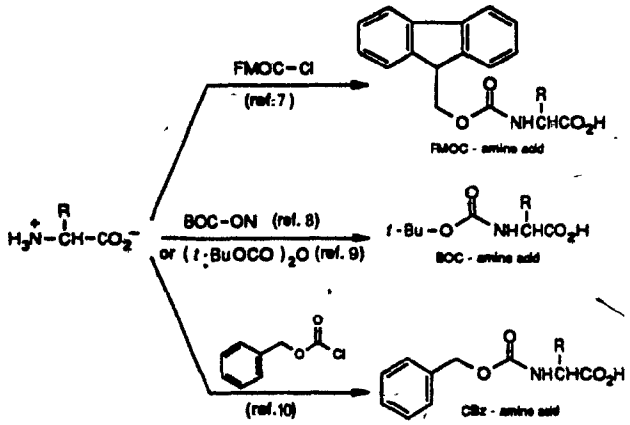

Figure A2.1 The protection methods for the α-amino group of the amino acids. FMOC: 9-fluorenylmethyloxycarbonyl; BOC-ON: 2-(*t*-bytyloxycarbonyl-oximino)-2-phenylacetonitrile; BOC: *tert*-butyloxycarbonyl; CBz: carbobenzoxy.

Ninhydrin Test: The primary amine groups can react with ninhydrin to form a blue-purple pigment on heating (Figure A2.2). The products formed with secondary amines, such as the amino group of proline, have a less intense color. This reaction can be used for a quantitative estimation of amino acids in small amounts. The UV detector of the HPLC system for the amino acid analysis also detects this colored compounds at 440 nm for proline and 570 nm for other amino acids.

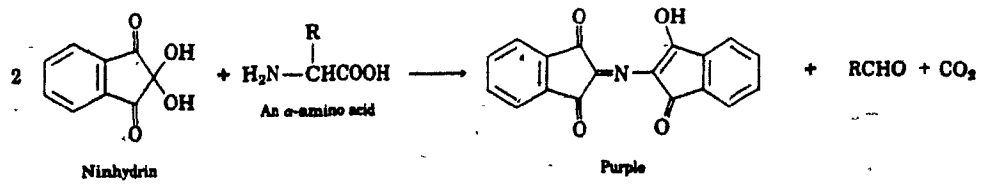

Figure A2.2 The reaction of amino acids with ninhydrin.

A2.2 Solid Phase Peptide Synthesis

For the Merrifield synthesis, a chloromethyl derivative of styrene-divinylbenzene copolymer is normally used. This polymer support forms an ester bond with the peptide sequence which ensures a complete cleavage of the peptide from the resin. Another kind of resin, often referred to as the Sheppard resin, is a water-swellable polyacrylamide resin with primary amine functional groups. The peptide remains on the resin after the synthesis.

The polyacrylamide resin (from Chemalog), which is a copolymer of dimethylacrylamide and N-acryl-1,6-diaminohexane crosslinked with bisacryl-1,2-diaminoethane (11%), can be used as the polymer support. Sequences of peptide can be synthesized onto the polymer using solid phase peptide synthesis techniques.

The flow chart of solid peptide phase synthesis is shown in Figure A2.3. The resin is first neutralized with an organic base, N,N-diisopropyl ethylamine, in dichloromethane (DCM). The anhydrides of the protected amino acids are prepared by reacting with DCC (1,3-dicyclohexyl-carbodiimide) in DCM. After filtering the urea formed as a by-product of the reaction, the anhydride solution is added to the resin and allowed to react for 3-9 hours. The completion of the coupling can be monitored by a negative ninhydrin test. After coupling, the resin is washed with DMF, DCM, etc. Finally the resin is reacted with 40% trifluoroacetic acid in DCM to remove the protecting group of the α-amino group. This is again followed by neutralization with DEA/DCM and washing. The entire procedure is automated by a computer controlled peptide synthesizer. An example of the programs used for the synthesis is depicted as in Table A2.1.

When the synthesis of the desired peptide sequence is finished, the resin is washed with DMF, DCM and anhydrous ether several times and dried before a complete deprotection. The deprotection is performed using an HF line made of Teflon material and equipped with safety supplies in a fumehood. The reaction flask containing the resin is pumped to vacuum. Anhydrous hydrofluoric acid is introduced into the vacuum and condensed with liquid nitrogen. The protecting groups of the amino acid side chains are removed by slowly stirring the resin in HF at 0°C for 60 minutes. After the evaporation of the HF under vacuum at room temperature, the resin is finally washed with anhydrous ether and dried under

vacuum. If the Merrifield resin is used, the peptide sequence are cleaved from the polymer support and can be purified and treated appropriately.

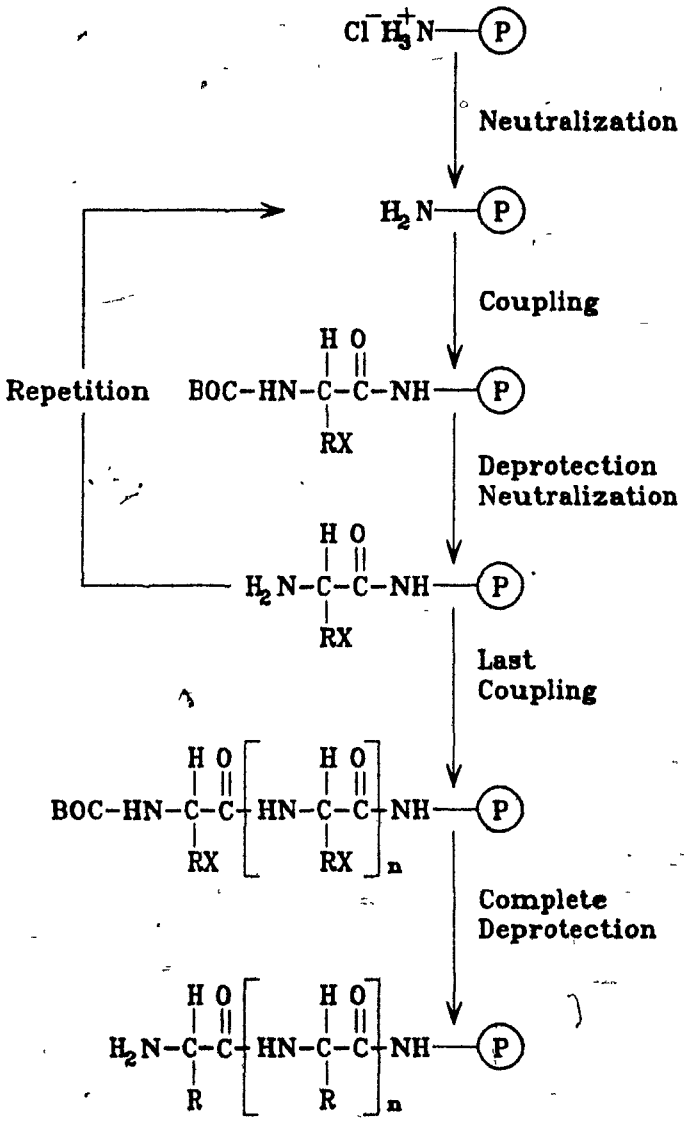

Figure A2.3 The reaction scheme for the solid phase peptide synthesis.

Table A2.1 The Computer Program for the Automated Peptide Synthesizer

Step	Operation	Reagent	Repetitions	Time (min)
1	Coupling	Anhydride of Amino Acid	1	> 180 (to completion)
2	Washing	DCM	2	1
3	Washing	DMF	1	1
4	Washing	DCM	3	1
5	Deprotection	40% TFA/DCM	1	20
6	Washing	DCM	2	1
7	Neutralization	5% DEA/DCM	1	5
8	Washing	DMF	2	1
9	Washing	DCM	4	2

The polyamide resin has primary amine functional groups in the form of hydrochloric acid. Thus, the total synthesis starts at Step 7 to neutralized the resin. Step 9 is followed by step 1 if another amino acid is to be added to the sequence. Upon completion of the peptide sequence, after Step 4, the resin is then washed with ether and dried before a complete deprotection on the HF line.

A2.3 Peptide Stability and Modifications of Peptides

The present studies on the interaction of bile acids and bile pigments with peptide-containing resins were limited to *in vitro* test. When these resins are applied for *in vivo* studies, the stability of peptides will become increasingly important. The stability of the peptides under the action of acids or enzymes and the methods used to improve the stability are discussed briefly in this section.

A2.3.1 Acidic and Enzymatic Hydrolysis of Peptides

It is well known that peptides undergo hydrolysis in the presence of specific enzymes (11), strong acids or bases. Concentrated acid (6N HCl) and high temperature are usually needed for the hydrolysis of peptides. At lower temperatures, it may take as long as several days for a partial hydrolysis of peptides. Considering the biological conditions in the human body, the main challenge is enzymatic hydrolysis rather than that with acids or bases.

Trypsin is the most specific proteolytic enzyme for peptides consisting of basic amino acids. It occurs as an inactive zymogen (trypsinogen) in the

pancreas. This zymogen can be activated by trypsin followed by the release of short peptide (12). The action of trypsin is limited almost exclusively to the peptide bonds associated with the carboxyl groups of lysine and arginine. The peptide bonds associated with the carboxyl group of tryptophan can also be partially hydrolyzed during long hydrolysis. If proline is coupled to the carboxyl group of lysine or arginine, the hydrolysis may not take place at all (12).

Like trypsin, other enzymes such as chymotrypsin and pepsin can also cause the cleavage of the peptide bonds with less specificity and a lower rate.

A2.3.2 The Enhancement of Peptide Stability

Over the years many methods have been studied to increase the stability of the peptide bond while maintaining the same biological function of the modified species.

The natually occuring α-amino acids are mostly chiral molecules. Most of the amino acids found in the human body are in the L-form. The peptide-hydrolyzing enzymes, of the proteases and peptidases, are generally specific for peptides having the L-α-amino acids in normal peptide linkage. D-amino acids do not occur in proteins, but some nonprotein peptides contain D-amino acids or other variations such as β-amino acids and γ-peptide bonds. The variations in structure protect the specialized peptides from enzymatic hydrolysis. The bacterial cell wall, which contains D-amino acids in its peptidoglycan structure, is resistant to the action of proteases (13). The peptide-hydrolyzing enzymes do not attack peptides consisting of D-amino acids because the scissile bond is not properly located relative to the catalytic site, as shown in Figure A2.4. In this enzyme-substrate complex of chymotrypsin and a peptide containing D-amino acids, the dihedral angles of the substrate must be adjusted for the cleavage of the peptide bond (14).

It is known that the hydrolysis of peptides by some enzymes is initiated at either the C-terminal or N-terminal (16). Therefore, the end groups can be selectively blocked chemically to prevent the hydrolysis by these enzymes. More often, it is the peptide bonds that are the target of hydrolytic enzymes. Hence, the stability of the peptides can be greatly enhanced by modifying the peptide linkages. Some of the methods used for the peptide backbone modifications have been summarized by Morley (17), thionation of the peptide bonds being one of the many available methods (18).

Oligopeptides consisting of mostly neutral amino acids have been thionated using a modified thionation reagent (19). The reaction is shown schematically in Figure A2.5. The final product can be purified by flash chromatography on a silica column with ethyl acetate-methanol as eluent. The geometry of the thiopeptide units is very close to that of the parent peptides, therefore adopting similar conformational properties (20).

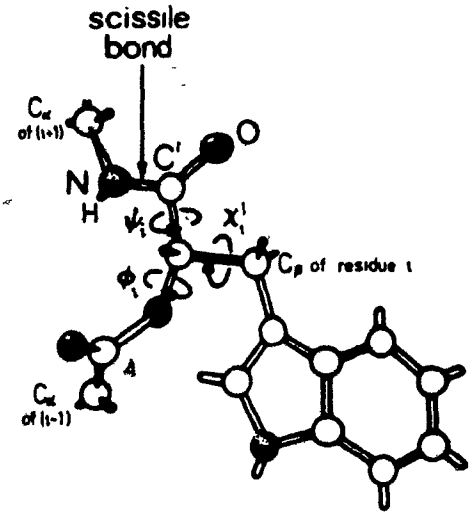

Figure A2.4 Substrate-binding to chymotrypsin (reference 15). Adjustments of the dihedral angles of the substrate have to be made for the cleavage of the peptide bond.

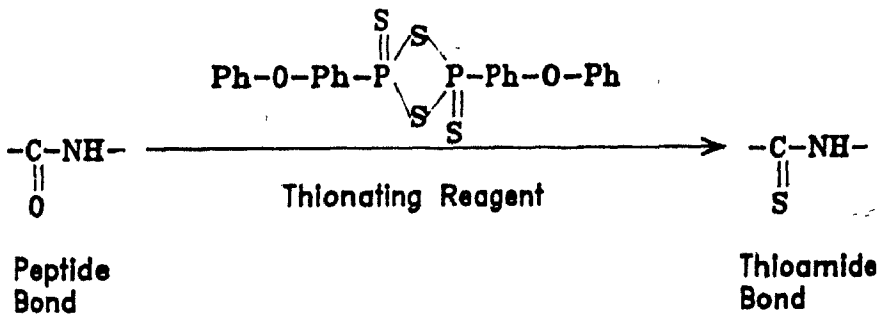

Figure A2.5 The thionation of the normal peptide bond.

A preliminary test for the thionation of a simple oligopeptide, diarginine, was done using the method developed by Belleau *et al.* (19). The diarginine was prepared following a procedure reported by Otsuka *et al.* (21) with modifications.

BOC-arginine was coupled with equal molarity of nitro-protected arginine methyl ester in a mixture of DMF and dichloromethane. The product was extracted and then precipitated from n-butanol. Thio-diarginine was prepared by reacting with this product and excess thionation reagent in dry THF. The reaction mixture was agitated at room temperature for at least 12 hours under nitrogen. Two overlapped spots were observed under the UV light on the TLC plate, after development with 5% ninhydrin in ethanol as eluent, indicating that the thioamide indeed formed in this reaction. Since the polarity of thio-diarginine did not differ much from that of diarginine, the separation of these two species was not satisfactory. The thiopeptides are usually amorphous, and thus very difficult, if not impossible, to crystallize, especially for the peptides consisting of amino acids with polar side chains. For peptides with polar side group, other separation methods such as HPLC could probably give better results.

A2.3.3 The Stability of the Peptide-Containing Resins

Enzymes are specific for the hydrolysis process. The peptides have to adopt a certain conformation to fit in the receptor of the enzyme. For the peptide containing resins, in general, it is possible that the enzymes are sterically hindered by the resin support, i.e., the accessibility of the peptide chain on the resin to enzymes is reduced by the presence of the backbone polymer. Therefore, it can be estimated that the stability of the peptide on the resin is enhanced compared with the polypeptides dissolved directly in solutions.

The poly-D-lysine coated resin exhibits the same, if not better, capacity and affinity for bilirubin. The D-amino acids can be used to replace the L-amino acids for the peptide resins, e.g., using poly-D-lysine instead of poly-L-lysine. It is expected that the peptide consisting of D-amino acids would be more resistant to the enzymatic hydrolysis.

The solid phase peptide synthesis technique can possibly be applied for the thionation. This can be accomplished by reacting the thionating reagent with the amino acid residues on peptide pendant immediately after coupling but before deprotection. If needed, the final thiopeptide can be cleaved from the resin for stability test or other experiments in solution.

The polymeric resins containing peptide sequences may demonstrate reasonable stability under normal conditions towards acidic or enzymatic

hydrolysis and degradation with all the available methods to enhance the stability of the peptides.

References

1. J.M. Stewart & J.D. Young, *Solid Phase Peptide Synthesis*, Pierce Chemical Company, 1984
2. R.C. Sheppard, **Continuous Flow Methods in Organic Synthesis**, *Chemistry in Britain*, 402, 1983
3. C. Birr, *Aspects of the Merrifield Peptide Synthesis*, Spring-Verlag, Berlin-Heidelburg, 1978
4. J. Meienhofer, **Peptide Synthesis: A Review of the Solid Phase Method**, p.45, in *Hormonal Proteins and Peptides, Vol. 2*, C.H. Li, ed., Academic Press, NY-London, 1973
5. R.B. Merrifield, *Fed. Proc.*, **21**, 412, 1962
6. R.B. Merrifield, *J. Am. Chem. Soc.*, **85**, 2149, 1963
7. L.A. Carpino & G.Y. Han, *J. Org. Chem.*, **37**, 3404, 1972
8. M. Itoh, D. Hagiwara & T. Kamiya, *Bull. Chem. Soc. Jpn.*, **50**, 718, 1977
9. D.S. Tarbell, Y. Yamamoto & B.M. Pope, *Proc. Natl. Acad. Sci. USA*, **69**, 730, 1972
10. M. Bergmann & L. Zervas, *Ber.*, **65**, 1192, 1932
11. **The Enzymes, Vol. 3, Hydrolysis: Peptide Bonds**, P.D. Boyer, ed., 3rd ed., Academic Press, NY-London, 1971
12. W.A. Schroeder, **Chap. 9, Methods for Partial Hydrolysis of the Peptide Chain**, p. 93, in *The Primary Structure of Proteins*, Happer & Row Publishers, NY-Evanston-London, 1968
13. A.L. Lehninger, p. 269, in *Biochemistry*, Worth Publishers, N.Y., 1975
14. D.W. Ingles & J.R. Knowles, *Biochem. J.*, **104**, 369, 1967
15. D.M. Blow, *Acc. Chem. Res.*, **9**, 145, 1976
16. W.N. Lipscomb, *Proc. Natl. Acad. Sci. USA*, **77**, 3875, 1980
17. J.S. Morley, *Trends Pharm. Sci.*, **1**, 463, 1980
18. W. Reid & E. Schmidt, *Ann. Chem.*, **695**, 217, 1966
19. G. Lajoie, F. Lepine, L. Maziak & B. Belleau, *Tetrahedron Lett.*, **24**, 3815, 1983
20. T.F.M. La Cour, H.A.S. Hansen, K. Clausen & S.-O. Lawesson, *Int. J. Pept. Prot. Res.*, **22**, 509, 1983
21. H. Otsuka, K. Inouye, M. Kanayama & F. Shinozaki, *Bull. Chem. Soc. Japan*, **39**, 882, 1966

Appendix 3

NMR Pulse Sequences

The development of the Fourier transform (FT) methods in NMR allows the introduction of a pulse sequence which is a series of radio frequency pulses with appropriate time delays between them. In modern FT nuclear magnetic resonance techniques, many pulse sequences are used for more sophisticated NMR experiments which provide very valuable information about the structure and conformation of the chemical substances.

A3.1 Spin-Lattice Relaxation Time (T_1) Measurement

For nuclei with spin quantum number I = 1/2, there are two energy levels in the Boltzmann distribution, the lower corresponding to a quantum number m = −1/2 and the upper to m = +1/2. The Boltzmann equation can then be expressed by

$$\frac{N^+}{N^-} = \exp\left(-\frac{\Delta E}{kT}\right) \qquad \text{(Equation A3.1)}$$

When the sample is outside a polarizing magnetic field, the difference in energy between the two levels is essentially zero. Therefore, the population N^+ and N^- must be equal. When the sample is placed in a magnetic field, the redistribution of population can be established after an interaction of the nuclei with the surroundings (the lattice). The time required for this adjustment serves as a measure of the rate at which the spin system returns to equilibrium with its environment and is therefore called the *spin-lattice relaxation time*, T_1.

The spin-lattice relaxation time is also referred to as the longitudinal relaxation time since it characterizes the rate that the longitudinal component (the *z*-component) of nuclear magnetization returns to its equilibrium value after being perturbed by a radio frequency pulse. In the NMR spectrum, the relaxations give rise to an exponential decay in the observed signals. The measured T_1 value is

actually the reciprocal of this exponential rate and represents the time after the perturbation that is required to recover 1–(1/e) or 63.2% of the magnetization lost as a result of the perturbation. There are many ways to measure the T_1 value, two common ones of which are the inversion-recovery method and the progressive saturation method. The inversion-recovery method was used in the presently reported experiment and is described in detail here.

In the inversion recovery method, the longitudinal component (the *z*-component) of the magnetization at equilibrium is perturbed by a single radio frequency pulse, which flips the *z*-component exactly 180°. After some time (referred to as delay time D_2) another pulse is applied to flip the magnetization 90° so that it lies in the *x-y* plane to be measured (Figure A3.1). The signal generated after this second pulse will be a measure of the value of the longitudinal magnetization present at that time. This value in turn will depend on the amount of recovery or relaxation that occurred during the time between the perturbing and the measuring pulse. The pulse sequence can be expressed by

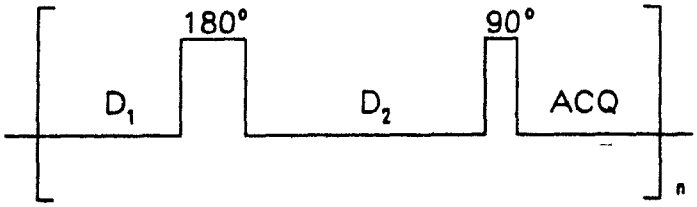

(The inversion-recovery pulse sequence)

where D_1 is the equilibrium time, which is chosen, together with signal accumulation time (ACQ), during which no actual data is acquired, to be at about five times the longest T_1 of interest to enhance the signal to noise ratio and for the equilibrium magnetization to recover; D_2 is the recovery time, which is usually set as an array of at least 5 points to cover a range of 0.1 to 3 times T_1. A 90° pulse is one whose duration is sufficient to tip the *z*-magnetization into the *x-y* plane.

The recovery of the longitudinal magnetization after the perturbing pulse can be measured as a function of time by repeating the above experiment over a range of different D_2 recovery times. The data analysis involves a three parameter least squares fit to an exponential curve as a function of this delay time from which the T_1 is calculated.

Since a sufficient number of transients must be accumulated for each spectrum, this method is time consuming compared with the other methods such as the progressive saturation, especially when used for such insensitive nucleus as ^{13}C. However, it is considered to be an accurate method for T_1 measurement since it is less critical to imperfect setting of the pulse angles. Even so, the pulse angles should be carefully calibrated prior to the experiment to eliminate errors in measurement.

If the T_1 of interest is very long, the *progressive saturation method* is preferable. Other methods such as COMB can also be used to enhance the accuracy and time efficiency of the measurements.

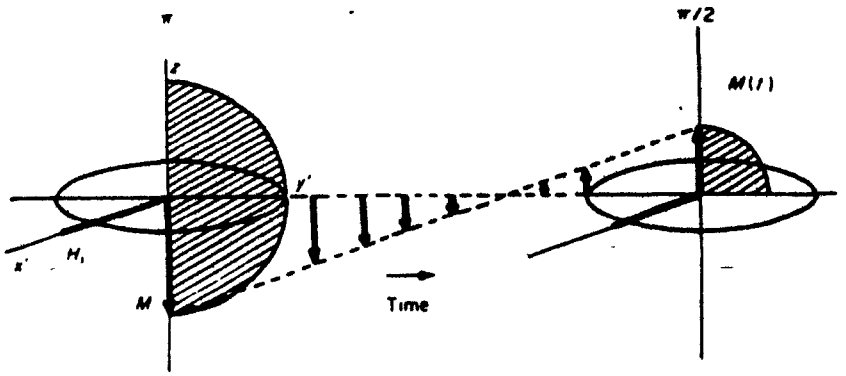

Figure A3.1 Diagram illustrating the principle of the inversion recovery experiment (reference 5).

A3.2 The INEPT (Insensitive Nuclei Enhanced by Polarization Transfer) Pulse Sequence

Certain nuclei which are most suitable for NMR measurement, such as ^{13}C, ^{15}N and ^{29}Si, suffer low natural abundance, long T_1's, and unfavorable gyromagnetic ratios. The sensitivity of these nuclei can be enhanced by transfer of polarization from protons to the insensitive nucleus.

For a two spin system consisting of a sensitive and an insensitive nucleus, e.g., ^1H-^{13}C or ^1H-^{15}N, the population of the energy levels in equilibrium is given by the Boltzmann law

$$N^+/N^- = \exp(-\Delta E / kT)$$

$$= \exp(-\gamma h B_0 / 2\pi kT)$$

$$= 1 - (\gamma h B_0 / 2\pi kT) \qquad \text{(Equation A3.2)}$$

where B_0 is the strength of the magnetic field, γ the gyromagnetic ratio, T the temperature, h the Planck constant, and k the Boltzmann constant.

The population difference between the two states E^+ and E^- is determined by the gyromagnetic ratio γ of the nucleus which changes its spin state during the transition E^+ to E^-. A larger population difference results for states involving the sensitive nucleus (usually ^1H, with large γ) than for those of the less sensitive nucleus (X, with small γ).

If the respective spin population are interchanged through a selective population inversion involving a ^1H transition, the absorption and emission for the X transition is enhanced. The Boltzmann distribution that determined the spin populations for ^1H now governs those of the less sensitive nucleus X. This phenomenon is know as polarization transfer.

Experimentally, population inversion can be achieved through a $180°_x$ pulse applied at the frequency of a ^1H line. The polarization transfer can also be achieved non-selectively through a proper pulse sequence. In the INEPT sequence, the transverse magnetization of the sensitive nucleus ^1H is modulated through coupling to the less sensitive nucleus X and the simultaneous application of two $180°_x$ pulses in the ^1H and X frequency regions. The vector arrangement obtained after the evolution period for the doublet components of the ^1H nucleus can be transformed into the characteristic arrangement of a selectively inverted spin system through application of a $90°_y$ pulse. This corresponds to a population inversion of one ^1H line and leads to polarization of the X lines. The INEPT pulse sequence is shown below:

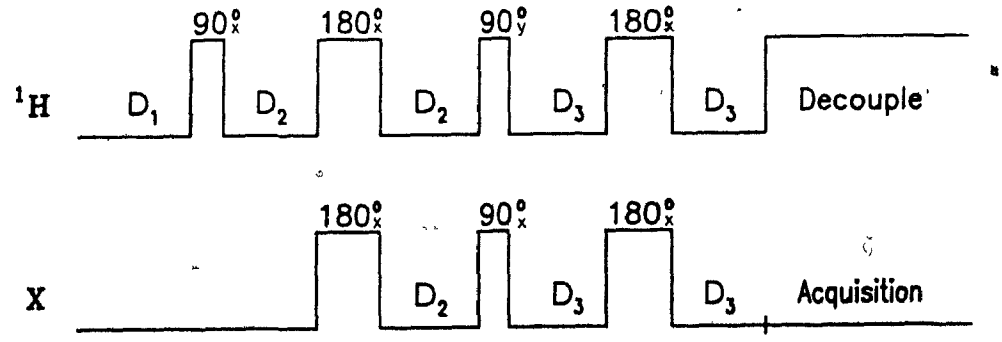

(The refocussed INEPT pulse sequence)

where D_1 is the preparation delay, D_2 the evolution delay, and D_3 the refocussing delay. The evolution delay of the INEPT pulse sequence is based on the particular X-H coupling constant and must be estimated if not known. A discrimination of the carbon types is made possible by the INEPT sequence, particularly CH's from CH_2's. Since the refocussing delay D_3 is dependent on the nature of the X-H multiplet, it is possible to adjust this delay to favor one type of multiplet, e.g., the CH doublet can be efficiently selected by setting this delay to 1/(4J). For the ^{15}N experiment, if different NH and NH_2 groups are present at least a second experiment must be performed.

The success of a polarization transfer experiment is determined largely by the relaxation time of sensitive nucleus A. This determines the time necessary for the perturbed spin system to return to the equilibrium state and must be long enough to prevent reestablishment of the normal Boltzmann distribution during the pulse sequence.

Using the INEPT pulse sequence, the intensity enhancement in suitable cases can be much higher than that obtained with the well-known nuclear Overhauser effect (NOE). Negative gyromagnetic ratio γ values are not disadvantageous because sensitivity enhancement for polarization transfer experiments is governed by the ratio γ_H/γ_X instead of the sum $1 + \gamma_H/2\gamma_X$, which is the maximum enhancement factor for the NOE experiments.

INEPT experiments have also been used to enhance ^{29}Si and metal nuclei by polarization transfer of ^1H and ^{31}P nuclei. In addition, the INEPT sequence has been used to measure the spin-lattice relaxation time of ^{13}C (10), ^{15}N (11,12), ^{29}Si (13), and was also applied to nuclei with spin quantum numbers which are greater than 1/2.

A3.3 The DEPT (Distortionless Enhancement by Polarization Transfer) Pulse Sequence

When analyzing ^{13}C NMR spectra of organic substances, it is always important to assign the signals of the different kinds of carbon atoms. The carbon atoms with different number of protons attached to them, i.e., methyl, methylene, methine and quaternary carbon atoms, can be differentiated by the DEPT pulse sequence.

The DEPT pulse sequence is less critical to the choice of the AX coupling constant and yields X multiplets without the artefacts involving relative intensity and line number observed with the INEPT method. The DEPT sequence is especially well suited for the assignment of resonance signals. For ^{13}C NMR spectra, the phases of the magnetization of quaternary C atoms and CH, CH_2, CH_3 groups are at the pulse angles θ of $\pi/4$, $\pi/2$, $\pi/3$ and $\pi/4$, respectively. The last proton pulse enables subspectra to be edited for CH, CH_2, CH_3 groups. For the detection of CH_2 and CH_3 groups, difference spectra must be used.

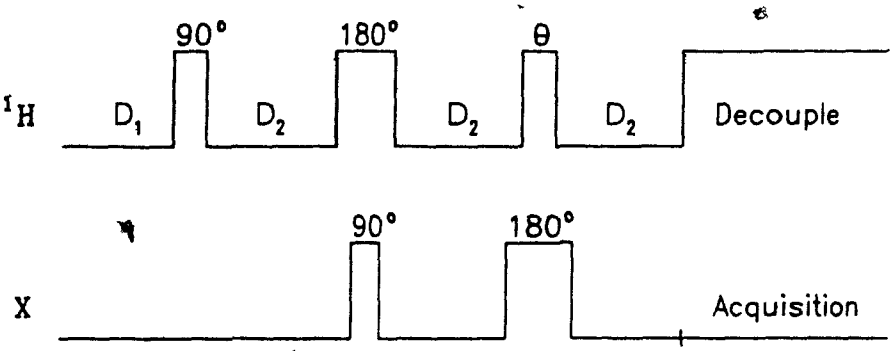

(The DEPT pulse sequence)

A3.4 The HETCOR (Two-Dimensional Heteronuclear Correlation) Pulse Sequence

In one-dimensional NMR spectroscopy, the FID (free induction decay) is obtained as a function of a single time variable, the detection time. In two-dimensional spectroscopy, an additional time variable, the evolution time, is introduced. A 2-D experiment consists of the acquisition of a series of FID's as a function of detection time with each member of the series differing from the previous member by a constant incremental value of the evolution time.

It is extremely useful in structure determination and in assignment of an NMR spectrum to correlate the ^{13}C spectrum with the proton spectrum. The 2-D heteronuclear correlation NMR spectrum, in which one axis is usually ^1H and the other is X (^{13}C or ^{15}N, etc.), allows one type of nucleus (e.g., X) to be assigned from a known assignment of the other type of nucleus (e.g., ^1H). The HETCOR sequence provides 2D data which correlates nuclear resonances of two nuclei, ^1H and X. The two domains correspond to the two nuclear chemical shift axes. The proton homonuclear splittings are retained, which permits the sorting out of

heavily overlapped proton spectra. The phase cycling requires a multiple of 4 for the number of transients to provide the equivalent of quadrature detection in the proton dimension, allowing the proton transmitter (the decoupler) to be placed in the center of the proton region.

The 2-D heteronuclear correlation experiment has a time sequence preparation-evolution-mixing-detection, which is most commonly used in 2-D NMR experiments. One type of 2-D correlated spectra is that in which both dimensions are coupled through coherent transfer of transverse magnetization (scalar correlation).

If the Larmor frequencies of two different types of nuclei, e.g. ^{1}H and ^{15}N, are related through scalar coupling, a 2-D heteronuclear correlation experiment can be performed. The pulse sequence generally used to produce heteronuclear correlated spectra also contains a polarization transfer and therefore leads to an enhancement of sensitivity. An evolution period t_1 is used for the precessional motion of the ^{1}H spins, and to measure the degree of precession with the X (^{15}N) channel. The transfer of information between A and X occurs in the mixing period, which is introduced between the evolution and the detection time. Coupled nuclei give signals with the coordinates H,X.

As illustrated in Figure A3.2, for ^{1}H-^{13}C correlation, a $90°_{x}$ ^{1}H pulse is applied to rotated the CH doublet in the *x*-*y* plane with different Larmor frequencies. Thereafter, both components of the proton doublet dephase in the *x*-*y* plane. The dephasing angle ϕ is defined by the magnitude of the CH coupling, whereas the phase shift φ is determined by the chemical shift of the protons (a-c). A $180°_{x}$ pulse in the ^{13}C channel irradiated after the first half period of the evolution time t_1 (d) inverts the population of the ^{13}C energy levels. As a result the two proton components exchange their coupling frequencies in order to refocus at the end of the evolution period t_1 (e). Chemical shift information is now contained in the phase angle φ. After a time $\Delta_1 = 1/(2J)$ (the first half of the mixing time) the angle ϕ is 180°. Both vectors are orientated antiparallel (f) and a $90°_{y}$ pulse transforms them into the +*z*-direction, and results in a polarization of proton magnetization (g). The chemical shift information is now given by the magnitude of the *z*-components, which depends on the phase angle φ, since the $90°_{y}$ pulse only affects the *x*-components of the vector. For $\varphi = (2N+1)\pi/2$ the longitudinal proton magnetization is equal to zero, whereas for $\varphi = 2N\pi/2$ it has

its maximum value. The polarization of the protons leads simultaneously to the polarization of ^{13}C magnetization, which can now be transformed into +y-magnetization by a $90°_x$ pulse (h). Due to their coupling with the attached protons, within the interval 1/(2J), both ^{13}C vectors refocus at the end of the mixing time (i). By switching on the proton decoupler, they can be detected as a singlet. The achieved polarization and thus the measured intensity, depends on the phase angle φ and is a direct function of the proton chemical shift (its Larmor frequency). In consequence, variation of the evolution period t_1 leads to amplitude modulation, which is a function of the proton chemical shift instead of the coupling. Thus, a second Fourier transformation in the t_1 domain provides maximum signals located at the chemical shifts of the coupled ^1H and ^{13}C nuclei.

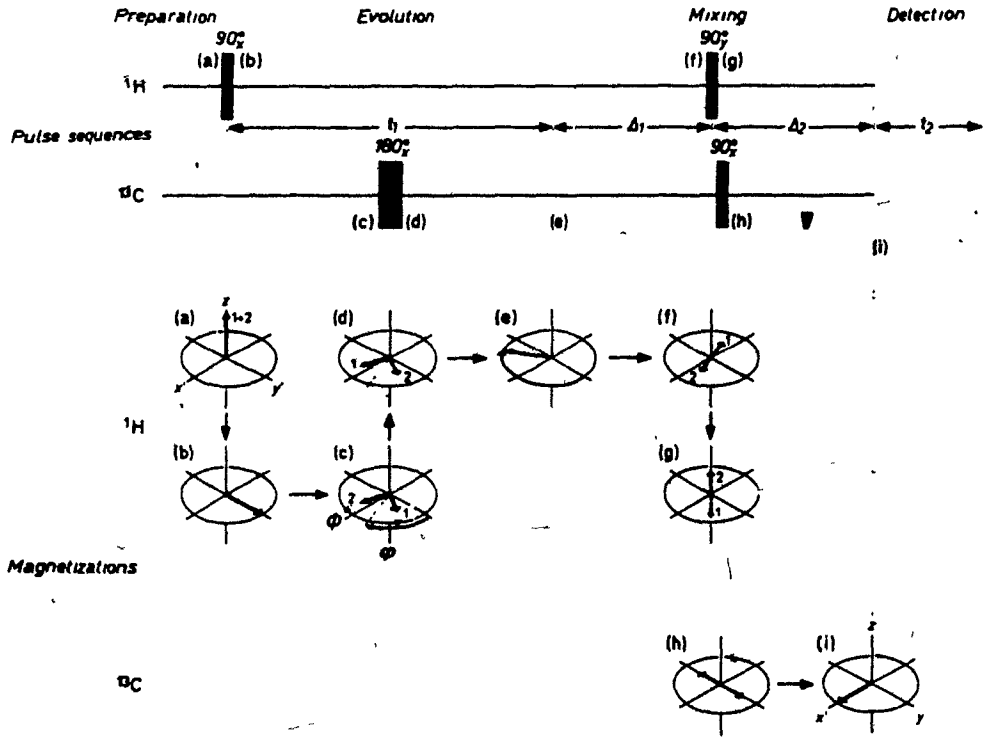

Figure A3.2 The HETCOR pulse sequence used for the heteronuclear correlation (X-^1H) experiment using the example of CH fragment (reference 7).

A3.5 The COSY (Two-Dimensional Homonuclear Correlation Spectroscopy) Pulse Sequence

The COSY pulse sequence (also referred to as HOMCOR) generates data which allows simultaneous correlation of all spin coupled protons when plotted in a two-dimensional array. The phase cycling should be a multiple of 4 of the number of transients to permit the equivalent of quadrature phase detection in the evolution period (D_2). The sequence is depicted in Figure A3.3.

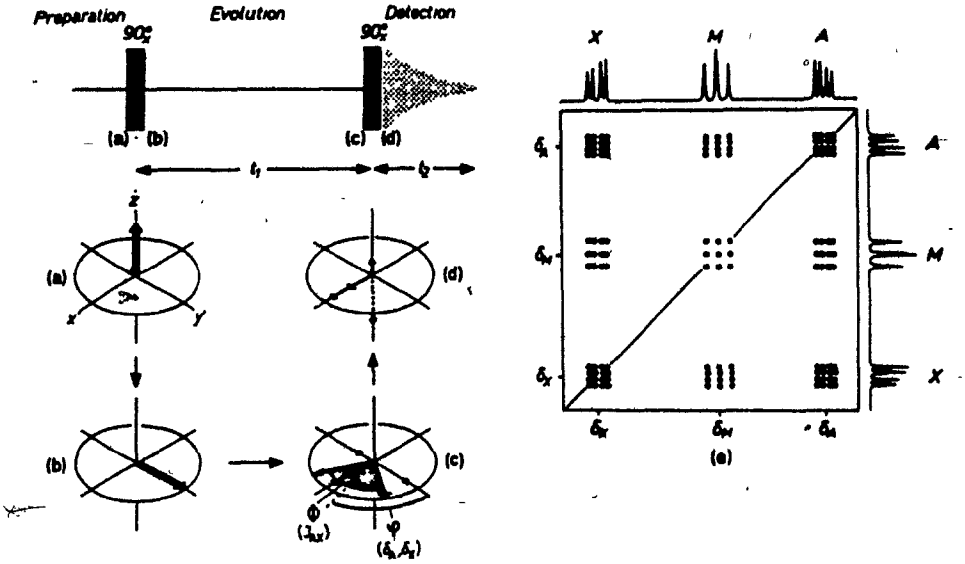

Figure A3.3 The COSY pulse sequence used for the homonuclear correlation (^{1}H-^{1}H) experiment (reference 7): (a-d) the COSY sequence; (e) an example of the COSY contour plot.

In the COSY sequence, a $90°_x$ pulse produces a transverse magnetization (a,b) immediately after the preparation delay. Because of A-X coupling, the magnetization vectors process away from each other in the *x-y* plane according to their Larmor frequency and their spin-spin coupling constants J (c). The second $90°_x$ pulse, which rotates the chemical shift dependent components of the doublet to the $\pm z$ axis (d), can be considered as a mixing pulse, but additional mixing time is not necessary since the protons are always coupled. For a non-coupled nucleus A ($J_{AX} = 0$), the second $90°_x$ pulse leads to a t_1-dependent modulation of the transverse magnetization that depends only on the Larmor frequency ν_A. The 2D spectrum therefore contains a signal on the diagonal (diagonal peak). If these peaks cause overlapping and thus are not desired, they can be eliminated by using

a mixing pulse of 45° or less. For the case $J_{AX} \neq 0$, the A magnetization through the scalar A-X interaction in the x-y plane also depends on the Larmor frequency ν_x. The 2D spectrum therefore contains two characteristic off-diagonal signals (cross peaks), which indicate a scalar spin-spin coupling between A and X. Smaller couplings can be emphasized in the COSY experiment by adding a delay to the evolution time.

References

1. M.L. Martin, G.J. Martin & J.-J. Delpuech, *Practical NMR Spectroscopy*, Heyden & Sons Ltd, London-Philadelphia-Rheine, 1980
2. E.D. Becker, *High Resolution NMR*, Academic Press, NY-London-Toronto, 1980
3. R.J. Abraham & P.Loftus, *Proton and Carbon-13 NMR Spectroscopy*, Heyden & Sons Ltd, London-Philadelphia-Rheine, 1980
4. J.W. Akitt, *NMR and Chemistry*, Chapman & Hall, London-NY, 1983
5. F.W. Wehrli & T.Wirthlin, *Interpretation of Carbon-13 NMR Spectra*, Heyden & Son Ltd., 1976
6. R. Benn & H. Gunther, **Modern Pulse Methods in High-Resolution NMR Spectroscopy**, *Angew. Chem. Ed. Engl.*, **22**, 350, 1983
7. E. Breitmaier & W. Voelter, *Carbon-13 NMR Spectroscopy*, 3rd, completely revised ed., VCH (F.R.Ger.), 1987

For INEPT

8. G. Morris & R. Freeman, *J. Am. Chem. Soc.*, **101**, 760, 1979
9. G. Morris, *J. Am. Chem. Soc.*, **102**, 428, 1980
10. G.A. Morris, *J. Mag. Reson.*, **41**, 185, 1980
11. J. Kowalewski & G.A. Morris, *J. Mag. Reson.*, **47**, 331, 1982
12. D. Marion, C. Garbay-Jauuregniberry & B.P. Roques, *J. Am. Chem. Soc.*, **104**, 5573, 1982
13. J. Kowalewski & G.A. Morris, *J. Mag. Reson.*, **47**, 331, 1982

For DEPT

14. D.M. Doddrell, D.T. Pegg & M.R. Bendall, *J. Mag. Reson.*, **48**, 323, 1982
15. O. Sorensen & R.R. Ernst, *J. Mag. Reson.*, **51**, 477, 1983

For HETCOR

16. A.A. Mandsley & R.R. Ernst, *Chem. Phys. Lett.*, **50**, 368, 1977
17. G. Bodenhauser & R. Freeman, *J. Mag. Reson.*, **28**, 471, 1977
18. A.A. Mandsley, L. Muller & R.R. Ernst, *J. Mag. Reson.*, **28**, 463, 1977
19. A.D. Bax & G.A. Morris, *J. Mag. Reson.*, **42**, 501, 1981

For HOMCOR (COSY)

20. W.P. Aue, E. Bartholdi & R.R. Ernst, *J. Chem. Phys.*, **64**, 2229, 1976
21. J. Jeener, *Ampere International Summer School*, Basko Polje, Yugoslavia, 1977
22. K. Nagayama, A. Kumar, K. Wuthrich & R.R. Ernst, *J. Mag. Reson.*, **40**, 321, 1980
23. A. Bax, R. Freeman & G. Morris, *J. Mag. Reson.*, **42**, 164, 1981

Appendix 4

The Computer Program for Adsorption Data Processing

A computer program providing detailed calculations and graphics was developed for the processing of the results for bile salt and bilirubin adsorptions. The program was first designed and written in BASIC, followed by several major revisions. The present version provides many convenient options for data storage and data manipulations.

In this program (EXPROC.NEW), experimental data can be read in from a previously saved file or entered manually and saved on the diskettes for later retrieval. Calculations are done on an adsorbate-resin mole/equivalent or weight/weight basis. The equilibrium concentration can be expressed by either mM or mg/dl. Different scales for graphics may be selected at the user's choice. It also generates a brief report of the experiment performed which easily fits into the user's record and saves time for the laborious calculations of the adsorption results. It has been used by many colleagues in the laboratory because of its convenience and user-friendliness.

```
1000 REM PROGRAM NAME EXPROC.NEW
1010 CLS : LOCATE 3, 1
1020 PRINT "       ************************************"
1030 PRINT "       *  Program to Process Adsorption Results        *"
1040 PRINT "       *              (NEW VERSION)                    *"
1050 PRINT "       *        EXPROC.NEW   COPYRIGHT                 *"
1060 PRINT "       *                                               *"
1070 PRINT "       *              by JULIAN ZHU                    *"
1080 PRINT "       *                May 1987                       *"
1090 PRINT "       ************************************"
1100 A$ = INPUT$ (1)
1110 LOCATE 13, 1
1120 PRINT "       The program is composed of the following sections:  "
1130 PRINT "    1) The entry of experimental parameters and data.      "
1140 PRINT "    2) The calculation of the experimental data.           "
1150 PRINT "    3) The printing and plotting of the calculated results.  "
1160 PRINT
1170 PRINT "       This program accepts a maximum of 50 groups of data.  "
1180 PRINT
1190 PRINT "       The data can be entered during program execution or  "
1200 PRINT "    they can be read from another disk by your own options.  "
1210 PRINT
1220 INPUT "    Do you want to enter experimental parameters?", A$
1230 CLS
1240 DIM CONCFR(50), WT(50), BEF(50), AFT(50)
1250 IF A$ = "N" OR A$ = "n" GOTO 1520
1260 PRINT "Enter experimental parameters----" : PRINT
1270 INPUT "Experiment number:          ", EXNUM$
1280 INPUT "Date (dd-mm-yy):            ", DAT$
1290 INPUT "Buffer and the pH:          ", PH$
1300 INPUT "Volume of ads. (ml):        ", VOL
1310 INPUT "Resin used:                 ", RESIN$
1320 INPUT "Resin capct.(mmol/g):       ", CAP
1330 REM INPUT "Substn. of resin (%):(RTN)", SUBST
1340 REM INPUT "Resin FW increase:  (RTN)", FWINCR
1350 INPUT "Sol'n conc.(mg/dl):  ", CONC
1360 PRINT "Which adsobate?     "
1370 PRINT "Type 1 for cholic acid;     "
1380 PRINT "    2 for cholic Na;        "
1390 PRINT "    3 for glycocholic acid; "
1400 PRINT "    4 for glycocholic Na;   "
1410 PRINT "    5 for bilirubin;        "
1420 PRINT "    6 for other (bile) acid."
1430 INPUT; ACID : PRINT
1440 IF ACID = 1 THEN ACID$ = "Cholic Acid              " : FW = 408.6
1450 IF ACID = 2 THEN ACID$ = "Cholic Na                " : FW = 430.57
1460 IF ACID = 3 THEN ACID$ = "Glycocholic Acid         " : FW = 465.6
1470 IF ACID = 4 THEN ACID$ = "Glycocholic Na           " : FW = 487.6
1480 IF ACID = 5 THEN ACID$ = "Bilirubin                " : FW = 585
```

```
1490 IF ACID = 6 THEN INPUT "Adsorbate used:", ACID$ : PRINT : INPUT "FW of
adsorbate:", FW : PRINT
1500 GOTO 1620
1510 REM ************************************************
1520 EXNUM$ = "X                    "
1530 DAT$  = "DD-MM-YY              "
1540 PH$   = "Tris 7.4              "
1550 RESIN$ = "I-COUNTER IONS       "
1560 CAP   = .23
1570 SUBST = .705
1580 ACID$ = "Cholic Acid           "
1590 FW    = 430.57
1600 CONC  = 10
1610 REM ************************************************
1620 INPUT "Do you want to print the parameters (Y/N)?", A$
1630 PRINT
1640 IF A$ = "N" OR A$ = "n" GOTO 1760
1650 LPRINT "Experiment number:  "; EXNUM$
1660 LPRINT "Date (dd-mm-yy):    "; DAT$
1670 LPRINT "Buffer and the pH:  "; PH$
1680 LPRINT "Adsorbate:          "; ACID$
1690 LPRINT "Resin used:         "; RESIN$
1700 REM LPRINT "Resin Substn (%):   ", SUBST
1710 LPRINT USING "Resin Capacity (mmol/g): ##.###"; CAP
1720 LPRINT USING "FW of the adsorbate:   ###.## "; FW
1730 LPRINT USING "Sol'n conc. (mg/dl):   ###.###"; CONC
1740 LPRINT USING "Volume of ads. (ml):    ##.## "; VOL
1750 LPRINT
1760 PRINT "TYPE  1  to enter one group of data each time;"
1770 PRINT "      2  to read data saved on a disk;       "
1780 PRINT "      3  to use data in the program as a sample."
1790 PRINT
1800 INPUT; FLAG
1810 ON FLAG GOTO 1820, 2130, 2260
1820 REM option #1 ***************************************
1830 PRINT : PRINT
1840 PRINT "         Enter one group of data.     "
1850 PRINT "         --Concentration (fraction);  "
1860 PRINT "         --Weight of resin (mg);      "
1870 PRINT "         --Adsorbance before ads.;    "
1880 PRINT "         --Adsorbance after  ads.;    "
1890 PRINT
1900 PRINT "         Enter 9999 when you finish data input."
1910 FOR I = 1 TO 50
1920 INPUT CONCFR(I), WT(I), BEF(I), AFT(I)
1930 IF CONCFR(I) = 9999 GOTO 1960
1940 N = N + 1
1950 NEXT I
1960 INPUT "Do you want to make corrections (Y/N)? ", Q1$
1970 IF Q1$="n" OR Q1$="N" GOTO 2030
1980 INPUT "Which one do you want to correct (#)?  ", CORR
```

```
1990 INPUT CONCFR(CORR), WT(CORR), BEF(CORR), AFT(CORR)
2000 INPUT "Any more corrections (Y/N)? ", Q2$
2010 IF Q2$="n" OR Q2$="N" GOTO 2030 ELSE GOTO 1980
2020 REM ************************************************
2030 REM save the data on the disk
2040 INPUT "Do you want to save your data on a disk (Y/N)? ", A$
2050 IF A$="n" OR A$="N" GOTO 2380
2060 INPUT "Put your disk in disk drive, press return.", B$
2070 INPUT "Name of your data file (A:FilNam.Ext) ?  ", C$
2080 OPEN "O", #2, C$
2090 FOR I=1 TO N
2100 WRITE#2, CONCFR(I), WT(I), BEF(I), AFT(I)
2110 NEXT I
2120 GOTO 2380
2130 REM option #2 ******************************************
2140 REM open data file on the disk and run the last part
2150 PRINT
2160 PRINT "What is the name of your data file?"
2170 INPUT "(Specify disk drive or directory): ", N$
2180 OPEN "I", #1, N$
2190 FOR I = 1 TO 50
2200 IF EOF(1) THEN 2240
2210 INPUT#1, CONCFR(I), WT(I), BEF(I), AFT(I)
2220 N = N + 1
2230 NEXT I
2240 CLOSE #1
2250 GOTO 2380
2260 REM option #3 ******************************************
2270 REM READ FROM THIS PROGRAM
2280 PRINT
2290 FOR I = 1 TO 50
2300 READ CONCFR(I), WT(I), BEF(I), AFT(I)
2310 IF CONCFR(I) = 9999 GOTO 2380
2320 N = N + 1
2330 NEXT I
2340 REM ************************************************
2350 REM order of data--concfr, wt of resin, abs bef, abs aft
2360 DATA .6,10,.2,.15,.8,10,.3,.23, 1,10,.4,.3, 9999,0,0,0
2370 REM ************************************************
2380 REM ***************CALCULATIONS**********************
2390 REM ************************************************
2400 CLS : LOCATE 5, 1
2410 PRINT "-------------------------------------------------------------"
2420 PRINT " CONC.  WT. OF   ABSORBANCE      Ceq       AMOUNT ADSORBED"
2430 PRINT " FRAC. RESIN(mg) BEFORE  AFTER  (mg/dl) (mM)  (mg/g) (mol/eq sites)"
2440 PRINT "-------------------------------------------------------------"
2450 CHANGE = 1 / (1 + .23 / 1000 * FWINCR * SUBST)
2460 NEWSUB = CHANGE * .23 / 1000 * SUBST
2470 FOR I = 1 TO N
2480 ADSD(I) =  (BEF(I) - AFT(I)) / BEF(I) * CONCFR(I) * CONC / 100 * VOL
2490 REMN(I) =  AFT(I) / BEF(I) * CONCFR(I) * CONC / 100 * VOL
```

```
2500 CEQ(I) = AFT(I) / BEF(I) * CONCFR(I) * CONC
2510 CEQM(I) = (CEQ(I) / 100 * 1000) / FW
2520 RADS(I) = ADSD(I) / WT(I) * 1000
2530 X (I) = RADS(I) / 1000 / FW / (CAP/1000)
2540 PRINT USING " ##.## "; CONCFR(I);
2550 PRINT USING " ##.## "; WT(I);
2560 PRINT USING "####.### "; BEF(I); AFT(I);
2570 PRINT USING "###.## "; CEQ(I);
2580 PRINT USING " #.#### "; CEQM(I);
2590 PRINT USING " ###.### "; RADS(I);
2600 PRINT USING "  ##.####"; X(I)
2610 NEXT I
2620 PRINT "-------------------------------------------------------------------" : PRINT
2630 INPUT "Do you want a hardcopy of this data sheet?", A$
2640 IF A$ = "N" OR A$ = "n" GOTO 2790
2650 LPRINT "-------------------------------------------------------------------"
2660 LPRINT " CONC.  WT. OF   ABSORBANCE      Ceq       AMOUNT ADSORBED"
2670 LPRINT " FRAC. RESIN(mg) BEFORE  AFTER  (mg/dl) (mM)  (mg/g) (mol/eq sites)"
2680 LPRINT "-------------------------------------------------------------------"
2690 FOR I = 1 TO N
2700 LPRINT USING " ##.## "; CONCFR(I);
2710 LPRINT USING " ##.## "; WT(I);
2720 LPRINT USING "####.### "; BEF(I); AFT(I);
2730 LPRINT USING "###.## "; CEQ(I);
2740 LPRINT USING " #.#### "; CEQM(I);
2750 LPRINT USING " ###.### "; RADS(I);
2760 LPRINT USING "  ##.####"; X(I)
2770 NEXT I
2780 LPRINT "-------------------------------------------------------------------" : LPRINT
2790 INPUT "Do you want to save these data onto a disk (Y/N)? ", D$
2800 IF D$ = "N" OR D$ = "n" GOTO 2900
2810 INPUT "Name of your file (specify diskdrive or directory)? ", F$
2820 OPEN "O", #3, F$
2830 WRITE#3, EXNUM$, DAT$, PH$, ACID$, RESIN$, CAP, FW, CONC, VOL
2840 FOR I=1 TO N
2850 WRITE#3, CONCFR(I), WT(I), BEF(I), AFT(I), CEQ(I), CEQM(I), RADS(I), X(I)
2860 NEXT I
2865 CLOSE #3
2870 REM ******************************************************
2880 REM ***************GRAPH PLOTTING*************************
2890 REM ******************************************************
2900 CLS : LOCATE 5, 1
2910 INPUT "    Do you want to chose scale ranges (Y/N)?", G$
2920 IF G$ = "N" OR G$ = "n" GOTO 3010
2930 PRINT
2940 PRINT " 1) Horizontal scale:                "
2950 INPUT "    Equilibrium concentration (mg/dl): ", CEQF
2960 INPUT "    Equilibrium concentration (mM):   ", CEQMF
2970 PRINT " 2) Vertical scale:                  "
2980 INPUT "    mol/eq. active sites:            ", XMOL
2990 INPUT "    mg/g of resin:                  ", RADSMG
```

```
3000 GOTO 3050
3010 CEQF = 10      'graph Ceq (mg/dl) scale
3020 CEQMF = .3     'graph Ceq (mM) scale
3030 XMOL = .2      'graph mol/eq pendant of the resin
3040 RADSMG = 20    'graph mg/g resin
3050 REM change for graphics
3060 FOR I = 1 TO N
3070 CEQG (I) =  80 + CEQ (I) * (550 / CEQF)
3080 CEQMG(I) =  80 + CEQM(I) * (550 / CEQMF)
3090  XG  (I) = 160 -  X  (I) * (140 / XMOL)
3100 RADSG(I) = 160 - RADS(I) * (140 / RADSMG)
3110 NEXT I
3120 REM CREATE GRAPH WITH THE ARRAY DATA
3130 LABEL1$="ADSORPTION ISOTHERM"
3140 LABEL2$="X"
3150 LABEL3$="Ceq (mM)"
3160 LABEL4$="Ceq (mg/dl)"
3170 PRINT
3180 CLS : LOCATE 4, 1
3190 PRINT "Press RETURN when you are ready to see the graph. "
3200 PRINT "Load the paper properly before doing a hardcopy. "
3210 PRINT "For a hardcopy, press SHIFT-PrtSc if GRAPHICS is loaded."
3220 PRINT : PRINT "MAKE YOUR CHOICE----"
3230 PRINT "TYPE  1 for a graph X (mol/eq active sites)-Ceq (mM);    "
3240 PRINT "      2 for a graph X (mg/g resin)-Ceq (mM);            "
3250 PRINT "      3 for a graph X (mol/eq active sites)-Ceq (mg/dl);"
3260 PRINT "      4 for a graph X (mg/g resin)-Ceq (mg/dl).         "
3270 PRINT "      5 to change scales for graphs.                    "
3280 PRINT "      6 to stop.                                        "
3290 INPUT; FLAG
3300 ON FLAG GOTO 3320, 3320, 3320, 3320, 2900, 3800
3310 REM ************************************************
3320 REM SET SCREEN TO HIGH RESOLUTION
3330 SCREEN 2
3340 CLS:KEY OFF
3350 L = LEN (LABEL1$)      'get length
3360 Q = INT ((80-L)/2)     'center on row
3370 IF Q <= 0 THEN Q = 1
3380 LOCATE 2, Q+4 : PRINT LABEL1$
3390 REM DRAW A BOX AROUND THE GRAPH AREA
3400 LINE (80,20)-(630,160),,B
3410 LOCATE 4,12 : PRINT RESIN$
3420 LOCATE 5,12 : PRINT "(#", EXNUM$; ")"
3430 REM GENERATE CIRCLES FOR DATA POINTS
3440 FOR I = 1 TO N
3450 IF FLAG = 1 THEN CIRCLE (CEQMG(I), XG  (I)), 3
3460 IF FLAG = 2 THEN CIRCLE (CEQMG(I), RADSG(I)), 3
3470 IF FLAG = 3 THEN CIRCLE (CEQG(I), XG  (I)), 3
3480 IF FLAG = 4 THEN CIRCLE (CEQG(I), RADSG(I)), 3
3490 NEXT I
3500 REM ************************************************
```

```
3510 REM LABEL X AXIS ************************************
3520 FOR I = 1 TO 10
3530 X = 80 + I * 55
3540 LINE (X,157) - (X,160)
3550 COLUMN = INT (3 + (X - 80) / 8)
3560 IF COLUMN > 78 THEN COLUMN = 78
3570 IF FLAG = 3 OR FLAG = 4 THEN GOTO 3620
3580 XLM = (CEQMF / 10) * (I - 1)
3590 LOCATE 22, COLUMN
3600 IF (XLM*100) MOD 5 = 0 THEN PRINT USING "#.##"; XLM
3610 GOTO 3650
3620 XL = (CEQF / 10) * (I - 1)
3630 LOCATE 22, COLUMN
3640 IF (XL*10) MOD 5 = 0 THEN PRINT USING "#.#"; XL
3650 NEXT I
3660 LOCATE 23, 42
3670 IF FLAG=1 OR FLAG=2 THEN PRINT LABEL3$ ELSE PRINT LABEL4$
3680 REM LABEL Y AXIS ************************************
3690 FOR I = 1 TO 11
3700 Y = 20 + (140 / 10) * (I - 1)
3710 LINE (80,Y) - (83,Y)
3720 ROW = INT (3 + (Y-20) / 7.5)
3730 IF ROW > 21 THEN ROW = 21
3740 IF FLAG = 1 THEN GOSUB 3820 ELSE GOSUB 3870
3750 NEXT I
3760 LOCATE 11, 2 : IF FLAG=1 OR FLAG=3 THEN PRINT "mol" ELSE PRINT "mg"
3770 LOCATE 12, 2 : IF FLAG=1 OR FLAG=3 THEN PRINT "---" ELSE PRINT "--"
3780 LOCATE 13, 2 : IF FLAG=1 OR FLAG=3 THEN PRINT " eq" ELSE PRINT " g"
3790 A$ = INPUT$ (1) : GOTO 3180
3800 SCREEN 0 : KEY ON : STOP
3810 REM *************************************************
3820 YL = ( XMOL / 10 ) * (11 - I)
3830 LOCATE ROW, 5
3840 IF (XMOL > .1) AND ((YL* 100) MOD 10 = 0) THEN PRINT USING "##.##"; YL
3850 IF (XMOL <= .1) AND ((YL*1000) MOD 10 = 0) THEN PRINT USING "##.##"; YL
3860 RETURN
3870 YL = (RADSMG / 10) * (11 - I)
3880 LOCATE ROW, 6
3890 IF (RADSMG > 30) AND (YL MOD 10 = 0) THEN PRINT USING "###"; YL
3900 IF (RADSMG <= 30) AND (YL MOD 5 = 0) THEN PRINT USING "###"; YL
3910 RETURN
3920 REM *************************************************
```

Appendix 5

Experimental Data

Figure 2.7

1) 0.005 M tris buffer
C_{eq} (mM), X (mol/eq)
0.0154, 0.0263
0.0236, 0.0416
0.0285, 0.0475
0.0445, 0.0686
0.0664, 0.1004
0.0846, 0.1223
0.1373, 0.1778

2) 0.005 M phosphate buffer
C_{eq} (mM), X (mol/eq)
0.0610, 0.0172
0.0947, 0.0289
0.1166, 0.0436
0.1742, 0.0599
0.2463, 0.0826
0.3003, 0.0945

3) 0.050 M phosphate buffer
C_{eq} (mM), X (mol/eq)
0.0103, 0.0033
0.0163, 0.0077
0.0233, 0.0114
0.0312, 0.0161
0.0346, 0.0207
0.0517, 0.0235
0.0678, 0.0277
0.0771, 0.0289
0.1077, 0.0328

Figure 2.8

1) NaC in 0.005 M tris buffer
C_{eq} (mM), X (mol/eq)
0.0199, 0.0044
0.0294, 0.0064
0.0399, 0.0087
0.0555, 0.0139
0.0699, 0.0169
0.0771, 0.0178
0.0978, 0.0220
0.1224, 0.0285

2) NaC in 0.005 M phosphate buffer
C_{eq} (mM), X (mol/eq)
0.0460, 0.0012
0.0666, 0.0042
0.0889, 0.0045
0.1370, 0.0045
0.1824, 0.0059
0.2289, 0.0065

3) NaGC in 0.005 M phosphate buffer
C_{eq} (mM), X (mol/eq)
0.0392, 0.0008
0.05955, 0.0011
0.0793, 0.0016
0.1122, 0.0040
0.1575, 0.0034
0.1975, 0.0040

Figure 2.9

1) with cholestyramine (Cl)
as in Figure 2.7, (1)

2) with cholestyramine (I)
C_{eq} (mM), X (mol/eq)
0.0094, 0.0070
0.0125, 0.0110
0.0184, 0.0157
0.0346, 0.0297
0.0422, 0.0367
0.0430, 0.0488
0.0617, 0.0853
0.1043, 0.1083
0.1069, 0.1267

Figure 2.10

1) NaC in 0.005 M tris buffer
as in Figure 2.7, (1)

2) NaGC in 0.005 M tris buffer
C_{eq} (mM), X (mol/eq)
0.0163, 0.0197
0.0216, 0.0324
0.0305, 0.0421
0.0430, 0.0603
0.0601, 0.0831
0.0640, 0.0884

3) NaC in 0.050 M phosphate buffer
as in Figure 2.7, (3)

4) NaGC in 0.050 M phosphate buffer
C_{eq} (mM), X (mol/eq)
0.0148, 0.0050
0.0167, 0.0063
0.0236, 0.0039
0.0513, 0.0067
0.0586, 0.0075
0.0765, 0.0081
0.0786, 0.0073
0.0846, 0.0093
0.0877, 0.0081
0.1081, 0.0106
0.1123, 0.0118
0.1147, 0.0116
0.1225, 0.0132
0.1324, 0.0121
0.1449, 0.0134
0.1602, 0.0140

Figure 2.11

1) TMG-P
C_{eq} (mM), X (mol/eq)
0.0412, 0.0094
0.0631, 0.0201
0.1245, 0.0274
0.1604, 0.0423
0.2048, 0.0437

2) TMG-Lys-Ala_3-P
C_{eq} (mM), X (mol/eq)
0.0365, 0.0164
0.0578, 0.0219
0.0801, 0.0216
0.1245, 0.0266
0.1561, 0.0344
0.1647, 0.0368
0.2665, 0.0464

3) TMG-Lys_3-Ala_3-P
C_{eq} (mM), X (mol/eq)
0.0408, 0.0097
0.0501, 0.0308
0.0768, 0.0259
0.1136, 0.0413
0.1552, 0.0350
0.1611, 0.0410
0.2077, 0.0422
0.2111, 0.0426
0.2686, 0.0437

4) TMG-Lys_5-Ala_3-P
C_{eq} (mM), X (mol/eq)
0.0327, 0.0255
0.0538, 0.0312
0.0760, 0.0319
0.1125, 0.0520
0.1357, 0.0721
0.1551, 0.0608
0.1913, 0.0783
0.1919, 0.0780
0.2520, 0.0757

5) TMG-Lys_5-Ala_3-P/ground
C_{eq} (mM), X (mol/eq)
0.0220, 0.0555
0.0387, 0.0685
0.0581, 0.0830
0.0930, 0.1155
0.1430, 0.1213
0.1889, 0.1369

Figure 2.12

1) TMG-P
C_{eq} (mM), X (mol/eq)
0.0409, 0.0044
0.0615, 0.0062
0.0870, 0.0044
0.1066, 0.0073
0.1284, 0.0084
0.1685, 0.0131
0.2137, 0.0144

2) TMG-Ala_3-P
C_{eq} (mM), X (mol/eq)
0.0410, 0.0094
0.0858, 0.0112
0.1067, 0.0148
0.1760, 0.0162

0.2250, 0.0159

3) TMG-Lys-Ala_3-P
C_{eq} (mM), X (mol/eq)
0.0466, 0.0113
0.1016, 0.0145
0.1203, 0.0234
0.1993, 0.0302
0.2661, 0.0251

4) TMG-Lys_3-Ala_3-P
C_{eq} (mM), X (mol/eq)
0.0429, 0.0042
0.0650, 0.0076
0.0825, 0.0135
0.1082, 0.0097
0.1698, 0.0195
0.2165, 0.0222

5) TMG-Lys_5-Ala_3-P
C_{eq} (mM), X (mol/eq)
0.0329, 0.0128
0.0525, 0.0132
0.0697, 0.0174
0.0904, 0.0183
0.1108, 0.0233
0.1439, 0.0326
0.1853, 0.0345

Figure 2.13

1) NaC in 0.005 M tris buffer
as in Figure 2.11 (5)

2) NaC in 0.005 M phosphate buffer
C_{eq} (mM), X (mol/eq)
0.0196, 0.0469
0.0337, 0.0610
0.0514, 0.0741
0.0850, 0.0933
0.1240, 0.1144
0.1587, 0.1341

Figure 2.14

1) NaC in 0.005 M phosphate buffer
as in Figure 2.13 (2)

2) NaGC in 0.005 M phosphate buffer
C_{eq} (mM), X (mol/eq)
0.0265, 0.0292
0.0374, 0.0461
0.0590, 0.0439
0.0870, 0.0677
0.1256, 0.0796
0.1542, 0.0986

2) NaGC in 0.005 M phosphate buffer
as in Figure 2.12 (5)

Figure 3.12

1) Carboxyl
$1/T \times 10^{-3}$ (K^{-1}), T_1 (sec)
3.35, 3.2
3.19, 3.8
3.05, 5.0
2.91, 6.9
2.79,10.9
2.74,14.9
2.68,17.1

2) 18-Methyl
$1/T \times 10^{-3}$ (K^{-1}), T_1 (sec)
3.35, 0.62
3.19, 0.78
3.05, 1.05
2.91, 1.18
2.79, 1.58
2.74, 1.98
2.68, 2.22

3) 19-Methyl
$1/T \times 10^{-3}$ (K^{-1}), T_1 (sec)
3.35, 0.63
3.19, 0.72
3.05, 0.79
2.91, 1.13
2.79, 1.33
2.74, 1.59
2.68, 1.98

4) 21-Methyl
$1/T \times 10^{-3}$ (K^{-1}), T_1 (sec)
3.35, 0.45
3.19, 0.56
3.05, 0.70
2.91, 1.04
2.79, 1.34
2.74, 1.65
2.68, 1.80

Figure 3.13

1) Carboxyl
$1/T \times 10^{-3}$ (K^{-1}), T_1 (sec)
3.35, 3.32
3.19, 4.35
3.05, 5.93

2.91, 7.22
2.83, 7.48
2.75, 9.69
2.68,12.06

2) 18-Methyl
$1/T \times 10^{-3}$ (K^{-1}), T_1 (sec)
3.35, 0.70
3.19, 0.91
3.05, 1.18
2.91, 1.53
2.83, 2.07
2.75, 2.33
2.68, 2.66

3) 19-Methyl
$1/T \times 10^{-3}$ (K^{-1}), T_1 (sec)
3.35, 0.59
3.19, 0.77
3.05, 1.20
2.91, 1.38
2.83, 1.60
2.75, 1.85
2.68, 2.23

4) 21-Methyl
$1/T \times 10^{-3}$ (K^{-1}), T_1 (sec)
3.35, 0.54
3.19, 0.64
3.05, 0.86
2.91, 1.15
2.83, 1.37
2.75, 1.56
2.68, 1.82

Figure 5.6

1) Resin 5-1
C_{eq} (mM), X (mg/g)
0.0156, 1.776
0.0398, 3.140
0.0645, 3.823
0.0974, 4.652
0.1303, 5.655
0.1631, 6.285

2) Resin 5-2
C_{eq} (mM), X (mg/g)
0.0068, 10.746
0.0209, 22.177
0.0427, 25.784
0.0625, 35.756
0.1027, 42.835
0.1153, 54.496
0.1355, 49.645

3) Resin 5-3
C_{eq} (mM), X (mg/g)
0.0109, 8.537
0.0337, 11.676
0.0350, 9.725
0.0574, 15.101
0.0627, 13.685
0.0885, 18.735
0.1202, 21.891
0.1229, 22.409
0.1502, 28,173
0.1624, 20.746

4) Resin 5-4
C_{eq} (mM), X (mg/g)
0.0088, 8.822
0.0193, 28.044
0.0394, 36.451
0.0597, 56.657
0.0868, 58.113
0.0930, 57.977
0.0953, 63.238
0.1099, 79.419
0.1119, 69.470
0.1248, 73.214

Figure 5.7

1) Resin 5-1
C_{eq} (mM), X (mol/eq lys residues)
0.0156, 0.1706
0.0398, 0.3015
0.0645, 0.3671
0.0974, 0.4467
0.1303, 0.5431
0.1631, 0.6036

2) Resin 5-2
C_{eq} (mM), X (mol/eq lys residues)
0.0068, 0.1038
0.0209, 0.2143
0.0427, 0.2492
0.0625, 0.3455
0.1027, 0.4139
0.1153, 0.5266
0.1355, 0.4797

3) Resin 5-3
C_{eq} (mM), X (mol/eq lys residues)
0.0109, 0.1564

0.0337, 0.2139
0.0350, 0.1782
0.0574, 0.2767
0.0627, 0.2507
0.0885, 0.3433
0.1202, 0.4011
0.1229, 0.4106
0.1502, 0.5162
0.1624, 0.3801

4) Resin 5-4
C_{eq} (mM), X (mol/eq lys residues)
0.0088, 0.0549
0.0193, 0.1746
0.0394, 0.2269
0.0597, 0.3527
0.0868, 0.3618
0.0930, 0.3609
0.0953, 0.3937
0.1099, 0.4944
0.1119, 0.4325
0.1248, 0.4558

Figure 5.8

1) Resin 5-5
C_{eq} (mM), X (mol/eq orn residues)
0.0109, 0.1284
0.0146, 0.1016
0.0353, 0.1374
0.0412, 0.1515
0.0604, 0.1490
0.0913, 0.1784
0.1226, 0.2281
0.1545, 0.2498

2) Resin 5-5
as in Figure 5.7 (2)

Figure 5.9

1) Lys-Ala_3-P
C_{eq} (mM), X (mol/eq lys residues)
0.015, 0.04
0.038, 0.08
0.079, 0.11
0.157, 0.19

2) Lys_2-Ala_3-P
C_{eq} (mM), X (mol/eq lys residues)
0.014, 0.025
0.034, 0.065
0.048, 0.105
0.065, 0.125
0.072, 0.105
0.099, 0.175
0.130, 0.280
0.132, 0.250

3) Lys_5-Ala_3-P
C_{eq} (mM), X (mol/eq lys residues)
0.009, 0.024
0.019, 0.060
0.029, 0.134
0.029, 0.140
0.044, 0.229
0.056, 0.280
0.104, 0.348

4) Resin 5-1
as in Figure 5.7 (1)

5) Resin 5-3
as in Figure 5.7 (3)

Figure 5.10

1) Resin 5-3 (methylated)
C_{eq} (mM), X (mg/g)
0.0098, 11.715
0.0321, 15.926
0.0346, 14.121
0.0597, 15.930
0.0883, 19.320
0.1482, 32.224

2) Resin 5-3
as in Figure 5.6 (3)

Figure 5.11a

1) Cholestyramine
C_{eq} (mM), X (mg/g)
0.022, 27.0
0.032, 32.0
0.044, 35.1
0.077, 34.4
0.111, 40.4

2) Resin 5-4
as in Figure 5.6 (4)

Figure 5.11b

1) Cholestyramine
C_{eq} (mM), X (mol/eq active sites)
0.022, 0.01399
0.032, 0.01658

0.044, 0.01818
0.077, 0.01782
0.111, 0.02093

2) Resin 5-4
as in Figure 5.7 (4)

Figure 5.12

1) 0°C
as in Figure 5.11b (1)

2) 10°C
C_{eq} (mM), X (mol/eq active sites)
0.012, 0.02010
0.021, 0.02222
0.029, 0.02383
0.044, 0.02580
0.072, 0.02549
0.087, 0.03108
0.094, 0.02730
0.104, 0.03263

3) 20°C
C_{eq} (mM), X (mol/eq active sites)
0.002, 0.02336
0.010, 0.03155
0.019, 0.03232
0.038, 0.03357
0.072, 0.03849
0.106, 0.03719

4) 25°C
C_{eq} (mM), X (mol/eq active sites)
0.005, 0.03362
0.012, 0.03621
0.032, 0.04201
0.063, 0.04564
0.109, 0.04652

Figure 5.13
$1/T \times 10^{-3}$ (K^{-1}), ln K
3.35, 6.44
3.41, 6.25
3.53, 5.93
3.66, 5.53

Appendix 6

Publications

Part of the research work has already been published or accepted for publication in scientific journals. These include the following:

(1) **A Study of the Interaction of Bilirubin with L-Lysyl-L-Lysine by NMR Spin-Lattice Relaxation Times**, co-authored with G.R. Brown and L.E. St-Pierre, *Can. J. Spectr.*, **32**, 49, 1987;

(2) **A Nitrogen-15 NMR Study of Bilirubin and Some Derivatives Using the INEPT Sequence**, co-authored with F. Sauriol, G.R. Brown and L.E. St-Pierre, *Can. J. Spectr.*, in press, 1988.

A Study of the Interaction of Bilirubin with L-Lysyl-L-Lysine by NMR Spin-Lattice Relaxation Time Determinations

X X. Zhu, G R Brown and L E St-Pierre

Contribution from Department of Chemistry, McGill University, Montreal, PQ, Canada H3A 2K6

Received: October 27, 1986 Accepted (in revised form): February 20, 1987

Résumé

L'interaction entre la bilirubine et l'oligopeptide, L-lysyl-L-lysine, dans le diméthyle sulfoxide a été étudiée en mesurant le temps de relaxation spin-réseau (T_1) des protons et des carbones-13 avec la technique d'inversion-recouvrement par transformee de Fourier. Des diminutions de T_1 ont été observées pour les groupes carboxyliques de la bilirubine apres l'addition de di-lysine Ces changements suggerent une liaison impliquant une rupture des ponts hydrogenes de la bilirubine et une interaction acide-base entre les groupes carboxyliques de la bilirubine et les groupes amines libres sur les chaînes latérales peptidiques Ceci est confirmé par les changements des C-13 T_1 de la di-lysine observés dans une solution tampon aqueuse de phosphate deutérée lors de l'addition de bilirubine

Abstract

The interaction between bilirubin and the oligopeptide L-lysyl-L-lysine in DMSO solution has been studied by measurements of the proton and carbon-13 spin-lattice relaxation times (T_1's) using the inversion-recovery Fourier transform technique. Decreases were observed in the T_1 values for the carboxyl groups of bilirubin upon adding the di-lysine These changes suggest a binding that involves the breakage of the intramolecular hydrogen-bonds of the bilirubin molecule and an interaction between the carboxyl groups of the bilirubin molecule and the free amine groups on the peptide side chains to form an acid-base linkage. This is confirmed by changes in the C-13 T_1's of di-lysine in deuterated aqueous phosphate buffer solution upon addition of bilirubin.

Introduction

The bilirubin in the human body is a product of the metabolism of hemoglobin of senescent red blood cells. Certain abnormalities in the catabolism process can result in hyperbilirubinemia, a disease frequently seen among newborns (1). Bilirubin has drawn much attention from researchers because of its biomedical importance.

The structure and conformation of bilirubin-IXα have been extensively studied by NMR and by other techniques (2). It is a tetrapyrrole compound with two propionic carboxyl groups. In its unconjugated form, shown in Figure 1, it has six intramolecular hydrogen bonds in the solid state as well as in certain organic solvents (3,4). Consequently, it is hydrophobic and in aqueous solution it has a very low solubility, that decreases as the pH of the solution decreases. It is virtually insoluble in water when the pH is below 7 (3).

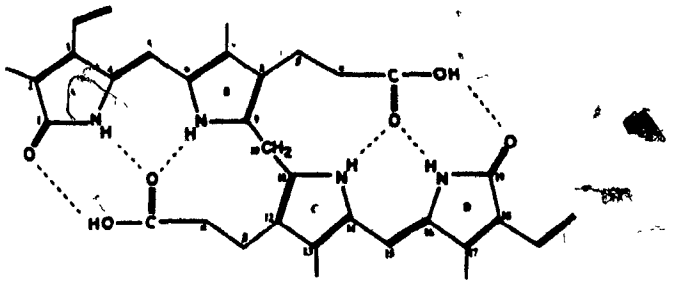

Figure 1. The struture of unconjugated bilirubin-IXα, intramolecular hydrogen bonded.

Serum albumin is known to be the natural carrier of bilirubin in the blood. It has been reported that each albumin molecule can strongly bind two bilirubin molecules, each of them located at a different binding site (3). Although the exact location of the binding sites on serum albumin has not been elucidated, evidence suggests that basic amino acids, such as lysine and arginine, must be at or close to the binding sites (5). This suggestion is supported by the observation that polymer resins with peptide pendants containing these two basic amino acids are very good adsorbents for bilirubin (6,7).

Although certain mechanisms have been proposed for the binding process, the precise details are currently not fully understood. Adsorption studies using polymeric supports with peptide pendants, indicate that the basicity of the amino acids in the pendants is an important feature (6). In addition, cooperative effects within the pendant are indicated, probably involving conformational changes of the peptides (8).

The association between bilirubin and oligopeptides has been studied indirectly by adsorption experiments, but NMR techniques, together with other experimental methods, should produce additional valuable information. The binding or interaction between two molecular species in solution increases the effective molecular weight, and hence, the size of the molecule. In solution, molecules bigger in size tumble less freely, corresponding to a longer correlation time Except for molecules with a very large molecular weight, such as polymers, this increase in correlation time generally leads to a decrease in the spin-lattice relaxation time (T_1) for a molecule undergoing mainly dipolar relaxation (9). This was demonstrated in a study of the binding of drugs such as sulfonamides to bovine serum albumin in aqueous solutions (10). It was found that the relaxation times for the protons on the functional groups involved in the binding decreased significantly. Subsequently, the binding of small ligands to macromolecules has also been explored (11).

The adsorption studies (7) of the binding between bilirubin and oligopeptide sequences gave incomplete information concerning the nature of the interaction and indicated the need for a closer investigation. The general principle of changes in relaxation times that result from binding can be applied to a study of the interaction of bilirubin with oligopeptides. This paper describes the determination of changes in the proton and carbon-13 spin-lattice relaxation times that result from the addition of a simple dipeptide, L-lysyl-L-lysine, to bilirubin. These permit a determination of the functional groups involved in the binding and offer some insight into the nature of the interactions.

Experimental

The proton experiments were performed using a Varian XL-200 NMR spectrometer with the samples contained in 5-mm NMR tubes, while carbon-13 experiments were done with samples in 10-mm tubes using a Varian XL-300 NMR spectrometer The inversion-recovery Fourier transform method (12) was used. Experimental parameters, e.g., the delay time array and irradiating pulse width, were calibrated prior to the experiment. A 180° pulse was applied nonselectively to all the signals to invert the magnetization. Immediately after the pulse, the magnetization was allowed to recover to its equilibrium value over a preselected period of time. For the carbon-13 experiments, a smaller spectral window was used to insure that the pulse was applied equally to all of the signals. The T_1 values were calculated using the computer software installed with the Varian instrument. The reported error for the proton T_1 values was always within ±5%, and in some cases < 1%. For the ^{13}C values of T_1 the errors tended to be larger, but still within 10%.

Bilirubin (Sigma) was used without purification based on high purity as shown by thin-layer chromatography and by HPLC, using methods described previously (13) Because bilirubin in the unconjugated form tends to precipitate in aqueous solutions (3), fully deuterated dimethyl sulfoxide (DMSO-d_6) was chosen as the solvent. The solutions were prepared immediately prior to the experiments and were covered with aluminum foil to prevent exposure to light. Degassed bilirubin solutions kept in a refrigerator remained stable for about one week.

L-Lysyl-L-lysine dihydrobromide, purchased from Vega Biochemicals, dissolves readily in phosphate buffer but is insoluble in organic solvents. To render it soluble in organic solvents it was converted to the salt of trifluoroacetic acid by dissolving it in trifluoroacetic acid (ca. 1 g in 5 ml), warming the solution to 35°C before it was poured into ethyl ether (45 ml). The resulting precipitate was filtered and washed with ether (14). The product was freeze-dried overnight before use and handled in a glove bag filled with dry nitrogen to avoid moisture.

The concentration of the bilirubin was kept in the range of 0.015 – 0.028 M (10 – 15 mg/ml) Relaxation times were measured at 20°C using solutions degassed by bubbling nitrogen through the NMR tube after which it was sealed. The degassing had little or no effect on the measured T_1 values. Following this measurement, sufficient di-lysine was added to obtain a molar ratio of about 1:10. After the resulting solution had been degassed, the second measurement was performed immediately to maintain the experimental conditions identical to those for the first measurement.

The measurements were generally repeated to ensure that the results were reproducible.

For the carbon-13 T_1 measurements of di-lysine, it was dissolved in 5-mm NMR tubes containing deuterated phosphate buffer (0.010 M, pH ≃ 7.8) because of its poor solubility in organic solvent. The concentration of di-lysine in buffer was about 0.20 M. The error for the measurements was < 5%.

Results and Discussion

(A) Proton T_1 Measurements of Bilirubin

The proton NMR spectrum of bilirubin in DMSO-d_6 is shown in Figure 2. The complete peak assignment has been published previously by several authors (4, 15-17). According to a recent NMR study by Kaplan and Navon (18), the intramolecular hydrogen bonds of bilirubin, observed in the solid state and in aqueous solutions, are disrupted by solvation in DMSO.

The stack plot of the relaxation process of bilirubin in DMSO-d_6, determined by the inversion-recovery Fourier transform technique, is shown in Figure 3a. Generally the protons on the more flexible side chains of the bilirubin molecule have longer T_1's than those on the backbone. Upon addition of di-lysine, the relaxation times of certain protons change, as shown by Figure 3b. The derived values of T_1, before and after mixing the di-lysine with bilirubin, for the affected protons are listed in Table I. In addition, small chemical shifts (ca. 0.010 ppm, usually downfield) are also observed.

The most significant change is for the T_1 of the carboxyl protons. The substantial decrease in their T_1 indicates an interaction of these carboxyl groups with the di-lysine. A strong selective broadening effect is also observed for these carboxyl protons. The DMSO used to prepare the solutions was not dried, since the use of drying reagents may introduce impurities (18). Consequently, the carboxyl protons are saturated with exchangeable protons from the water in solution prior to the addition of di-lysine. Therefore, the broadening effect is indicative of an exchange between the carboxyl protons and the exchangeable protons of the di-lysine. It gives added evidence of a specific interaction of the bilirubin moiety with the di-lysine. This is verified by carbon-13 NMR studies which are discussed later.

It is of particular note that the T_1 values for the protons of the NH groups, i.e., the pyrrole and the lactam protons, remain unchanged, within experimental error. On this basis it would appear that their

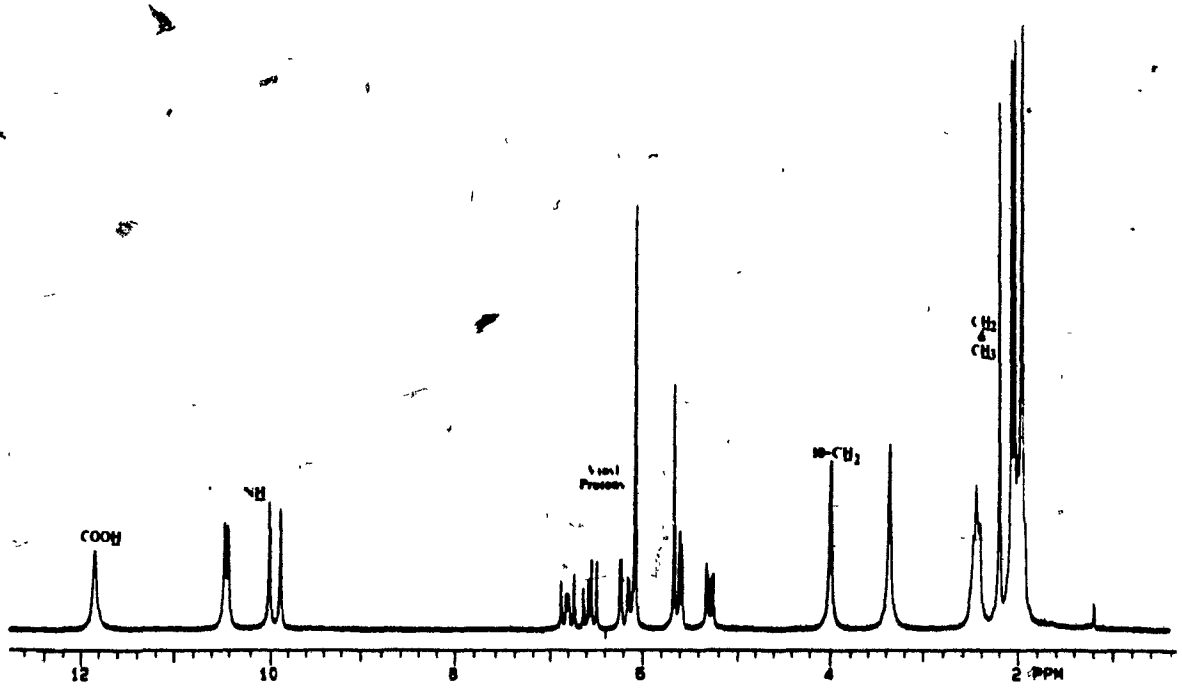

Figure 2. The proton NMR spectrum of bilirubi-IXα in DMSO-d_6.

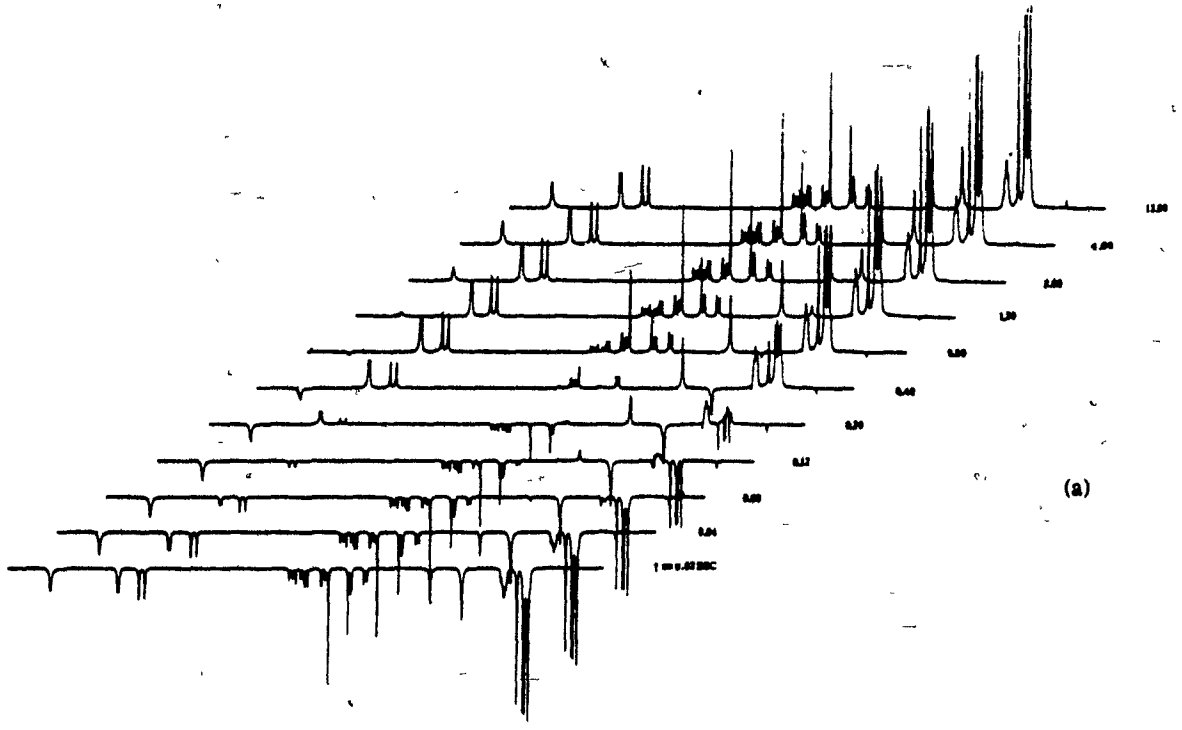

Figure 3. Proton spin-lattice relaxation time plots; 16 transients collected per spectrum; t, delay time: a) T_1 measurement of 0.017 M bilirubin in DMSO-d_6; b) T_1 measurement of 0.017 M bilirubin in DMSO-d_6 with di-lysine, bilirubin/di-lysine molar ratio 10:1.5.

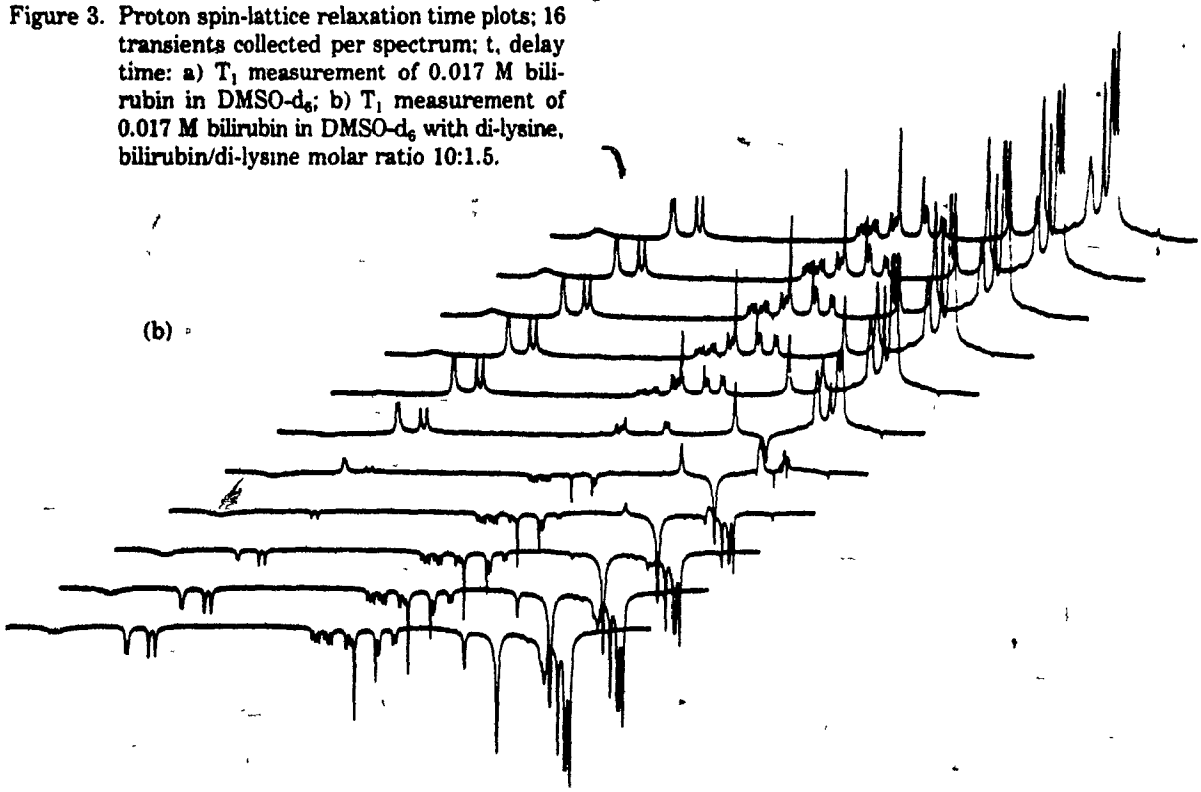

Table I Changes in Proton T_1 Values (in sec) of Bilirubin (BR) upon Addition of Di-Lysine (DL)

Proton	BR	BR + DL	Difference (%)
Carboxyl	1.48	0 87	−41 (1)
	1 49	0 81	−46 (2)
10-methylene	0.14	0 16	+14
	0.14	0 15	+ 7
α-propionic methylene	0.21	0.25	+19
	0.21	0 25	+19
β-propionic methylene	0.15	0.17	+13
	0.15	0 17	+13
7- & 13-methyl	0 41	0 33	−20
	0 41	0 33	−20
	0 40	0.32	−20
	0.40	0 32	−20
2-methyl	0 37	0 32	−14
	0 36	0.31	−14
17-methyl	0 45	0.39	−13
	0 45	0 38	−16

Note. The two groups of data correspond to the following samples.
(1) 0.015 M BR/DMSO, BR/DL molar ratio 10:1 0,
(2) 0.017 M BR/DMSO, BR/DL molar ratio 10:1 5

involvement in the interaction of di-lysine with bilirubin is limited, if there is any at all. Similarly, the vinyl groups on the backbone, carbons C-4, C-5 and C-15, C-16 of bilirubin do not seem to be involved.

The protons of the methyl groups at carbons C-2, C-7, C-13 and C-17 show a significant decrease in T_1 value. This decrease can be attributed to an increase in rigidity that results from the formation of a complex of bilirubin with di-lysine. In solution all four methyl groups on the free bilirubin molecule point toward the environment and can tumble freely. The increase in correlation time and resulting decrease in the T_1 values are consistent with complex formation upon addition of di-lysine. It is particularly interesting to notice that the percentage decrease of T_1 values for the methyl protons on C-7 and C-13 is greater than those for the methyl protons on C-2 and C-17, which are further away from the propionic side chains with the carboxyl groups.

In the case of the binding of two small molecules, where only one correlation time is applicable, only decreases in relaxation times would normally be expected under the extreme narrowing condition. Surprisingly, a small *increase* was observed for the T_1's of the methylene protons, i.e., for protons on the C-10 bridge and on the propionic chains. It is important to note that bilirubin, with a molecular weight of 585, is a relatively large molecule. Upon binding with di-lysine it becomes a complex, the various portions of which may have different correlation times. Consequently, the changes in relaxation time that result from the interaction with di-lysine may differ for the various parts of the molecule. Due to conformational changes of the molecule, the spin-lattice relaxation times for the various groups may involve increases as well as decreases. Thus, the increase in T_1 for the C-10 methylene protons may reflect an increase in correlation time for conditions where the correlation time lies beyond the limit of the extreme narrowing condition, calculated from ^{13}C relaxation times to be approximately 10^{-10} to 10^{-9} seconds. This is supported by the simultaneous increase in T_1 for the propionic methylene protons.

On the other hand, the increase in T_1 of the C-10 methylene protons due to the addition of the oligopeptide suggests that these protons gained freedom, possibly as a result of further dissociation of the intramolecular hydrogen bonds. These hydrogen bonds are known to be between opposite halves of the bilirubin molecule and the binding of di-lysine to a carboxyl group on one half of the bilirubin molecule would certainly disrupt such interactions. The solvation effect of the bilirubin molecules by DMSO is certainly less significant than the binding between bilirubin and the basic peptide.

(B) Carbon-13 T_1 Measurements of Bilirubin

A complete assignment of the carbon-13 nuclear magnetic resonance spectrum of bilirubin in DMSO has been published previously (18,19). Values of T_1 for those carbons of bilirubin affected by the addition of di-lysine are given in Table II.

The carbons of the carboxyl groups on the propionic side chains show a large decrease in T_1. This decrease confirms the earlier suggestion that the decrease in T_1 for the carboxylic protons is not due merely to the broadening effect arising from the proton exchange process. Furthermore, it also indicates that the nature of the interaction is not exclusively hydrogen bonding Since the bilirubin molecules in DMSO solution are already solvated, as a result of the formation of hydrogen bonds with DMSO, it seems unlikely that the mere substitution of this hydrogen bond by another with di-

Table II Changes in C-13 T_1 Values (in sec) of Bilirubin (BR) upon Addition of Di-Lysine (DL)

Carbon	BR	BR + DL	Difference (%)
Carboxyl	2.28	1.69	−26 (1)
10-methylene	0 09	0 11	+22 (2)
α-propionic methylene	0 13	0.12	− 7.7 (2)
β-propionic methylene	0 09	0 11	+22 (2)
7- & 13-methyl	1.33	1.06	−25 (1)

Samples: (1) 0.028 M BR/DMSO, BR/DL molar ratio 10:2.2;
(2) 0.028 M BR/DMSO, BR/DL molar ratio 10:1.5

lysine would result in a significant change in T_1. Therefore, it would seem more probable that this is an acid-base interaction. This will be discussed further in the following section

It is of interest to recall that the di-lysine was added to the bilirubin in the form of the salt of trifluoroacetic acid. Studies by FTIR of this salt dissolved in carefully dried DMSO solution failed to indicate the presence of the free amine group of di-lysine indicating that, under these conditions, the salt is largely undissociated. However, when the solution was prepared with undried DMSO, as was done for the NMR studies, the IR spectra gave clear evidence that the amino groups on the peptide side chains exist as free primary amine groups This would facilitate the formation of the salt bonds with bilirubin in the solution.

Comparison of the changes in T_1, as determined from the proton NMR spectra with those from the ^{13}C spectra indicates similar trends. The methylene group on the central bridge, position 10, is again a very useful sensor in studying the conformation of the bilirubin molecules in solution. The C-10 bridge carbon shows an increased T_1 relaxation time (Table II), as seen in previous T_1 measurements for attached protons, which supports the suggestion that the binding with the peptide involves a complete dissociation of the intramolecular hydrogen bonds of the bilirubin molecule so that the central carbon becomes less restricted and thus has a longer relaxation time. Furthermore, the increase in T_1 for the β-carbon on the propionic chain demonstrates that side chain becomes more flexible when bilirubin is bound to di-lysine Meanwhile, the T_1 for the α-carbons on these two side chains shows a slight decrease, or remains unchanged within experimental error This is consistent with the smaller increase observed for the T_1's of these protons relative to those of the β-carbon.

Since both bilirubin and di-lysine have two functional groups, some of the bilirubin molecules can be complexed together through the di-lysine linkage, forming a complex having a large effective molecular weight. This in turn leads to an increase in the correlation time for the C-10 methylene which now is on the backbone of the complex. The correlation time for the central bridge methylene group of bilirubin is calculated to be approximately 10^{-10} to 10^{-9} seconds and is on the border of the extreme narrowing condition. The increase for the C-10 carbon T_1 value is larger than that for the corresponding protons, as shown in Tables I and II. This discrepancy can be explained by the dependence on frequency of the T_1 values in the range where the correlation time falls around the minimum of T_1. It should also be pointed out that the measurement error for carbon-13 T_1 values is greater than that for the proton T_1's. However, repeated experiments demonstrate the same tendency upon addition of varying amounts of di-lysine

Generally the carbons on the bilirubin backbone show a decrease in the relaxation time as expected. This is obviously due to the increase of the molecular weight resulting from the formation of a complex. The methyl carbons also relax faster in the presence of di-lysine, that is also consistent with the results for the proton T_1's. This is also true for the vinyl carbons at positions 3 and 18.

(C) Carbon-13 T_1 Measurements for Di-Lysine

In the previous section, it has been suggested that the binding between bilirubin and di-lysine is an acid-base binding. The most likely binding would be between the side chain amino groups of di-lysine and the carboxyl groups of bilirubin.

To determine the involvement of di-lysine, experiments were performed in which small quantities of bilirubin were added to excess di-lysine. As mentioned previously, to obtain a concentration of di-lysine sufficient for these experiments, the dipeptide was dissolved in deuterated phosphate buffer This allowed observation of changes in T_1 for carbons of the di-lysine. Table III demonstrates that the T_1 for the carbon adjacent to the side chain amine group is reduced in the presence of bilirubin. This is unequivocal evidence of the involvement of the side chain amine group in the binding of bilirubin to di-lysine and strongly supports the existence of the ammonium carboxylate salt bond.

Both groups of data in Table III demonstrate a decrease of T_1 for this carbon atom The reason for the relatively small change could be the very low solubility of bilirubin in aqueous buffer solution. Consequently, the amount of bilirubin in solution was sufficient to interact with only a very small fraction of the di-lysine. Alternatively, the formation of complex requires the disruption of the extensive intramolecular hydrogen bonds of bilirubin in aqueous solution. Hence, a considerably smaller change would be expected than in DMSO solvent.

Table III Changes in T_1 value (in sec) of the Carbon Adjacent to the Amino Group on the Side Chain of Di-Lysine (DL) upon Addition of Bilirubin (BR)

	DL	DL + BR	Difference (%)
Relaxation Time	1.04	0 96	−7 7 (1)
	1 02	0 98	−4 0 (2)

Note: The two groups of data correspond to the following samples
(1) 0.185 M DL/buffer, DL/BR molar ratio 1000:6.
(2) 0 210 M DL/buffer, DL/BR molar ratio 1000:4.

Summary

From this study, it can be concluded that in the polar organic solvent, DMSO, the remarkable decrease of the relaxation time for the carboxyl group of the bilirubin molecule indicates that this group is involved in an interaction with di-lysine. On the other hand, the decrease of the T_1 for the carbon adjacent to the amino groups on the di-lysine side chains provides evidence that the basic amino groups are involved in the binding. This is in agreement with the results of adsorption experiments in which it was found that an increase in the number of amino acids in the peptide pendants attached to the solid-polymer support increases the amount of bilirubin adsorbed (7). The nature of the interaction is predominantly salt binding. The interaction process involves the dissociation of the intramolecular hydrogen bonds of the bilirubin molecule and the formation of the ammonium carboxylate salt bond between bilirubin and the peptide.

Acknowledgments

The authors are grateful to Dr. F. Sauriol for assistance in performing the NMR experiments and to Prof. D.F.R. Gilson for helpful discussions. X.X.Z. wishes to express his gratitude to the Chinese Ministry of Education for a scholarship and to McGill University for the Clifford C.F. Wong Fellowship. Support in the form of operating grants from NSERC and FCAR is gratefully acknowledged.

References

1 K.-S. Lee, and L.M. Gartner, "Fetal bilirubin metabolism and neonatal jaundice", in "Bile pigments and jaundice, molecular, metabolic and medical aspects", ed., J.D. Ostrow, Dekker, N.Y., 1986, p. 373.
2 M.S. Stoll, "Formation, metabolism, and properties of pyrrolic compounds appearing in the gut", in "Bilirubin, Vol. II; Metabolism", ed., K.P.M. Heirwegh and S.B. Brown, CRC Press, Inc., Florida, 1982, p. 103.
3 R. Brodersen, "Binding of bilirubin to albumin", CRC Crit. Rev. Clin. Lab. Sci., CRC Press, Inc., Cleveland, 1980, p. 305.
4. A.F. McDonagh, "Bile pigments bilatrienes and 5, 15-biladienes", in "The porphyrins", Vol. VI, Part A, ed., D. Dolphin, Academic Press, 1979, p. 403.
5 C. Jacobsen, Eur. J. Biochem., *27*, 513 (1972).
6 D.S. Henning, G.A. Lajoie, G.R. Brown, L.E. St-Pierre, and S. St-Pierre, Int. J. Artif. Organs, *7*, 209 (1984).
7 D.S. Henning, G.R. Brown, and L.E. St-Pierre, Int. J. Artif. Organs, *9*, 33 (1986).
8 M. Bouvier, G.R. Brown, and L.E. St-Pierre, in press, Aug., Can. J. Chem.
9 R.J. Abraham and P. Loftus, "Proton and carbon-13 NMR spectroscopy", Heyden & Son Ltd., 1980, pp. 128-129.
10. O. Jardetzky and N.G. Wade-Jardetzky, Mol. Pharmacol., *1*, 214 (1965).
11 P.J. Andree, J. Mag. Reson., *29*, 419 (1978).
12. M.L. Martin, J.J. Delpuech, and G.J. Martin, "Practical NMR spectroscopy", Heyden & Son Ltd., 1980, pp. 254-256.
13 J.J. McCarthy, S.A. McClintock, and W.C. Purdy, Anal. Lett., *17 (16B)*, 1843 (1984).
14 M.M. Ponpipom, R.L. Bugianesi, J.C. Robbins, T.W. Doebber and T.Y. Shen, J. Med. Chem., *24*, 1393 (1981).
15 C.C. Kuenzle, Biochem. J., *119*, 395 (1970).
16. M.S. Stoll, N. Vicker, C.H. Gray and R. Bonnett, Biochem. J., *183*, 139 (1979).
17 D. Kaplan and G. Navon, Isr. J. Chem., *23*, 177 (1983).
18 D. Kaplan and G. Navon, Biochem. J. *201*, 605 (1982).
19 P.E. Hansen, H. Thuesen, and R. Brodersen, Acta Chim. Scand., *B33*, 281 (1979).

A Nitrogen-15 NMR Study of Bilirubin and Some Derivatives Using the INEPT Pulse Sequence

X.X. Zhu, F. Sauriol, G.R. Brown and L.E. St-Pierre
Department of Chemistry
McGill University
801 Sherbrooke St. W.
Montreal, PQ, Canada H3A 2K6

Résumé

Les spectres de RMN de l'azote-15 de la bilirubine et de quelques-uns de ses dérivés, tel le diester de méthyl de la bilirubine, la bilirubine ditaurine conjuguée et la biliverdine, ont été enregistrés à l'aide de la séquence INEPT. Des expériences de corrélation hétéronucléaire ^{15}N-^{1}H en RMN bidimensionnelle ont permis l'assignation des signaux d'azote-15. L'étude de l'interaction entre la bilirubine et le chlorure de triméthylbenzylammonium, à l'aide de la RMN de l'azote-15, a montré que ce sont les groupes NH pyrroles qui sont impliqués dans cette interaction, comme on peut le constater par la diminution des signaux pyrroles dans le spectre de RMN INEPT de l'azote-15.

Abstract

The nitrogen-15 NMR spectra of bilirubin and some of its derivatives such as bilirubin dimethyl ester, bilirubin ditaurine conjugate and biliverdin, in DMSO have been recorded using the INEPT pulse sequence. To assign the ^{15}N peaks, two dimensional ^{15}N-^{1}H heteronuclear correlation NMR experiments were performed. The interaction between bilirubin and benzyltrimethylammonium chloride is indicated by the diminution of the pyrrole nitrogen peaks in the ^{15}N INEPT spectrum.

Introduction

Bilirubin, a natural bile pigment formed by the catabolism of hemoglobin, has drawn much attention from researchers because of its biomedical importance, especially as related to jaundice. The increasing interest in phototherapy and hemoperfusion studies of bilirubin in recent years has stimulated the investigation of the structure and conformation of the bile pigments by a variety of physical techniques (1), but especially by NMR.

It is well known that bile pigments are tetrapyrrole compounds with two propionic carboxyl groups. A structure for bilirubin was first suggested by Fischer *et al.* in 1941 (2). Subsequently, modifications to that structure were proposed by many researchers (1) and Fig. 1a gives the currently accepted structure. The two carboxyl groups readily form six intramolecular hydrogen bonds with the pyrrole and lactam groups (Fig. 1c). As a result of the formation of these intramolecular hydrogen bonds, bilirubin is very hydrophobic. Therefore, it is not surprising that bilirubin is practically insoluble in aqueous solutions, except in strongly alkaline solutions that disrupt the hydrogen bonds. It dissolves with limited solubility in some organic solvents, such as dimethylsulfoxide (DMSO) and chloroform.

The structure and conformation of bilirubin in DMSO and chloroform have been studied extensively by proton and carbon-13 NMR. With the development of the powerful Fourier transform NMR technique, researchers have been able to confirm the hydrogen-bonded structure and conformation for some of the bile pigments and their related derivatives. These studies has been reviewed by Kaplan and Navon (3).

In addition to the protons and the carbon atoms, there are also four nitrogen atoms in the molecules of bile pigments, two of which are on the pyrrole rings and the remaining two on the lactam rings. The study of these nitrogen atoms, by NMR, can give interesting information concerning the conformation of bilirubin. Furthermore, the chemical shifts of ^{15}N are known to be more sensitive to environment than those of proton and ^{13}C. Consequently, the ^{15}N chemical shifts may offer a good probe for the study of the interactions of bilirubin with various other molecules.

Although nitrogen-14 is the most abundant isotope, it is not ideal for NMR studies because of the line broadening (up to several kHz) associated with its quadrupolar nature. The nitrogen-15 nucleus has a spin of 1/2, but its low natural abundance (only 0.365%) and unfavorable gyromagnetic ratio (-2.7112×10^7) make it very difficult to detect (4). However, it is possible to obtain sharp ^{15}N lines, especially when sufficient sample is available and an appropriate pulse sequence is applied. Modern enhancement techniques, such as the INEPT (Insensitive Nuclei Enhanced by Polarization Transfer) and DEPT (Distortionless Enhancement by Polarization Transfer) sequences, can be used to improve the signal. For example, Hansen *et al.* have recently reported the nitrogen-15 NMR spectrum for bilirubin in DMSO, obtained by use of a pulse sequence called SINEPT (5). The commonly used INEPT pulse sequence (6) can easily be applied to obtain enhanced nitrogen-15 NMR spectra.

In a previous study of the interaction between bilirubin and di-lysine, using ^{1}H and ^{13}C spin-lattice relaxation time measurements, interesting information was presented on the binding of bilirubin with oligopeptides, which is of importance in biomedical research (7). In the present paper we report the complete assignment of the ^{15}N spectra of bilirubin and some of the related pigments, as determined by the use of two-dimensional heteronuclear correlation experiments. Studies of the interaction of bilirubin with benzyltrimethylammonium chloride, based on the ^{15}N spectra, are also presented and compared with the interaction of bilirubin with di-lysine.

Results and Discussion

Spectral Assignments

As expected, four signals, in pairs of two, were detected in the decoupled ^{15}N spectrum of bilirubin IXα in DMSO using the INEPT techniques (Fig. 2). The peaks in the ^{15}N spectrum of bilirubin were partially assigned by Hansen and Jakobsen in 1984 (5). That assignment is confirmed by the data obtained by a ^{15}N-^{1}H heteronuclear correlation experiment (Fig. 2). Thus, based on the proton assignment reported by Kaplan and Navon (3), the pair located at the upper field, –249.59 and –249.02 ppm, correlate with the protons of the lactam groups, at positions 21 and 24 respectively, while the other pair at the lower field, –231.39 and –231.07 ppm, belong to the two pyrrole groups positions 22 and 23. However, since the two pyrrole protons signals at 10.46 and 10.49 ppm, respectively, were not differentiated from one another, it is not possible to make a complete assignment of the ^{15}N spectrum of bilirubin (5).

To obtain the information required for this assignment, the spectrum is compared with those of its derivatives and some other related bile pigments. The proton NMR spectrum of bilirubin dimethyl ester has been published previously by Trull *et al.*, with peak assignments based on a comparison with the spectra of pyrromethenones, including a separation of the pyrrole protons (8). The ^{15}N spectrum of bilirubin dimethyl ester (Fig. 3) is nearly identical to that of bilirubin. For the pyrrole nitrogens, there is a small downfield shift of 0.24 and 0.22 ppm, while the two lactam nitrogen atoms show a slight upfield shift of 0.11 and 0.10 ppm (Table 1). Interestingly, these changes in the chemical shift for ^{15}N signals are in accordance with the changes observed in the proton chemical shift; pyrrole protons shift downfield by 0.07 ppm, lactam protons shift upfield by 0.02 ppm, as shown in Table 2.

The similarity of the ^{15}N spectra indicates that in DMSO-d_6 both bilirubin and its dimethyl ester assume identical conformations, as suggested by earlier researchers (8,9). The intramolecular hydrogen bonds of bilirubin are disrupted in DMSO and as a consequence there is no NOE (nuclear Overhauser enhancement) effect on the NH protons from the carboxyl protons (9). However, in chloroform solutions, the derived values for the NOE effect indicate that bilirubin retains the intramolecular hydrogen bonds (10). In DMSO solutions, the intramolecular hydrogen bonds of bilirubin are disrupted and intermolecular hydrogen bonds are formed with the DMSO molecules, similar to those of bilirubin dimethyl ester. This solvation effect in DMSO makes both bilirubin and the ester adopt similar conformations. The similarity in conformation for these two compounds in DMSO is also characterized by similar spin-lattice relaxation times for the central bridge methylene groups, as reported by Kaplan and Navon (9).

The 2-D correlation spectrum for bilirubin dimethyl ester permits the complete assignment of its ^{15}N spectrum (Fig. 3). The ^{1}H and ^{15}N spectra of bilirubin and bilirubin dimethyl ester are very similar in both dimensions, as seen in a comparison of Figs. 2 and 3. The peaks in the contour plot appear at the same relative positions, so that the assignments for these compounds should be the same. Therefore, it may be concluded that, in the bilirubin ^{15}N spectrum, the pyrrole nitrogen signal that appears at the lower field belongs to the 22 NH while the one at the upper field side belongs to the NH of the 23 position (Table 1). Hence, in the proton spectrum the relative signal positions are reversed: the 22 NH proton appears at 10.49 ppm, the 23 NH proton at 10.46 ppm.

The ^{15}N spectrum of conjugated bilirubin (ditaurate sodium salt) was also recorded (Table 1). The two signals for lactam nitrogen remained unchanged. The pyrrole nitrogen signals were both shifted upfield by 0.41 ppm, obviously due to the sustitution on the propionic side chains. The ditaurine amide nitrogen appeared as a sharp signal at –264.43 ppm. The correlation of the 2-D ^{15}N-^{1}H spectrum of the bilirubin conjugate is identical to those of bilirubin and bilirubin dimethyl ester.

Biliverdin samples required a longer acquisition time than the other bile pigment samples, due to the relatively longer spin-lattice relaxation time of the NH groups. In the ^{15}N NMR spectrum of biliverdin, three sharp signals were detected. The signals at –246.11 and –246.17 ppm correspond to the two lactam NH groups, while the other at –245.44 ppm corresponds to the pyrrole NH group (Table 1). This assignment was also confirmed by a ^{15}N-^{1}H correlation experiment. The difference between the chemical shifts of these two lactam ^{15}N peaks is only 0.06 ppm, much smaller than expected from the structural difference of the respective groups. This is indicative of similar chemical environments for both rings A and D in spite of the structural difference for these two rings, as shown in Fig. 1b. This result is consistent with a reported fast proton exchange process between rings B and C, as determined by fluorescence (11). However, the rate of the exchange is still slow enough to allow the detection of the single pyrrole NH group of biliverdin at –245.44 ppm.

Interaction Studies

A previous study of proton spin-lattice relaxation times suggested that bilirubin interacts with di-lysine by forming an acid-base linkage through the carboxyl groups of bilirubin and the amino groups on the lysine side chains while the lactam and pyrrole groups of bilirubin have shown little evidence of involvement in any interaction with di-lysine (7). It is of interest to investigate further the interaction of bilirubin with oligopeptides, such as di-lysine, which is known to interact with bilirubin (12), by considering the ^{15}N chemical shifts. The addition of di-lysine does not result in significant changes to the ^{15}N spectrum of bilirubin in DMSO (Fig. 4b). The chemical shifts for the lactam nitrogens remained unchanged within experimental error and the signals of the pyrrole nitrogen were detected to be shifted downfield about 0.08 and 0.10 ppm, respectively. The changes for the pyrrole groups of bilirubin correspond to the involvement of the nearby carboxyl groups in the interaction. This is consistent with the results obtained by the

proton spin-lattice relaxation time measurements (7), which indicated that the NH groups of the bilirubin molecules were little involved in the interaction with the oligopeptide.

The interaction of amines with bilirubin is of considerable interest since it is known that cholestyramine adsorbs bilirubin and some other biocompounds, albeit with limited capacity and poor biocompatibility (13). This material has benzyltrimethyl quaternary ammonium functional groups on a crosslinked polystyrene backbone. To obtain insight into the interaction of bilirubin with quaternary ammonium functional groups of cholestyramine, studies were made of the effect on the ^{15}N NMR spectrum of bilirubin upon addition of benzyltrimethylammonium chloride, which closely resembles the functional groups of cholestyramine.

The signals of the two pyrrole nitrogens diminished significantly when benzyltrimethylammonium chloride was added (Fig. 4c). Since the proton signals were used to enhance the intensity of the ^{15}N peaks in INEPT, this behavior is consistent with the absence of the proton on these groups. Note that there is also a chemical shift change of about 1 ppm accompanied with the diminution of the pyrrole ^{15}N signals. It is possible that the diminution could be caused by proton exchange, since moisture and other exchangeable protons existed in the solution. Benzyltrimethylammonium chloride itself is very hygroscopic. The drying of the mixture with molecular sieves was attempted but it caused precipitation.

To study the effect of the presence of water, small amounts of distilled water were deliberately added to the bilirubin solution in DMSO-d_6. No significant change was found for the ^{15}N signals (Fig. 4d). On the other hand, the addition of inorganic salts or acids caused precipitation of bilirubin. In fact, the proton exchange rate of pyrrole NH group of bilirubin has been reported to be much lower than that of the lactam NH group (10). Evidently, the addition of benzyltrimethylammonium chloride accelerates the proton exchange process of the pyrrole groups, while the lactam groups are less affected. This suggests a specific interaction between the quaternary ammonium salt and the pyrrole NH groups of bilirubin.

As expected, proton spectra of bilirubin in DMSO with water and with benzyltrimethylammonium chloride were characterized by the disappearance of the carboxylic proton signals on the propionic side chains. The two adjacent pyrrole NH proton peaks of bilirubin in DMSO-d_6 gradually collapse into one single broad peak upon the addition of benzyltrimethylammonium chloride. In contrast, upon addition of water to bilirubin solution, the pyrrole protons gave two separate peaks, as in pure bilirubin samples. The signals of the four NH protons in the sample of bilirubin with benzyltrimethylammonium chloride are broadened, along with significant changes in chemical shifts (Fig. 5). This downfield shift is possibly due to the deshielding effect of the π-electrons of the benzene ring when the benzene ring is aligned with the pyrrole rings of bilirubin upon interaction. Since there is a rapid proton exchange involving the pyrrole groups of bilirubin, as evidenced by the ^{15}N spectrum, it is unlikely that this deshielding is caused by increased hydrogen bonding.

Unlike di-lysine, benzyltrimethylammonium chloride is very soluble in DMSO so that a considerable amount can be added to the bilirubin solution. It is possible that the ionized form of benzyltrimethylammonium chloride interacts not only with the carboxyl groups of bilirubin but also with the pyrrole groups. However di-lysine interacts only with the propionic acid groups of bilirubin.

Conclusions

The ^{15}N and proton spectra of bilirubin and some of the related derivatives have been assigned by 2-D ^{15}N-^{1}H heteronuclear correlation with the results shown in Tables 1 and 2. The similar conformations of bilirubin and bilirubin dimethyl ester in DMSO are confirmed by the ^{15}N studies. The proton exchange between the two pyrrole rings of biliverdin molecule is identified by the ^{15}N spectrum. The ^{15}N study has also confirmed that the involvement of the NH groups of bilirubin in the interaction with di-lysine is negligible. The addition of a quaternary ammonium

salt (benzyltrimethylammonium chloride) selectively accelerates the proton exchange of pyrrole groups of bilirubin, indicating that the pyrrole NH groups are involved in the interaction.

Materials and Experimental

Bilirubin IXα, purchased from Sigma, was of high purity as determined by thin layer chromatography and high performance liquid chromatography (14). Biliverdin IXα was also purchased from Sigma with a 85% purity. Bilirubin dimethyl ester and bilirubin conjugate (ditaurate sodium salt) were purchased from Porphyrin Products (Utah, USA). The bilirubin dimethyl ester commercial product was impure as checked by t.l.c. test. The compounds were used without further treatment or purification since the NMR spectra of these compounds indicated acceptable purity for the experiments.

L-Lysyl-L-lysine dihydrobromide (Vega) was converted to trifluroacetic acid salt, using a procedure described in an earlier report (7). Benzyltrimethylammonium chloride was purchased from Aldrich.

The solution of bile pigments in DMSO-d_6 was prepared in 10 mm NMR tubes. The solution was filtered carefully in a glove bag filled with dry nitrogen and was degassed with nitrogen for about 10 minutes. This process was performed in a dark room, using a dim red light when necessary.

The nitrogen-15 spectra, recorded with a Varian XL-300 NMR spectrometer operating at a ^{15}N frequency of 30.406 MHz, were on a scale with nitromethane set as the 0 ppm reference. The detected ^{15}N signals all appeared upfield relative to CH_3NO_2, therefore, acquiring a negative sign. The stability of the magnetic field was verified by recording the ^{15}N spectra of dimethylacetamide (90% with DMSO-d_6) with and without an external reference. A very small change (ca. 0.02 ppm) was detected, indicating an acceptable stability for the magnetic field.

The refocussed INEPT pulse sequence as shown below was used to detect the ^{15}N signal. The delays used in the sequence were based on an average value of $^1J_{NH}$ (95 Hz) observed for bilirubin (5). The value of t_D in all cases was 2.63 ms ($1/(4\,^1J_{NH})$). The refocussing period (t_R) was also set to 2.63 ms to maximize the detection of the NH groups. One of the advantages of the INEPT experiment is that the repetition rate of the sequence is based on the short proton spin-lattice relaxation times of the NH groups, thus permitting the use of a short preparation delay (D_1) of 0.4 to 0.5 seconds.

$$^1H \quad D_1\text{-}(\pi/2)_x\text{-}t_D\text{-}(\pi)_x\text{-}t_D\text{-}(\pi/2)_y\text{-}t_R\text{-}(\pi)_x\text{-}t_R\text{-DEC}$$
$$^{15}N \quad (\pi)\text{-}t_D\text{-}(\pi/2)\text{-}t_R\text{-}(\pi)\text{-}t_R\text{-ACQ}$$

(The refocussed INEPT pulse sequence)

Two-dimensional heteronuclear correlation experiments were then conducted to assign the nitrogen peaks for the bile pigments. The spin-lattice relaxation times for the pyrrole and lactam protons of these molecules were determined previously by the inversion recovery technique. Proper delay time and pulse width were calibrated prior to the experiment and were carefully chosen to optimize the spectrum.

Acknowledgement

The authors wish to thank Dr. A. Natasohn for helpful discussions on general topics of NMR experiments. XXZ thanks McGill University for providing the Clifford C.F. Wong Fellowship and the Dalbir Bindra Fellowship. Financial support from the National Sciences and

Engineering Research Council of Canada and the Quebec Government (FCAR Fonds) is gratefully acknowledged.

References

1. A.F. McDonagh, "Bile Pigments: Bilatrienes and 5,15-Biladienes", in The Porphyrins, Vol. VI, Part A, D. Dolphin, ed., Academic Press, 1979
2. H. Fischer, H. Plienenger & O. Weissbarth, *Z. Physiol. Chem.*, **268**, 197 (1941)
3. D. Kaplan & G. Navon, *Isr. J. Chem.*, 23, 177 (1983)
4. G.J. Martin, M.L. Martin & J.-P. Gouesnard, Chapter 1 in ^{15}N-NMR Spectroscopy, Springer-Verlag, Berlin-Heidelberg-New York, 1981
5. P.E. Hansen & H.J. Jakobsen, *Org. Mag. Reson.*, 22, 668 (1984)
6. (a) G.A. Morris & R. Freeman, *J. Am. Chem. Soc.*, **101**, 760 (1979); (b) G.A. Morris, *J. Am. Chem. Soc.*, **102**, 428 (1980)
7. X.X. Zhu, G.R. Brown & L.E. St-Pierre, *Can. J. Spectr.*, 32, 49 (1987)
8. F.R. Trull, J-S. Ma, G.L. Landen & D.A. Lightner, *Isr. J. Chem.*, 23, 211 (1983)
9. D. Kaplan & G. Navon, *Biochem. J.*, 201, 605 (1982)
10. D. Kaplan & G. Navon, *J. Chem. Soc., Perkin Trans. II*, 1374 (1981)
11. S.E. Braslavsky, A.R. Holzwarth & K. Schaffner, *Angew. Chem. Int. Ed. Engl.*, **22**, 656 (1983)
12. D.S. Henning, G.R. Brown & L.E. St-Pierre, *Intern. J. Artif. Org.*, 9, 33 (1986)
13. S. Sideman, L. Mor & M. Brandes, *Trans. Am. Soc. Art. Intern. Organs*, **25**, 497 (1979)
14. J.J. McCarthy, S.A. McClintock & W.C. Purdy, *Anal. Lett.*, 17 (16B), 1843 (1984)

Table 1 ^{15}N Chemical Shifts of Bile Pigments in DMSO-d_6

Compound	Chemical Shift (ppm) 21	22	23	24
Bilirubin	-249.59	-231.07	-231.39	-249.02
BRDME	-249.70	-230.83	-231.17	-249.12
BR Ditauride	-249.56	-231.48	-231.80	-249.02
Biliverdin	-246.17		-245.44	-246.11
BR + Dilysine	-249.53	-230.99	-231.29	-249.00

BR: Bilirubin; BRDME: Bilirubin Dimethyl Ester.

Table 2 ^{1}H Chemical Shifts of Bile Pigments in DMSO-d_6

Compound	Chemical Shift (ppm) 21	22	23	24
Bilirubin	10.05	10.49	10.46	9.93
BRDME	10.03	10.56	10.53	9.91
BR Ditauride	10.07	10.44	10.40	9.94
Biliverdin	10.79		10.67	10.79
BR + Dilysine	10.08	10.56	10.53	9.95
BR + BTMACl	10.33	10.80	10.80	10.20
BR + Water	10.04	10.49	10.46	9.91

BR: Bilirubin; BRDME: Bilirubin dimethyl ester; BTMACl: Benzyltrimethylammonium Chloride.

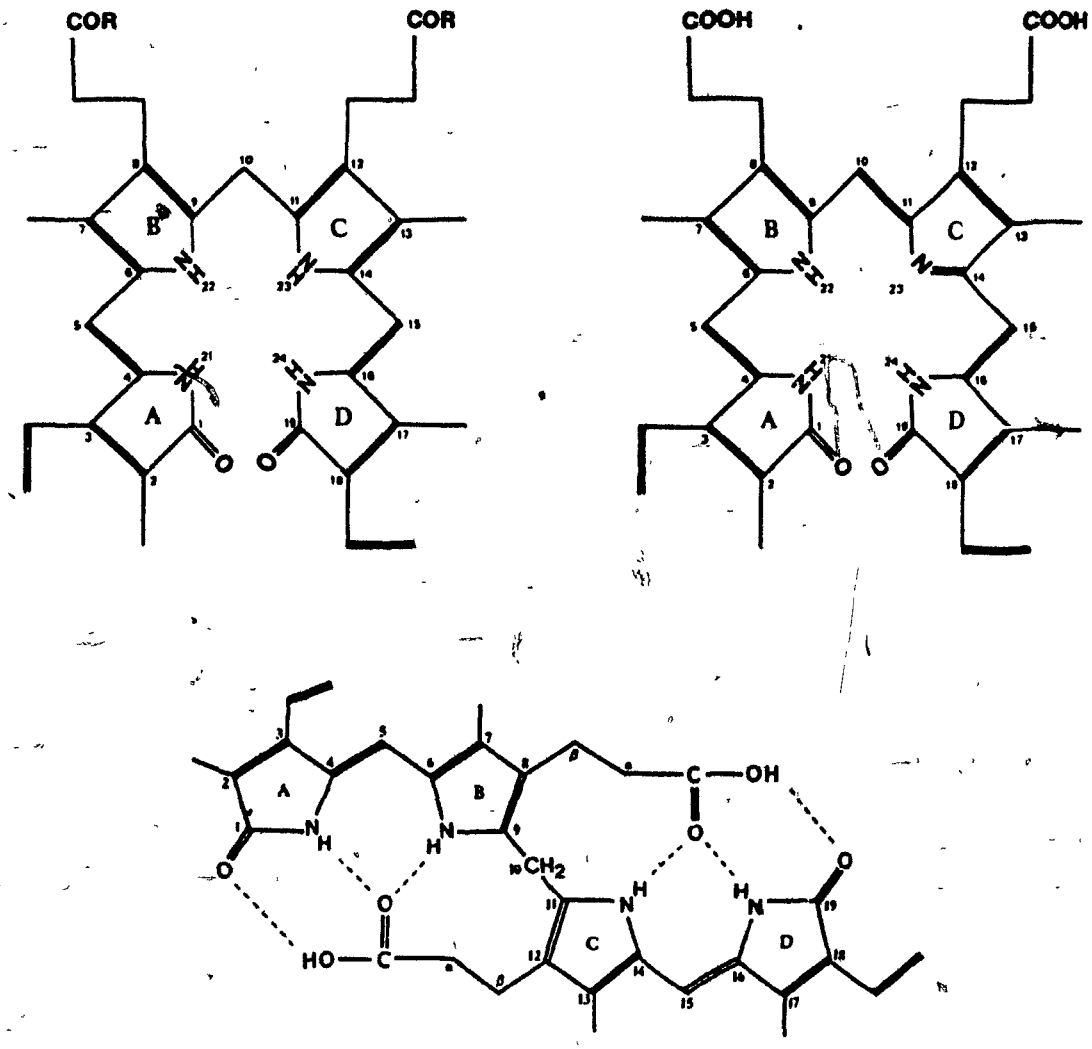

Fig. 1 The structure of bile pigments: (a) R = OH, bilirubin IXα; R = OCH_3, bilirubin dimethyl ester; R = $NHCH_2CH_2SO_3H$, bilirubin ditaurine conjugate; (b) Biliverdin IXα; (c) Intramolecularly hydrogen bonded bilirubin IXα.

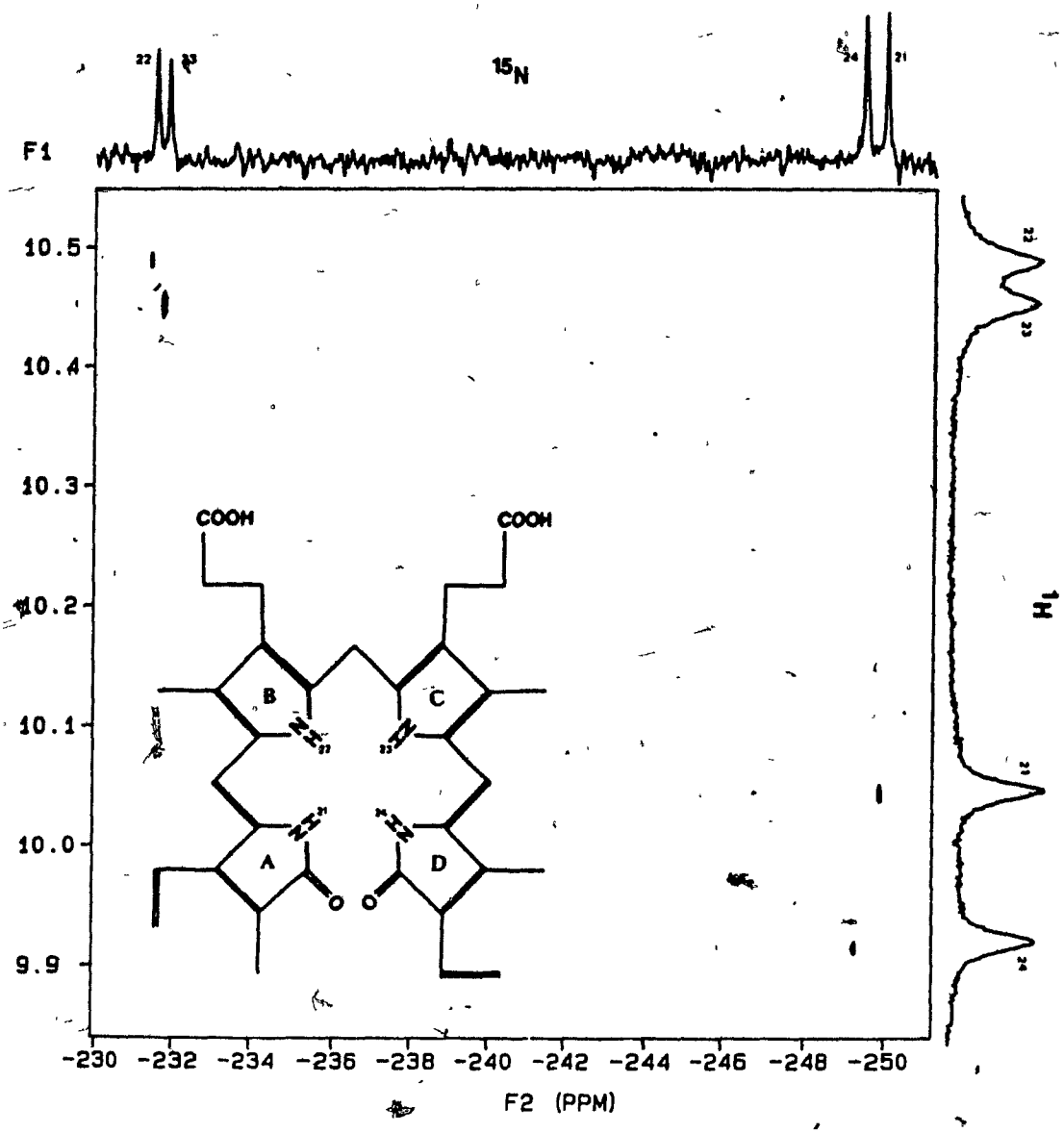

Fig. 2 The 2-D (^{15}N-^{1}H) spectrum of bilirubin in DMSO-d_6.

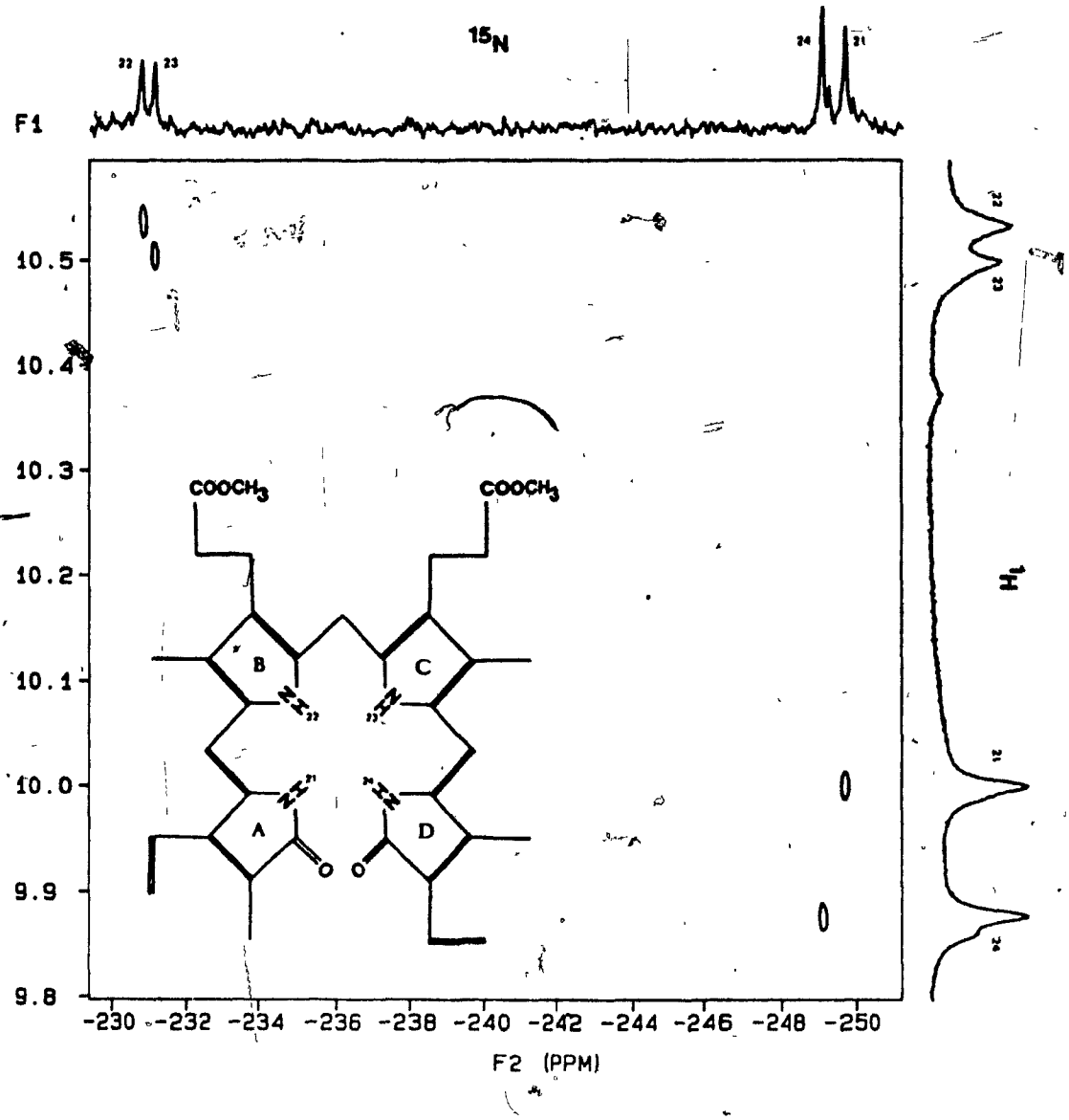

Fig. 3 The 2-D (^{15}N-^{1}H) spectrum of bilirubin dimethyl ester in DMSO-d_6.

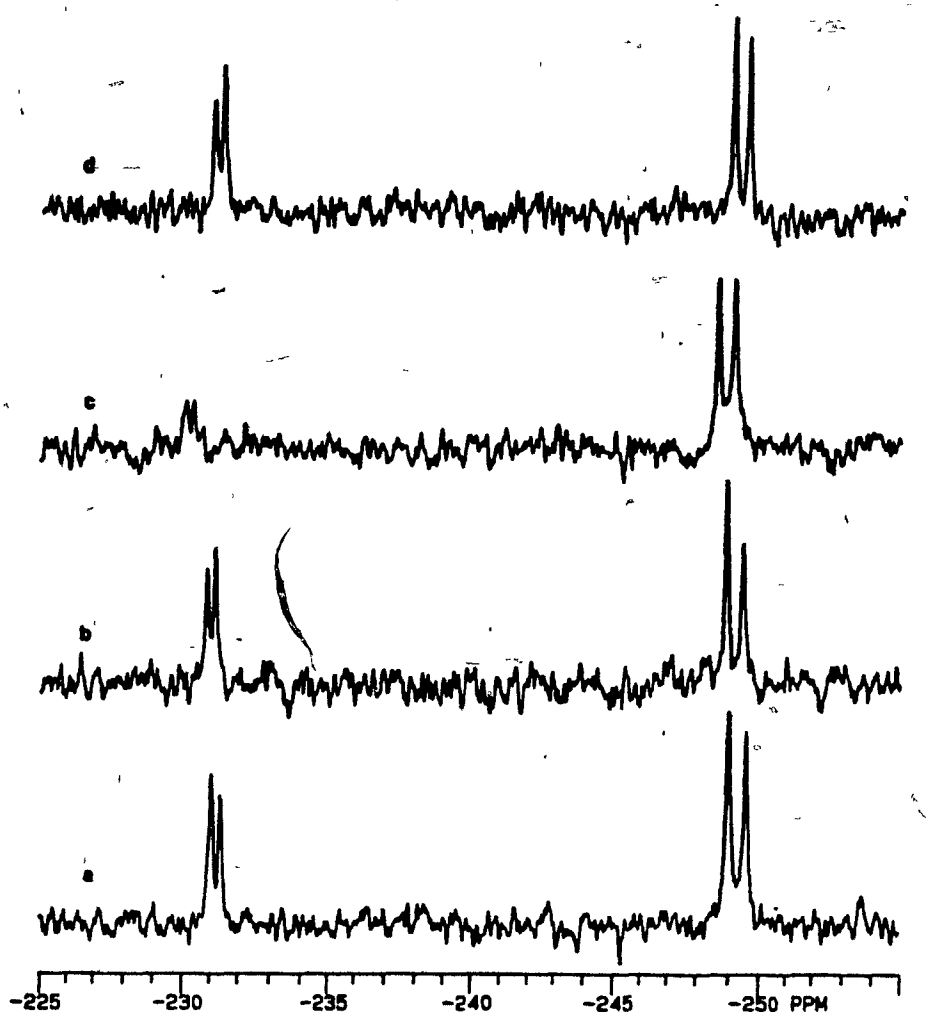

Fig. 4 The ^{15}N spectrum of (a) bilirubin; (b) bilirubin + di-lysine; (c) bilirubin + benzyltrimethylammonium chloride; (d) bilirubin + water. Solvent: DMSO-d_6.

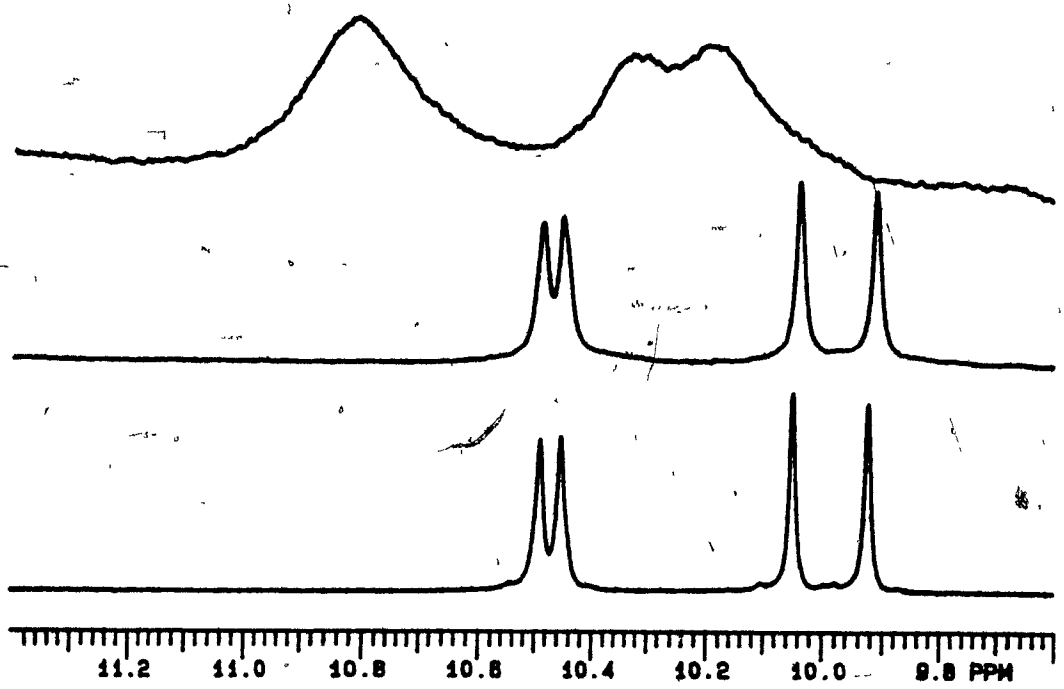

Fig. 5 The ^1H spectra of the NH groups: (a) Bilirubin; (b) Bilirubin + Water; (c) Bilirubin + Benzyltrimethylammonium Chloride. Solvent: DMSO-d_6.